



**Università
degli Studi
di Ferrara**

DOCTORAL COURSE IN "CHEMICAL SCIENCE"
CYCLE XXXV

DIRECTOR Prof. Alberto Cavazzini

**Design, synthesis and biological evaluation of
novel anticancer agents able to target the
hBAG3 protein**

Scientific/Disciplinary Sector (SDS) CHIM/08

Candidate

Dott. Federica Budassi

Supervisor

Prof. Romeo Romagnoli

Co-Supervisor

Dr. Colin P. Leslie

Years 2019/2022

CONTENTS

1. INTRODUCTION.....	7
1a - Impact	7
1b - The BAG proteins family	9
1c - The BAG/HSP70 complex.....	11
1d - BAG3 and its multiple roles in cancer.....	15
1e - The role of BAG3 in apoptosis escape	17
1f – Small molecules targeting BAG3-HSP70 PPI.....	21
1g - PROTAC (Proteolysis Targeting Chimera).....	25
1h - Advantages of PROTACs.....	29
1i - Elements of PROTAC design.....	30
1l - Targeting apoptosis with PROTACs.....	33
2. AIMS OF THE THESIS	35
3. DISCUSSION AND BIOLOGICAL RESULTS	37
3a - SAR exploration on position 3 of the 2,4-thiazolidinedione	41
3b – SAR exploration on position 5 of the 2,4-thiazolidinedione	51
3c - Thiazolidinedione “core” replacement and exploratory derivatives.....	62
3d - <i>In vitro</i> cell viability assay of the most relevant BAG3 inhibitors.....	69
3e - <i>In vitro</i> synergistic studies on HD-MB03 R cells.....	71
3f - PROTACs.....	73
4. CONCLUSIONS AND FUTURE PLANS.....	84
5. EXPERIMENTAL PROCEDURES.....	86
6. REFERENCES.....	142
7. ACKNOWLEDGEMENTS	150

ABBREVIATIONS

ADP	Adenosine 5'-diphosphate
APAF1	Apoptotic protease activating factor-1
ATP	Adenosine 5'-triphosphate
BAG	BCL-2 associated athanogene
BAK	BCL-2 antagonist/killer
BAX	BCL-2 associated X protein
BCL-2	B-Cell lymphoma 2
BCL-XL	B cell lymphoma extra-large
BCL-W	B cell lymphoma w
BD	BAG domain
BFL1	BCL2-related isolated from fetal liver 1
BID	BH3-interacting domain death agonist
BIM	BLC-2-interacting mediator of cell death
Boc	'Butyloxycarbonyl
CHIP	C-terminus of the HSC70-interacting protein
CHX	Cyclohexane
Conc.	Concentration
CRBN	Cereblon
DAD	Diode-array detector
DC₅₀	Half-maximal degradation concentration
DCM	Dichloromethane
DIPEA	N,N-Diisopropylethylamine
DMF	N,N-dimetilformammide
D_{max}	Maximum dose
EC₅₀	Half maximal effective concentration
EGF	Epidermal growth factor
Eq.	Equivalent
EtOAc	Ethyl acetate
EWG	Electron withdrawing group
HATU	O-(7-Azabenzotriazol-1-yl)-N,N,N',N'-tetramethyluronium hexafluorophosphate
HBA	Hydrogen bond acceptor
HBD	Hydrogen bond donor
HFIP	Hexafluoro-2-propanol
HSC70	Heat shock cognate 71 kDa
HSF	Heat shock elements
HSF	Heat shock transcription factor
HSP70	Heat shock protein 70-kilodalton
HSP40	Heat shock protein 40-kilodalton
HPLC	high performance liquid chromatography
HTS	High throughput screening
IAP	Inhibitor of apoptosis protein
IC₅₀	Half maximal inhibitory concentration
IFS	Immunofluorescence
IMiDS	immunomodulatory imide drugs
IPV	Ile-Pro-Val

Kd	Dissociation constant
LC-MS	Liquid chromatography mass spectrometry
LHS	Left-hand-side
MCL1	Myeloid cell leukaemia 1
MeCN	Acetonitrile
MeOH	Methanol
MDM2	Murine double minute 2
MOA	Mechanism of action
MOMP	Mitochondrial outer membrane permeabilization
MW	Molecular weight
NB	No binding
NBD	Nucleotide binding domain
ND	Not determined
NEF	Nucleotide exchange factor
NF-κB	Nuclear factor kappa-light-chain-enhancer of activated B cells
NLS	Nuclear localization sequence
NOE	Nuclear Overhauser effect
PEG	Polyethylene glycol
PDA	Photodiode array
PLC-γ	Phospholipase C- γ
POI	Protein of interest
PPI	Protein-protein interaction
Ppm	Parts per million
PROTAC	Proteolysis targeting chimera
PSA	Polar surface area
PUMA	p53 upregulated modulator of apoptosis
PxxP	Prolin-rich
Ref.	Reference
Rt	Retention time
ROS	Reactive oxygen specie
RU	Resonance unit
SAR	Structure-activity relationship
SBD	Substrate binding domain
SCX	Strong cation exchange
SD	Standard deviation
SEM	Standard error of the mean
SH3	SRC homology 3
sHSP	small heat shock proteins
S_N	Nucleophilic substitution
S_NAr	Nucleophilic aromatic substitution
SPR	Surface plasmon resonance
TEA	Triethylamine
TFA	Trifluoroacetic acid
THF	Tetrahydrofuran
TIC	Total ion current
TLC	Thin layer chromatography
Tm	Melting temperature
TNF	Tumor necrosis factor
TSA	Thermal shift assay
UBL	Ubiquitin-like
UPLC	Ultra-performance liquid chromatography

UPS	Ubiquitin-Proteasome System
VECC	Vincristine, Etoposide, Cisplatin and Cyclophosphamide
VHL	Von Hippel-Lindau
WHO	World Health Organization
WW	Tryptophan-tryptophan
ΔT_m	Thermal shift

1. INTRODUCTION

1a - Impact

Cancer is a large group of diseases that can start in almost any organ or tissue of the body when abnormal cells grow uncontrollably and go beyond their usual boundaries to invade adjacent parts of the body and/or spread to other organs.¹ According to estimates from the World Health Organization (WHO), in 2020 cancer was the second leading cause of death globally before the age of 70 years, after ischemic heart disease, accounting for an estimated 10 million deaths. The most frequent types of cancer (in terms of new cases) were breast (2,26 million cases), lung (2,21 million cases), colon and rectum (1,93 million cases) and prostate (1,41 million cases).¹

Each year, approximately 400,000 children develop cancer. Leukemias, followed by brain and nervous system cancers and lymphomas, are the most prevalent malignant diseases in subjects aged 14 years or younger.² Medulloblastoma, the most common pediatric brain tumor, is the first cause of cancer related deaths in children.³ The overall risk of developing cancer between the age of 0-74 years is 20.2% and in the next four decades, cancer deaths are expected to have a two-fold increase. Therefore, malignancies will become the leading causes of mortality around the world immediately after the year 2030.²

Drug resistance is the principal limiting factor for achieving cures in patients with cancer. Although tumours went into remission quickly when treated with conventional chemotherapeutics, they developed resistance, resulting in disease relapse and progression. The initial solution to the problem of resistance to single-agent chemotherapy was the combined administration of agents with non-overlapping mechanisms of action. At the turn of the century, the successes achieved with polychemotherapy had reached a steady state with no appreciable improvements. Surgery, radiotherapy and polychemotherapy were clearly not enough to cure many tumour types.⁴ Therefore, the current challenge is to define the molecular mechanism and key cellular events that sustain the acquired resistance to therapy. This project is focused on targeting the predominant BCL-2 associated athanogene (BAG) family member, BAG3, responsible for therapy resistance and consequent relapse in cancer. In the last ten years, the BAG family members have become a focus of numerous cancer-related studies. BAG proteins can exert a pro-tumorigenic role, acting as oncogenes

whose overexpression is reported in many tumor types and is frequently associated with cell transformation, tumor recurrence, and drug resistance. In addition, BAG proteins are involved in many oncogenic protein-protein interactions (PPIs) with molecular co-chaperones or signalling molecules making them potential therapeutic targets for cancer treatment.⁵

1b - The BAG proteins family

The BCL-2 associated athanogene (BAG) family is a multifunctional group of proteins, that participate in the regulation of several physiological processes, such as autophagy, apoptosis, and protein homeostasis.⁶⁻¹³ The origin of the name “BAG” (BCL-2 associated athanogene) comes from the founding member of this family, BAG1 which shares a high functional similarity with BCL-2 (B-cell lymphoma 2, an anti-apoptotic protein involved in the regulation of the intrinsic pathway of apoptosis which presents also oncogenic properties) enhancing its anti-apoptotic effects.^{5,13-16} The BAG family genes are evolutionarily conserved, with homologues found in many species, from yeast to animals and plants.¹⁷⁻²¹ The human BAG family of proteins contains six members (BAG1-BAG6) sharing a conserved C-terminal region called the “BAG” domain (BD) (which presents a 40-60% sequence homology among this protein family), a bundle of three α -helices (of 30-40 amino acids each), that allows them to interact with the 70 kDa heat-shock protein (HSP70), assisting it in the maintenance of protein homeostasis (Fig. 1.1).²¹

Proteins that share the BAG domain are also characterized by their interaction with a variety of other partners (e.g., steroid hormone receptors, Raf-1 and Akt), involved in the regulation of several cellular processes, including cell proliferation, stress response, apoptosis, autophagy, cytoskeleton re-organization, aberrant angiogenesis and epithelial to mesenchymal transition.

While BAG5 represent an exception in the BAG family because it consists of five BAG domains (that constitute almost the entire protein),²² the remaining BAG family members possess only a single BAG domain sharing however several specialized protein domains.⁵ BAG3, for example, has multiple protein-protein interaction motifs such as proline-rich repeat (PxxP), tryptophan–tryptophan (WW) domains and two Ile-Pro-Val (IPV) motifs. The proline-rich repeat is involved in the binding to the SRC homology 3 (SH3) domain of Protein Phospholipase C- γ (PLC- γ) and forms an epidermal growth factor (EGF)- regulated ternary complex.²³ The WW region preferentially binds to PxxP containing proteins and is essential in chaperone-assisted autophagy. The two IPV motifs are involved in the interaction with the small heat shock proteins (sHSP) family to stimulate macroautophagy and inhibit protein aggregation.⁵

BAG1 and BAG6 have one ubiquitin-like (UBL) domain that targets HSP70 clients to the proteasome, regulating therefore their degradation.¹¹ As the BAG domain of BAG6 presents a low sequence homology with the classical BAG domain (it is a shorter version consisting

of only 47 amino acids, where some of the essential residues conserved in the other BAG domains are missing) it can't interact with HSP70.

To increase the BAG family complexity, a single *BAG1* mRNA gives rise to four protein isoforms (BAG1, BAG1S, BAG1M and BAG1L) that differ in size due to their diverse N-termini. The longest isoform, BAG1L, contains a nuclear localization sequence (NLS) at the N-terminal region, which is responsible for its nuclear localization while the remaining BAG1 isoforms are preferentially localized in the cytoplasm in normal conditions.⁵

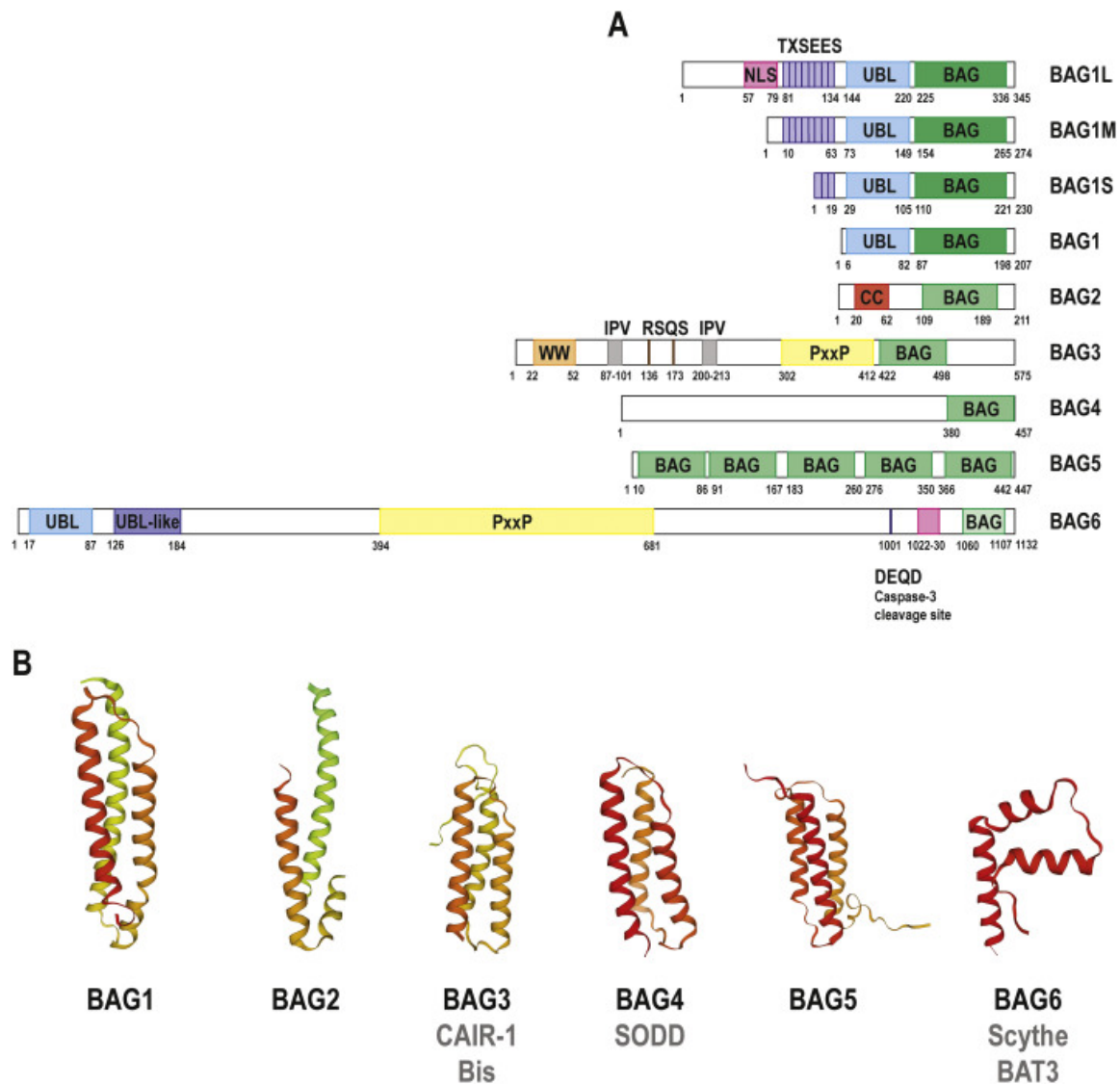


Figure 1.1: A, Protein domains compositions of the human BAG family members. Conserved BAG domains (green), ubiquitin-like (UBL) domains (blue), PxxP repeats (yellow), nuclear localization sequence (NLS) (pink), WW domain (orange) and IPV sequence (grey) are shown. B, Structural comparison of human BAG domains. Ribbon model of hBAG1, hBAG2, mBAG3, hBAG4, hBAG5 and hBAG6 BAG domains.⁵

1c - The BAG/HSP70 complex

HSP70 belongs to an evolutionary conserved family of proteins which play essential roles in cell survival and protein homeostasis, preventing misfolding and aggregation of newly synthesized or unfolded proteins.

HSP70 proteins have two major functional domains (Fig. 1.2):

- The N-terminal, nucleotide binding domain (NBD): a V-shaped structure composed of two lobes that enclose the ATP-binding site. This ATPase domain binds ATP with high affinity and slowly hydrolyzes it to ADP.
- The C-terminal, substrate binding domain (SBD): a peptide binding site made from two subdomains, respectively the beta-sheet and the alpha-helical.²⁴

Functional allosteric interactions take place between the NBD and the SBD: the hydrolysis of ATP in the NBD drives conformational changes in the SBD, and substrate-induced conformational changes are transmitted from the SBD to the NBD interface.²⁵

HSP70 adopts an open conformation when ATP is bound to its NBD, allowing the accommodation of the client protein in its SBD. The binding of the substrate to the HSP70/ATP complex stimulates ATP hydrolysis, which results in a conformational change in the SBD, that locks the hydrophobic region of HSP70, resulting in a more stable complex with the bound substrate. The subsequent nucleotide exchange and the rebinding of a new ATP molecule triggers the release of the substrate from the complex.²⁴

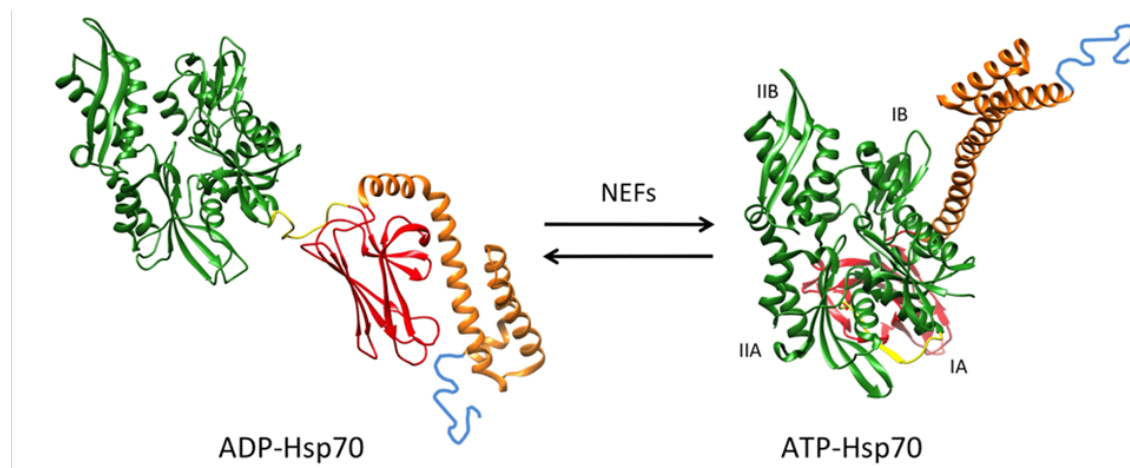


Figure 1.2: HSP70 in the closed (HSP70/ADP) and open (HSP70/ATP) conformations. The NBD (in green) and the two subdomains of SBD (in red and orange) are shown (Picture adapted from ref. ²⁵).

Different co-chaperones regulate the activity of HSP70 by modulating its ATP-consuming cycle. HSP70 has a very low ATPase activity by itself, but its rate can be increased by the

interaction with a family of co-chaperones, the HSP40 proteins. BAG proteins act as nucleotide exchange factors for HSP70 stimulating its ATPase rate and promoting substrate release from the chaperone. Their BAG domain promotes nucleotide release from HSP70 by opening the nucleotide binding cleft upon binding to the ADP-bound state. Because of the excess of ATP over both ADP and BAG proteins in the eukaryotic cytosol, ATP will enter the nucleotide-binding pocket and displace bound BAG protein, resulting in an acceleration of nucleotide exchange.²⁵

The crystal structure of the BAG1 binding domain in complex with the HSC70 (Heat shock cognate 71 kDa protein; a member of the Hsp70 family) ATPase domain gives useful information about the main interactions that occur between these two chaperones (Fig. 1.3). Among the three-helix bundle that forms the BAG domain, helices 2 and 3 contact subdomains IB and IIB of the NBD.²⁴

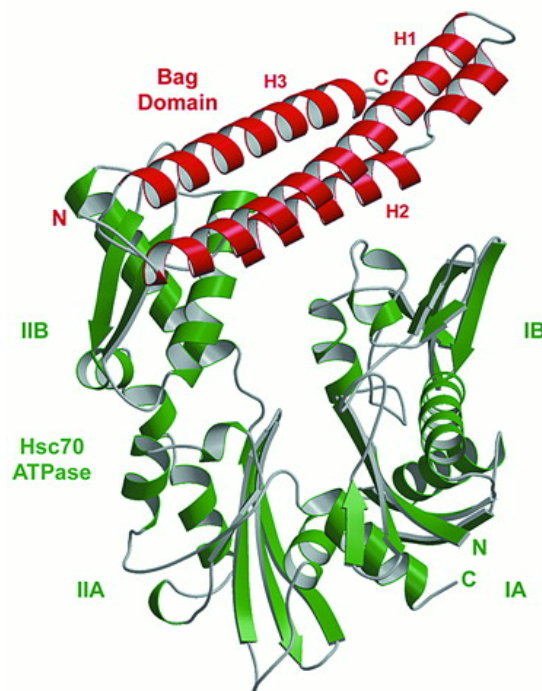


Figure 1.3: Representation of the BAG domain/HSC70 complex: in red the backbones of the BAG domain and in green the ATPase domain of HSC70.²⁴

Binding of the BAG domain to the ATPase domain is mediated by electrostatic interactions, mainly exploiting residues Glu212, Asp222, Arg237, and Gln245 in BAG1 (Figure 1.4). These residues are highly conserved in all BAG proteins, and their individual replacement with alanine results in a reduced affinity for the HSC70 ATPase domain. The main residues of HSC70 involved in the interaction with BAG1 are Arg261 and Glu283 (Fig. 1.4). All HSC70 residues involved in the interaction with BAG1 are absolutely conserved in all cytosolic forms of eukaryotic HSP70 proteins.²⁴

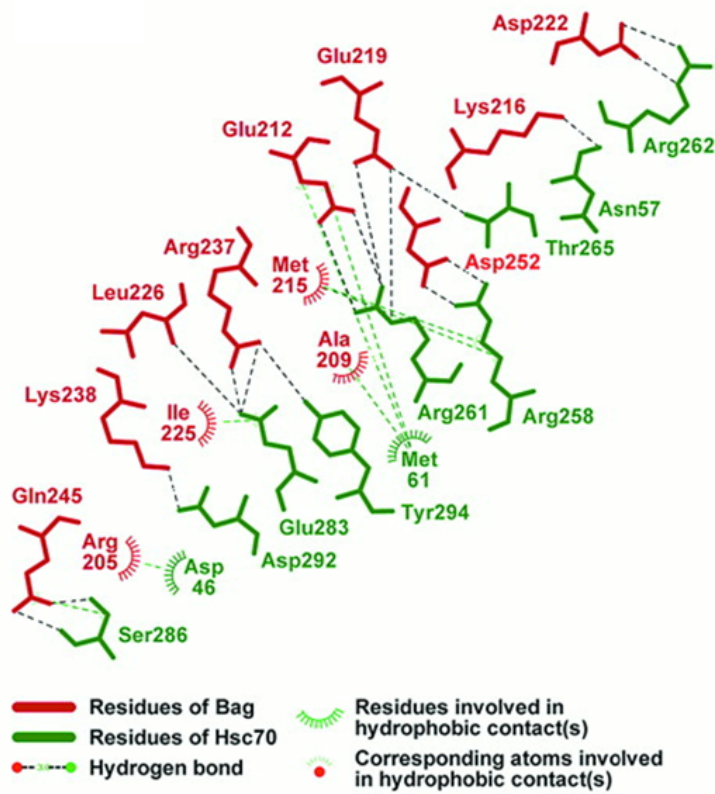


Figure 1.4: Representation of the interactions between HSC70 and the BAG domain. In red the residues of BAG and in green the residues of HSC70.²⁴

As described, BAG proteins act as nucleotide exchange factors (NEF) for HSP70 by stabilizing the nucleotide-free state of the ATPase. The consequence of the BAG proteins binding to the HSP70 ATPase domain is a 14° rotation of subdomain IIB (Fig. 1.5 and Fig.1.6). This new conformation is incompatible with high-affinity nucleotide binding, resulting in the release of the nucleotide (ADP).²⁴

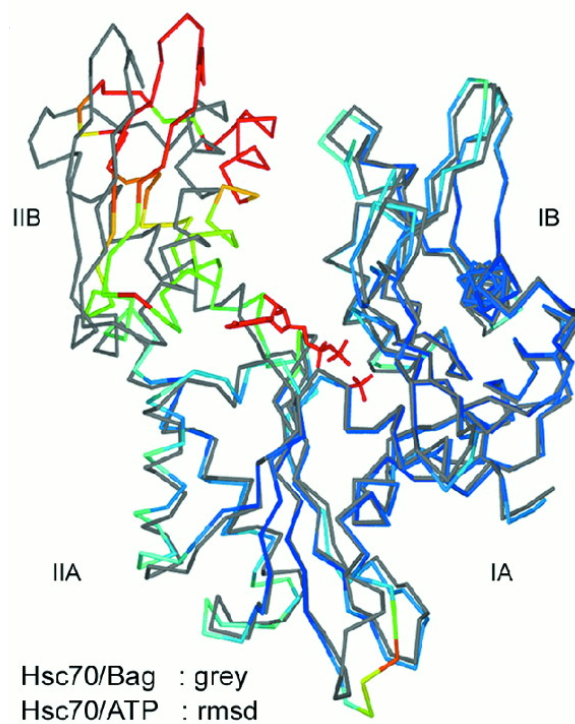


Figure 1.5: Superposition of the HSC70/ATP complex (coloured) with the HSC70/BAG complex (in grey). The main changes in the ATPase domain induced by binding of the BAG domain occur in residues of subdomains IA and IIB that orient the adenosine moiety of the nucleotide. This leads to an opening of the nucleotide-binding cleft with consequent release of the nucleotide (ADP).²⁴

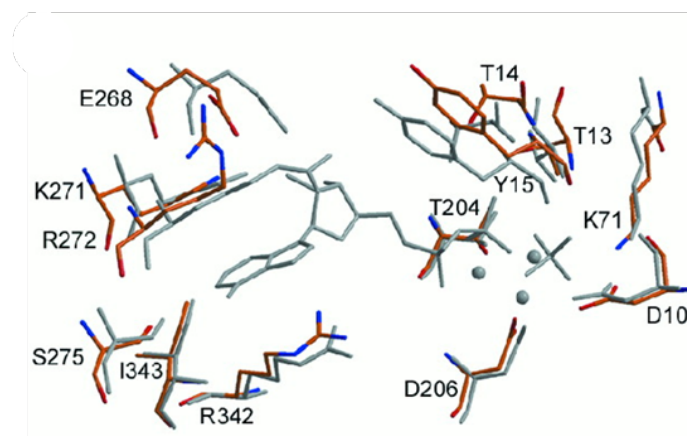


Figure 1.6: Superposition of the HSC70 side chains involved in ATP binding and hydrolysis. The ATP bound state is drawn in gray; the conformation of the respective residues in the BAG domain/HSC70 complex is drawn in orange.²⁴

1d - BAG3 and its multiple roles in cancer

The multifunctional HSP70 co-chaperone and anti-apoptotic protein BAG3 is a well investigated member of the BAG protein family and represents the main target of this project. BAG3 is a 74 KDa cytoplasmatic protein, particularly concentrated in the rough endoplasmatic reticulum. As mentioned in chapter 1b, the protein shares with the other members of the family the evolutionary conserved BAG domain that binds the ATPase domain of HSP70 and allows them to act as nucleotide exchange factors.^{9,12} Lacking a crystal structure of the BAG3/HSP70 complex, the information about how BAG3 and HSP70 interact comes from a published homology model built using the crystal structure of the homologous BAG1/HSP70 complex (Fig. 1.7).^{8,18} This homology model gives useful information about the salient interactions that occur between the two proteins. As in the case of the BAG1/HSC70 complex (see chapter 1c, Fig. 1.4),²⁴ salt bridges play a pivotal role, particularly those between Asp456 (BAG3) and Arg262 (HSP70), and between Arg480 (BAG3) and Asp285(HSP70).⁸

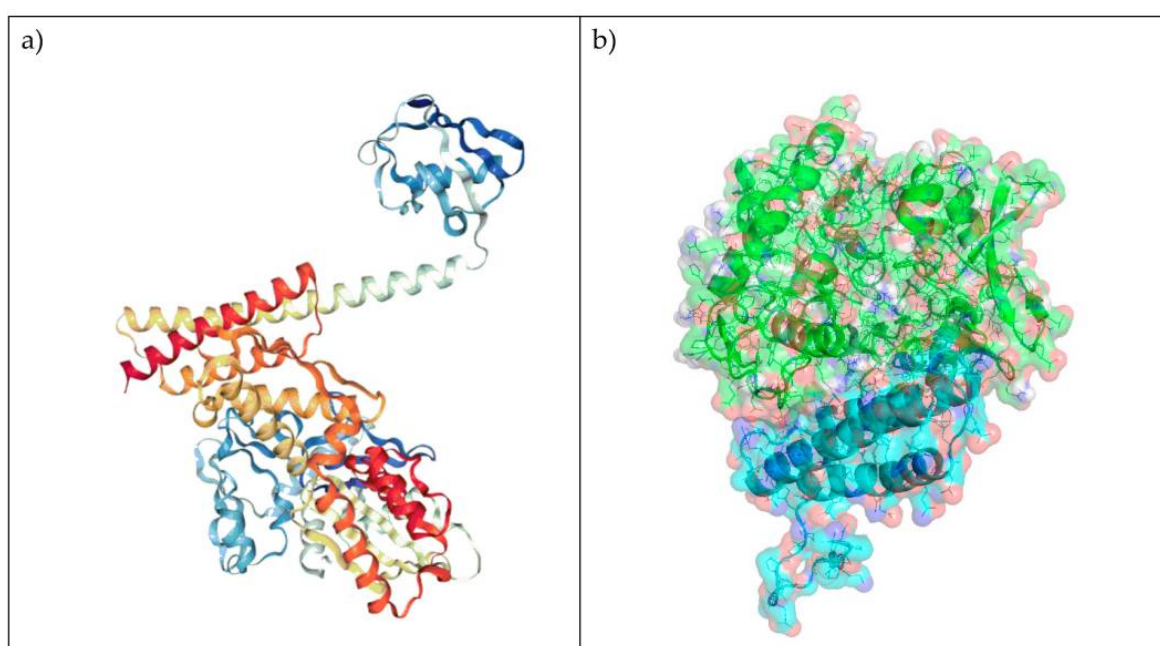


Figure 1.7: a) crystal structure of BAG1/HSP70 complex; b) Homology model of BAG3 (cyan) bound to HSP70 (green).⁸

The complex between BAG3 and HSP70 selectively binds to a wide variety of client proteins controlling their turnover via the two major protein degradation pathways, proteasomal degradation and macroautophagy. By regulating the levels of several substrates, BAG3 can exert many key physiological functions, including an involvement in cellular stress

responses, proteostasis, cell death regulation, development, and cytoskeletal dynamics.^{6,7,12} In addition to its physiological function, BAG3 is also involved in several pathological conditions, including cancer.^{6,7} Indeed, BAG3 is found to be over-expressed in many neoplastic cell types and tumours,⁸ e.g., in lymphocytic leukemia,^{26,27} medulloblastoma,²⁸ glioma,²⁹ thyroid,³⁰ lung,³¹ colorectal,³² breast,³³ liver,³⁴ and pancreatic^{35,36} cancer. In malignant diseases, BAG3 mostly exerts oncogenic functions and is known to regulate several key hallmarks of cancer, including cell survival, adhesion, metastasis, angiogenesis, enhanced autophagic activity, and apoptosis escape.¹²

In several neoplastic cell types, it was recently shown that stressful stimuli, such as elevated temperature, oxidants, heavy metals, and chemotherapeutic drugs, induced upregulation of BAG3 and heat shock proteins (HSPs).^{6,8} The heat shock transcription factors (HSFs), in response to those stimuli, acquire DNA binding activity to the heat shock elements (HSE) present in the *bag3* gene, thereby mediating its transcription. Among the BAG family, the oncogene BAG3 is the only one reported to be inducible by stressors.^{8,9}

Under physiological conditions, BAG3 is expressed at low basal levels and BAG1 can positively cooperate with HSP70 and CHIP (C-terminus of the HSC70-interacting protein) to transfer, through its ubiquitin-like domain, client proteins to the proteasome leading to their degradation.³⁷⁻³⁹ Under stress conditions, an accumulation of misfolded proteins occurs, leading to an induced overexpression of BAG3. The increased levels of BAG3 can interfere with the BAG1 mediated delivery of client proteins to proteasome degradation by competing with BAG1 for binding to the ATPase domain of HSP70. In this way BAG3 can influence the intracellular levels of several client proteins.⁷⁻⁹

1e - The role of BAG3 in apoptosis escape

One of the mechanisms that can sustain uncontrolled proliferation of tumor cells and their survival despite the presence of toxic drug insults and/or stress conditions is apoptosis escape. The imbalance between pro-survival and pro-apoptotic factors is a common trait of tumor cells that allow them to avoid apoptosis triggering.

Apoptosis is an evolutionarily conserved cell death pathway responsible for the programmed killing of cells during normal development, maintenance of tissue homeostasis and cancer prevention. To maintain normal physiology and tissue function, dysfunctional or no longer necessary damaged cells are constantly removed via apoptosis and ideally replaced by new healthy cells. On the other hand, the abnormal survival and accumulation of damaged or superfluous cells leads to pathologies like cancer.⁴⁰

Apoptosis is a cascade of highly regulated and controlled biochemical events, which culminates in the activation of caspases (cysteine-aspartic proteases) which degrade cellular components to prepare dying cells for clearance by phagocytes with minimal stress to surrounding cells and tissues. Apoptosis is mediated via two distinct pathways: the extrinsic and the intrinsic one. The intrinsic pathway, mediated by mitochondria, is highly regulated by the B Cell lymphoma 2 (BCL-2) family proteins, that include both pro-apoptotic and pro-survival (anti-apoptotic) members (Fig. 1.8).⁴⁰

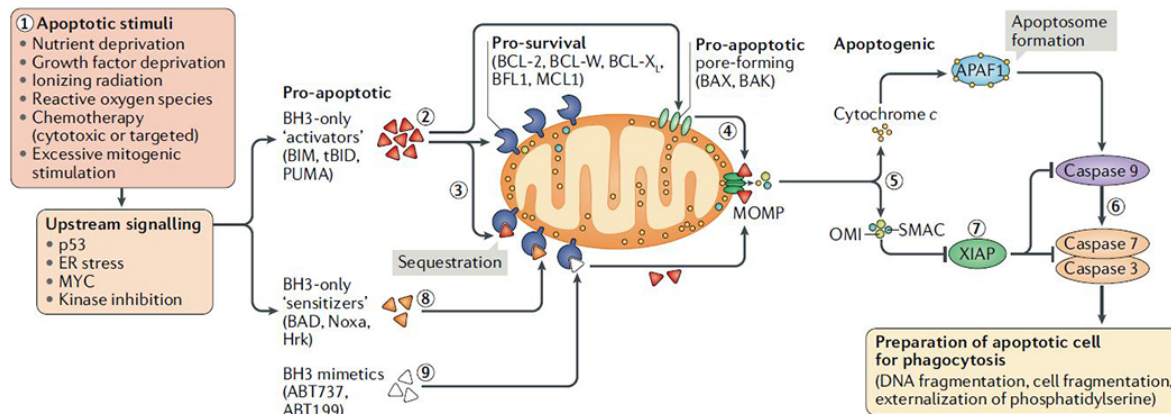


Figure 1.8: The mitochondrial apoptosis pathway.

In the intrinsic pathway the apoptosis cascade is triggered by damage signals or cellular stress. The first step is the upregulation/activation of pro-apoptotic proteins: BCL-2-interacting mediator of cell death (BIM), BH3-interacting domain death agonist (BID) and p53 upregulated modulator of apoptosis (PUMA). These proteins can be bound and sequestered by the pro-survival proteins or, when these pro-survival proteins are saturated or absent, can activate the pro-apoptotic proteins BCL-2 associated X protein (BAX) and BCL-2 antagonist/killer (BAK). After their activation, BAX and BAK form pores that causes the mitochondrial outer membrane permeabilization (MOMP), resulting in the release of apoptogenic molecules (including cytochrome c, OMI and SMAC) from the mitochondrial intermembrane space. This is the irreversible 'point of no return' in the apoptosis cascade. When cytochrome c is released, it binds to the cytosolic protein Apoptotic protease activating factor-1 (APAF1) to create a protein complex called apoptosome, which can recruit, cleave, and activate the pro-caspase 9. Once activated, this initiator caspase cleaves and activates pro-caspases into the effector caspases 3 and 7 and trigger a cascade of events which leads to cell dismantling. The cell fragments (called apoptotic bodies) are then removed by phagocytes.⁴⁰

Countering this pro-apoptotic chain of events are the pro-survival (anti-apoptotic) BCL-2 family proteins: B cell lymphoma 2 (BCL-2), B cell lymphoma extra-large (BCL-XL), B cell lymphoma w (BCL-W), BCL2-related isolated from fetal liver 1 (BFL1) and Myeloid cell leukaemia 1 (MCL1). These proteins can block apoptosis by binding and sequestering activated BAX or BAK. Apoptosis occurs when, pro-survival proteins within the cell are overwhelmed and BAX and/or BAK activated. This is where the balance between pro-survival and pro-apoptotic proteins comes into play.⁴⁰

Cell transformation to a malignant state is a stressful event associated with accumulating DNA damage, aberrant growth signals and excessive pressure to support the rapid and uncontrolled cell growth. In these conditions, apoptosis escape plays a critical role in the continued proliferation of cancer cells, and the ability to suppress apoptosis is one of the hallmarks of cancer. Cancer cells can evade apoptosis by the heterogeneous over-expression of pro-survival BCL-2 family proteins (BCL-2, MCL1, BCL-XL, BFL1 and BCL-W). Therefore, the pro-apoptotic family members (BIM, BID, BAX, BAK, Noxa, PUMA, and Hrk) cannot express their function, providing an obstruction in cell death signalling.

Apoptosis escape also enable cancer cells to develop resistance to cytotoxic drugs and ionizing radiation and for too many patients, the inability to eradicate all malignant cells results in the selection and expansion of the resistant ones with consequent resistance to therapy.

Among molecules that regulate apoptosis, a role is emerging for BAG3, a protein with the ability to sustain directly the anti-apoptotic function of BCL-2. Under physiological conditions, BAG3 is constitutively present in very few cell types, including cardiomyocytes and skeletal muscle cells. However, stress conditions can induce BAG3 expression by the activation of the transcription factor HSF1, which regulates the activity of the *bag3* gene promoter (as discussed in chapter 1d). BAG3 overexpression contributes to apoptosis escape by promoting cell survival signalling in complex with HSP70. BAG3 binds to the NBD of HSP70, releasing the client protein from the chaperone and counteracting proteasome-mediated degradation. When these client proteins have anti-apoptotic function, the result is the obstruction in the apoptosis pro-death signalling, leading to cell survival. Resistance to cell death caused by defects in apoptotic pathways and overexpression of anti-apoptotic proteins is a general hallmark of cancer.^{6,8}

Conversely, BAG3 down-modulation (by phosphorothioate antisense oligodeoxynucleotide) resulted in enhancement of cytochrome c release, caspase activation and consequent reduction of tumor growth.⁹

BAG3 has a stabilizing effect on some pro-survival BCL-2 proteins, including BCL-2, BCL-XL, and MCL-1. The formation of the BAG3/HSP70 complex with these anti-apoptotic proteins reduced their proteasomal turnover, leading to an enhanced anti-apoptotic capacity and prevention of apoptosis induction. In the case of MCL-1, neuroblastoma cells were adopted as a model to demonstrate that the BAG3 interaction with MCL-1 and Hsp70 may prevent or destabilize the binding of MCL-1 to HSP70, reducing the delivery of MCL-1 to the proteasome and supporting the anti-apoptotic activity of MCL-1.^{8,41}

In osteo-sarcoma and melanoma cells, BAG3 protects IKK- γ from proteasome delivery and this results in sustained NF-kB activation and cell survival.^{8,42} A different mechanism has been observed in glioblastoma cells, in which BAG3 retains BAX, a pro-apoptotic protein, in the cytosol, preventing its mitochondrial translocation and in this way protecting tumor cells from apoptosis.^{8,29} The HSP70-BAG3 complex modulates the activity of several other key drivers of cancer, including the transcription factors FoxM1, Hif1 α , the translation regulator HuR, the cell-cycle regulator p21 and Akt, with possible implications for tumor cell survival, cellular metabolism, stemness, and proliferation.⁸

1f - Small molecules targeting BAG3-HSP70 PPI

BAG3 and HSP70 are stress-inducible proteins that are required for cancer development at several steps and are frequently found to be overexpressed in tumour cells. BAG3 has been shown to collaborate with HSP70 in regulating cancer development through multiple pathways, promoting cancer cell survival, proliferation, metastasis, and apoptosis escape. Targeting the active site of HSP70 with small molecule competitive inhibitors has proven relatively challenging, because the site is located in a deep groove in its nucleotide-binding domain (NBD) and partly because of the high affinity of HSP70 for ATP. Therefore, inhibition of the HSP70–BAG3 protein–protein interaction (PPI) may provide an alternative way to target this chaperone. In line with these observations, blocking the HSP70–BAG3 interaction using mutations, knockdowns, or first-generation small molecules has selective antiproliferative activity in cancer cells, suggesting that this could be a noncanonical way to interrupt both HSP70 and BAG3 functions.⁴³

These PPIs have been successfully inhibited using molecules that bind to allosteric sites. BAG3 binds to the NBD of HSP70 but the affinity for this interaction is significantly weakened (13-fold) in the presence of ADP, suggesting that stabilizing the ADP-bound state of HSP70 might be one way of allosterically blocking the HSP70–BAG3 contact.

MKT-077 was identified as the first allosteric HSP70 inhibitor among a series of benzothiazole rhodacyanines (Fig. 1.9). It binds to a deep allosteric pocket in the NBD of HSP70 and stabilizes it in the ADP-bound form, disrupting the PPI with BAG3. However, despite the antitumor activity exhibited during preclinical studies ($EC_{50} \sim 2.2 \mu\text{M}$ in MCF7 breast cancer cells), MKT-077 was retired during phase I clinical trials due to its renal accumulation and rapid metabolism ($t_{1/2} < 5 \text{ min}$).⁴⁴

The optimization of the MKT-077 scaffold led to the identification of new compounds with improved drug-like properties (Fig. 1.9). Among them, JG-98 was found to be 7-fold more metabolically stable ($t_{1/2} = 37 \text{ min}$) and 3-fold more potent than MKT-077 in cell cytotoxicity assay ($EC_{50} \sim 0.4 \mu\text{M}$ in MCF7 breast cancer cells). In an *in vitro* assay, JG-98 strongly inhibited the interactions between HSP70 and BAG3 (IC_{50} value of $1.6 \pm 0.3 \mu\text{M}$) and did not present any renal toxicity.⁴³

However, further studies demonstrate that JG-98 was also a good inhibitor of the HSP70-BAG1 and HSP70-BAG2 complexes (with IC_{50} values of $0.6 \pm 0.1 \mu\text{M}$ and $1.2 \pm 0.1 \mu\text{M}$, respectively) so, it is likely that treatment with JG-98 would impact other pathways which contribute to its anti-proliferative activity. Further advancement of this compound was

limited also by its modest potency and relatively poor pharmacokinetics in animal models.

43

A structure- and potency- guided design strategy was employed to optimise further JG-98. The best of the resulting compounds, JG-231 and JG-294 (Fig. 1.9), had sub-micromolar potency ($EC_{50} \sim 0.1 \mu\text{M}$ in MCF7 breast cancer cells), presented better pharmacokinetic proprieties and were relatively less toxic to nontransformed cells. The metabolic stability of JG-231 and JG-294 was substantially improved ($t_{1/2} > 60 \text{ min}$) but their low solubility and photoreactivity remain significant liabilities. Therefore, it cannot be excluded that off-target based mechanisms of these compounds are involved in their antiproliferative and proapoptotic effects, as they lack sufficient specificity.⁴⁵

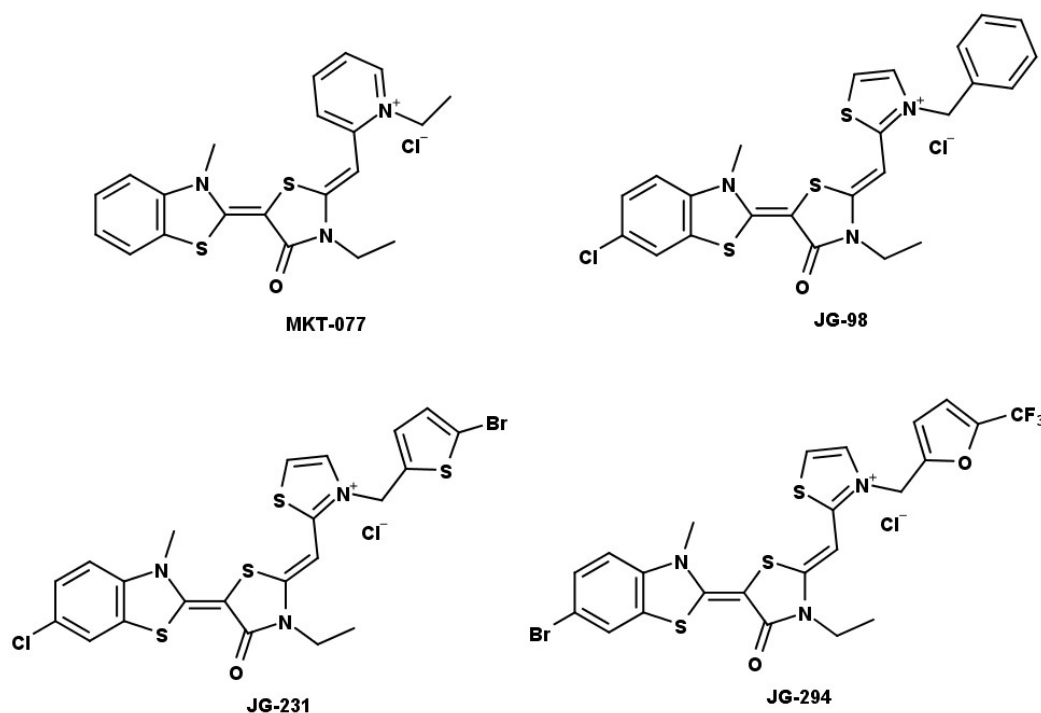


Figure 1.9: Structures of the allosteric HSP70 inhibitors MKT-077, JG-98, JG-231 and JG-294.

44-45

By performing high-throughput screening for inhibitors of PPIs between HSP70 and its co-chaperones, the group of Taylor discovered ‘compound R’, the founder of a new series of 2-aminothiazoles (Fig. 1.10).⁴⁶ Compound R inhibits the HSP70/BAG PPI and showed an antiproliferative activity in the micromolar range ($EC_{50} \sim 5.8 \mu\text{M}$) on a breast cancer cell line (MDA-MB-231). From the SAR exploration performed on the “right” side of this molecule emerged IT2-144 (Fig. 1.10), which had an EC_{50} of $\sim 2.7 \mu\text{M}$ in suppressing growth of MDA-MB-231 cells. Further studies suggested that IT2-144 might bind to the same allosteric site on HSP70 that is occupied by the benzothiazole-rhodacyanines (e.g., MKT-077 and JG-98).⁴⁶

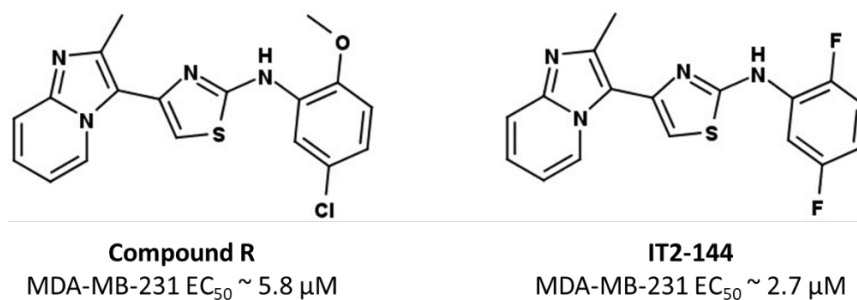


Figure 1.10: Structures of compound R and its analogue IT2-144 and their antiproliferative activities (as EC_{50} values) on a breast cancer cell line (MDA-MB-231).⁴⁶

An alternative strategy to prevent the HSP70/BAG3 PPI is the development of high-affinity direct BAG3 inhibitors. Terracciano *et al.* described the first example of a selective BAG3 domain modulator of BAG3. The authors employed a structure-based virtual screening approach, followed by experimental validation and chemical modification to report the 2,4-thiazolidinedione derivative reported in Fig. 1.11.⁴⁷

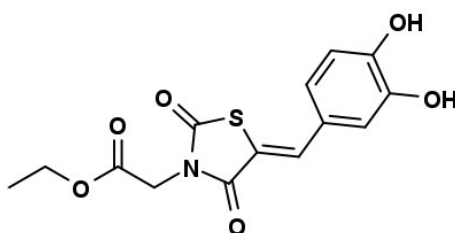


Figure 1.11: Chemical structure of the 2,4-thiazolidinedione derivative reported by Terracciano *et al.*⁴⁷

During preliminary assays, this 2,4-thiazolidinedione showed the ability to selectively bind BAG3 ($K_d = 11.1 \pm 3.9 \text{ nM}$) and its BAG domain ($K_d = 6.4 \pm 2.2 \text{ nM}$), with respect to other members of the BAG family (BAG4 and BAG1). As BAG3 has been reported to be overexpressed in melanoma cells (A375), the antiproliferative activity of this compound was first tested on the human melanoma cancer cell line A375 obtaining an $IC_{50} \sim 16.6 \mu\text{M}$. Then, the same compound was tested on a small panel of cancer cell lines known to be able to overexpress the BAG3 protein [pancreatic carcinoma (Panc-1), breast cancer (MCF7), prostate cancer (PC3) and lung cancer (A549) cells] wherein it displayed variable antiproliferative activities.⁴⁷

Further in silico-screening of compounds that share the 2,4-thiazolidinedione scaffold was recently performed by the same group. Among this new series of compounds, the two 2,4-thiazolidinedione derivatives shown in Fig. 1.12 present the best binding affinity for BAG3 and its isolated BAG domain. Both these molecules also showed promising antiproliferative

activity, with IC_{50} values in the micromolar range in both human melanoma (A375) and human cervical adenocarcinoma (HeLa) cell lines.⁴⁸

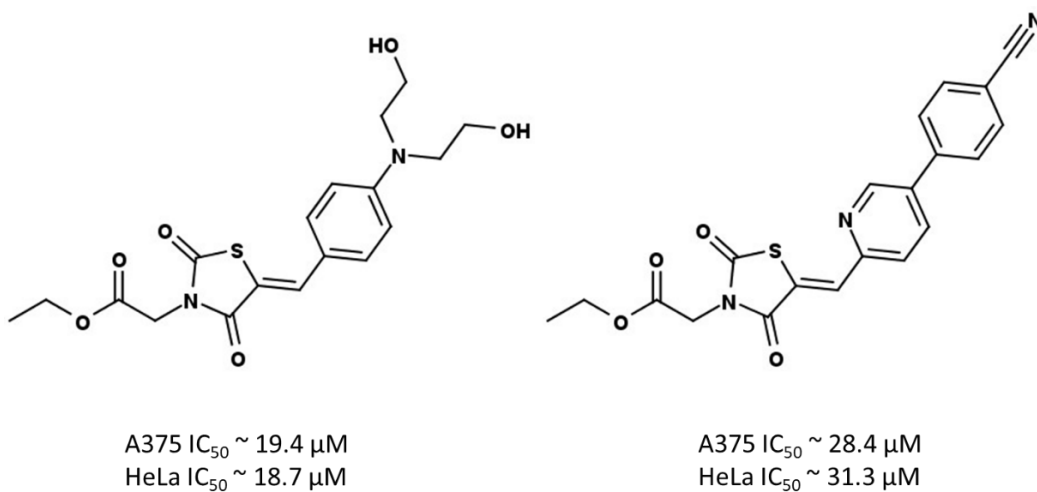


Figure 1.12: Best compounds that emerged from the second collection of 2,4-thiazolidinedione derivatives and their antiproliferative activity (reported as IC_{50} value) in both A375 and HeLa cell lines.⁴⁸

1g - PROTAC (Proteolysis Targeting Chimera)

PROTAC technology is a novel therapeutic approach based on the induction of target protein degradation by the ubiquitin-proteasome system (UPS). The proteasome is a cellular complex responsible for the proteolytic degradation of proteins tagged for destruction via the addition of specific chains of the 8.5 kDa protein ubiquitin. As reported in Fig. 1.13, ubiquitin tags are delivered to target proteins via an initial conjugation to an E1 ubiquitin-activating enzyme followed by transfer to an E2 ubiquitin-conjugating enzyme which then relies on a large family of adaptor proteins (ubiquitin E3 ligases) to deliver their ubiquitin chain to the desired protein. The ubiquitin transfer to target protein, mediated by the E3 ligase, is driven by the proximity of the ligase complex and by the presence of specific recognition elements. Appropriately, ubiquitinated proteins are then recognized by the proteasome and proteolytically cleaved. The promiscuous nature of this proximity-induced enzymatic ubiquitin transfer offers the opportunity to use artificial systems to mimic this process and induce non-physiological degradation.⁴⁹

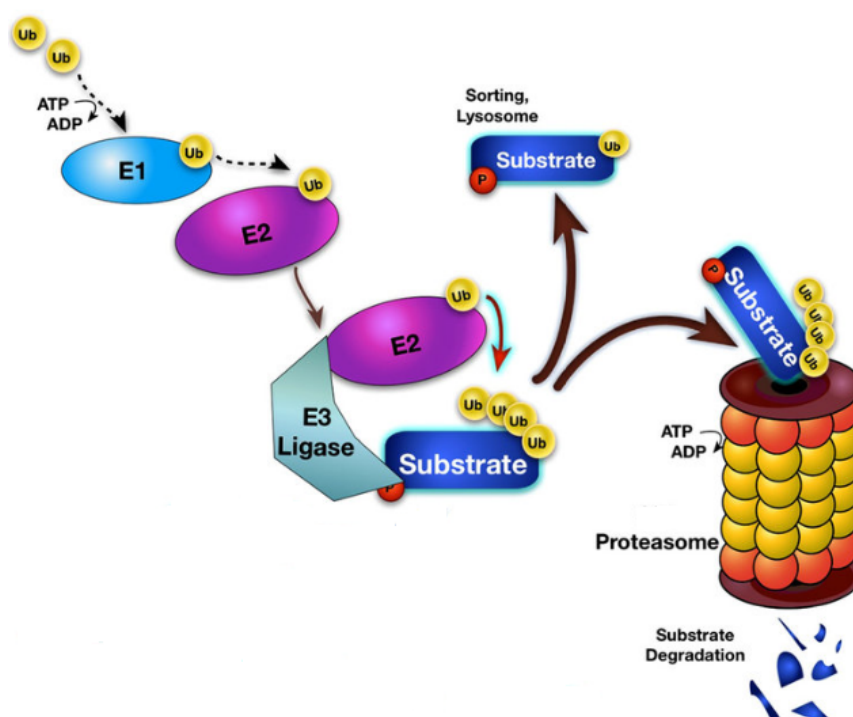


Figure 1.13: Scheme of the ubiquitin-proteasome system (picture adapted from ref.⁵⁰).

PROTACs are hetero-bifunctional small molecules made of a ligand binding to the target protein, a ligand binding to the E3 ubiquitin ligase, and a linker for conjugating these two elements. They are designed to bind the target protein and the ubiquitylation machinery

simultaneously to form a ternary complex in which proximity facilitates the ubiquitin transfer (Fig. 1.14).

PROTAC presents a catalytic mode of action, so that one PROTAC molecule is able to remove many target proteins from the cell. In this way they can promote target protein degradation at low exposures, and hence they overcome the receptor occupancy limitation of traditional inhibitors, in which the protein function is modulated via temporary inhibition.⁵¹

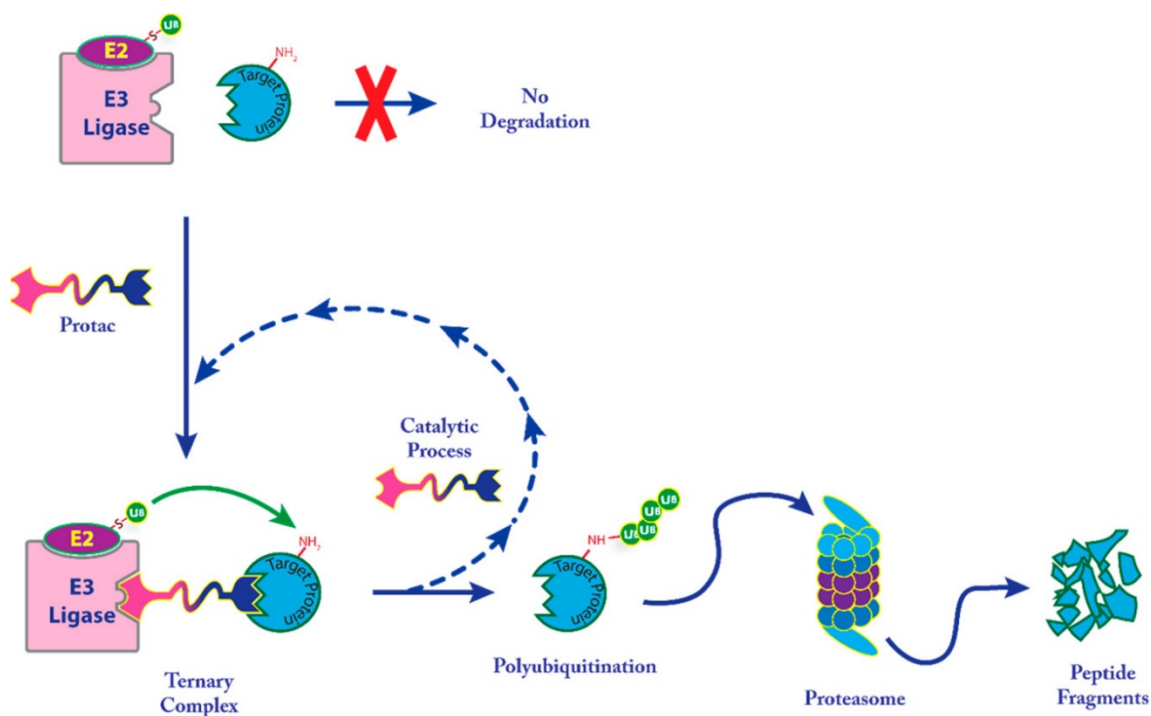


Figure 1.14: PROTAC ternary complex with E3 ligase and target protein, and catalytic mechanism of action.⁴⁹

PROTACs present characteristic bell-shaped dose-response curves, also called the “Hook effect” (Fig. 1.15), in which ineffective binary complexes (PROTAC-Target protein or PROTAC- E3 ligase) are observed at high concentrations of PROTAC and these compete with effective ternary complexes (Target protein-PROTAC- E3 ligase).^{52,53}

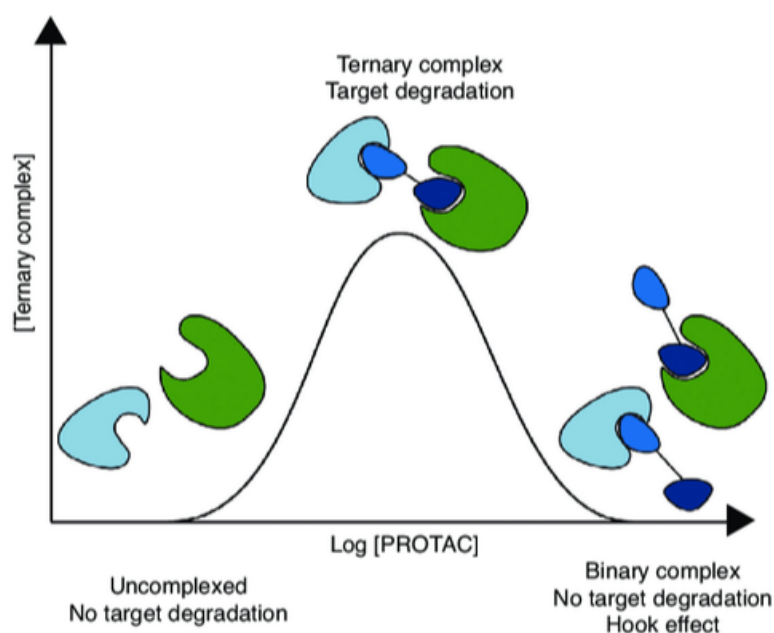


Figure 1.15: Hook effect as a function of PROTAC concentration.⁵³

To achieve successful protein degradation a PROTAC molecule must go through several steps. First the PROTAC must be able to reach the appropriate intracellular compartment where both the ligases and the target protein reside. This can be challenging due to the larger molecular size of PROTACs (800-1500 Da) that can affect their cell permeability. However, many PROTACs are capable of efficiently entering cells and achieving sufficient concentration to exploit their functions. PROTACs can enter cells only by a slow passive process since no specific active routes for their uptake are known. If the PROTAC can get into the cell, then it must be able to form the ternary complex with both the target protein and the E3 ligase to enable the ubiquitin transfer. Favourable or repulsive interactions between the target protein and E3 ligase may affect ternary complex formation. The term cooperativity is used to describe these PPIs. Stabilizing PPIs (positive cooperativity) can promote the formation of the ternary complex while destabilizing PPIs (e.g., undesired steric clashes) can abrogate the ternary complex formation (negative cooperativity).⁵³ The PROTAC linker can also contribute to generate positive cooperativity interaction with the target protein. Once the ternary complex is formed, it must bring the two proteins into an appropriate conformation, which enables the ubiquitin transfer to an acceptor site (usually a lysine residue on the surface of the target protein). The rate of the ubiquitin transfer must be faster than the dissociation of ternary complex and should also overcome any competitive removal of ubiquitin by deubiquitinase enzymes. Proteins can be functionalized with multiple ubiquitins, forming chains of vary lengths and topologies. The pattern of ubiquitin residues should facilitate the recognition by the proteasome to initiate the degradation

process. At this point the PROTAC may dissociate from its bound protein, ready to repeat the cycle again. To achieve the desired pharmacological effect, the degradation rate must be faster than the de novo resynthesis rate of the target protein.⁴⁹

1h - Advantages of PROTACs

PROTACs present numerous advantages versus traditional small molecule antagonists. First, they usually have a higher cellular potency driven by their catalytic mechanism of action (MOA). As PROTACs act catalytically to start a degradation cascade, a low level of target occupancy may be sufficient to maintain a rate of protein degradation that quickly depletes target proteins to afford the desired pharmacological effect. Therefore, usually their cellular EC_{50} values are much lower than the intrinsic target binding K_d . Another consequence of this catalytic MOA is a profound time-dependence of degradation, with greater protein depletion seen over time. Once the pre-existing reservoir of cellular protein is depleted, the PROTAC need only degrade a smaller pool of de novo resynthesized protein to maintain its effect. Even after the complete clearance of the PROTAC, cells may still require a significant period of time to re-establish their pool of protein resulting in a greatly extended duration of action. The extended duration of action, coupled with the high potency, allows low drug exposure, low dose, and long dosing interval.⁴⁹

When a highly selective ligand was incorporated into a PROTAC a highly selective degradation was often observed. However, the PROTAC technology can also provide enhanced selectivity beyond that of the protein of interest (POI) ligand. Favourable PPIs can stabilize the ternary complex accessing specific geometries that favour ubiquitin transfer to some substrates over others. Even the linker can yield productive interactions leading to selective stabilization of ternary complexes. PROTACs can also achieve cell or tissue selectivity even when their target protein is ubiquitously expressed. They achieve this goal by targeting the proteins to an E3 ligase that is differentially expressed in tumor cells compared with normal tissues. This high selectivity can reduce the on-target side effects and the toxicity of classical small molecule inhibitors.⁵⁴

Finally, the PROTAC technology has the potential to develop molecules capable of modulating challenging non-traditional drug targets (e.g., targets that does not present a specific catalytically active site or target with larger protein interfaces). Since PROTAC technology only requires binders that temporarily mediate ternary complex formation, low affinity ligands for the target protein can be incorporated into a PROTAC. As the ligand itself doesn't need to possess a specific function, it can bind anywhere on the target protein. This had a significant impact on drug discovery: proteins previously described as undruggable can now be investigated as they are degradable, thus offering new opportunities to develop treatments for diseases with currently unmet medical need.^{53,55,56}

1i - Elements of PROTAC design

A modular approach can be applied to PROTAC design, in which they can be divided into their three constituent parts: the target ligand, the linker and the E3 ligase ligand.⁵⁶ To date, most of the reported PROTACs have been developed starting from a well-characterized ligand, often an inhibitor, as the target protein recruiting moiety. The crystal structure of the ligand bound to its target protein and/or available ligand structure activity relationship (SAR) information has been used to guide PROTAC design (e.g., to identify a suitable linker attachment point on the ligand). As mentioned before, PROTAC technology does not need high affinity target ligands to ensure high efficacy, since it only requires binders that temporarily mediate ternary complex formation, binding anywhere on the target protein.

Another challenge in PROTAC development is choosing which E3 ligase is better to recruit. There are approximately 600 known E3 ligases. To date, only a few of them have been employed for use with PROTACs, which is largely due to the lack of suitable ligands for many of the ligases.⁵⁶ Among the four most characterized E3 ligases there are: Von Hippel-Lindau (VHL), cereblon (CRBN), murine double minute 2 (MDM2) and inhibitor of apoptosis protein (IAP). The most potent small molecules developed to selectively bind these ligases are shown in Fig. 1.16. Among them, the hydroxyproline VH032 is a high-affinity ligand commonly used to recruit VHL ($K_d = 185$ nM), while thalidomide and its analogues, such as lenalidomide and pomalidomide, are potent ligands for CRBN, with dissociation constants of ~ 250 nM, ~ 178 nM and ~ 157 nM, respectively. Methylbestatin and a higher-affinity derivative of LCL161, are the ligands most used to recruit IAP. Nutlin-3 has been used to target MDM2.

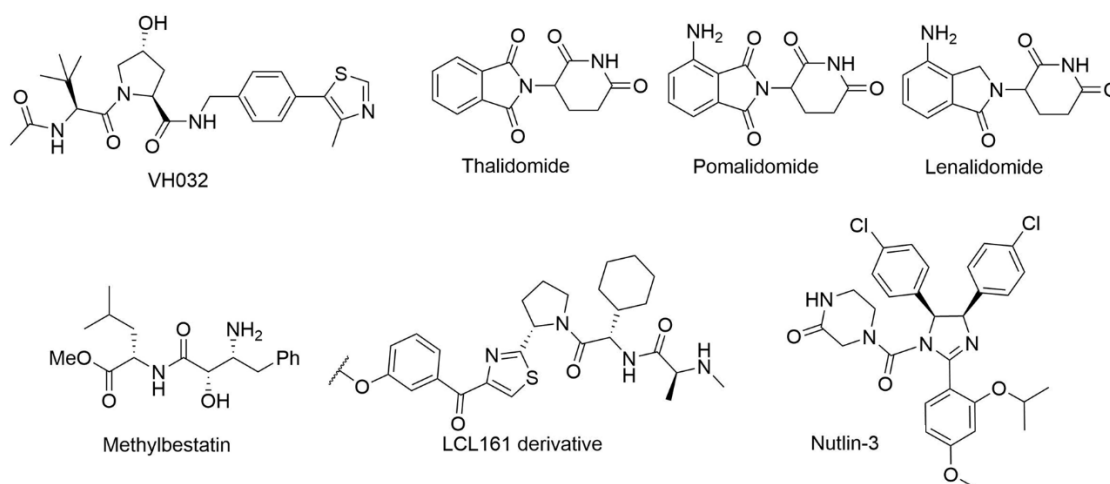


Figure 1.16: Commonly used E3 ubiquitin ligases ligands.⁵⁷

The linker composition, particularly its length and attachment point, is very important for achieving ternary complex formation, degradation activity, and target selectivity. The specific nature of the linker can also affect the physio-chemical properties of the PROTAC. The most common motifs incorporated into PROTAC linker structures are PEG and alkyl chains of varying lengths (Fig. 1.17). They have many advantages including: high synthetic accessibility and commercial availability, flexibility, and the possibility to easily tune their length. Flexibility can be crucial to find a potent compound because it allows the adoption of suitable conformations for productive ternary complex formation. When considering linker length, usually there is a minimum distance required between the two ligands for a PROTAC to be effective. This requirement derives from the need to avoid steric repulsion between the ligands and either of the proteins, or between the two proteins when they are both bound to the PROTAC. Alterations in linker length can also be used to impart selectivity for degradation of different proteins. Using diverse combinations of PEG and alkyl motifs also allows for tuning of important physical properties such as polar surface area (PSA) and lipophilicity which in turn have implications on solubility and cell permeability. Other linker motifs include alkynes, triazoles and saturated heterocycles such as piperazine and piperidine, which are able to impart some rigidity and to modulate physical properties (Fig. 1.17). These linkers provide the most likely route to optimise the solubility of PROTACs, such as by replacement of more traditional alkyl and PEG moieties with saturated nitrogen heterocycles (ionisable piperidine/piperazine) or other polar rigidifying groups, which could also benefit permeability.⁵⁷

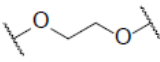
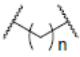
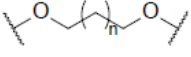
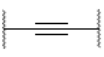
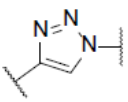
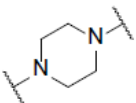
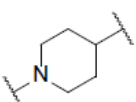
Structure	Linker motif
	PEG
	Alkyl
	Other Glycol
	Alkyne
	Triazole
	Piperazine
	Piperidine

Figure 1.17: Common motifs incorporated into PROTAC linker structures (picture adapted from ref.⁵⁷).

11 - Targeting apoptosis with PROTACs

The upregulation of anti-apoptotic proteins (e.g., BCL-2 and BCL-X_L) or downregulation of pro-apoptotic factors (e.g., Puma, Bax) enable cancer cells to evade apoptosis triggering and permit them to survive under stressful conditions, supporting their abnormal survival, therapeutic resistance, and cancer recurrence. Therefore, designing a PROTAC that directly targets anti-apoptotic proteins could initiate programmed cell death of cancer cells and improve their response to anticancer drugs. A successful example of this strategy has been reported by Zhou *et al.*⁵⁴ who developed a selective and safer BCL-X_L PROTAC.

BCL-X_L is a member of the BCL-2 family of proteins with anti-apoptotic functions and is frequently found overexpressed in tumor cells with consequent evasion of apoptosis and resistance to cancer therapy. As BCL-X_L is a well validated target for cancer, extensive drug discovery efforts were conducted which led to the development of the potent small molecule inhibitor ABT263 (a BCL-2 and BCL-X_L dual inhibitor) reported in Fig. 1.18. ABT263 was not approved by the FDA because the inhibition of BCL-X_L induces on- target and dose-limiting thrombocytopenia.

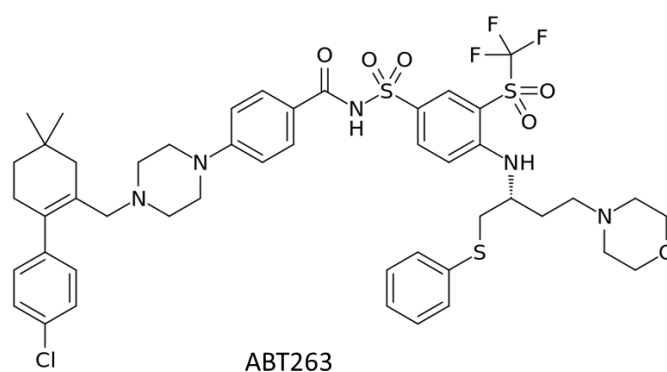
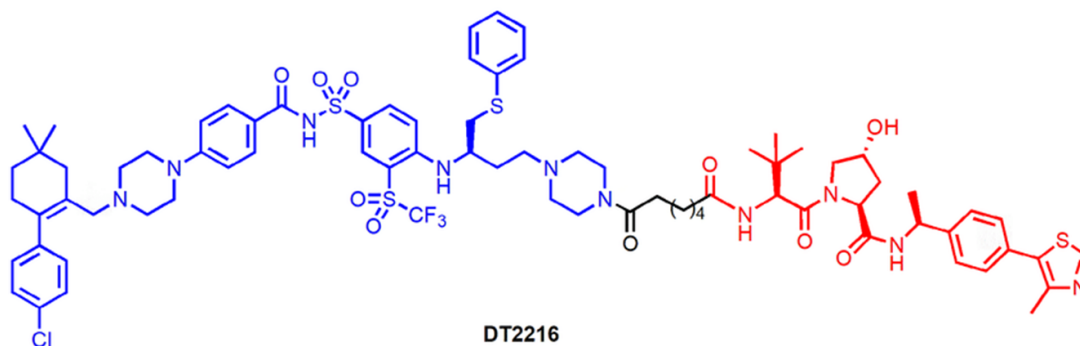


Figure 1.18: Structure of ABT263.⁵⁴

To reduce the toxicity of ABT263, Zhou *et al.* converted it into DT2216 (Fig. 1.19), a BCL-X_L PROTAC, that targets BCL-X_L to the VHL E3 ligase for degradation. VHL E3 ligase is differentially expressed in tumor cells compared to normal tissue. As PROTACs rely on a E3 ligase to induce protein degradation, they can achieve cell/tissue selectivity even when their target protein is ubiquitously expressed. As VHL is minimally expressed in platelets, DT2216 presented reduced platelet toxicity compared with ABT263. It was also found that DT2216 presents a high potency in inducing BCL-X_L degradation in MOLT-4 (T-cell acute lymphoblastic leukemia) cells with a DC₅₀ of 63 nM and a D_{max} of 90.8%.

The effect of this PROTAC on the viability of MOLT-4 cells was therefore evaluated in comparison with ABT263. DT2216 ($EC_{50} = 52$ nM) was four-fold more cytotoxic to MOLT-4 cells than ABT263 ($EC_{50} = 191$ nM). These findings confirm that this PROTAC has improved antitumor potency and reduced toxicity compared to ABT263.⁵⁴



*Figure 1.19: Structure of DT2216.*⁵⁴

2. AIMS OF THE THESIS

The main objective of this PhD is to target BAG3 and its protein-protein interaction with HSP70 through the development of high-affinity small molecule BAG3 inhibitors. New derivatives were designed and synthesized starting from compound **1a** (Fig. 2.1), a hit compound reported in the literature (Terracciano *et al.*⁴⁷) that is able to bind the ‘BAG domain’ of BAG3, modulating its activity and preventing its PPIs with HSP70. To perform a SAR (structure-activity relationship) expansion, new chemical groups were introduced and/or replaced in the hit compound **1a** to improve its binding affinity for BAG3 and anti-proliferative activity against different cancer cell lines (alone or in combination with consolidated anticancer drugs).

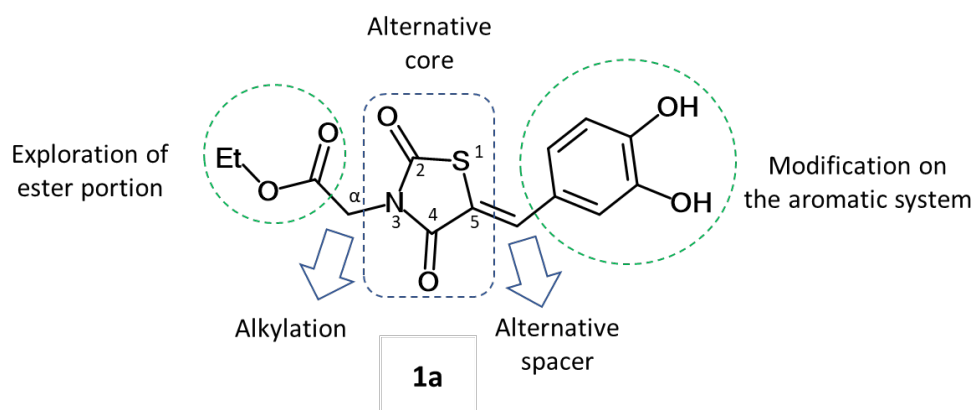


Figure 2.1: SAR exploration on compound **1a** (Terracciano *et al.*⁴⁷).

Once the biological activity of the hit compound **1a** was confirmed, the SAR exploration started from the 3 position of the 2,4-thiazolidinedione core. Substituents of varying steric bulk were introduced to explore how much space there is around the ester group and at the position α to its carbonyl. The ester function was also replaced with amides and other functional groups such as lactones and ethers. Subsequently, the SAR exploration was focused onto replacement of the catechol ring, in order to understand if the two hydroxy groups are necessary to retain the binding affinity to BAG3 (as hydrogen bond donors) or if they can be substituted with other groups. Then, the reduction and the methylation of the double bond at the 5 position of the 2,4-thiazolidinedione was considered to verify if these modifications are tolerated while removing a possible metabolic hot spot. Finally, some explorative core replacements were considered to access a new series of BAG3 modulators,

allowing the discovery of a new proprietary class of inhibitors. The compounds synthesized were tested for their BAG3 binding affinity and antiproliferative activity.

As the down-modulation of BAG3 (mediated by specific small interference RNA) has been shown to reduce tumor growth by suppressing its anti-apoptotic activity, the second purpose of this PhD is to design and synthesize PROTACs able to form effective ternary complexes with the target protein (BAG3) and an E3 ubiquitin ligase. Such process would lead to the ubiquitination and degradation of BAG3, thereby restoring death by apoptosis in tumor cells. As already mentioned, PROTACs exhibit a catalytic mechanism of action and do not require a ligand with a high binding affinity for the target protein. Furthermore, the binder does not necessarily need to possess a biological activity. These features make the PROTAC technology particularly attractive for the development of novel anticancer drugs directed against BAG3. The information gained from the SAR exploration around the 2,4-thiazolidinedione series were used to design and develop several PROTACs.

3. DISCUSSION AND

BIOLOGICAL RESULTS

Ethyl 2-[(5Z)-5-[(3,4-dihydroxyphenyl) methylidene]-2,4-dioxo-1,3-thiazolidin-3-yl]acetate (**1a**) is the first selective BAG domain modulator of BAG3 reported in the literature, with a high selectivity for BAG3 respect to other similar BAG family members, such as BAG1 and BAG4. As already discussed, this compound was discovered by the group of Terracciano via a HTS screening campaign and its biological characterization was also reported. In the preliminary Surface Plasmon Resonance (SPR) assays this compound showed a high binding affinity for BAG3 ($K_d = 11.1 \pm 3.9$ nM) and for its isolated BAG domain ($K_d = 6.4 \pm 2.2$ nM). The compound was also evaluated in an *in vitro* cytotoxicity assay on melanoma cells (A375) (known to overexpress BAG3) where it showed an IC_{50} value in the micromolar range ($IC_{50} = 16.6 \pm 1.5$ μ M).⁴⁷ To confirm the data reported by Terracciano *et al.*, this work started with the synthesis in house and the *in vitro* biological characterization of the hit compound **1a**.

The synthetic route reported in Fig. 3.1 involves two steps, the first one is a S_N2 reaction between the commercially available 2,4-thiazolidinedione and ethyl bromoacetate. This is followed by a Knoevenagel condensation of intermediate **2a** with 3,4-dihydroxybenzaldehyde. Compound **1a** was obtained in a good yield (64%) and tested in the preliminary screenings.

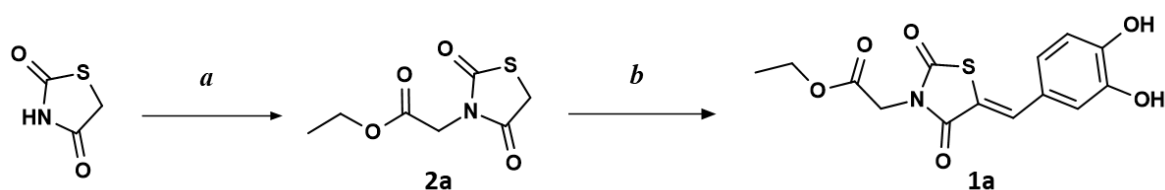


Figure 3.1: Synthesis of compound **1a**. Conditions: a) ethyl bromoacetate (1 eq.), potassium carbonate (2 eq.), MeCN, 25 °C, 18 h; b) 3,4-dihydroxybenzaldehyde (1 eq.), piperazine (0.5 eq.), acetic acid (0.5 eq.), toluene, reflux, 18 h.

To confirm the BAG3-binding capability of the reference compound **1a**, a thermal shift assay (TSA) was initially performed in collaboration with Prof. Giampietro Viola (Dept. of Woman's and Child's Health, University of Padova, Italy). The TSA is a spectroscopic technique that measures the temperature-dependent denaturation of a protein in solution and is used to study the thermal stabilization of a protein upon ligand binding. The assay measures the melting temperature (T_m) of a protein, which is the temperature at which the concentration of protein in the native state is equal to the concentration of protein in the unfolded state. Protein denaturation is monitored via an increase in fluorescence of SYPRO Orange dye which binds to hydrophobic residues that become exposed when the target protein unfolds (Fig. 3.2). Ligand binding to the target protein leads to increased stability and an increase in melting temperature (Fig. 3.3). This change in T_m , called thermal shift (ΔT_m), is used to identify binders ($\Delta T_m > 0$) from not-binders ($\Delta T_m \leq 0$).⁵⁸ As reported in Fig. 3.4, compound **1a** showed positive values in the TSA ($T_m = 51.2$ °C; $\Delta T_m = 3$ °C) and these results confirm its ability to bind BAG3.

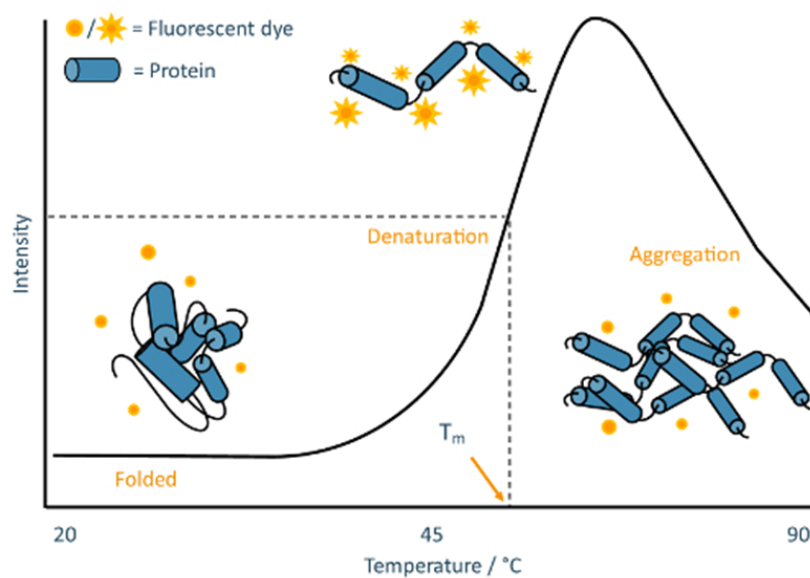


Figure 3.2: Melt curve obtained from a TSA experiment. It represents the “two-state” protein unfolding: the folded state (low fluorescence intensity) and the unfolded state (high fluorescence intensity).⁵⁹

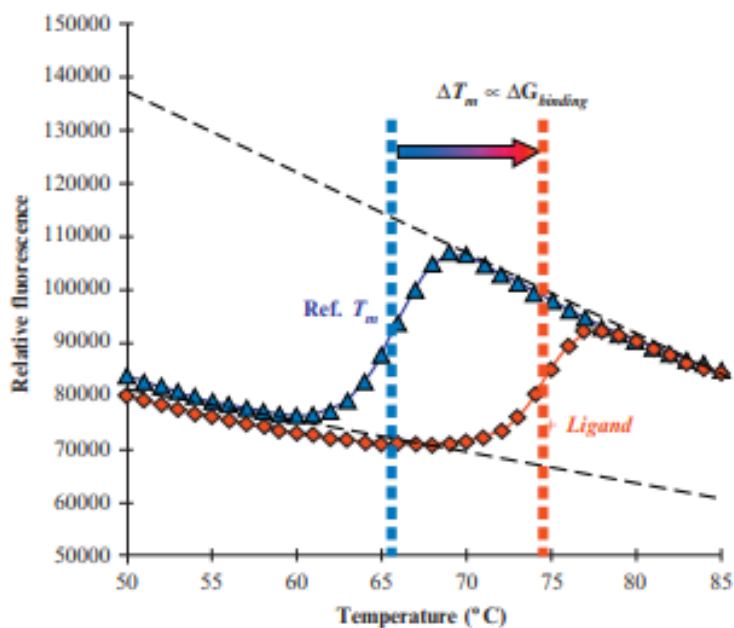


Figure 3.3: Melt curves of an enzyme alone or in the presence of a fixed concentration of its ligand. The shift in melting temperature is the result of the added binding energy to ΔG_U from the ligand.⁶⁰

Compound	Curves	T _m (°C)	ΔT_m (°C)
DMSO	grey	48,3	
		48,1	
		48,3	
1a	light blue	51,2	3

Figure 3.4: *In vitro* results of TSA for compound **1a**. T_m and relative ΔT_m were calculated by JTSA software. For data analysis, the reference control (i.e., BAG3 and 2% vehicle) was tested in triplicate and the mean of the T_m was calculated.

Then a SPR assay (Fig. 3.5) was performed as primary screening in collaboration with Prof. Marco Rusnati (Dept. of Molecular and Translational Medicine, University of Brescia, Italy) to evaluate the BAG3-binding efficacy of the reference compound **1a** and its newly synthesized derivatives. In this method, the target protein is immobilised onto a biosensor surface. The drug ligand is then continuously flowed across the biosensor surface, where it binds to the immobilised protein. Binding is measured as a change in resonance units (RUs) on the biosensor surface. Measuring the increase in binding over time for a given ligand concentration gives the association rate (k_{on}). The drug ligand can then be washed off the protein by switching to buffer alone once the drug flow has stopped. The ligand dissociation rate (k_{off}) is calculated by tracking the progression of the decline in bound ligand. The affinity of the ligand for the receptor (the equilibrium dissociation constant, K_d) is calculated from

the kinetic association and dissociation rates ($k_{\text{off}}/k_{\text{on}}$) for several different ligand concentrations.

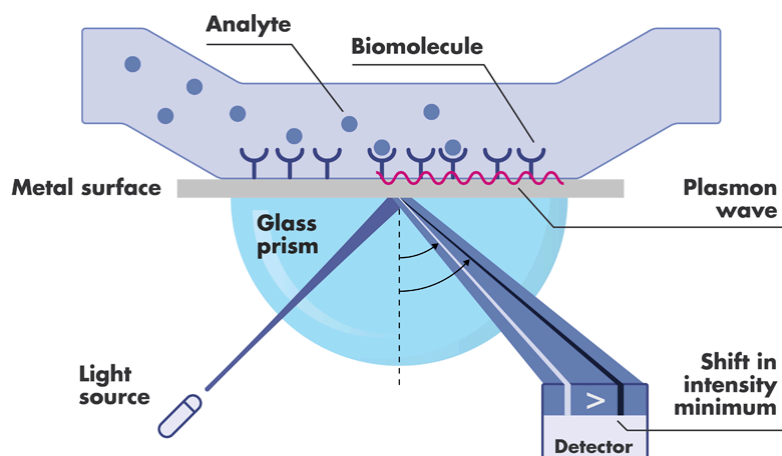


Figure 3.5: SPR analysis is an optical method measuring changes in the mass of biomolecules immobilized on a metal film. When an analyte binds those biomolecules, the refractive index of the metal film changes, resulting in a changed reflection angle of light. (Imagine from: <https://www.reactionbiology.com>, 13-Dec-2022).⁶¹

All the putative BAG3 inhibitors were initially injected onto the BAG3-containing biosensor at a single dose of 50 μM and the analysis was repeated 3-10 times for each compound. The amount of compound that specifically bound the immobilized BAG3 was measured as resonance unit (RU). A further dose-dependent binding analysis at increasing concentrations was performed for the best scoring compounds and the dissociation constant (K_d) values (that are inversely proportional to the affinity of the interaction) were calculated. Also compound **1a** was initially tested at a concentration equal to 50 μM . As expected, very small chemical compounds give rise to very low SPR signals (few RU units), while the presence of DMSO increases significantly the aspecific binding (over hundreds of RU). Despite these limitations, a specific binding can be appreciated with compound **1a**: 8.8 ± 0.9 RU. The compound was then subjected to a further dose-dependent binding analysis at increasing concentrations and the K_d value was calculated: 233 ± 58 μM . The difference between this result and those reported by Terracciano *et al.* ($K_d = 11.1 \pm 3.9$ nM) was attributed to the fact that the Terracciano group employed the non-glycosylated protein obtained from *E. Coli* for their experiment instead of the glycosylated protein.

3a - SAR exploration on position 3 of the 2,4-thiazolidinedione

The SAR exploration was initially focused on the Left-Hand-Side (LHS) of the hit molecule **1a**, by considering point changes on the ester chain and on the α -position of the ester carbonyl group (Fig. 3.6).

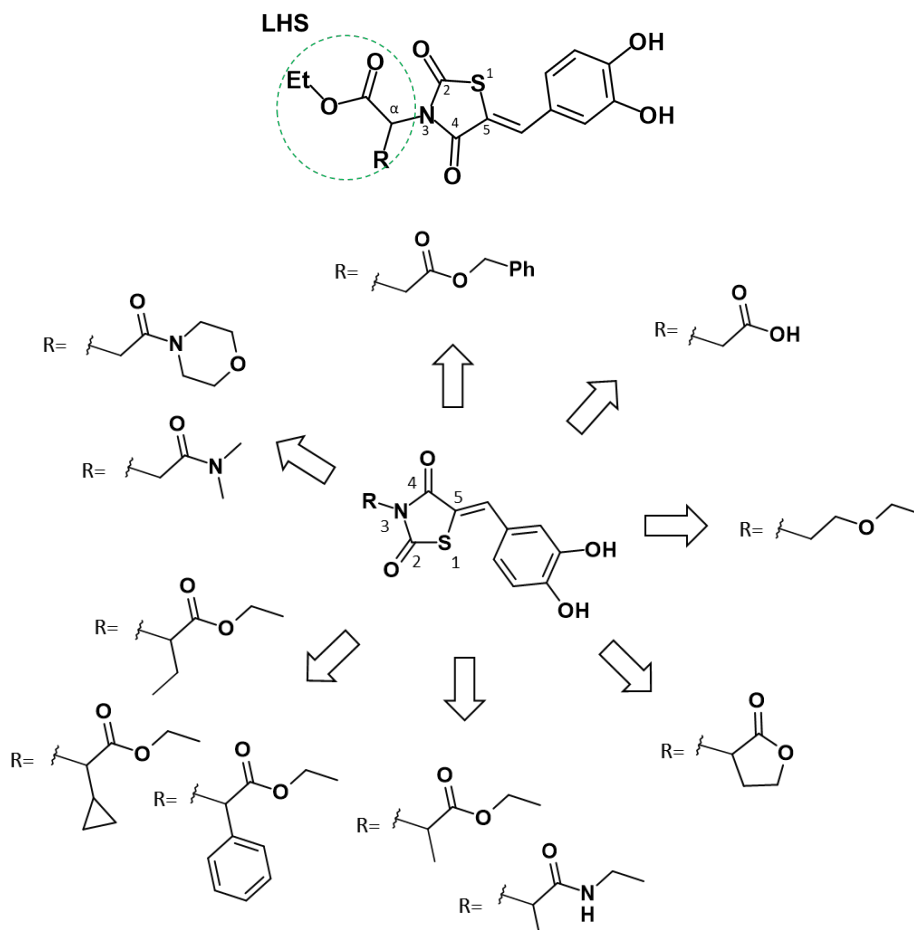


Figure 3.6: Designed derivatives for the SAR exploration on the LHS of the thiazolidinedione series.

The replacement of the ethyl ester with a bulky and flexible substituent like a benzyl ester can give useful information about the extent of hydrophobic interactions needed to increase the binding surface within the protein. Or conversely, the introduction of an acidic functionality, like a carboxylic acid, could reveal if a positive ionic interaction or hydrogen bonding could take place with the surrounding amino acid sidechains. The ether analogue was designed to verify if the carbonyl group of the ester is essential for binding to the protein, in particular to see whether the loss of planarity, due to the removal of the -C=O, the increased flexibility, and the removal of a putative hydrogen bond acceptor (HBA) could be tolerated. The five member lactone ring was designed as a cyclized version of the ethyl ester, to block the flexible ethyl group in a rigid conformation and to study the space around the carbonyl.

Esters are well-known to be metabolically unstable groups, because esterases (enzymes belonging to the class of hydrolases) catalyze the reaction of hydrolysis of the ester bond (Fig. 3.7). These enzymes are widely expressed by most living organisms and are found ubiquitously distributed in the human body. They play different metabolic roles including digestive, inflammatory and detoxification processes. Some enzymes, such as acetylcholinesterase, recognize a specific substrate (acetylcholine) while other esterases are non-specific (pseudocholinesterases) and catalyze the hydrolysis reaction of a wider range of molecules. Similarly, amides can be hydrolyzed by enzymes called amidases (an enzymatic family belonging to the class of hydrolases capable of specifically hydrolyzing the amide bond, Fig. 3.7), but the ester hydrolysis reaction is much faster than the amide hydrolysis reaction. In conclusion, a drug which is an ester, is hydrolyzed more quickly, therefore, its duration of action is much lower than a drug of amide origin.⁶²

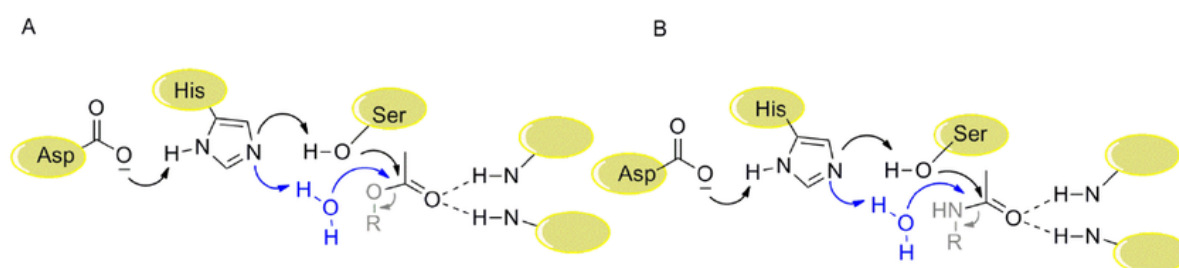


Figure 3.7: Reaction mechanism of esterase (A) and amidase (B). The two enzymes share a common mechanism, in which a Ser, which is activated by a His-Asp dyad, serves as nucleophile. Subsequently, acylesterase and acylamidase adducts are hydrolyzed by an activated water molecule.⁶³

Hydrolase activities are known to be important in the phase I metabolism of xenobiotics. Such enzymes are known from both microsomes and the soluble cytoplasm but are more commonly found in the latter.⁶² As replacing a labile ester linkage with an amide group is known to impart an improved stability to the molecule, secondary and tertiary amides were designed to prevent future problems due to this metabolic hot spot.

As part of the LHS exploration, also the introduction of alkyl groups in the α -position of the carbonyl was considered to obtain information about the space available in this region and if positive hydrophobic interactions can occur with the protein surface. Starting with small substituents, such as methyl and ethyl groups, then expanding to larger substituents, such as the bulkier cyclopropyl and phenyl groups, five analogues were designed.

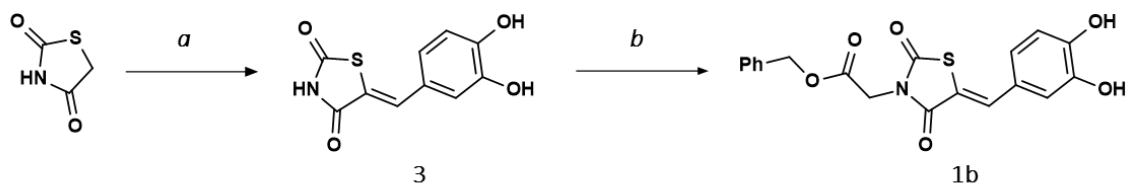
For the functionalization of position 3 of the 2,4-thiazolidinedione ring with different alkyl chains using the convergent approach reported in the synthetic route A of Fig. 3.8 was

initially considered. The common intermediate **3** was synthesized in excellent yield (486 mg, 80% yield) by a Knoevenagel condensation of 2,4-thiazolidinedione with 3,4-dihydroxybenzaldehyde in the presence of a catalytic amount of piperidine. In the second step, compound **3** was employed in a S_N2 reaction with benzyl bromoacetate in the presence of potassium carbonate. Although the outcome of the reaction resulted in a complicated profile the final compound **1b** was however isolated in a low yield (17%). This low yield could be attributed to side reactions due to the presence of the catechol moiety which competes in the S_N2 with the nitrogen of 2,4-thiazolidinedione reducing the amount of desired product.

To avoid this shortcoming, for the synthesis of the other derivatives (**1c-f**) a different approach was considered (Fig. 3.8, synthetic route B). The alkylation of the 2,4-thiazolidinedione was performed as the first step obtaining the intermediates **2c-f**, which were then used in the condensation step with 3,4-dihydroxybenzaldehyde, affording compounds **1c-f** in good yields.

A similar synthetic route was adopted for the synthesis of derivatives **1h-n** (Fig. 3.9) which present a substituent in the α -position of the carbonyl. For this set of compounds, the S_N2 reaction was performed with secondary alkyl halides in the presence of sodium hydride (pK_a = 35) rather than potassium carbonate (pK_a = 10). Sodium hydride is a more effective base in the presence of bulkier secondary alkyl halides due to its small size and because its pK_a is much higher. The acidic hydrolysis of the ester group of compound **1a** afforded the corresponding carboxylic acid **1g** as reported in Fig. 3.8.

Synthetic route A:



Synthetic route B:

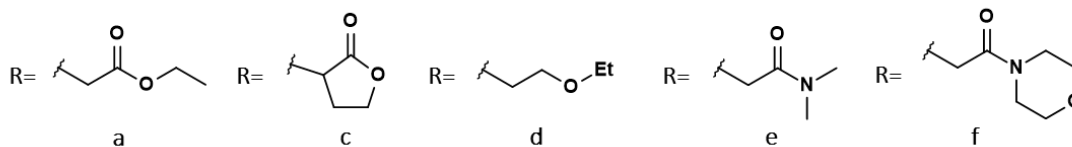
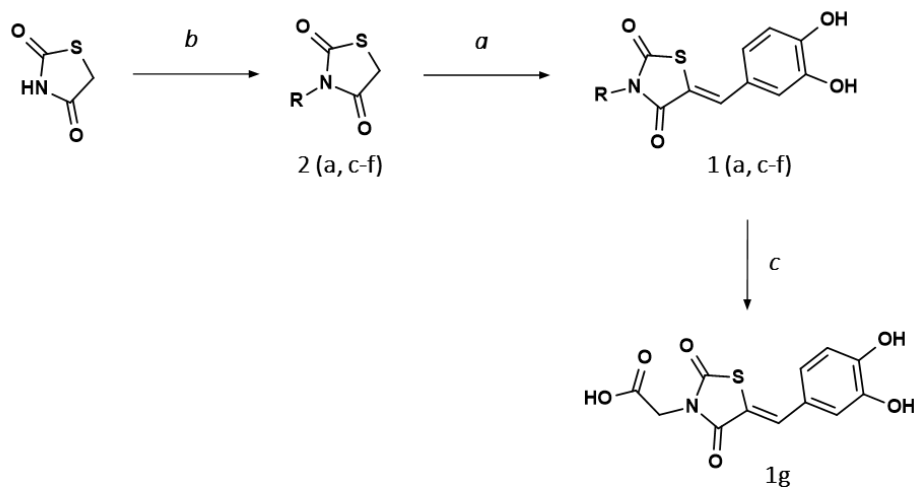


Figure 3.8: Synthesis of compounds **1a-g**. Conditions: a) 3,4-dihydroxybenzaldehyde (1 eq.), piperazine (0.5 eq.), acetic acid (0.5 eq.), toluene, reflux, 18 h; b) alkyl bromide (1 eq.), potassium carbonate (2 eq.), MeCN, 25 °C, 18 h; c) 6M hydrochloric acid, acetic acid, 120 °C, 2 h, for compound **1a**.

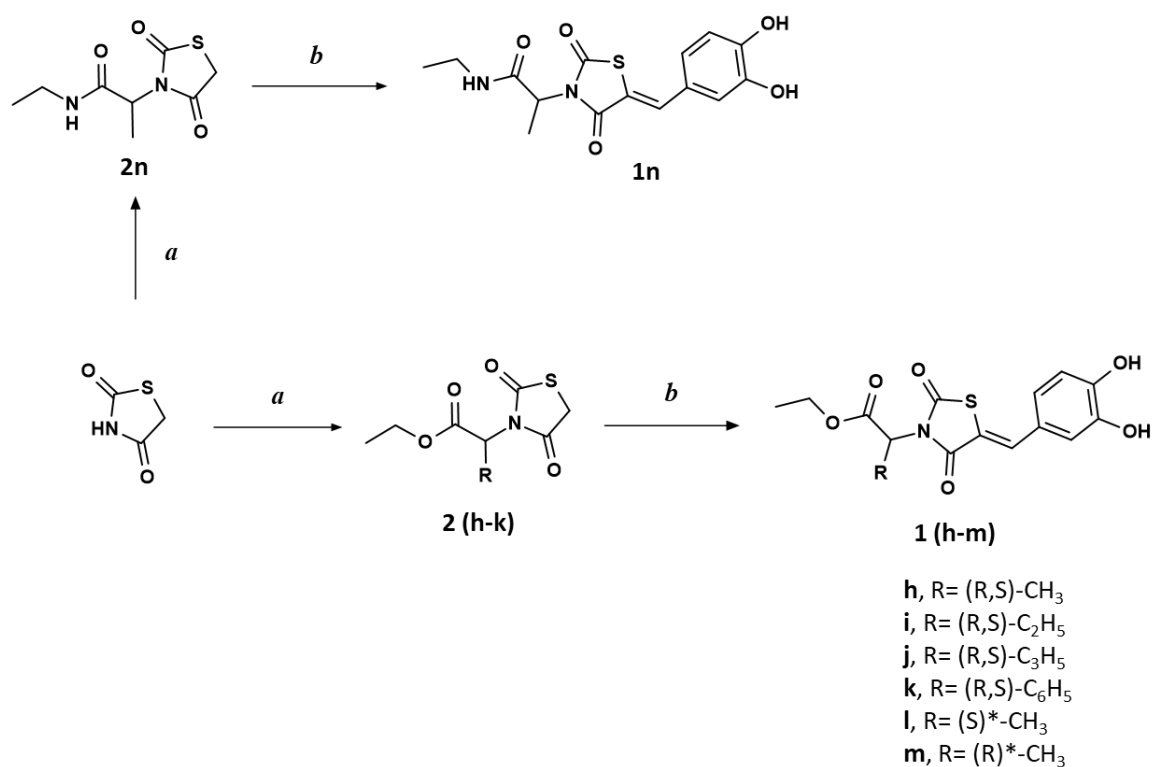


Figure 3.9: Synthesis of compounds **1h-n**. Conditions: a) Alkyl halide (1 eq.), sodium hydride (1.1 eq.), MeCN, 25 °C, 18 h; b) 3,4-dihydroxybenzaldehyde (1 eq.), piperazine (0.5 eq.), acetic acid (0.5 eq.), toluene, reflux, 18 h. *Stereochemistry arbitrarily assigned.

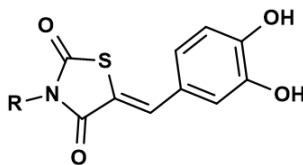
All these compounds were subjected to an initial SPR screening, performed at a single concentration of 50 μ M (Fig. 3.10 and 3.11).

The substitution of the ethyl ester of compound **1a** with the benzyl ester of compound **1b**, had a detrimental effect on the binding affinity possibly due to the steric clash of this bulky and rotatable substituent. The cyclization of the ethyl ester to the corresponding racemic lactam **1c** leads to a drop of binding affinity (< 5 RU) which can be attributed to the lack of free space around the carbonyl. In addition, the hydrolysis of the carbonyl group to the corresponding carboxylic acid **1g** had a detrimental effect on the binding affinity indicating that the carboxylic acidic moiety is not tolerated in this position. Of note, the binding of compound **1d** (where the carbonyl group of the ethyl ester was removed affording the corresponding ethyl ether) could not be evaluated because its binding was irreversible and destroyed the biosensor surface.

As part of the SAR exploration on the LHS, the ethoxy group of the ester was replaced with different amines, affording the corresponding amides. The first amide derivative synthesized, **1e**, which bears the dimethyl amine, completely lost binding affinity for BAG3, while the morpholine derivative **1f** showed an improved binding capacity compared to the reference compound **1a**. This improved binding affinity could be explained by the establishment of a new positive interaction with the protein, where the morpholine oxygen can act as a hydrogen bond acceptor (HBA).

The introduction of a methyl group in the α -position of the ethyl acetate moiety, as in compound **1h**, was well tolerated. This decoration leads to the introduction of a chiral center in the molecule. To verify if there is any selectivity towards the two enantiomers, the racemate was resolved by a semi-preparative HPLC chiral separation. The primary SPR assay showed that enantiomer **1l**, has a comparable binding affinity with the racemate while the binding affinity of the other enantiomer **1m** is still under evaluation. Also, the corresponding ethyl amide **1n** was synthesized as reported in Fig. 3.9, but the compound did not show any binding affinity for BAG3. These results could be attributed to the presence of an additional hydrogen bond donor (HBD) in the amide derivative, which may lead to unfavorable interactions with the protein. The encouraging results obtained with **1h** led us to verify if larger substituents could be tolerated in this position. The SAR analysis revealed that as steric hindrance at the α -position of the acetic chain increases from methyl to cyclopropyl (**1j**), the binding affinity improves, whereas the introduction of a phenyl group (**1k**) decreases the binding affinity, indicating that bulkier substituents than cyclopropyl are less tolerated in that position thus providing an idea of the amount of space available in this region of the binding site. As reported in Fig. 3.11, compounds **1h** and **1j** show BAG3

binding affinities of ~10.7 RU and ~12.7 RU respectively and are the most promising lead compounds among this series.



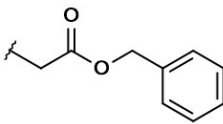
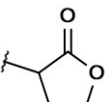
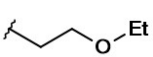
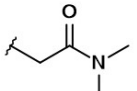
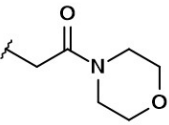
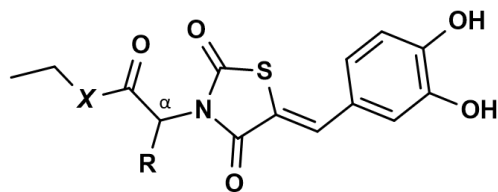
Compound	R	number of measurements	RU (mean + SEM)
1a	-CH ₂ CO ₂ Et	16	8.8 ± 0.9
1b		3	NB
1c		3	3.9 ± 1.0
1d		3	ND
1e		3	NB
1f		9	10.8 ± 1.2
1g	-COOH	3	NB

Figure 3.10: *In vitro* SPR analysis of compounds **1a-g**. Compound **1a** was used as reference. New compounds were injected onto the BAG3-containing biosensor at the single concentration of 50 μ M and the analysis was repeated 3-9 times for each compound. NB = No Binding. ND = Not Determined. SEM = Standard error of the mean.



Compound	R	X	number of measurements	RU (media + SEM)
1a	H	O	16	8.8 ± 0.9
1h	(R,S)-CH ₃	O	6	10.7 ± 2.0
1l	(S)*-CH ₃	O	3	8.4 ± 0.9
1n	(R,S)-CH ₃	NH	3	NB
1i	(R,S)-C ₂ H ₅	O	5	9.9 ± 0.7
1j	(R,S)-C ₃ H ₅	O	7	12.7 ± 1.4
1k	(R,S)-C ₆ H ₅	O	5	9.8 ± 1.3

Figure 3.11: *In vitro* SPR analysis of compounds **1a**, **1h-l**, and **1n-k**. Compound **1a** was used as reference. New compounds were injected onto the BAG3-containing biosensor at the single concentration of 50 μ M and the analysis was repeated 3-7 times for each compound. NB = No Binding. SEM = Standard error of the mean.

Given the encouraging results obtained with compounds **1f** and **1h**, further amide analogues were designed maintaining the methyl group in the α -position of the carbonyl group (see compounds **1p-s**, Fig. 3.12). The first amide, **1p** was designed to verify if the morpholine and the α methyl group could have a synergistic effect on the binding affinity. The piperidine derivative **1q**, which presents a $-\text{CH}_2-$ instead of the morpholine oxygen, was exploited to verify if the oxygen of **1f** can effectively make a positive interaction with the protein, in which case a loss of binding affinity is expected for this derivative. Some variations on the morpholine ring were also considered, like the spiro derivative **1s**. The spiro piperidine **1r** was proposed to verify if two HBA were tolerated.

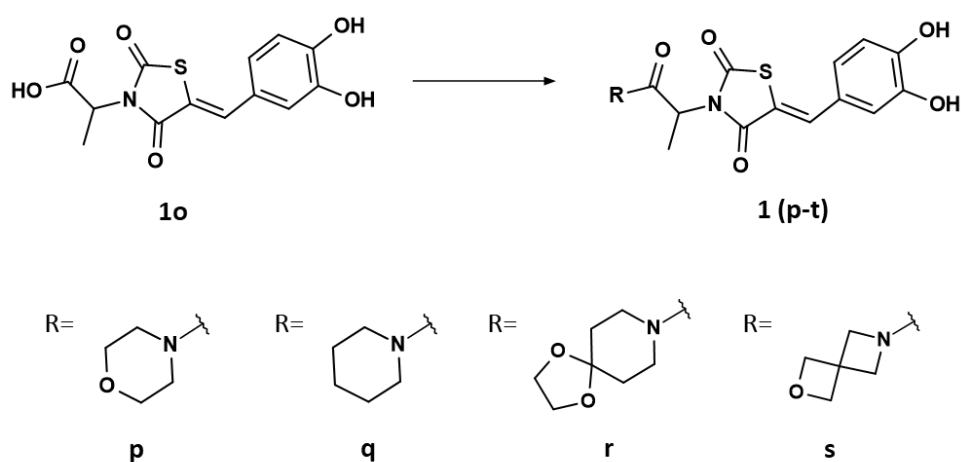
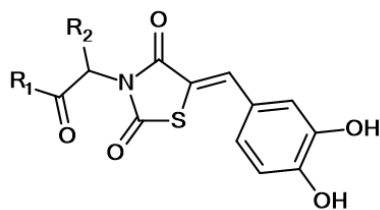


Figure 3.12: Synthesis of compounds **1p-s**. Conditions: secondary amine (1 eq.), HATU (1 eq.), TEA (1 eq.), DMF (1 eq.), 25 °C, 4 h.

These amides were synthesized as reported in Fig. 3.12, where the carboxylic acid **1o** (whose synthesis is reported in Fig. 3.41) was used to perform an amide coupling with different secondary amines, in the presence of O-(7-azabenzotriazol-1-yl)-N,N,N',N'-tetramethyluronium hexafluorophosphate (HATU) as coupling agent and triethylamine (TEA) as base. All the final amides were obtained as racemic mixtures due to the presence of a chiral center.

The results of the SPR assay, reported on Fig. 3.13, showed a complete loss of binding affinity for **1p** and **1s** and a substantial drop for **1r** (5.3 RU). The only compound which retains a good binding with the protein was **1q**. These results taken together suggest that the oxygen of the morpholine is not necessary to retain a good BAG3-binding efficacy, but it is helpful only in the case in which it is placed in the right position. Furthermore, no substituent bulkier than morpholine or piperidine are tolerated.



Compound	R ₁	R ₂	number of measurements	RU (media + SEM)
1a	-OCH ₂ CH ₃	H	16	8.8 ± 0.9
1f		H	9	10.8 ± 1.2
1n	-NHCH ₂ CH ₃	(R,S)-CH ₃	3	NB
1p		(R,S)-CH ₃	3	NB
1q		(R,S)-CH ₃	8	10.4 ± 1.0
1r		(R,S)-CH ₃	3*	5.3 ± 0.1
1s		(R,S)-CH ₃	3	NB

Figure 3.13: *In vitro* SPR analysis of compounds **1a**, **f**, **n**, **p-s**. Compound **1a** was used as reference. New compounds were injected onto the BAG3-containing biosensor at the single concentration of 50 μ M and the analysis was repeated 3-9 times for each compound. NB = No Binding. SEM = Standard error of the mean. *One value discarded.

3b - SAR exploration on position 5 of the 2,4-thiazolidinedione

The SAR exploration on the right-hand-side (RHS) of the 2,4-thiazolidinedione series (Fig. 3.14), was initially focused on the replacement of the catechol ring with more suitable moieties. Catecholic compounds are known to be highly reactive molecules and the catechol (1,2-dihydroxybenzene) nucleus can undergo a variety of chemical reactions, as reported in Fig. 3.15.⁶⁴

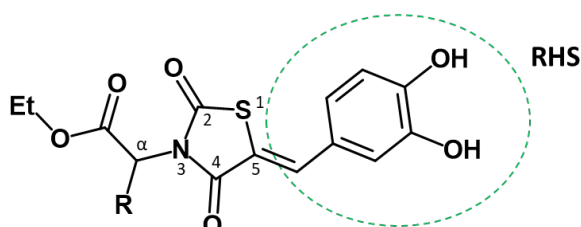


Figure 3.14: The RHS of the thiazolidinedione series (highlighted in the green circle).

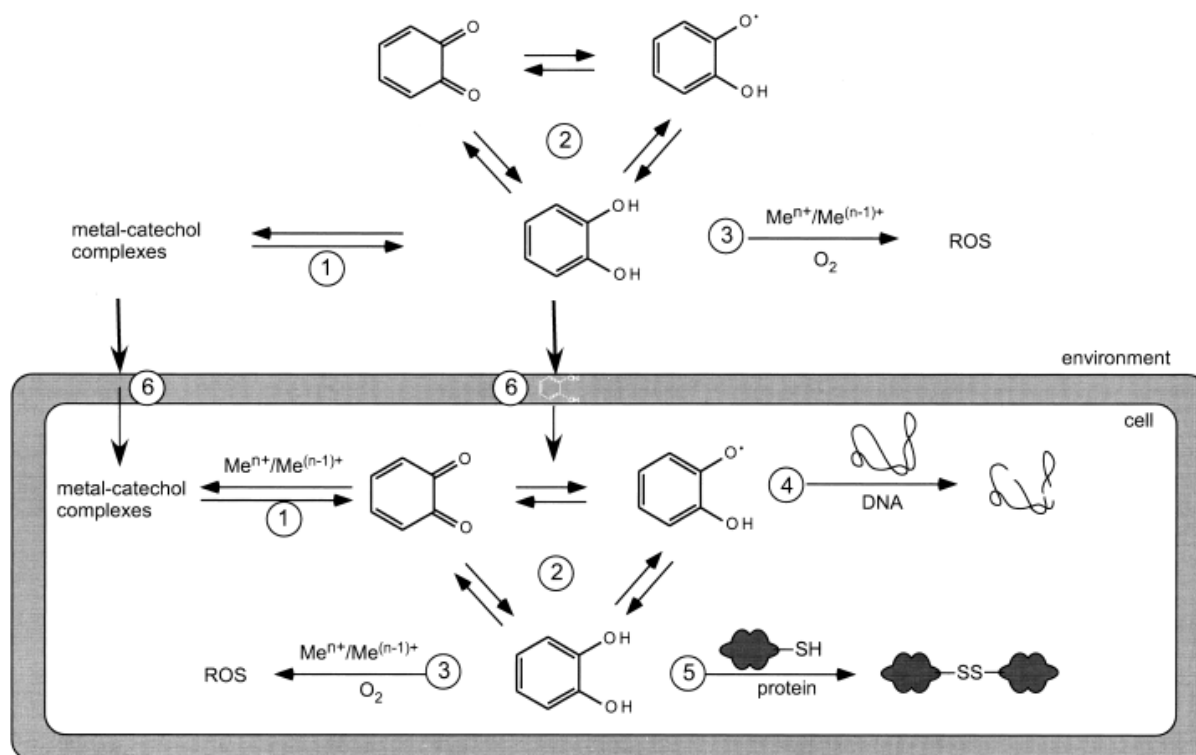


Figure 3.15: Catechol chemical reactions in the environment and in cells. Chemical reactions: 1, Heavy metals complex formation; 2, Redox cycling; 3, Generation of reactive oxygen species (ROS) in the reaction with heavy metals and oxygen. Molecular mechanisms of actions in cells: 4, DNA damage (for example, strand breaks and the formation of DNA adducts); 5, protein damage (for example, protein cross-linking via disulphide groups).⁶⁴

Catechols can undergo redox reactions, cycling between catechols, and can form semiquinone radicals and *ortho*-benzoquinone (Fig. 3.16). Under physiological conditions catechol is not auto-oxidized, except in the presence of heavy metals (e.g. copper). Several enzymes can catalyse the oxidation of catechol to benzoquinone, such as the copper-containing superoxide dismutase, some haem-containing peroxidases and tyrosinase. When catechol is oxidized enzymatically or in the presence of oxygen and heavy metals, one electron is transferred to molecular oxygen, consequently superoxide (O_2^-) is formed. In the presence of heavy metals (e.g., copper, iron), superoxide is further reduced to hydrogen peroxide (H_2O_2) and hydroxyl radicals ($\cdot OH$). These reactive oxygen species (ROS) can be harmful to cells and organisms because they can damage macromolecules such as DNA and proteins if they are not eliminated.⁶⁴

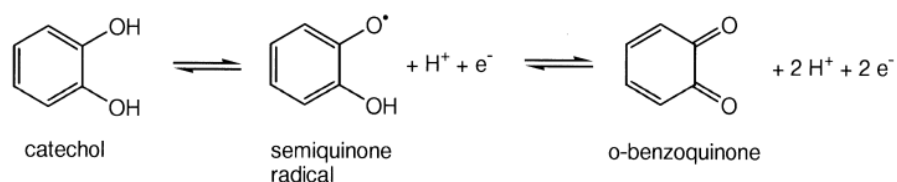


Figure 3.16: Redox cycling of catechol.⁶⁴

The DNA damage can be either due to DNA-adduct formation by the catechols or their reaction intermediates or it can be due to the formation of ROS causing an oxidation of DNA bases and/or DNA strand breaks. Oxidized catechols also react with sulfhydryl groups of proteins and glutathione (Fig. 3.17). Catechol thereby binds either directly to sulfhydryl groups and inactivates the protein, or protein and glutathione radicals are produced. These radicals might subsequently lead to protein cross-linking and glutathione dimer formation. As glutathione is an important reductant in cells, a dimer formation can change the redox status of the cell, thereby producing oxidative stress. It has been shown that also the ϵ -amino groups of lysine react with oxidized catechols.⁶⁴

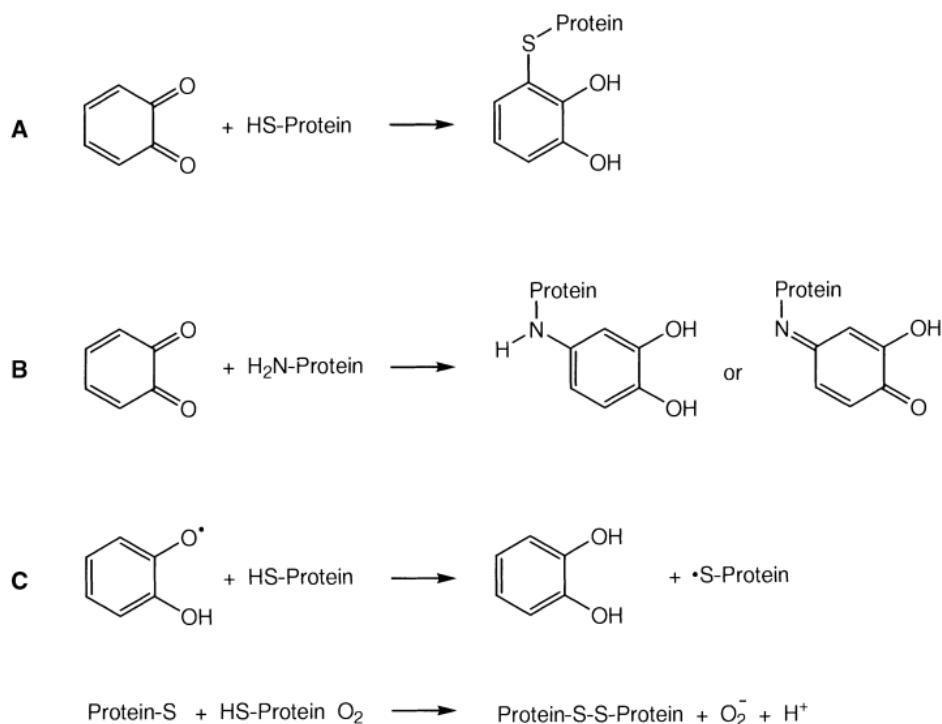


Figure 3.17: Catechol-protein interactions can have three forms: *A.* Oxidized catechol reaction with sulfhydryl groups; *B.* Oxidized catechol reaction with amino groups; *C.* Reduction of the semiquinone radical by a sulfhydryl group and subsequent protein cross-linking in the presence of oxygen.⁶⁴

The replacement of the catechol moiety with alternative aromatic patterns is fundamental to avoid all these possible side reactions. In the first set of derivatives described, the left portion of molecule **1a** is kept fixed, so the SAR changes only concern the catechol ring (Fig. 3.18). To verify if the two-hydroxy groups were both essential to retain the BAG3 binding affinity, the two phenolic derivatives, **4a** and **4b**, were designed. In either compound, an acidic -OH group is still present and can act as HBD/HBA and can possibly be involved in ionic interactions with the protein. The 3-fluorophenol derivative **4c** was designed to evaluate the effect of an electron withdrawing substituent (fluorine) instead of an electron releasing group (hydroxyl). The *meta*-fluorine can also act as HBA and mask the *para*-hydroxyl with an intramolecular hydrogen bond. The effect of an electron withdrawing group (EWG), such as a fluorine or chlorine, was also examined in the *para*-fluorine derivative **4d** and in the 3,4-dichloro derivative **4e**. The di-methoxy derivative **4f** and its cyclised version **4g** were designed to further evaluate if the two-hydroxy groups present in the catechol ring are involved in some specific HBD interactions with the protein. Both the compounds possess two HBA groups, such as the *ortho*-methoxy pyridine derivative **4h**.

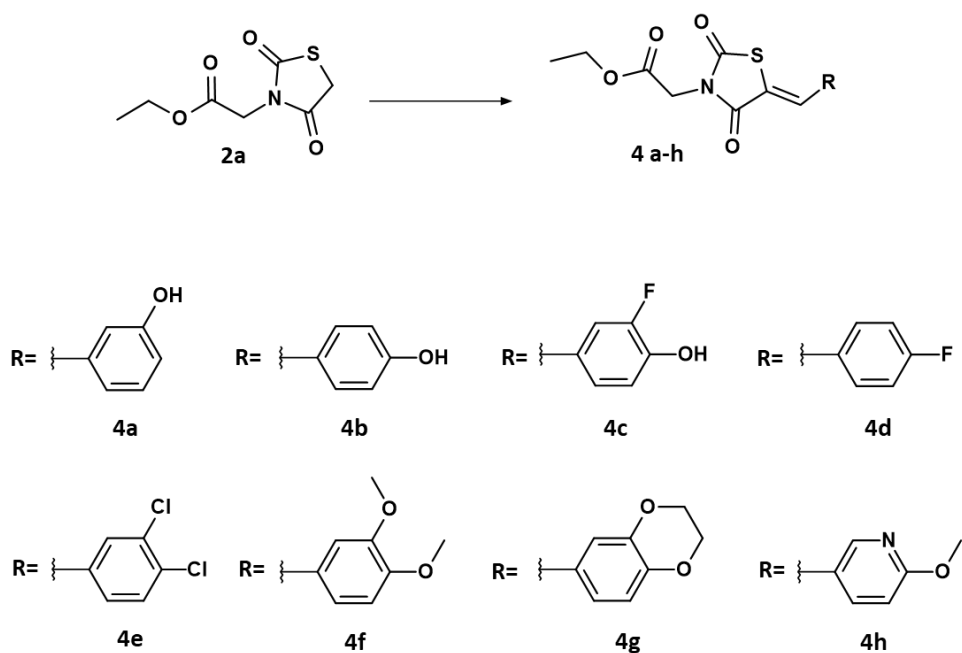


Figure 3.18: Structures and synthesis of compounds **4a-h**. Conditions: aromatic aldehyde (1 eq.), piperazine (0.5 eq.), acetic acid (0.5 eq.), toluene, reflux, 18 h.

All the described compounds were synthesized following the general synthetic scheme reported in Fig. 3.18. The synthesis of intermediate **2a** was already discussed at the beginning of the chapter (see Fig. 3.1). **2a** was then condensed under Knoevenagel conditions to afford compounds **4a-h** in good yield.

This set of compounds was tested in the primary *in vitro* SPR assay at a single concentration of 50 μ M but none of them showed any binding affinity for BAG3. Some hypotheses were formulated to explain their complete loss of affinity:

- A single hydroxy group is not sufficient to maintain the interaction with BAG3.
- Either a single HBD (*para*-hydroxy or *meta*-hydroxy) or HBA (*para*-fluorine) are not enough to retain the binding affinity.
- The alkylation of both the *meta*- and *para*- hydroxyl groups of the catechol lead to loss of affinity. It is possible that at least one of the two hydroxyl groups acts as HBD or is involved in ionic interactions. It is also possible that there is little space in this area and the increased steric hindrance is not tolerated for this reason.
- Electron withdrawing groups, such as fluorine and chlorine, are not well tolerated in either *meta*- or *para*- positions.

To verify these hypotheses further analogues were designed, as reported in Fig. 3.19. As the SAR exploration on the LHS had shown that a methyl group in the α -position of the ethyl ester was well tolerated, this change was introduced in this set of derivatives.

Further derivatives which bear EWGs, such as fluorine and chlorine, on both *meta*- and *para*-positions were designed. In compound **5a** the fluorine and the hydroxy group were inverted from those of compound **4c**, to verify if this reversed pattern of HBD/HBA is well tolerated. As the fluorine is a small substituent, whose dimension is comparable to a hydrogen atom, further analogues with larger groups, such as chlorine, were considered. In compound **5b** the *meta*-hydroxy group of the catechol is replaced with a chlorine, while in compound **5c** the *para*-hydroxy moiety has been replaced with a chlorine. In the 2,6-difluoro and 2,6-dichloro phenol derivatives, **5d** and **5e**, a second EWG near the *para*-hydroxy group was introduced to increase the acidity of the latter.

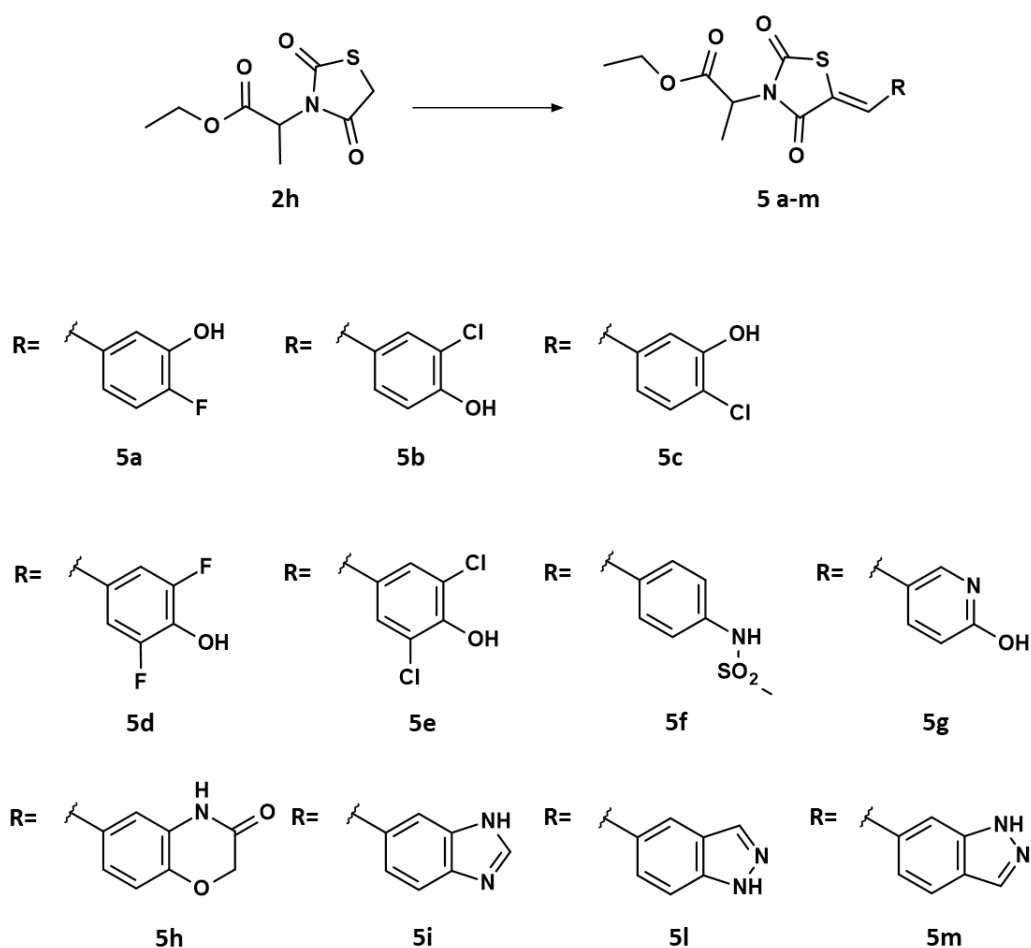


Figure 3.19: Structures and synthesis of compounds **5a-m**. Conditions: aromatic aldehyde (1 eq.), piperazine (0.5 eq.), acetic acid (0.5 eq.), toluene, reflux, 18 h.

Other mild acidic groups and HBD/HBA moieties were introduced to replace the catechol, such as the sulphonamide **5f** and the hydroxy pyridine **5g**. Compound **5h** is a derivative of **4g** where a HBA was replaced with a HBD by substitution with an amide group.

The benzimidazole **5i** and the two indazole derivatives **5l** and **5m** are some examples of catechol bioisosteres replacement. These alternative moieties have been reported in the literature as effective catechol replacements.^{65,66}

Catechols can form an intramolecular hydrogen-bond to create a second ring. In both benzimidazole and indazole this H-bond ring is mimicked by a covalent ring structure (Fig. 3.20).

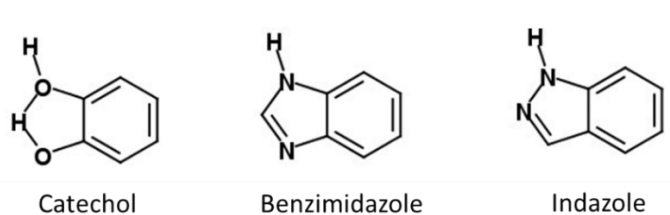
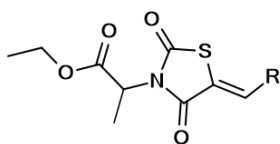


Figure 3.20: Catechol intramolecular H-bond and its bioisosteres.^{65,66}

This set of compounds was synthesized from intermediate **2h**, as reported in Fig. 3.19, by Knoevenagel condensation with the appropriate aromatic aldehydes and then tested at a single concentration of 50 μM in the *in vitro* SPR assay (data reported in Fig. 3.21). Among the entire set of compounds, six derivatives (**5c**, **5e**, **5f**, **5i**, **5l**, **5m**) showed a signal in the SPR analysis, but for five of them the signal was under the cut-off of 5 RU. The only compound that showed a good binding affinity for BAG3 was **5i** (~ 7.95 RU).



Compound	R	number of measurements	RU (media + SEM)
1h		6	10.7 ± 2.0
5a		3	NB
5b		3	NB
5c		3	1.3 ± 0.3
5d		3	NB
5e		3	4.9 ± 0.3
5f		3	3.3 ± 0.1
5g		3	NB
5h		3	NB
5i		8	8.0 ± 1.1
5l		3*	2.0 ± 0.2
5m		3*	1.6 ± 0.2

Figure 3.21: *In vitro* SPR analysis of compounds **1h** and **5a-m**. Compound **1h** was used as reference. The compounds were injected onto the BAG-3-containing biosensor at the single concentration of 50 μ M and the analysis was repeated 3-8 times for each compound. NB = No Binding. SEM = Standard error of the mean. *One measure discarded.

In parallel with the last set of compounds also a few morpholine derivatives were considered. As the morpholine derivative **1f** showed an improved binding capacity (~ 10.8 RU) with respect to its ester analogue **1a** (~ 8.8 RU), the two morpholine derivatives **6a** and **6b** were designed to verify if the low SPR signal (< 5 RU) detected for the two compounds **5e** and **5f** could be improved. For the synthesis of these two analogues intermediate **2f** was condensed with the respective aldehydes, as reported in Fig. 3.22.

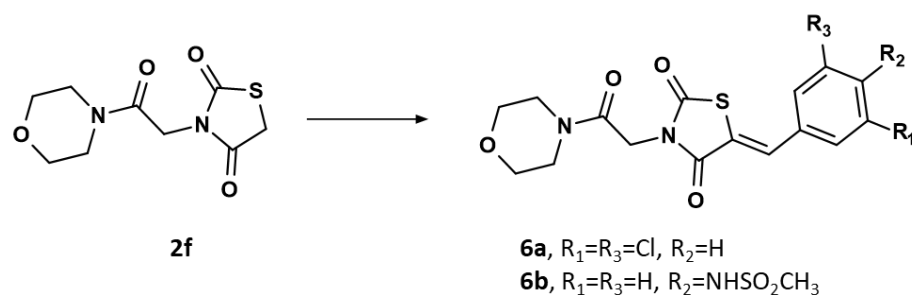


Figure 3.22: Structures and synthesis of compounds **6a** and **6b**. Conditions: aromatic aldehyde (1 eq.), piperazine (0.5 eq.), ethanol, reflux, 8 h.

Finally, the catechol ring attachment point was switched, affording the 2,3-dihydroxyphenyl derivative **9** (Fig. 3.23). This compound also presented two of the most promising LHS modifications reported in this work: the morpholine instead of the methoxy group of the ester and the methyl group in the α -position of the ester. The compound was synthesized in three steps, the first one involved the acidic hydrolysis of the ester intermediate **2h** to the corresponding carboxylic acid **7** which was converted into the amide **8** by using morpholine as amine and HATU and TEA as coupling reagents. Finally, this intermediate was condensed under Knoevenagel conditions with 2,3-dihydroxybenzaldehyde affording the desired compound **9**.

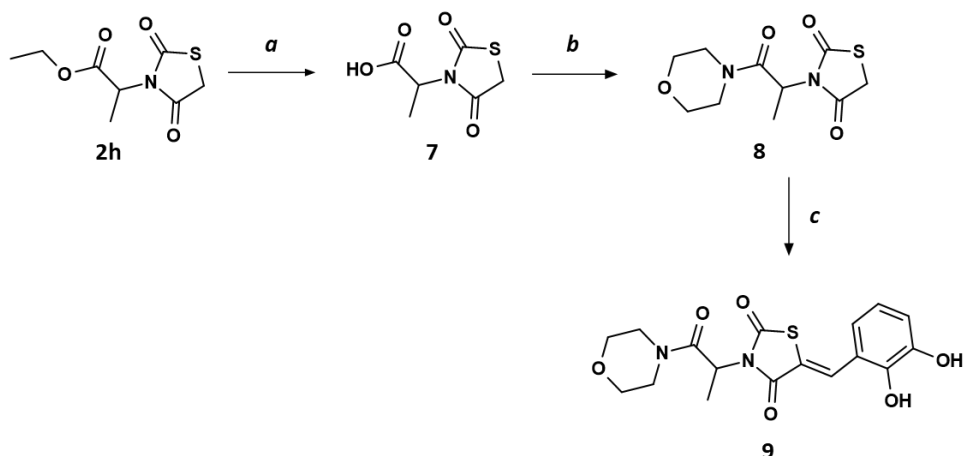


Figure 3.23: Structure and synthesis of compound **9**. Conditions: a) HCl 6M, acetic acid, 120 °C, 1h; b) morpholine (1 eq.), HATU (1 eq.), TEA (1 eq.), DMF (1 eq.), 25 °C, 4h; c) 2,3-dihydroxybenzaldehyde (1 eq.), piperazine (0.5 eq.), acetic acid (0.5 eq.), toluene, reflux, 18 h.

The results of the primary SPR assay for these three compounds (Fig. 3.25) showed a loss of binding affinity for both **6a** and **6b**, and an increase for **9** with a value of ~12 RU. These results and those reported on Fig. 3.21, give useful SAR information, and confirmed some of the hypotheses formulated previously:

- Electron withdrawing groups, such as fluorine and chlorine, are not tolerated on either *meta*- or *para*- positions.
- A mild acidic group alone is not sufficient to retain the binding affinity.
- In general, the catechol ring replacement is not tolerated. Two exceptions are represented by a bioisosteric replacement with the benzimidazole and the shift of the *para*-hydroxy group to the *ortho*-position.
- The bioisosteric replacement of the catechol ring worked well in the case of the benzimidazole but was less tolerated in the case of the two indazole moieties which showed a binding affinity < 5 RU.

Given the encouraging results obtained with compound **9**, another two derivatives were designed and synthesized (Fig. 3.24). Compound **5o** is the ethyl ester derivative of compound **9** and compound **5n** is a 2,4-dihydroxyphenyl derivative of compound **5o**. These two novel compounds are currently being tested and the biological results are not yet available.

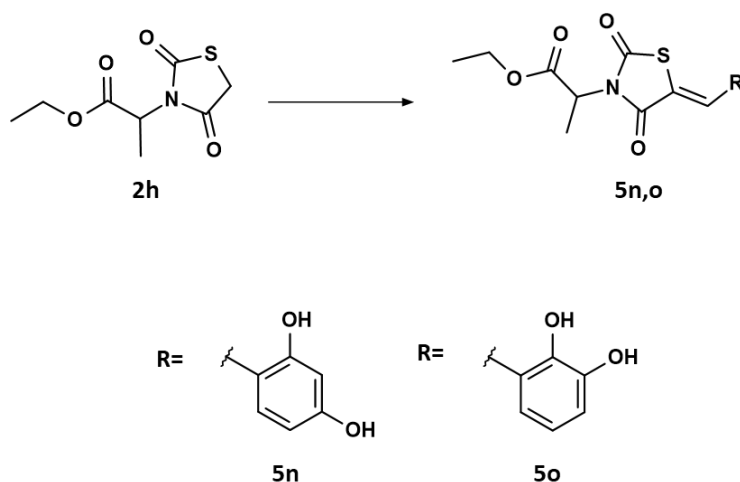
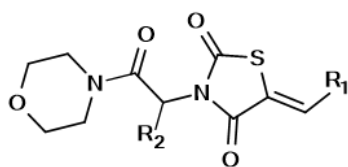


Figure 3.24: Structures and synthesis of compounds **5n** and **5o**. Conditions: aromatic aldehyde (1 eq.), piperazine (0.5 eq.), ethanol, reflux, 18 h.



Compound	R1	R2	number of measurements	RU (media + SEM)
1f		H	9	10.8 ± 1.2
6a		(R,S)-CH ₃	3	NB
6b		(R,S)-CH ₃	3	NB
9		(R,S)-CH ₃	6	12.1+0.7

Figure 3.25: *In vitro* SPR analysis of compounds **1f**, **6a**, **b** and **9**. The compounds were injected onto the BAG3-containing biosensor at the single concentration of 50 μ M and the analysis was repeated 3-9 times for each compound. Compound **1f** was used as reference. NB = No Binding. SEM = Standard error of the mean.

To complete the SAR exploration on the RHS, the double bond of compound **1a** was reduced by hydrogenation, affording compound **10** (Fig. 3.26). The transformation from a sp² carbon to a sp³ leads to an increase in the degrees of freedom of the system, which switches from a rigid double bond in the Z configuration to a rotatable single bond.

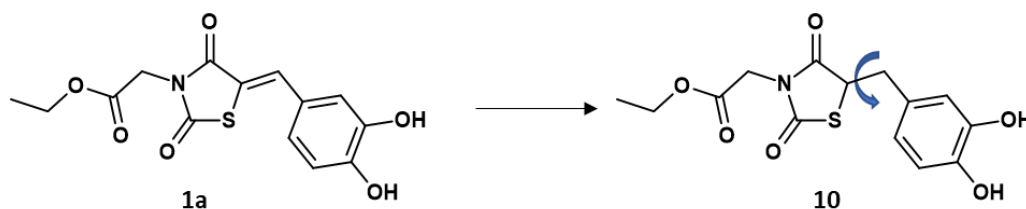


Figure 3.26: Structure and synthesis of compound **10**. Conditions: Pd/C 10% wet, molecular hydrogen (6 atm), ethanol, 25 °C, 18 h.

Another modification investigated is the introduction of a methyl group on the double bond to give compound **12**. This compound was synthesized according to Fig. 3.27. Initially the direct Knoevenagel condensation of intermediate **2a** with 3,4-dihydroxyacetophenone was tried but no reaction occurred. So, the condensation step was performed on 2,4-thiazolidinedione, affording intermediate **11**, which was then alkylated with ethyl bromoacetate under the usual S_N2 conditions affording the desired product **12**. In the primary SPR assay both compounds **10** and **12** did not show any binding affinity for BAG3. This means that a sort of reduced rotation is required, such as a double bond in the Z configuration, and the presence of substituents is not tolerated.

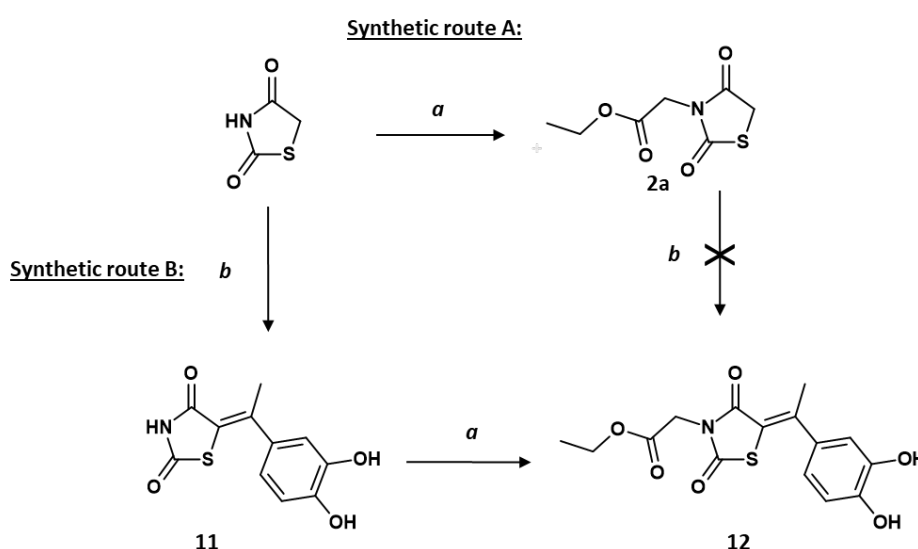


Figure 3.27: Structure and synthesis of compound **12**. Conditions: a) ethyl bromoacetate (1 eq.), potassium carbonate, (2 eq.) MeCN, 25 °C, 18 h; b) 3,4-dihydroxyacetophenone (1 eq.), piperazine (0.5 eq.), acetic acid (0.5 eq.), toluene, 100 °C, 18-36 h.

3c - Thiazolidinedione “core” replacement and exploratory derivatives

As part of the SAR exploration, the 2,4-thiazolidinedione core was replaced with alternative heterocycles, such as hydantoins, thiazole, and quinoline cores with the aim of obtaining a new series of compounds.

The hydantoin core, also called glycolylurea, presents a nitrogen in place of the sulphur atom of the thiazolidinedione core. Two derivatives were designed, the first one with the free NH, and the second one its N-methylated analogue. For their synthesis the following synthetic scheme was employed (Fig. 3.28). The first step is a S_N2 reaction on the hydantoin core with ethyl 2-bromopropanoate in the presence of potassium carbonate. The reaction was selective for the succinimide-like nitrogen affording the common intermediate **13** which was then condensed with the 3,4-dihydroxybenzaldehyde in the Knoevenagel conditions, to give **14**. Intermediate **13** was also methylated, in the presence of potassium carbonate and iodomethane, affording intermediate **15**, which was then condensed with 3,4-dihydroxybenzaldehyde, affording compound **16** as a 1:2 mixture of Z/E geometric isomers.

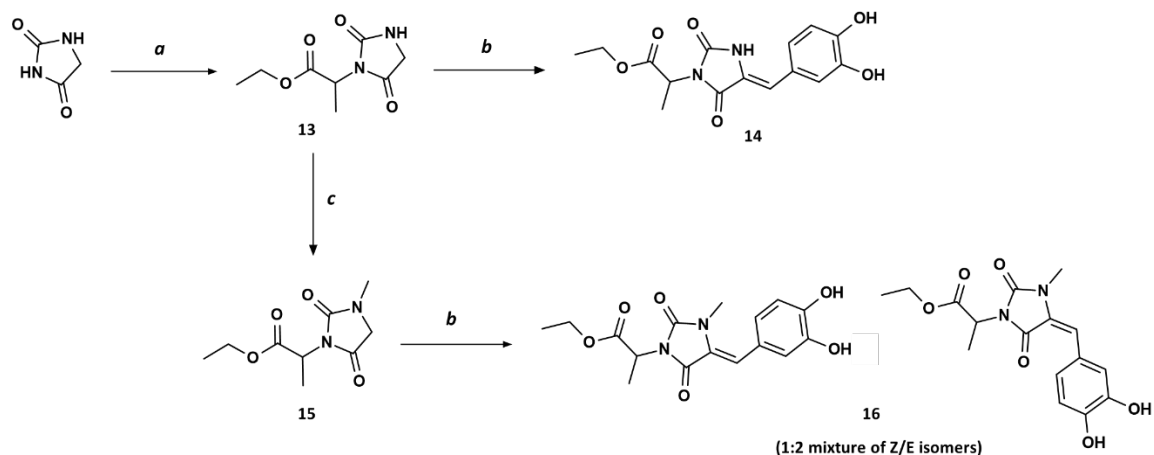


Figure 3.28: Synthesis of compounds **14** and **16**. Conditions: *a*) ethyl 2-bromopropanoate (1 eq.), potassium carbonate, (2 eq.), THF, 85 °C, 18 h; *b*) 3,4-dihydroxybenzaldehyde (1 eq.), piperazine (0.5 eq.), acetic acid (0.5 eq.), toluene, reflux, 18 h; *c*) Iodomethane (1.1 eq.), potassium carbonate (1 eq.), DMF, 25 °C, 18 h.

The thiazole derivative **17** (Fig. 3.29A) was designed as an aromatic replacement of the 2,4-thiazolidinedione core of compound **1a**. The double bond in position 5 was replaced by the oxygen of a phenoxy group and the catechol ring was replaced with a *para*-hydroxyphenyl group to reduce the electronic density of the aromatic ring.

As shown in the model reported in Fig. 3.29B the minimum energy conformation of this exploratory compound overlaps well with compound **1a**. The compound was synthesized in two steps starting from commercially available ethyl 2-aminothiazole-4-acetate (Fig. 3.30). The first step is the Sandmeyer bromination of the aminothiazole, affording intermediate **18**, which then reacts with 1,4-dihydroxybenzene in a nucleophilic aromatic substitution (S_NAr) reaction affording the desired compound **17**.

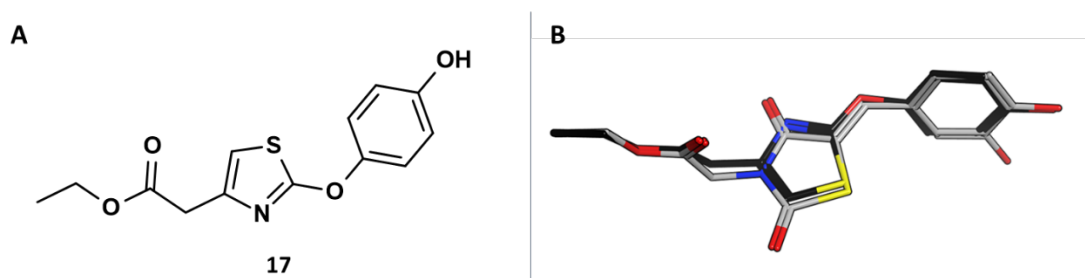


Figure 3.29: A, Structure of compound **17**. B, Minimum energy conformation of compound **17** (in black) and its superimposition with compound **1a** (in grey).

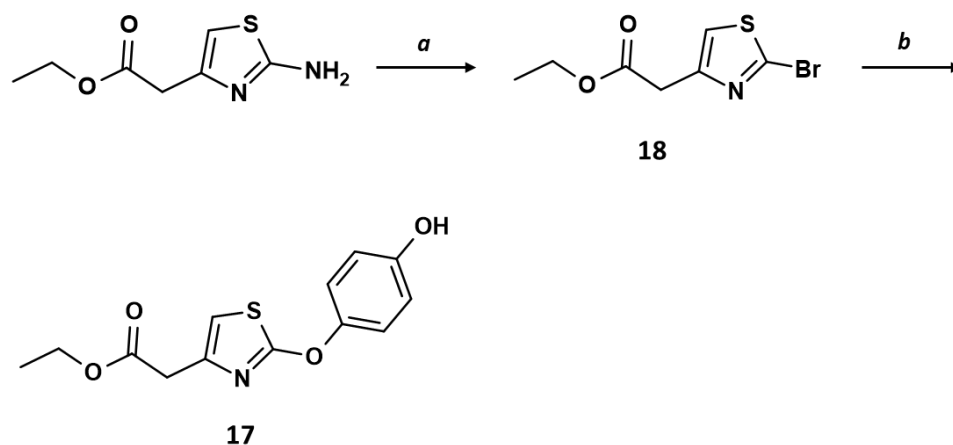


Figure 3.30: Synthesis of compounds **17**. Conditions: a) *t*-butyl nitrite (0.75 eq.), Copper (II) bromide (0.6 eq.), MeCN, 25 °C, 18 h; b) 1,4-dihydroxybenzene (1 eq.), potassium carbonate (1 eq.), DMF, 140 °C, 18 h.

Finally, also a few examples of (iso)quinoline derivatives were designed (Fig. 3.31). The superimposition of the calculated minimum energy conformation of these (iso)quinolines with compound **1a** showed a good overlapping although the quinoline derivative seems to remain flatter.

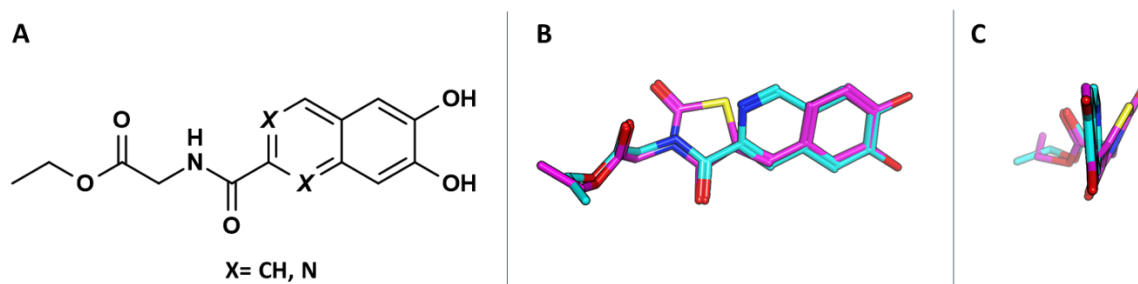


Figure 3.31: A, Structure of designed (iso)quinoline derivatives. B, C, Minimum energy conformation of a quinoline derivative (light blue) and its superimposition with compound **1a** (magenta).

The first quinoline derivative, compound **19**, was synthesized following the synthetic scheme reported in Fig. 3.32. The first step is the condensation of the aniline (3,4-dimethoxyaniline) and ethyl vinyl ether in the presence of a catalytic amount of iodine affording the 2-methylquinoline intermediate **20**. In this reaction, the iodine species acted with a dual behaviour: molecular iodine serves as an oxidant, while its reduced form, hydrogen iodide, activates the vinyl ether. The redox reaction between these iodine species enables the use of a catalytic amount of iodine in this synthetic method. A plausible mechanism for this reaction is reported in Fig. 3.33.⁶⁷ Then the methyl group of intermediate **20** was oxidized to a carboxylic acid in the presence of selenium dioxide, affording compound **21**. The two methoxy groups were then demethylated with hydrogen bromide affording **22** which was coupled with glycine ethyl ester in the presence of HATU and N,N-diisopropylethylamine (DIPEA) yielding compound **19**.

These four compounds were finally tested in the SPR assay at a single concentration of 50 μM (Fig. 3.34). Among this set of compounds only **17** showed a binding affinity for BAG3, but it was less than 5 RU. However, the compound was further characterized in the cell viability assay (Fig. 3.35) and resulted not to be cytotoxic in the four cancer cell lines tested, for this reason the compound was not characterized or pursued further.

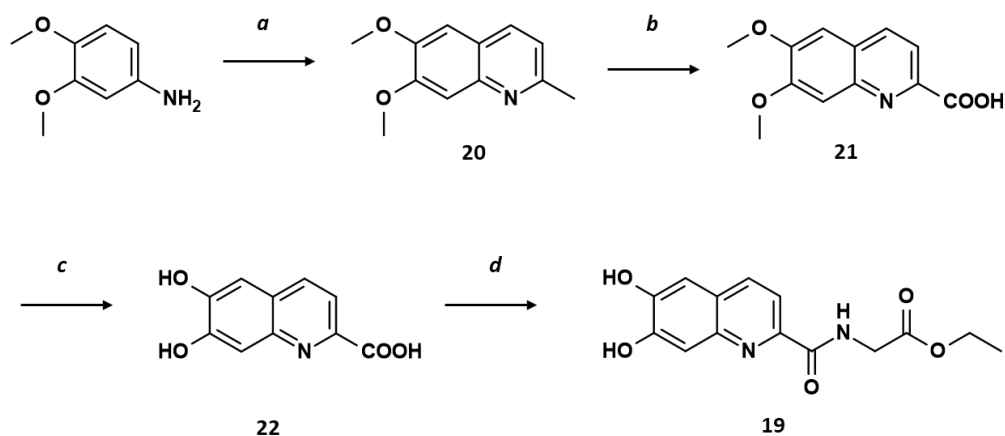


Figure 3.32: Synthesis of compound **19**. Conditions: a) ethyl vinyl ether (2eq.), iodine (0.05 eq.), dry toluene, 80 °C, 3 h; b) selenium dioxide (3 eq.), pyridine, 115 °C, 4 h; c) hydrogen bromide (48% w/w in water) (3 eq.), 120 °C, 2 days; d) Glycine ethyl ester hydrochloride (1 eq.), HATU (1 eq.), DIPEA (2 eq.), DMF, 25 °C, 1 h.

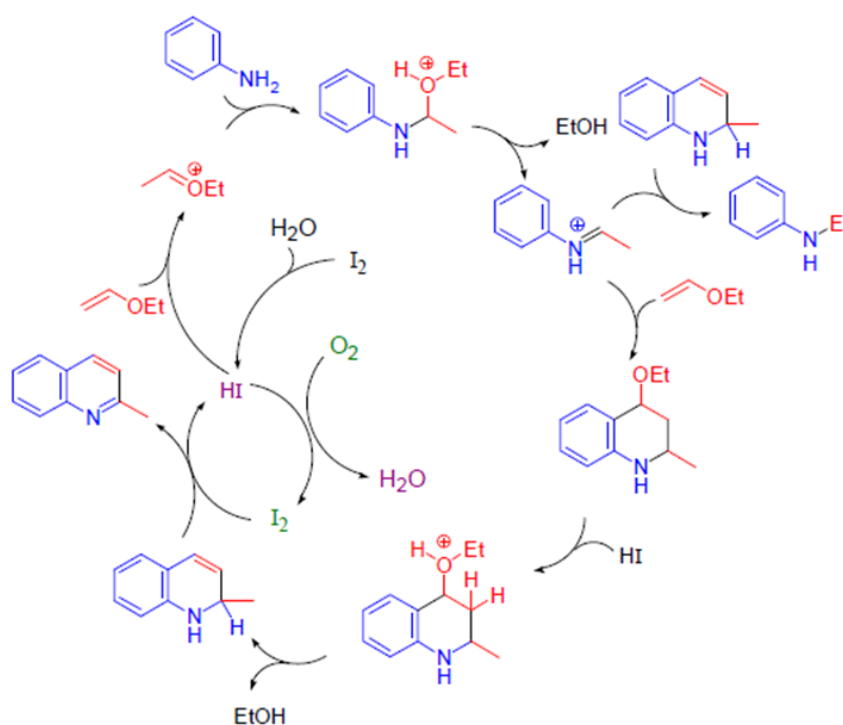


Figure 3.33: Proposed mechanism. At first, iodine generates a trace amount of hydrogen iodide by reacting with water present in the reaction mixture, initiating the reaction by activating the vinyl ether. Aniline attacks the activated vinyl group, leading to an *N,O*-acetal, from which ethanol is eliminated to afford the iminium intermediate. This iminium reacts with another molecule of vinyl ether followed by intramolecular cyclization to afford the tetrahydroquinoline. Dihydroquinoline is then obtained after ethanol elimination. Aromatization by molecular iodine affords the final quinoline. In this process, iodine is reduced to hydrogen iodide, which is then oxidized again to molecular iodine upon contact with air.⁶⁷

Compound	number of measurements	RU (media + SEM)
1a	16	8.8 ± 0.9
14	3	NB
16	3	NB
17	3	< 5
19	6	NB

Figure 3.34: *In vitro* SPR analysis of compounds **1a**, **14**, **16**, **17** and **19**. Compound **1a** was used as reference. New compounds were injected onto the BAG3-containing biosensor at the single concentration of 50 μ M and the analysis was repeated 3-6 times for each compound. NB = No Binding. SEM = Standard error of the mean.

Compound	IC ₅₀ (μ M)			
	HD-MB03	HD-MB03 R	RS4;11	A549
1a	14.82	68.75	6.39	42.49
17	>100	>100	>100	>100

Figure 3.35: *In vitro* inhibitory effects of compounds **1a** and **17**. Compound **1a** was used as reference. IC₅₀ = Half maximal inhibitory concentration; HD-MB03 human medulloblastoma cancer; HD-MB03 R human medulloblastoma cancer resistant; RS4;11 human acute leukemia; A549 human lung adenocarcinoma.

As described above, the primary *in vitro* SPR screening (performed at the single concentration of 50 μ M) identified 17 compounds that were able to bind BAG3. In detail, **1c**, **1r**, **5c**, **5e**, **5f**, **5l**, **5m** and **17** showed a very limited quantitative binding (below 5 RU). Instead, compounds **1f**, **1h**, **1l**, **1i**, **1j**, **1k**, **1q**, **5i** and **9** showed a higher binding capacity (> 8 RU) and were then subjected to further dose-dependent binding analysis to calculate the affinity of their interaction with BAG3. Increasing concentrations of each compound were injected onto the sensorchip and their K_d values (that are inversely proportional to the affinity of the interaction) were calculated (Fig. 3.36).

In the experimental conditions adopted, the interaction with surface-immobilized BAG3 was dose-dependent for all the compounds tested but it was saturable only for compound **9**. However, also with no clear saturation binding reached, the software embedded in the Biacore X100 instrument provided a K_d value expected on the basis of the curve's trend. The only exception is that of derivative **1i**, that binds BAG3 by following a convex binding isotherm, which is typical of unspecific low affinity interaction. This compound was not characterized further in the next *in vitro* assays. In other compounds, such as **1h**, **1j**, **1q** and **9**, the introduction of a substituent in the α -position of the ester group is tolerated. Instead, compound **1k**, which presents a bulky phenyl group in that position, showed a detrimental effect on the binding affinity for BAG3. The single enantiomer **1l** of compound **1h** showed a similar K_d value with respect to the racemate. The replacement of the catechol ring with its imidazole bioisostere **5i** and its 2,3-dihydroxybenzyl isomer **9** is well tolerated. The replacement of the ester group with the amides **1f**, **1q** and **9** had positive impact on the binding affinity. In agreement with its capacity to reach a saturation binding, **9** is the compound endowed with the highest BAG3 binding affinity (with a K_d that is 2-7 times lower than those of all the other compounds). This SPR analysis demonstrates that the best compounds from this work bind to BAG3 to a similar extent (**1h**, **1l**, **1j**, **1k**, **5i**), or even stronger than (**1f**, **1q** and **9**) the hit compound **1a** described by Terracciano *et al.*

Compound	Structure	BAG3 Kd ± SD (μM)
1a		233 ± 58
1f		152 ± 25
1h		286 ± 86
1i		ND
1j		204 ± 32
1k		366 ± 93
1l		270 ± 82
1q		150 ± 39
5i		198 ± 82
9		45 ± 6

Figure 3.36: *K_d* values of the interaction of the compounds **1a**, **f**, **h-l**, **q**, **5i** and **9** with sensorchip immobilized BAG3. *SD* = standard deviation. *ND* = Not Determined.

3d - *In vitro* cell viability assay of the most relevant BAG3 inhibitors

Compounds that showed a good binding affinity for BAG3 (> 8 RU) in the primary SPR assay were then evaluated for their *in vitro* antiproliferative activity against four different cancer cell lines known to overexpress BAG3: human medulloblastoma cancer (HD-MB03), human medulloblastoma cancer resistant to the VECC (Vincristine, Etoposide, Cisplatin and Cyclophosphamide) treatment (HD-MB03 R), human acute leukemia (RS4;11) and human lung adenocarcinoma (A549). The cell viability assays were performed in collaboration with Prof. Giampietro Viola (Dept. of Woman's and Child's Health, University of Padova, Italy). As mentioned above, compound **1i** was not characterized further due to its aspecific binding to BAG3. The inhibitory effects, expressed as IC_{50} values, of the entire set of compounds including the reference compound **1a** were in the micromolar range, with the best results shown by compound **9** (Fig. 3.37).

The IC_{50} values of compound **1a** are respectively: $14.8 \mu\text{M}$ in HD-MB03, $68.7 \mu\text{M}$ in HD-MB03 R, $6.4 \mu\text{M}$ in RS4;11 and $42.5 \mu\text{M}$ in A549. Compound **5i** was not cytotoxic on three out of four cancer cell lines ($IC_{50} > 100 \mu\text{M}$) and showed only a low inhibitory effect in the HD-MB03 with an IC_{50} of $42.5 \mu\text{M}$, so it was not further considered in the discussion.

Compared to reference compound **1a** ($IC_{50} = 14.8 \mu\text{M}$), similar IC_{50} values on HD-MB03 were detected for **1j** ($IC_{50} = 15.5 \mu\text{M}$), **1k** ($IC_{50} = 17.6 \mu\text{M}$), **1q** ($IC_{50} = 13.9 \mu\text{M}$) and **9** ($IC_{50} = 11.2 \mu\text{M}$) while the other compounds were less cytotoxic. Instead, all the compounds tested have an enhanced inhibitory effect on HD-MB03 R with respect to compound **1a** ($IC_{50} = 68.7 \mu\text{M}$), with the best results shown by **1k** ($IC_{50} = 17.5 \mu\text{M}$), **1j** ($IC_{50} = 20.5 \mu\text{M}$) and **9** ($IC_{50} = 18.2 \mu\text{M}$). Moreover, all the compounds tested showed a comparable cytotoxicity on the RS4;11 cells with IC_{50} values between 5 and $10 \mu\text{M}$ (except **1f**, which is less toxic than the reference **1a**). Compound **1f** ($IC_{50} = 49.4 \mu\text{M}$) showed a similar cytotoxicity on A549 cells with respect to the reference compound **1a** ($IC_{50} = 42.5 \mu\text{M}$), while the other compounds showed an improved inhibitory effect (IC_{50} values comprised in the range between 28 and $33 \mu\text{M}$).

Compound	IC ₅₀ (μM)			
	HD-MB03	HD-MB03 R	RS4;11	A549
1a	14.8	68.7	6.4	42.5
1f	33.1	34.6	24.8	49.4
1h	25.3	33.7	5.1	32.5
1j	15.5	20.5	6.8	28.1
1k	17.6	17.5	9.5	33.3
1l	21.2	34.9	7.0	29.9
1q	13.9	55.0	8.6	29.4
5i	42.5	>100	>100	>100
9	11.2	18.2	6.7	28.0

Figure 3.37: *in vitro* antiproliferative effects of compounds **1a**, **f**, **h**, **j-l**, **q**, **5i** and **9** in four different cancer cell lines: human medulloblastoma cancer (HD-MB03), human medulloblastoma cancer resistant to the VECC treatment (HD-MB03 R), human acute leukemia (RS4;11) and human lung adenocarcinoma (A549). VECC treatment is unable to induce expression of membrane pumps. Cell viability was evaluated by resazurin assay after 72h of treatment. The percentages of cell viability were normalized to untreated cells. Data are represented as the means ± SEM of at least three independent experiments. IC₅₀ = Half maximal inhibitory concentration.

3e - *In vitro* synergistic studies on HD-MB03 R cells

As discussed, this series of 2,4-thiazolidinedione scaffold-based molecules did not demonstrate high cytotoxicity on the cancer cell lines tested but as BAG3 overexpression is involved in drug resistance mechanisms, it was hypothesized that these compounds could be used in combination with consolidated anticancer drugs to overcome the drug resistance phenomena in resistant cancer cells and to restore their cytotoxicity with a synergistic effect. These *in vitro* synergistic studies were performed in collaboration with Prof. Giampietro Viola (Dept. of Woman's and Child's Health, University of Padova, Italy).

The efficacy of the most relevant BAG3 binders identified by SPR was evaluated in combination with the chemotherapy VECC (Vincristine, Etoposide, Cisplatin and Cyclophosphamide) treatment on HD-MB03 VECC resistant cells (HD-MB03 R). Compound **4g** (that did not bind to BAG3 according to SPR data), was selected as negative control. According to the reported non-cytotoxicity of BAG3 inhibitors ($IC_{50} > 10 \mu\text{M}$), HD-MB03 R cells were treated with a fixed dose of the selected BAG3 inhibitors ($10 \mu\text{M}$) and scalar dilution of VECC. From this cell viability assay it emerged that compounds **1d**, **1h**, **1j**, **1k** and **1l** have a strong synergistic effect with chemotherapy on this *in vitro* MB resistant cell model (Fig. 3.38). A similar synergistic effect was observed also with the reference compound **1a**. Compound **1f** did not show any synergistic effect and further investigations are ongoing to understand this behaviour. As expected, compound **4g** did not show any relevant synergistic effect in reducing HD-MB03 VECC resistant cell viability (Fig 3.38). These data support the hypothesis that the specific inhibition of BAG3 may impact tumor chemotherapy resistance. Compound **9** and its ethyl ester derivatives **5n** and **5o**, are still under evaluation for they synergistic effects and the data will be published as soon as they will be available.

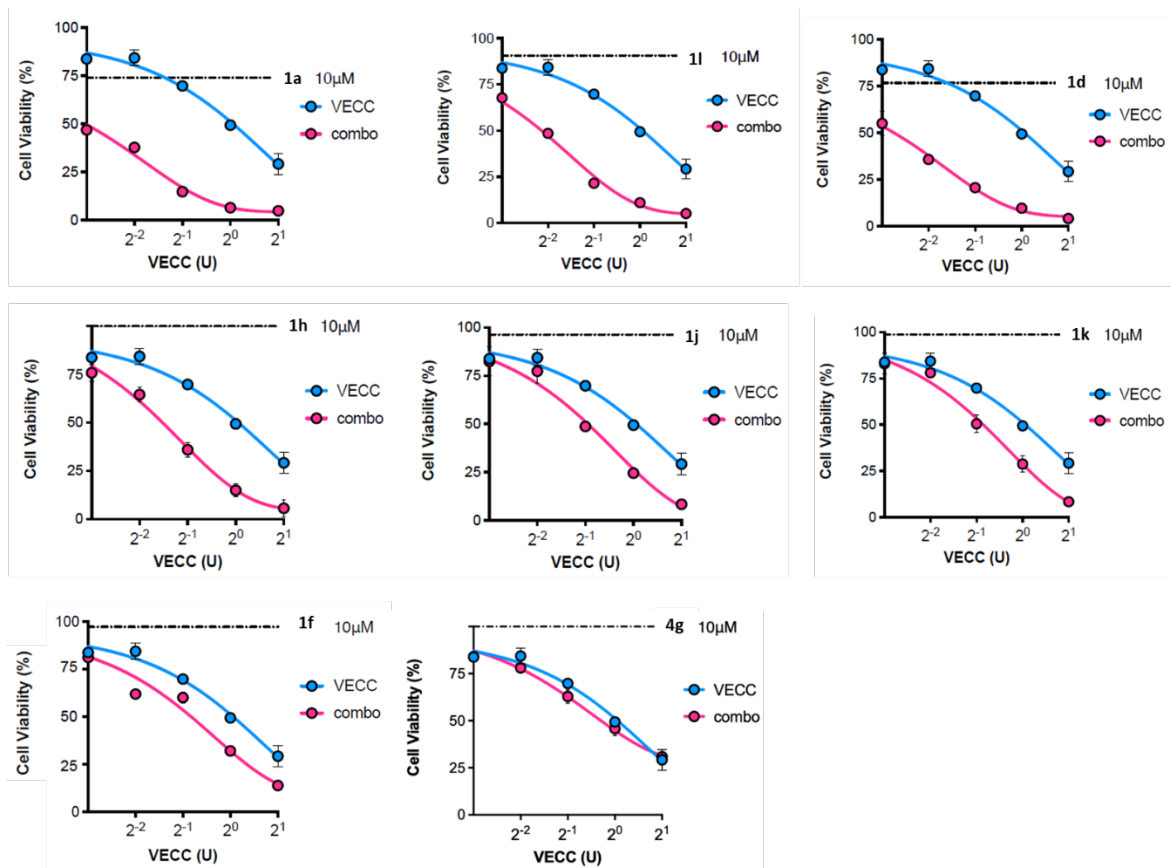


Figure 3.38: Putative BAG3 inhibitors/VECC combination in HD-MB R cell lines. Cell viability was evaluated by resazurin assay after 72h of treatment. Cells were treated for 72 h with a fixed dose of BAG3 putative inhibitor in combination with scalar dilutions of VECC. The percentages of cell viability were normalized to untreated cells. Data are represented as the means \pm SEM of at least three independent experiments. The blue dotted line indicates the effect on cell viability induced by VECC single treatment. The red dotted line indicates the effect on cell viability induced by a specific BAG3 inhibitor in combination with VECC treatment.

3f - PROTACs

PROTAC is an emerging novel technology for the development of small-molecule therapeutics that can induce the degradation of abnormally expressed disease-associated proteins. As mentioned above, in the current work PROTAC technology was used to circumvent some limitations of the available 2,4-thiazolidinedione series, namely their weak binding affinity for BAG3 (in the micromolar range) and low cytotoxicity. As PROTACs present a catalytic mechanism of action and do not require a ligand with a high binding affinity for the target protein, this technology resulted particularly advantageous for these purposes. In the absence of an X-ray crystal structure of human BAG3 (either alone or with its co-chaperone), the SAR studies performed on the 2,4-thiazolidinedione series were used to formulate hypotheses of the regions of the structure suitable for use as the linker attachment point.

The SAR exploration on the 5 position of the 2,4-thiazolidinedione series demonstrated that, in general, catechol ring replacement is not tolerated, and two hydroxy groups must be present to retain the binding affinity. Moreover, all the changes on the 2,4-thiazolidinedione 'core' resulted to be detrimental for binding affinity. The 3 position is the only region where some modifications, such as the introduction of a morpholine or piperidine, are tolerated. Due to these results the 3 position was selected as the linker attachment point. The BAG3 ligand should also have a suitable functional group that can be exploited as attachment point for the linker, therefore a secondary amine or a ketone, was introduced in the devised region. As discussed in chapter 1i, PEG chains are the most common motifs incorporated into PROTACs and they were selected as linker motifs for this application because they allow modulation of important physical properties such as PSA and lipophilicity which in turn have implications on solubility and cell permeability. Flexibility can also be crucial to identify a potent compound because greater flexibility can allow the compound to adopt suitable conformations for productive ternary complex formation- accordingly, different linker lengths were selected (PEG2-PEG4) in this work. The designed PROTACs must have a certain permeability to be able to enter into the cell. In order to do so, their PSA should be lower than 260 and their molecular weight (MW) less than 1000 Da and the HBD count should be kept to the minimum possible. Cereblon (CRBN) and Von Hippel-Lindau (VHL) were selected as target E3 ubiquitin ligases because they are usually found overexpressed in different tumor types.⁶⁸ Considering all these factors, three PROTACs were designed, as reported in Fig. 3.39.

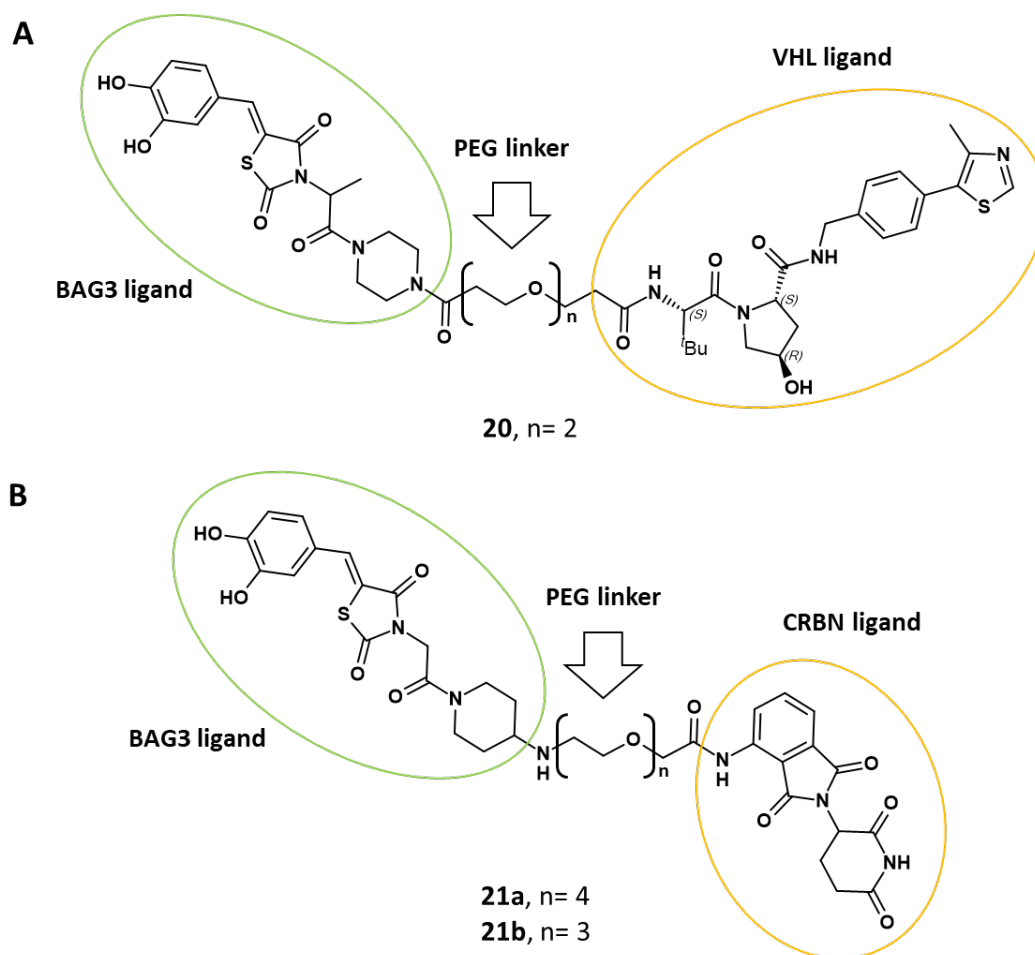


Figure 3.39: PROTACs designed.

The first PROTAC synthesized, compound **20** (Fig. 3.39A), has a built-in high-affinity feature VH032 ($K_d = 185$ nM) which allows recruitment of the VHL E3 ligase and a piperazine derivative of the herein described compound **1q** ($K_d = 150 \pm 39$ μ M) as BAG3 ligand. The replacement of the piperidine with piperazine was necessary to have a linker attachment point for the PEG2 linker. The MW (963.35) and PSA (248.55) of compound **20** fulfil the requirements for permeability (data calculated with Marvin Sketch).

The other two PROTACs, **21a** and **21b** (Fig. 3.39B), exploit the pomalidomide ($K_d \sim 157$ nM), a thalidomide derivative, to recruit the E3 Ligase CRBN. Although thalidomide is notorious for its teratogenic effect in infants when the drug was prescribed to pregnant women for relieving pregnancy nausea, in recent years it has been experiencing a revival of sorts. In fact, after being withdrawn from the market, thalidomide and its analogues were found to possess multiple other functions, such as antiinflammation, anti-angiogenesis, and immune modulation and after years of carefully designed clinical trials they were approved as immunomodulatory drugs (IMiDs) for the treatment of multiple myeloma. However, their

molecular target and the MoA of their anticancer effect were discovered years later and CRBN, a component of the E3 complex, was identified as the cellular target of the IMiDs. Based on these findings, thalidomide and its analogues (Fig. 3.40) are now widely used as ligands of CRBN for the design of bifunctional PROTACs.^{69,70} Those ligands share some advantages, such as the specific and strong binding affinity for CRBN, acceptable physicochemical characteristics (such as molecular weight, solubility, lipophilicity, lack of metabolic hot spots) and permeability.⁷¹

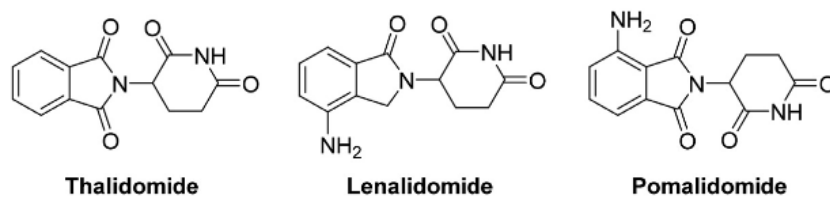


Fig. 3.40: Representative small-molecule ligands of E3 ligase used for CRBN PROTACs.

PROTACs **21a** and **21b** are derivatives of compound **1f**, a BAG3 ligand, where instead of the morpholine, a piperidone was introduced to provide a ketone group for the linker attachment point. The MW of PROTAC **21b** is 822.25 and its PSA is 250.52 while the MW of PROTAC **21a** is 866.28 and its PSA is 259.75 (data calculated with Marvin Sketch). These data suggest the achievement of an acceptable permeability. However, all the PROTACs herein described present from four to five HBD, this elevated number of HBD could negatively affect the PROTACs permeability.

The Synple Chem technology was used for the synthesis of these three PROTACs. It consists of an automated synthesizer that uses pre-packed cartridges containing all the reagents needed for the reactions of interest and a chip containing the method for the synthesis. The use of Synple Chem proved to be particularly advantageous as cartridges containing the ligands for the E3 ligase enzyme (VHL or CRBN) already connected with PEG chains are commercially available. The cartridges and methods supplied with the Synple Chem synthesizer therefore allowed preparation of the designed PROTACs in an automated fashion, reducing the number of steps and the time required in comparison to an exclusively traditional synthesis. It also avoids the need to manipulate difficult-to-manage intermediates thanks to the support on solid phase.

The first synthetic route developed to obtain compound **20** is reported in Fig. 3.41 and was designed with the aim to use the Synple Chem technology at the end of the synthesis, to perform an amide coupling between the advanced intermediate **26** and the partial PROTAC in the form of a 2,3,5,6-tetrafluorophenyl ester (Fig. 3.42) contained in the cartridge (P062-PEG2-AE-VHL).

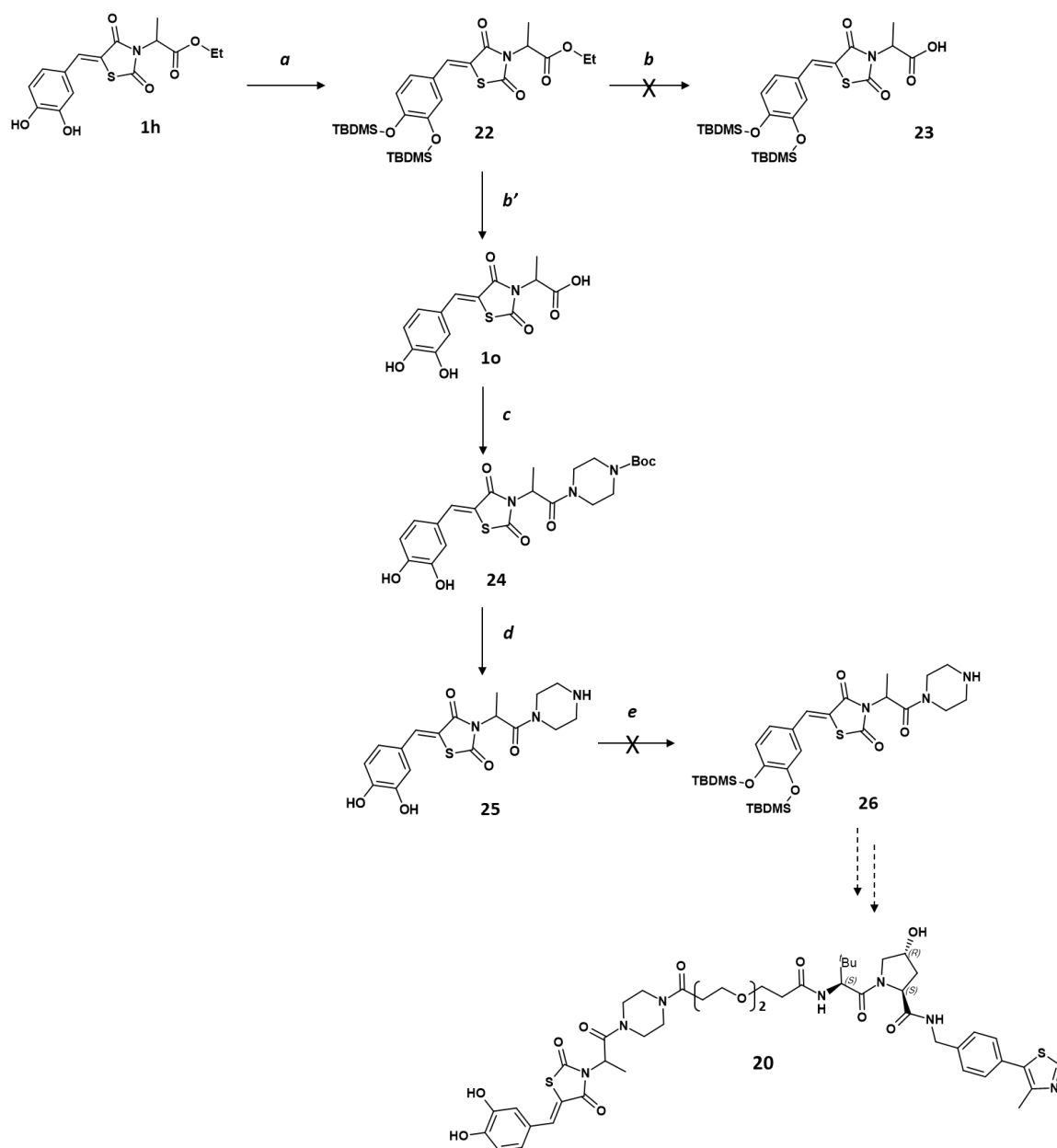


Fig. 3.41: First synthetic route developed for the synthesis of compound **20**. Conditions: a) *N,N*-dimethyl-4-pyridinamine (0.1 eq.), TEA (2.5 eq.), tert-butyldimethylchlorosilane (2.5 eq.), dry DMF, 25 °C, 1 h; b) lithium hydroxide hydrate (or sodium hydroxide) (1 eq.), H₂O/THF 1:1, 25 °C, 1 h; b') 12 M hydrochloric acid (22 eq.), acetic acid, 100 °C, 2 h; c) 1-Boc-piperazine (1 eq.), HATU (1 eq.), DIPEA (2 eq.), 0 °C → 25 °C, 1 h; d) TFA/DCM 1:1, 25 °C, 1 h; e) *N,N*-dimethyl-4-pyridinamine (0.1 eq.), TEA (3.5 eq.), tert-butyldimethylchlorosilane (2.5 eq.), dry DMF, 25 °C, 1 h.

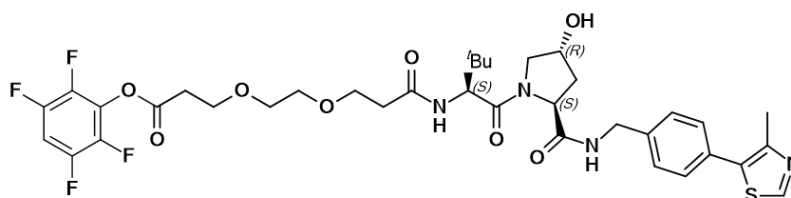


Fig. 3.42: The partial PROTAC in the form of a 2,3,5,6-tetrafluorophenyl ester.

Some chemistry-limitations, related to the use of this cartridge and the method for the synthesis of PROTACs by amide bond formation, include:

- Scale (up to 0.1 mmol).
- Solvents (protic solvents are not suitable for this reaction since they will react with the partial PROTAC reagent to give the correspondent ester. The amine starting material must be soluble in DCM and needs to be converted to its free-base before the reaction).
- Acidic functional groups (will cause the product to be retained by the resin in the purification step. Some phenols also be partially or completely trapped).

Starting from the previously described compound **1h**, the first step of this synthesis required the protection of the catechol ring to mask the acidity of its phenol groups. Tert-butyldimethylchlorosilane was used as protecting agent, affording intermediate **22**.

Several attempts to perform the hydrolysis of the ester group under basic conditions (LiOH and NaOH) were performed without success. Although basic conditions would have been more convenient, as the protecting groups would have been retained, the hydrolysis had to be performed in acid conditions. The reaction worked well but as expected it also caused the deprotection of the catechol ring, affording compound **1o**. With the intention of reprotecting the catechol ring before the PROTAC coupling, this carboxylic acid was used to perform the following amide coupling with 1-Boc-piperazine, in the presence of HATU and DIPEA, giving compound **24**, which was Boc-deprotected with trifluoroacetic acid (TFA) giving intermediate **25**. An attempt to protect the catechol ring of **25** with tert-butyldimethylchlorosilane was made, but the protecting groups were found to be highly labile on this catechol moiety and deprotection occurred during the work-up of the reaction. This synthetic route was therefore abandoned.

Subsequently, another synthetic route was developed for the synthesis of compound **20** (Fig. 3.43), where the first step is an amide coupling performed with the Synple Chem technology using a cartridge which contains the partial PROTAC in the form of a 2,3,5,6-tetrafluorophenyl ester (Fig. 3.42). Such an activated ester readily reacts with the secondary amine of 1-Boc-piperazine to form an amide bond. 1-Boc-piperazine was selected as starting

material for the first reaction because it fit well with the chemistry limitations related to the use of the Synple Chem cartridge and method (it was an amine commercially available as its free-base, it is soluble in DCM and does not present any acidic functionality). The first step worked well, affording intermediate **27** in acceptable yield (36%), which was then Boc-deprotected in the presence of trifluoroacetic acid to give intermediate **28** as a trifluoroacetate salt. Finally, **28** was reacted with compound **1o** in an amide coupling, in the presence of HATU and DIPEA, to afford the desired product **20**.

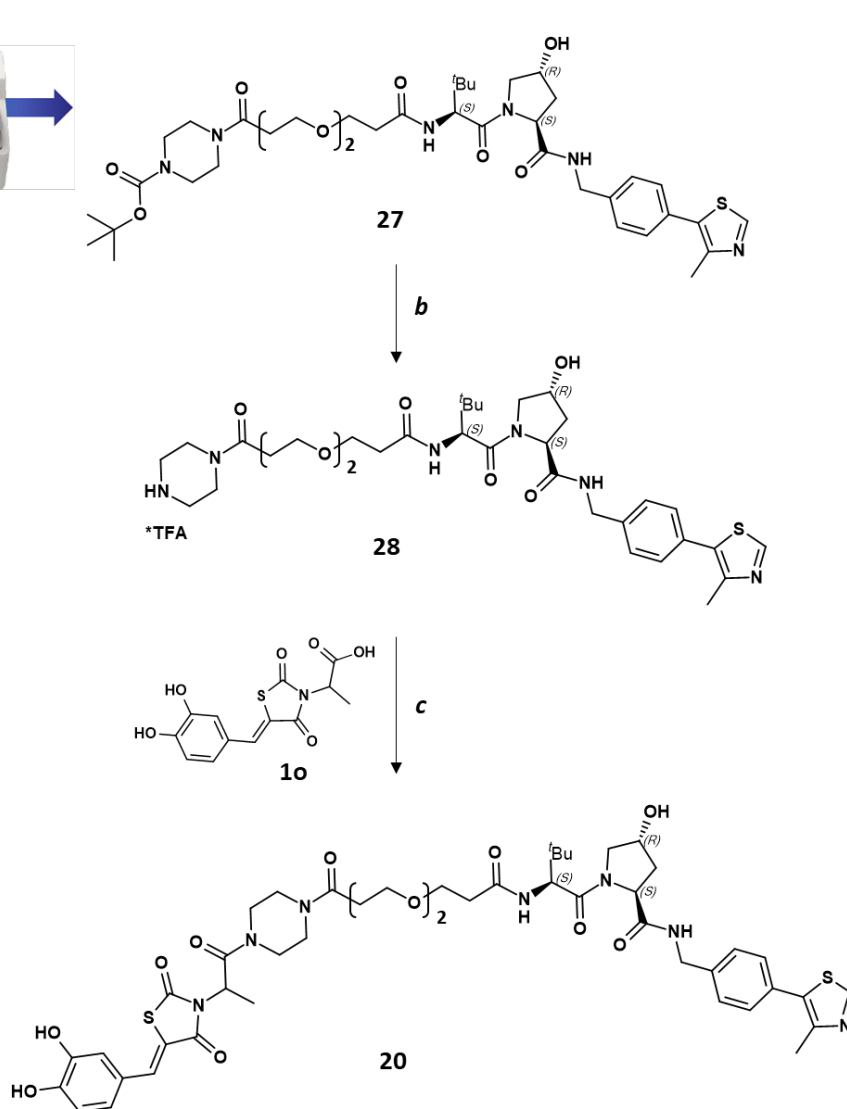


Fig. 3.43: Synthesis of compound **20**. Conditions: a) Synple Chem console, cartridge P062-PEG2-AE-VHL, dry DCM, 25 °C; b) TFA/dry DCM 1:1, 0 °C → 25 °C, 1 h; c) Compound **1o** (1 eq.), HATU (1 eq.), DIPEA (2.5 eq.), dry DMF, 0 °C → 25 °C, 4 h.

For the synthesis of compounds **21a** and **21b**, a different synthetic approach was considered as alternative PROTAC cartridges were available for the Synple Chem. The first synthetic route developed to obtain compound **21a** is reported in Fig. 3.44. The route was designed with the aim to use the Synple Chem technology at the beginning of the synthesis, to perform a reductive amination between N-Boc-4-piperidone and the partial PROTAC in the form of an amine salt (Fig. 3.45) contained in the cartridge (P004-CRBN-PEG4).

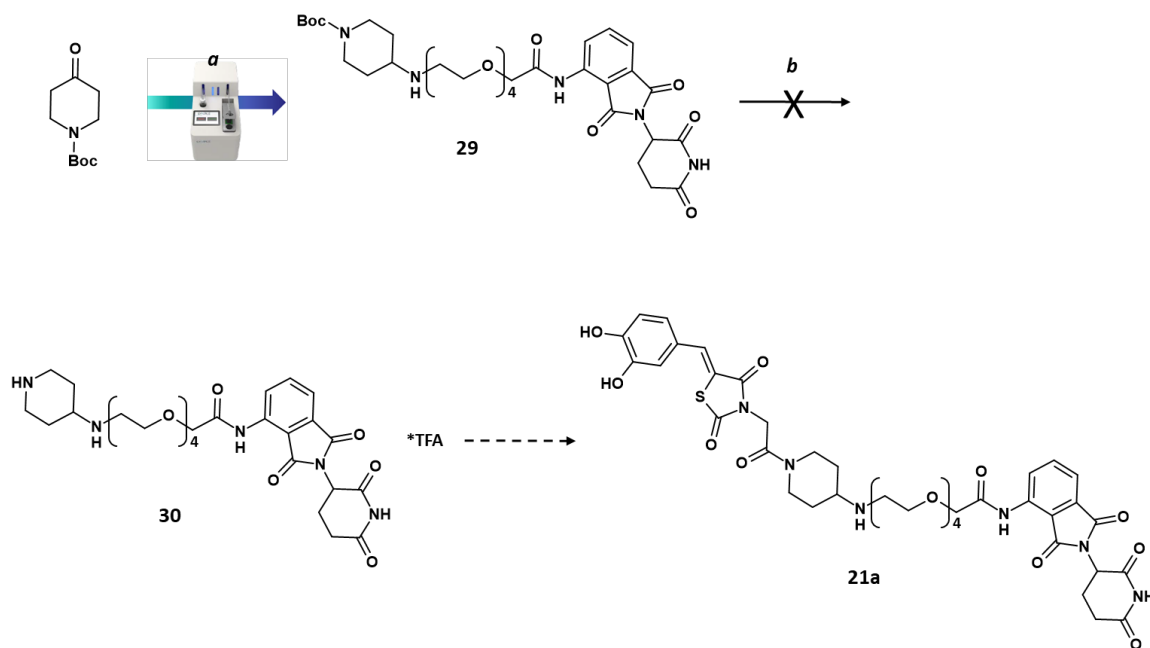


Fig. 3.44: First synthetic route performed for the synthesis of compound **21a**. Conditions: a) Synple Chem console, cartridge P004-CRBN-PEG4, dry DCM/hexafluoro-2-propanol 3:1, 25 °C; b) TFA/dry DCM 1:1, 0 °C → 25 °C, 1 h.

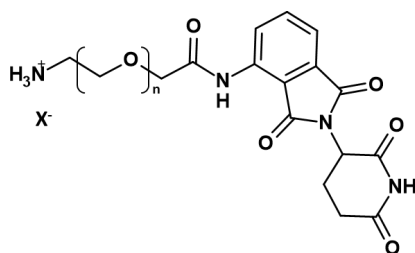


Fig. 3.45: partial PROTAC in the form of an amine salt.

Some chemistry-limitations, related to the use of this cartridge and the method for the synthesis of PROTACs by reductive amination, include:

- Scale (up to 0.1 mmol).
- Solubility (the starting material must be soluble in the 3:1 mixture of dichloromethane/hexafluoro-2-propanol. Insoluble starting material will lead to no, or low, conversion).

- Boc deprotection: a certain extent of Boc deprotection occurred in rare cases when Boc containing starting materials are employed. This can be avoided by disabling the SCX purification step.
- Stability of CRBN ligand (CRBN ligand is not stable in MeOH at 40°C, with a half-life of ~ 30 min. The by-product formation occurred by imide opening).

As the starting material (N-Boc-4-piperidone) fit well with all these criteria, the first reaction worked and intermediate **29** was obtained as a mixture with its Boc-deprotected derivative. To obtain compound **30**, this mixture was subjected to a deprotection step with trifluoroacetic acid, but the reaction presented a dirty profile and was abandoned.

Another synthetic route was therefore developed for the synthesis of compound **21a** (Fig. 3.46).

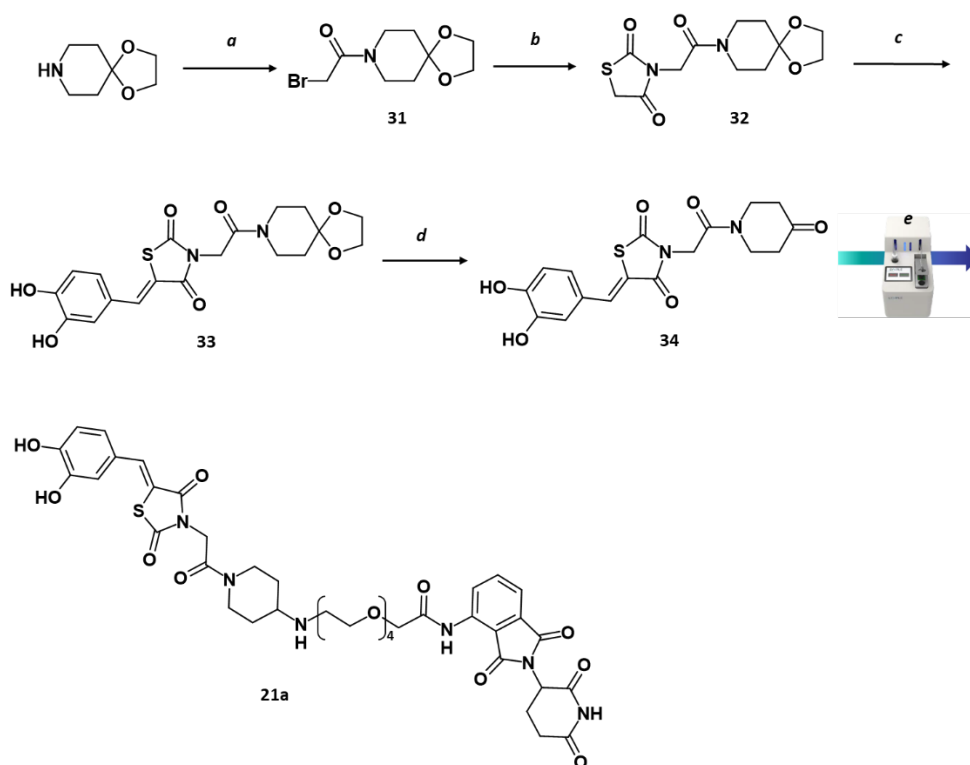


Fig. 3.46: Second synthetic route for the synthesis of compound **21a**. Conditions: a) 2-Bromoacetyl bromide (1.2 eq.), potassium carbonate (1.5 eq.), DCM, water, 25 °C, 18 h; b) 2,4-thiazolidinedione (1 eq.), potassium carbonate (2 eq.), MeCN, 25 °C, 18 h; c) 3,4-dihydroxybenzaldehyde (1 eq.), piperidine (0.5 eq.), ethanol, reflux, 8 h; d) 6 M hydrochloric acid, MeCN, 80 °C, 4 h; e) Synple Chem console, cartridge P004-CRBN-PEG4, dry DCM/hexafluoro-2-propanol 3:1, 25 °C.

Starting from the 1,4-dioxaspiro[4.5]decane, the first reaction was the acylation of the piperidine nitrogen with 2-bromoacetyl bromide, affording compound **31** which was then subjected to a S_N2 reaction with 2,4-thiazolidinedione. Intermediate **32** was condensed with

3,4-dihydroxybenzaldehyde in Knoevenagel conditions and then the acetal protecting group of compound **33** was removed in the presence of 6 M hydrochloric acidic solution, affording the ketone **34**. Finally, this intermediate was used to perform the reductive amination on the Synple Chem console using the P004-CRBN-PEG4 cartridge. The reaction worked well, affording the desired compound **21a** in acceptable yield (17 %).

Compound **34** was also a common intermediate for the synthesis of compound **21b**, where a P003-CRBN-PEG3 cartridge was used to perform the reductive amination, as reported in Fig. 3.47. Also, in this case the reaction worked well affording the final PROTAC **21b** in acceptable yield (33%).

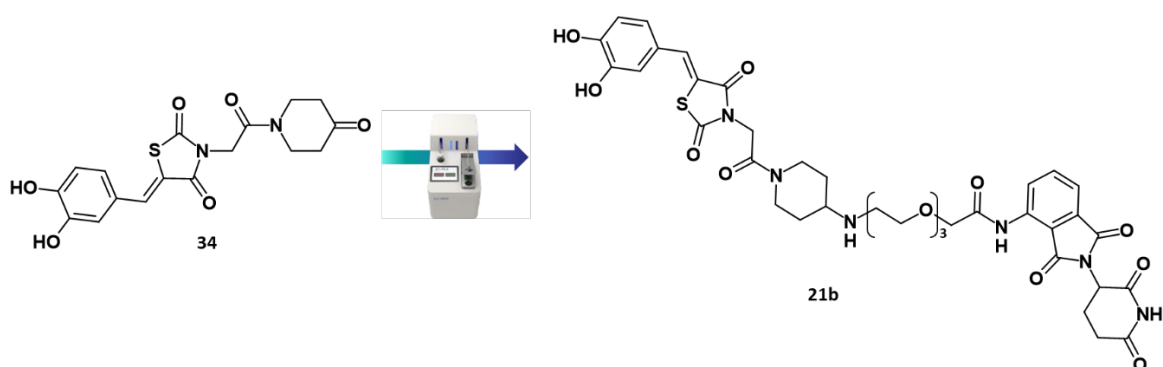


Fig. 3.47: Synthesis of compound **21b**. Conditions: Synple Chem console, cartridge P003-CRBN-PEG3, dry dichloromethane/hexafluoro-2-propanol 3:1, 25 °C.

The three PROTACs were then evaluated for their *in vitro* inhibitory effects on four cancer cell lines but none of them showed any cytotoxicity (Fig. 3.48).

Compound	IC ₅₀ (μM)			
	HD-MB03	HD-MB03 R	RS4;11	A549
20	>100	>100	>100	>100
21a	>100	>100	>100	>100
21b	>100	>100	>100	>100

Figure 3.48: *in vitro* inhibitory effects of compounds **20** and **21a,b** in four different cancer cell lines. IC₅₀ = compound concentration required to inhibit tumor cells proliferation by 50%; HD-MB03 human medulloblastoma cancer; HD-MB03 R human medulloblastoma cancer resistant; RS4;11 human acute leukemia; A549 human lung adenocarcinoma.

The PROTACs were then tested in cell culture by either Western Blot assay (Fig. 3.49) or Immunofluorescence (IFS) analysis (Fig. 3.50) to verify their efficacy in terms of BAG3 protein degradation. Western Blot is a technique that allows the identification of a specific protein in a mixture of proteins extracted from cells or tissues, through the recognition by specific antibodies. To facilitate that recognition, the protein mixture is first separated according to size (or MW) using gel electrophoresis. Subsequently, the recognition of the protein is carried out using a specific antibody. The VHL-based PROTAC (**20**) was incubated with Reed-Sternberg (RS) cells for 24 h at decreasing dilution 1:2 from 50 μM. As determined by Western Blot, no significant reduction in the level of BAG3 was observed.

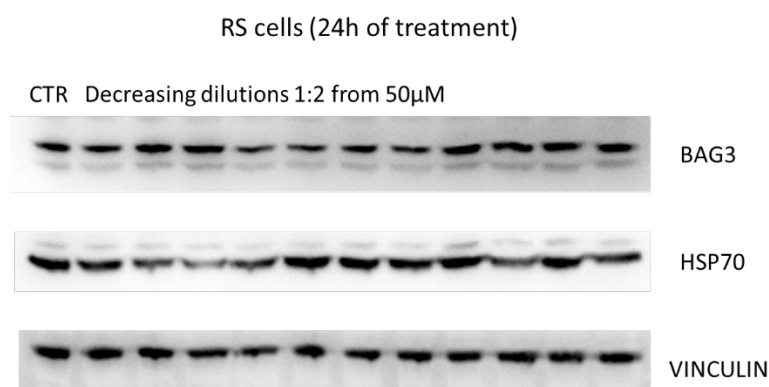


Fig. 3.49: Western Blot analysis of BAG3 protein levels in RS cells. The VHL-based PROTAC (**20**) was incubated with RS cells for 24h at decreasing dilution 1:2 from 50 μM.

IFS is a technique used to identify, in a tissue or cellular context, the presence of specific antigens, using the respective antibodies that are rendered fluorescent with a fluorochrome (such as fluorescein, a dye which under the action of ultraviolet rays emits green light). The CRBN-based PROTACs **21a** and **21b** were incubated with HD-MB cells for 48 h at a single concentration of 50 μ M. As determined by immunoblot assay, no degradation of BAG3 was observed compared to the control (Fig. 3.50).

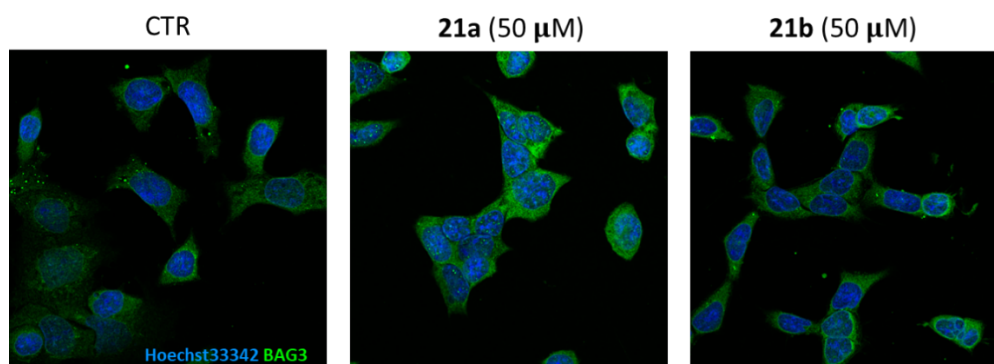


Fig. 3.50: CRBN-based PROTACs **21a** and **21b** incubated with HD-MB cells for 48 h at 50 μ M.

4. CONCLUSIONS AND FUTURE PLANS

BAG3 and HSP70 are stress-inducible proteins that are required for cancer development at several steps and they are frequently found overexpressed in tumour cells.

BAG3 overexpression contributes to apoptosis escape by promoting cancer cell survival signalling in complex with HSP70.

Starting from compound **1a** (Terracciano *et al.*⁴⁷), which can selectively bind the ‘BAG domain’ of BAG3, and applying different consolidated medicinal chemistry strategies (e.g., point substitutions, cyclization and bioisosteric replacements) a set of small molecules has been successfully synthesized. These derivatives have been tested in the primary *in vitro* screenings to analyse their BAG3 binding affinity by means of a SPR assay, generating a SAR which led to the identification of compounds **1f** and **9**. These compounds are endowed with the highest binding capacity (> 10 RU), indeed they display higher affinity than the reference compound **1a**. In both compounds introduction of the morpholine amide in place of the ethyl ester group has a beneficial impact on the binding affinity. Moreover, in compound **9** the introduction of a substituent in the α -position of the amide group and replacement of the catechol ring with its 2,3-dihydroxybenzyl isomer are well tolerated. The compounds with intermediate-to-high BAG3-binding capacity were subjected to additional concentration-dependent binding screening to calculate the affinity of their interaction with BAG3. This SPR analysis demonstrated that the best compounds from this work bind to BAG3 to a similar extent (**1h**, **1l**, **1j**, **1k**, **5i**), or even stronger than (**1f**, **1q** and **9**) the hit compound **1a** described by Terracciano *et al.* (Fig. 3.36).

The most effective compounds have also been evaluated for their antiproliferative activity on four different cancer cell lines, showing IC₅₀ values in the micromolar range (Fig. 3.37), with the best results displayed by compound **9**. These compounds will also be tested on peripheral blood mononuclear cells (PBMC) to ensure their non-cytotoxicity on non-tumoral cells. Finally, the efficacy of some of the most relevant BAG3 binders was analysed in combination with VECC chemotherapy on HD-MB03 resistant cells. From this cell viability assay it emerged that **1h**, **1l**, **1j** and **1k** have a strong synergistic effect with VECC chemotherapy (Fig. 3.38). These data support the hypotheses that the specific inhibition of BAG3 may impact tumor chemotherapy resistance. Further studies are still ongoing with the last compounds synthesized, such as compound **9** and its derivatives, to verify if they could display a synergistic effect. Since the effect of BAG3 on cell survival is partially mediated

by the interaction with HSP70, also the influence of these compounds on the BAG3-HSP70 PPI will be object of further investigations. The results of these studies will be published as soon as they are available.

Finally, a PROTAC strategy has been successfully applied to the BAG3 ligands and three PROTACs were designed and synthesized. PROTACs are small-molecules able to induce the degradation of abnormally expressed disease-associated proteins. This emerging technology was used to try to circumvent some limitations of the 2,4-thiazolidinedione series, namely their weak binding affinity for BAG3 and low cytotoxicity. Although these PROTACs did not show significant effects in the primary assays, further studies in this field are still ongoing to verify their efficacy and the results will be published as soon as they are available.

5. EXPERIMENTAL PROCEDURES

Materials and methods

All the reagents and solvents were obtained from commercial sources and used as supplied. The Synple Chem console with the appropriate cartridges (which contain the desired reagents) were employed for the automated steps in PROTAC synthesis and the reactions were performed under N₂ with anhydrous conditions.

¹H nuclear magnetic resonance (NMR) spectroscopy was carried out using one of the following instruments: a Bruker Avance 400 or a Bruker Avance III 400. The spectra were acquired in the stated solvent at around room temperature (unless otherwise stated), and chemical shifts (δ) are reported in parts per million (ppm) relative to the residual solvent peak. In all cases, NMR data were consistent with the proposed structures.

Characteristic chemical shifts (δ) are given in ppm using conventional abbreviations for designation of major peaks: e.g., s, singlet; d, doublet; t, triplet; q, quartet; dd, doublet of doublets; dt, doublet of triplets; and br, broad.

When thin layer chromatography (TLC) has been used it refers to silica gel TLC using Merck precoated aluminum-backed silica gel 60 F₂₅₄ plates with UV at 254 nm. TLC plates were stained using KMnO₄.

Column chromatography purifications were performed using an automatic flash chromatography (FC) system (Biotage SP1 or Isolera) over Biotage Sfär KP-Amino D 50 μ m cartridges or Biotage Sfär Silica D 60 μ m 100 Å cartridges. Reversed phase flash chromatography purifications were performed using Biotage Sfär C18 D 30 μ m 100 Å cartridges.

Chromatography purifications were also performed by preparative TLC plates on PLC silica gel 60 F₂₅₄ 0.5 mm (20 x 20 cm) plates (Merck).

Liquid Chromatography-Mass Spectrometry (LC-MS): Total ion current (TIC) and diode-array detector (DAD) UV chromatographic traces together with MS and UV spectra associated with the peaks were taken on an UPLC/MS Acquity™ system equipped with a photodiode array (PDA) detector and coupled to a Waters single quadrupole mass spectrometer operating in alternated positive and negative electrospray ionization mode. Compound UPLC/MS retention times (R_t) were obtained using the following methods.

Method A: Acquity UPLC CSH C18 column (50 mm × 2.1 mm, 1.7 μm particle size) at 40 °C, a linear gradient from 3 to 100% B over 2 min [A = 0.1% v/v solution of HCOOH in water, B = 0.1% v/v solution of HCOOH in acetonitrile (MeCN)] and a flow rate of 0.9 mL/min.

Method B: Acquity UPLC Peptide BEH C18 column (50 mm × 2.1 mm, 1.7 μm particle size) at 40 °C, a linear gradient from 3 to 60% B over 4 min [A = 0.05% v/v solution of TFA in water, B = 0.05% v/v solution of TFA in MeCN] and a flow rate of 0.7 mL/min.

LC-MS was used for monitoring the reactions and for the characterization of intermediates and final compounds.

When high-performance liquid chromatography (HPLC) purification was performed, compounds were purified using a semipreparative MDAP Fractionlynx (Waters) equipped with a mass spectrometry detector (MS: ZQ2000). Method used: XSelect semipreparative column C-18 CSH (30 × 100 mm, 5 μm, from Waters), solvent A = 0.1% v/v solution of HCOOH in water, B = CH₃CN, gradient from 35.0% B1 to 55.0% B1 in 10min, flow rate of 40 mL/min. Detection: UV/Vis detection range 210 nm to 350 nm, MS(ES+/ES-) Scan range 100 to 1000 AMU.

The resolution of racemates was performed on a semipreparative chiral HPLC 1100 from Agilent. Method used: Column Chiralpak IC (25 x 2.0 cm, 5 μ, from Chiral Technologies Europe, Daicel group), mobile phase: n-Hexane/(Ethanol + 0.1% HCOOH) 85/15 % v/v, flow rate 17 ml/min, DAD detection 220 nm, Loop 550 μL.

To verify the enantiomeric excess of the resolved enantiomers these analytical chiral HPLC conditions were employed: Column Chiralpak IC (25 x 0.46 cm, 5 μ), mobile phase n-Hexane/(Ethanol + 0.1% HCOOH) 85/15 % v/v, flow rate (ml/min) 1.0, DAD 220 nm Loop 20 μL.

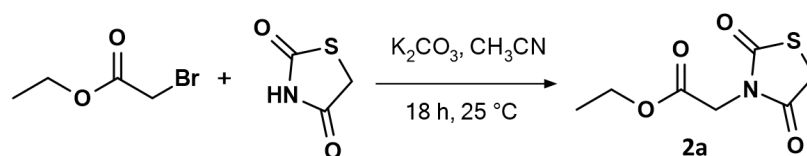
When stereochemistry is not stated, the compounds with a chiral centre are racemic mixtures. When a racemic mixture is solved into separated enantiomers, the stereochemistry has been arbitrarily assigned.

General procedures and synthesis

GP1 - General procedure for Knoevenagel condensation of N-substituted-2,4-thiazolidinedione with an aromatic aldehyde:

To a stirring solution of N-substituted-2,4-thiazolidinedione (1 eq.) and aromatic aldehyde (1 eq.) in dry toluene (0.34 M), piperidine (0.5 eq.) and acetic acid (0.5 eq.) were added at room temperature. The mixture was heated under reflux and left stirring overnight. After cooling to room temperature, the reaction was diluted with EtOAc and washed with water. The organic phase was dried over Na₂SO₄, filtered, and concentrated under *vacuum*. The purification was performed by flash chromatography using the gradient conditions reported below and the final products were characterized by ESI-MS and NMR spectra. The reaction was monitored by analytical LC-MS (A/a by UV and ESI-MS).

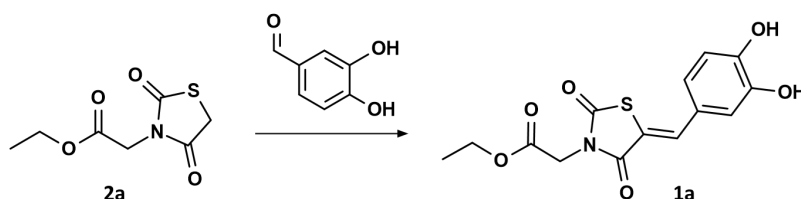
Synthesis of Ethyl 2-(2,4-dioxo-1,3-thiazolidin-3-yl)acetate (**2a**)



To a stirring suspension of thiazolidine-2,4-dione (2 g, 17.08 mmol) and potassium carbonate (4.73 g, 34.22 mmol) in dry MeCN (300 mL), ethyl 2-bromoacetate (1.89 mL, 17.08 mmol) was added dropwise at room temperature under nitrogen atmosphere. After 18 h, the reaction was concentrated in *vacuo* and the residue partitioned between EtOAc and water. The aqueous phase was extracted with EtOAc (3 x), then the organic phases were collected, dried over Na₂SO₄, filtered, and concentrated under *vacuum*. The residue was purified by flash chromatography (cartridge: Biotage sfär Silica D 25 g; gradient conditions: EtOAc in CHX, from 0% to 40%, 8 CV) to afford the title compound **2a** (2.82 g, 13.88 mmol, 81% yield) as a colourless oil.

¹H NMR (400 MHz, Chloroform-d) δ 4.37 (s, 2H), 4.25 (q, J = 7.1 Hz, 2H), 4.06 (s, 2H), 1.31 (t, J = 7.1 Hz, 3H). C₇H₉NO₄S; UPLC-MS acidic (method A) r.t. 0.64 min, MS (ESI) m/z = 204.0 [M+H]⁺.

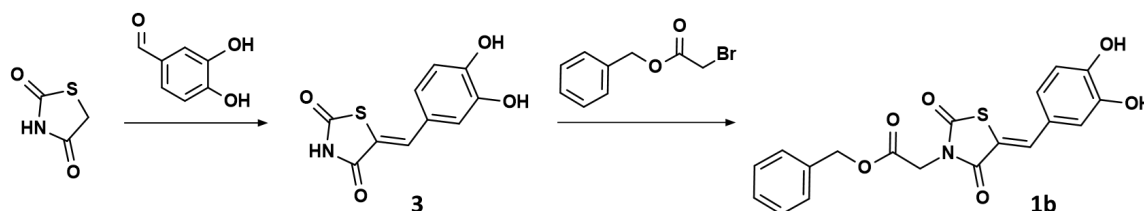
Synthesis of ethyl 2-[(5Z)-5-[(3,4-dihydroxyphenyl)methylidene]-2,4-dioxo-1,3-thiazolidin-3-yl]acetate (1a)



Compound **1a** was obtained from compound **2a** (250 mg, 1.23 mmol) and 3,4-dihydroxybenzaldehyde (172 mg, 1.24 mmol), by following the general procedure GP1, as a yellow solid (255 mg, 0.79 mmol, 64% overall isolated yield after purification by reversed phase flash chromatography); Cartridge: Biotage sfär C18 D 30 g, gradient conditions: MeCN in water, in presence of 0.1% HCOOH, from 2% to 100%, 10 CV.

^1H NMR (400 MHz, DMSO- d_6) δ 9.70 (s, 2H), 7.81 (s, 1H), 7.07 – 6.99 (m, 2H), 6.89 (d, J = 8.0 Hz, 1H), 4.47 (s, 2H), 4.17 (q, J = 7.1 Hz, 2H), 1.21 (t, J = 7.1 Hz, 3H). ^{13}C NMR (100 MHz, DMSO- d_6) δ 167.56, 167.23, 165.52, 149.79, 146.45, 135.40, 124.94, 124.40, 117.00, 116.79, 115.91, 62.04, 42.55, 14.41. $\text{C}_{14}\text{H}_{13}\text{NO}_6\text{S}$; UPLC-MS acidic (method A) r.t. 0.89 min, MS (ESI) m/z = 324.1 $[\text{M}+\text{H}]^+$.

Synthesis of benzyl 2-[(5Z)-5-[(3,4-dihydroxyphenyl)methylidene]-2,4-dioxo-1,3-thiazolidin-3-yl]acetate (1b)



(5Z)-5-[(3,4-dihydroxyphenyl)methylidene]-1,3-thiazolidine-2,4-dione (3)

To a stirring solution of thiazolidine-2,4-dione (300 mg, 2.56 mmol) and 3,4-dihydroxybenzaldehyde (357 mg, 2.59 mmol) in dry toluene (1.9 mL), piperidine (22 mg, 0.26 mmol) and acetic acid (15 mg, 0.26 mmol) were added. The resulting mixture was heated under reflux and left stirring overnight. Then, the reaction was cooled to room temperature, and the yellow solid precipitate was recovered by filtration, washed with DCM, water, and then dried under reduced pressure to afford compound **3** (486 mg, 2.05 mmol, 80% yield) as a yellow solid.

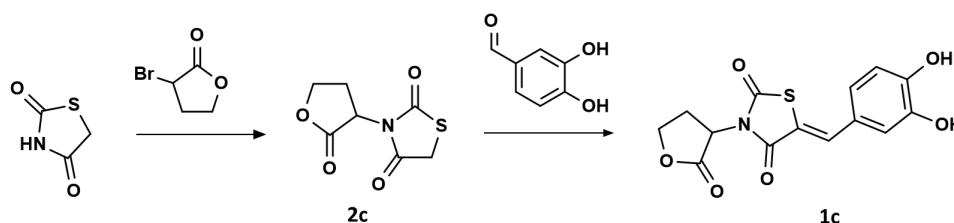
^1H NMR (400 MHz, DMSO- d_6) δ 12.41 (s, 1H), 9.78 (s, 1H), 9.42 (s, 1H), 7.59 (s, 1H), 6.99 (d, J = 2.2 Hz, 1H), 6.95 (dd, J = 8.3, 2.2 Hz, 1H), 6.86 (d, J = 8.2 Hz, 1H). $\text{C}_{10}\text{H}_7\text{NO}_4\text{S}$; UPLC-MS acidic (method A) r.t. 0.64 min, MS (ESI) m/z = 238.1 $[\text{M}+\text{H}]^+$.

Benzyl 2-[(5Z)-5-[(3,4-dihydroxyphenyl)methylidene]-2,4-dioxo-1,3-thiazolidin-3-yl] acetate (1b)

To a stirring suspension of compound **3** (30 mg, 0.13 mmol) and potassium carbonate (17 mg, 0.13 mmol) in dry DMF (2 mL), 2-bromoacetic acid (phenylmethyl) ester (20 μ L, 0.13 mmol) was added dropwise under nitrogen atmosphere at room temperature. After 18 h, the reaction was concentrated in vacuo and the residue partitioned between EtOAc and water. Then, the aqueous phase was extracted with EtOAc (2 x), the organic phases were collected, dried over Na₂SO₄, filtered, and concentrated under reduced pressure. The residue was subjected to direct phase flash chromatography (cartridge: Biotage sfär Silica D 10 g, gradient conditions: EtOAc in CHX, from 0% to 100%, 10 CV) to afford compound **1b** (8.3 mg, 0.022 mmol, 17% yield) as a yellow solid.

¹H NMR (400 MHz, DMSO-*d*₆) δ 7.81 (s, 1H), 7.44 – 7.29 (m, 5H), 7.07 – 6.99 (m, 2H), 6.88 (d, *J* = 8.0 Hz, 1H), 5.20 (s, 2H), 4.55 (s, 2H). Structure confirmed also by 2D NMR analysis. C₁₉H₁₅NO₆S; UPLC-MS acidic (method A) r.t. 1.06 min, MS (ESI) *m/z* = 386.1 [M+H]⁺.

Synthesis of (5Z)-5-[(3,4-dihydroxyphenyl)methylidene]-3-(2-oxoxolan-3-yl)-1,3-thiazolidine-2,4-dione (1c)



3-(2-oxoxolan-3-yl)-1,3-thiazolidine-2,4-dione (2c)

To a stirring suspension of thiazolidine-2,4-dione (40 mg, 0.34 mmol) and potassium carbonate (142 mg, 1 mmol) in dry DMF (2.5 mL), 3-bromo-2-oxolanone (113 mg, 0.68 mmol) was added at room temperature. Then, the reaction was heated to 50 °C and left stirring for 18 h. The reaction mixture was left reach room temperature and then partitioned between EtOAc and water. The aqueous phase was extracted with EtOAc (2 x), the organic phases were collected, dried over Na₂SO₄, filtered, and concentrated under *vacuum*. The residue was subjected to direct phase flash chromatography (cartridge: Biotage sfär Silica D 10 g; gradient conditions: EtOAc in CHX, from 0% to 100%, 12 CV) to afford compound **2c** (19 mg, 0.094 mmol, 28% yield) as a colourless oil.

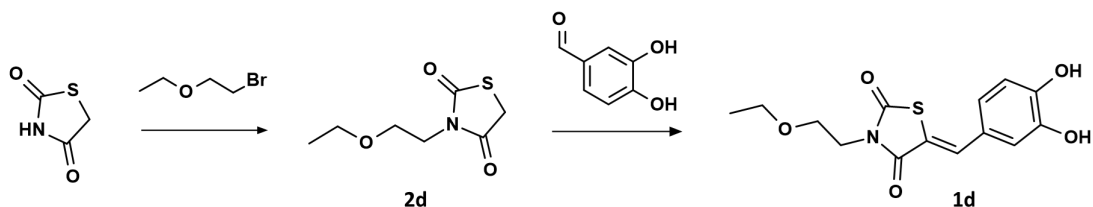
^1H NMR (400 MHz, DMSO- d_6) δ 5.08 – 5.01 (m, 1H), 4.61 (td, J = 9.2, 2.4 Hz, 1H), 4.46 – 4.30 (m, 1H), 4.03 (s, 2H), 2.71 – 2.62 (m, 1H), 2.58 – 2.48 (m, 1H). $\text{C}_7\text{H}_7\text{NO}_4\text{S}$; UPLC-MS acidic (method A) r.t. 0.42 min, MS (ESI) m/z = 201.9 $[\text{M}+\text{H}]^+$.

(5Z)-5-[(3,4-dihydroxyphenyl)methylidene]-3-(2-oxoxolan-3-yl)-1,3-thiazolidine-2,4-dione (1c)

Compound **1c** was obtained from compound **2c** (19 mg, 0.094 mmol) and 3,4-dihydroxybenzaldehyde (13 mg, 0.094 mmol), by following the general procedure GP1 (conc. 0.035 M instead of 0.34 M), as a yellow solid (14 mg, 0.044 mmol, 46% overall isolated yield after purification by direct phase flash chromatography); Cartridge: Biotage sfär Silica D 10 g, gradient conditions: EtOAc in CHX, from 0% to 100%, 10 CV.

^1H NMR (400 MHz, DMSO- d_6) δ 7.80 (s, 1H), 7.07 – 6.98 (m, 2H), 6.90 – 6.86 (m, 1H), 5.40 (t, J = 10.0 Hz, 1H), 4.51 (td, J = 8.8, 2.6 Hz, 1H), 4.42 – 4.32 (m, 1H), 2.62 – 2.53 (m, 1H), 2.49 – 2.43 (m, 1H). ^{13}C NMR (100 MHz, DMSO- d_6) δ 172.86, 167.34, 165.21, 149.84, 146.45, 135.68, 125.00, 124.42, 117.02, 116.82, 115.57, 66.60, 50.57, 25.59. $\text{C}_{14}\text{H}_{11}\text{NO}_6\text{S}$; UPLC-MS acidic (method A) r.t. 0.76 min, MS (ESI) m/z = 322.1 $[\text{M}+\text{H}]^+$.

Synthesis of (5Z)-5-[(3,4-dihydroxyphenyl)methylidene]-3-(2-ethoxyethyl)-1,3-thiazolidine-2,4-dione (1d)



3-(2-ethoxyethyl)-1,3-thiazolidine-2,4-dione (2d)

To a stirring suspension of thiazolidine-2,4-dione (100 mg, 0.85 mmol) and potassium carbonate (236 mg, 1.71 mmol) in a mixture of dry MeCN (1 mL) and DMF (1 mL), 1-bromo-2-ethoxyethane (100 μL , 0.85 mmol) was added at room temperature. Then, the reaction was heated to 75 $^\circ\text{C}$ and left stirring for 2 h. The reaction was concentrated under reduced pressure and the residue was partitioned between EtOAc and water. The aqueous phase was extracted with EtOAc (2x) and the organic layers were collected, dried over Na_2SO_4 , filtered, and concentrated under *vacuum*. The residue was subjected to direct phase flash chromatography (cartridge: Biotage sfär Silica D 10 g; gradient conditions: EtOAc in CHX, from 0% to 100%, 8 CV) to afford compound **2d** (102 mg, 0.54 mmol, 63% yield) as a white solid.

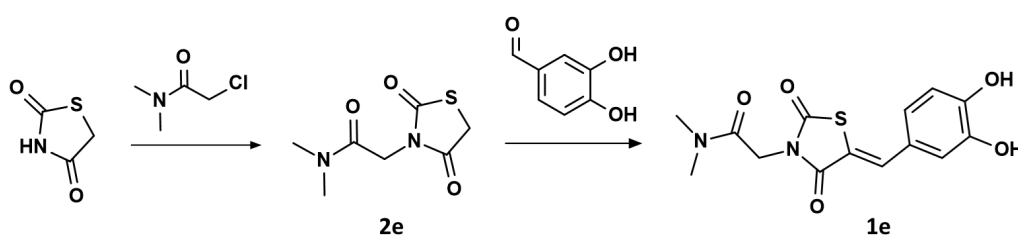
^1H NMR (400 MHz, $\text{DMSO-}d_6$) δ 4.21 (s, 2H), 3.65 (t, $J = 5.9$ Hz, 2H), 3.48 (t, $J = 5.8$ Hz, 2H), 3.41 (q, $J = 7.0$ Hz, 2H), 1.05 (t, $J = 7.0$ Hz, 3H). $\text{C}_7\text{H}_{11}\text{NO}_3\text{S}$; UPLC-MS acidic (method A) r.t. 0.60 min, MS (ESI) $m/z = 190.0$ $[\text{M}+\text{H}]^+$.

(5Z)-5-[(3,4-dihydroxyphenyl)methylidene]-3-(2-ethoxyethyl)-1,3-thiazolidine-2,4-dione (1d)

Compound **1d** was obtained from compound **2d** (100 mg, 0.48 mmol) and 3,4-dihydroxybenzaldehyde (66 mg, 0.48 mmol), by following the general procedure GP1, as a yellow solid (67 mg, 0.215 mmol, 45% overall isolated yield after purification by direct phase flash chromatography and then by reversed phase flash chromatography); *First column purification*: cartridge: Biotage sfär Silica D 25 g; gradient conditions: EtOAc in CHX, from 0% to 100%, 10 CV; *Second column purification*: cartridge: Biotage sfär C18 D 12 g; gradient conditions: MeCN in water, in presence of 0.1% HCOOH, from 2% to 100%, 10 CV.

^1H NMR (400 MHz, $\text{DMSO-}d_6$) δ 7.75 (s, 1H), 7.07 – 6.96 (m, 2H), 6.87 (d, $J = 8.1$ Hz, 1H), 3.80 (t, $J = 5.8$ Hz, 2H), 3.56 (t, $J = 5.8$ Hz, 2H), 3.43 (q, $J = 7.0$ Hz, 2H), 1.05 (t, $J = 7.0$ Hz, 3H). ^{13}C NMR (100 MHz, $\text{DMSO-}d_6$) δ 167.86, 166.20, 149.39, 146.37, 134.34, 124.66 (2C), 116.94, 116.75, 116.63, 66.04, 65.66, 41.29, 15.43. $\text{C}_{14}\text{H}_{15}\text{NO}_5\text{S}$; UPLC-MS acidic (method A) r.t. 0.88 min, MS (ESI) $m/z = 310.0$ $[\text{M}+\text{H}]^+$.

Synthesis of 2-[(5Z)-5-[(3,4-dihydroxyphenyl)methylidene]-2,4-dioxo-1,3-thiazolidin-3-yl]-N,N-dimethylacetamide (1e)



2-[(2,4-dioxo-1,3-thiazolidin-3-yl)-N,N-dimethylacetamide (2e)

To a stirring suspension of thiazolidine-2,4-dione (100 mg, 0.85 mmol) and potassium carbonate (236 mg, 1.71 mmol) in a mixture of dry MeCN (4 mL) and dry DMF (1 mL), 2-chloro-N,N-dimethylacetamide (0.09 mL, 0.85 mmol) was added at room temperature. The reaction was heated to 75 °C and left stirring for 2 h. Then, the reaction was concentrated in vacuo, the residue was taken up in EtOAc and washed with water. The aqueous phase was extracted with EtOAc (2 x) and then the organic phases were collected, dried over Na_2SO_4 , filtered and concentrated under *vacuum*. The residue was subjected to direct phase flash

chromatography (cartridge: Biotage sfär Silica D 10 g; gradient conditions: EtOAc in CHX, from 0% to 100%, 8 CV) to afford compound **2e** (135 mg, 0.67 mmol, 78% yield) as a white solid.

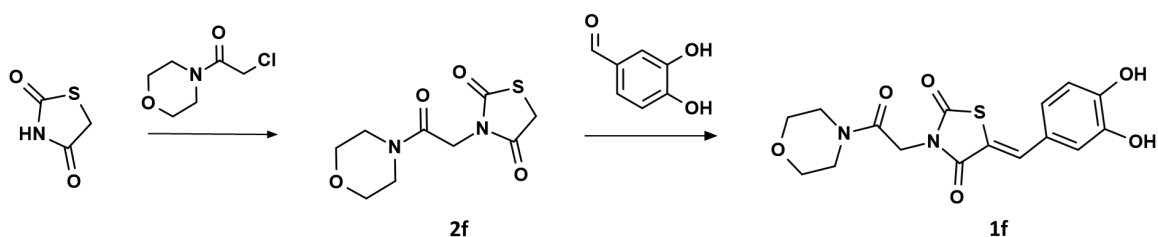
^1H NMR (400 MHz, DMSO- d_6) δ 4.38 (s, 2H), 4.30 (s, 2H), 3.02 (s, 3H), 2.82 (s, 3H). $\text{C}_7\text{H}_{10}\text{N}_2\text{O}_3\text{S}$; UPLC-MS acidic (method A) r.t. 0.40 min, MS (ESI) $m/z=203.0$ $[\text{M}+\text{H}]^+$.

2-[(5Z)-5-[(3,4-dihydroxyphenyl)methylidene]-2,4-dioxo-1,3-thiazolidin-3-yl]-N,N-dimethylacetamide (1e)

Compound **1e** was obtained from compound **2e** (50 mg, 0.25 mmol) and 3,4-dihydroxybenzaldehyde (34 mg, 0.25 mmol), by following the general procedure GP1, as a yellow solid (58 mg, 0.18 mmol, 73% overall isolated yield after purification by trituration in MeOH, DCM, and Water).

^1H NMR (400 MHz, DMSO- d_6) δ 7.76 (s, 1H), 7.08 – 6.97 (m, 2H), 6.88 (d, $J=8.1$ Hz, 1H), 4.54 (s, 2H), 3.05 (s, 3H), 2.84 (s, 3H). ^{13}C NMR (100 MHz, DMSO- d_6) δ 167.78, 165.94, 164.89, 149.61, 146.42, 134.70, 124.77, 124.53, 116.91, 116.77, 116.50, 43.05, 36.21, 35.66. $\text{C}_{14}\text{H}_{14}\text{N}_2\text{O}_5\text{S}$; UPLC-MS acidic (method A) r.t. 0.69 min, MS (ESI) $m/z=323.0$ $[\text{M}+\text{H}]^+$.

Synthesis of (5Z)-5-[(3,4-dihydroxyphenyl)methylidene]-3-[2-(morpholin-4-yl)-2-oxoethyl]-1,3-thiazolidine-2,4-dione (1f)



3-[2-(morpholin-4-yl)-2-oxoethyl]-1,3-thiazolidine-2,4-dione (2f)

Batch 1:

To a stirring suspension of thiazolidine-2,4-dione (100 mg, 0.85 mmol) and potassium carbonate (236 mg, 1.71 mmol) in a mixture of dry MeCN (4 mL) and dry DMF (1 mL), 2-chloro-1-(morpholin-4-yl)ethan-1-one (0.11 mL, 0.85 mmol) was added at room temperature. The reaction was heated to 75 °C and left stirring for 2 h. The reaction was concentrated in vacuo, then taken up in EtOAc and washed with water. The aqueous phase was extracted with EtOAc (2 x) and then the organic phases were collected, dried over Na_2SO_4 , filtered and concentrated under *vacuum*. The residue was subjected to direct phase flash chromatography (cartridge: Biotage sfär Silica D 10 g; gradient conditions: EtOAc in

CHX, from 0% to 100%, 10 CV) to afford compound **2f** (142 mg, 0.58 mmol, 68% yield) as a white solid.

¹H NMR (400 MHz, DMSO-*d*₆) δ 4.42 (s, 2H), 4.31 (s, 2H), 3.61 (t, J = 4.7 Hz, 2H), 3.56 (t, J = 4.9 Hz, 2H), 3.51 (t, J = 4.8 Hz, 2H), 3.41 (t, J = 4.9 Hz, 2H). C₉H₁₂N₂O₄S; UPLC-MS acidic (method A) r.t. 0.42 min, MS (ESI) m/z= No ionization.

Batch 2:

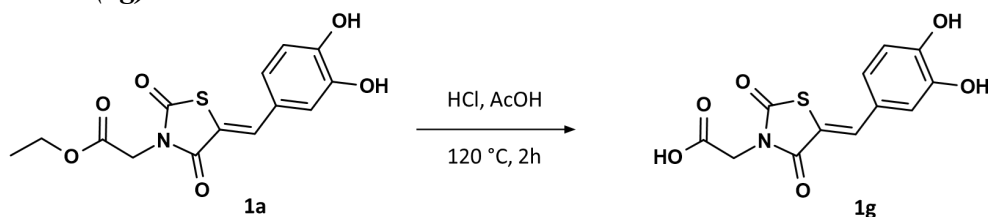
To a stirring suspension of thiazolidine-2,4-dione (1 g, 8.54 mmol) and potassium carbonate (2.36 mL, 17.1 mmol) in dry MeCN (51 mL), 2-chloro-1-(morpholin-4-yl)ethan-1-one (1.4 g, 8.54 mmol) was added at room temperature. The reaction mixture was heated to 80 °C and stirred for 18 h. Solvents were removed under reduced pressure, then water was added, and the resulting mixture was extracted with DCM (3x). The combined organic layers were dried over Na₂SO₄, filtered, and concentrated in vacuo to afford compound **2f** (1.87 g, 7.66 mmol, 90% yield) as a colourless oil. C₉H₁₂N₂O₄S; UPLC-MS acidic (method A) r.t. 0.42 min, MS (ESI) m/z= No ionization.

(5Z)-5-[(3,4-dihydroxyphenyl)methylidene]-3-[2-(morpholin-4-yl)-2-oxoethyl]-1,3-thiazolidine-2,4-dione (1f)

Compound **1f** was obtained from compound **2f** (62 mg, 0.25 mmol) and 3,4-dihydroxybenzaldehyde (35 mg, 0.25 mmol), by following the general procedure GP1, as a yellow solid (66 mg, 0.18 mmol, 72% overall isolated yield after purification by trituration in MeOH, DCM, and Water).

¹H NMR (400 MHz, DMSO-*d*₆) δ 7.76 (s, 1H), 7.09 – 6.96 (m, 2H), 6.88 (d, J = 8.1 Hz, 1H), 4.59 (s, 2H), 3.66 – 3.61 (m, 2H), 3.60 – 3.51 (m, 4H), 3.46 – 3.41 (m, 2H). ¹³C NMR (100 MHz, DMSO-*d*₆) δ 167.77, 165.92, 163.96, 149.61, 146.43, 134.76, 124.79, 124.52, 116.93, 116.78, 116.46, 66.37 (2C), 44.99, 42.88, 42.39. C₁₆H₁₆N₂O₆S; UPLC-MS acidic (method A) r.t. 0.69 min, MS (ESI) m/z= 365.1 [M+H]⁺.

Synthesis of 2-[(5Z)-5-[(3,4-dihydroxyphenyl)methylidene]-2,4-dioxo-1,3-thiazolidin-3-yl]acetic acid (1g)



Batch 1:

A mixture of compound **1a** (50 mg, 0.15 mmol), glacial acetic acid (1.55 mL) and concentrated hydrogen chloride (0.47 mL, 5.58 mmol) was stirred at 120 °C for 2 h. The reaction was left reach room temperature, diluted with water and extracted with EtOAc. The organic phase was separated, dried over Na₂SO₄, filtered, and concentrated under reduced pressure. The residue was purified by reversed phase flash chromatography (cartridge: Biotage sfär C18 D 12 g; gradient conditions: MeCN in water, in presence of 0.1% HCOOH, from 2% to 100%, 10 CV) to give the title compound, **1g** (21 mg, 0.071 mmol, 46% yield), as a yellow solid.

¹H NMR (400 MHz, DMSO-*d*₆) δ 13.39 (s, 1H), 9.92 (s, 1H), 9.50 (s, 1H), 7.80 (s, 1H), 7.06 – 7.00 (m, 2H), 6.89 (d, *J* = 8.1 Hz, 1H), 4.34 (s, 2H). ¹³C NMR (100 MHz, DMSO-*d*₆) δ 168.51, 167.62, 165.67, 149.60, 146.41, 135.12, 124.84, 124.53, 117.02, 116.79, 116.24, 42.70. C₁₂H₉NO₆S; UPLC-MS acidic r.t. 0.70 min, MS (ESI) *m/z*= 296.1 [M+H]⁺.

Batch 2:

A mixture of compound **1a** (185 mg, 0.57 mmol), glacial acetic acid (5.74 mL) and concentrated hydrogen chloride (1.72 mL, 20.7 mmol) was stirred at 120 °C for 2 h. The reaction was left reach room temperature and precipitation of a yellow solid was observed. The solid was recovered by filtration and then washed with water and MeCN to afford the title compound, **1g** (105 mg, 0.36 mmol, 62% yield) as a yellow solid.

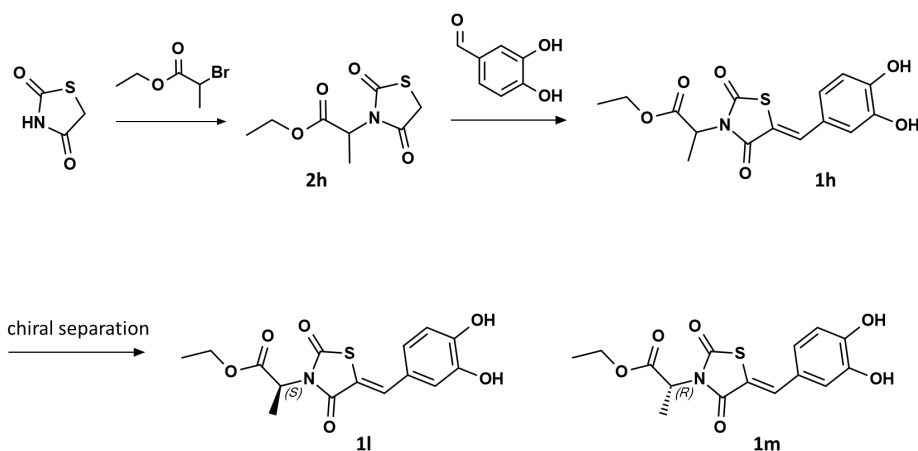
¹H NMR (400 MHz, DMSO-*d*₆) δ 13.39 (s, 1H), 9.93 (s, 1H), 9.50 (s, 1H), 7.80 (s, 1H), 7.09 – 6.99 (m, 2H), 6.89 (d, *J* = 8.1 Hz, 1H), 4.34 (s, 2H). C₁₂H₉NO₆S; UPLC-MS acidic r.t. 0.72 min, MS (ESI) *m/z*= 296.1 [M+H]⁺.

Batch 3:

A mixture of compound **1a** (2.39, 7.39 mmol), glacial acetic acid (18 mL) and concentrated hydrogen chloride (6.16 mL, 73.92 mmol) was stirred at 120 °C for 5 h. The reaction was left reach room temperature and precipitation of a yellow solid was observed. The solid was recovered by filtration and then washed with water to afford the title compound, **1g** (2 g, 6.77 mmol, 92% yield), as a yellow solid.

¹H NMR (400 MHz, DMSO-*d*₆) δ 13.38 (s, 1H), 9.92 (s, 1H), 9.50 (s, 1H), 7.80 (s, 1H), 7.07 – 7.00 (m, 2H), 6.89 (d, *J* = 8.1 Hz, 1H), 4.35 (s, 2H). C₁₂H₉NO₆S; UPLC-MS acidic (method A) r.t. 0.70 min, MS (ESI) *m/z*= 294.0 [M-H]⁻.

Synthesis of ethyl 2-[(5Z)-5-[(3,4-dihydroxyphenyl)methylidene]-2,4-dioxo-1,3-thiazolidin-3-yl]propanoate (1h), ethyl (2S)-2-[(5Z)-5-[(3,4-dihydroxyphenyl)methylidene]-2,4-dioxo-1,3-thiazolidin-3-yl]propanoate (1l) and ethyl (2R)-2-[(5Z)-5-[(3,4-dihydroxyphenyl)methylidene]-2,4-dioxo-1,3-thiazolidin-3-yl]propanoate (1m)



Ethyl 2-(2,4-dioxo-1,3-thiazolidin-3-yl)propanoate (2h)

Batch 1:

To a solution of thiazolidine-2,4-dione (200 mg, 1.71 mmol) in dry DMF (1 mL), sodium hydride (as a 60% dispersion in mineral oil; 75 mg, 1.88 mmol) was added under N₂ atmosphere at 0 °C, and the resulting reaction mixture was left stirring for 10 min. Then the reaction was left reach room temperature and 2-bromopropanoic acid ethyl ester (0.21 mL, 1.88 mmol) was added dropwise. After stirring overnight, the reaction mixture was diluted with water and then extracted with EtOAc (2 x). The combined organic phases were collected, dried over Na₂SO₄, filtered, and concentrated under reduced pressure. The residue was subjected to direct phase flash chromatography (cartridge: Biotage sfär Silica D 25 g; gradient conditions: EtOAc in CHX, from 0% to 40%, 8 CV) to afford compound **2h** (300 mg, 1.38 mmol, 81% yield) as a colourless oil.

¹H NMR (400 MHz, DMSO-*d*₆) δ 4.91 (q, J = 7.1 Hz, 1H), 4.38 – 4.21 (m, 2H), 4.17 – 4.04 (m, 2H), 1.41 (d, J = 7.1 Hz, 3H), 1.15 (t, J = 7.1 Hz, 3H). C₈H₁₁NO₄S; UPLC-MS acidic (method A) r.t. 0.75 min, MS (ESI) m/z= 218.0 [M+H]⁺.

Batch 2:

To a solution of thiazolidine-2,4-dione (500 mg, 4.27 mmol) in dry DMF (2.5 mL), sodium hydride (as a 60% dispersion in mineral oil; 188 mg, 4.7 mmol) was added under N₂ atmosphere at 0 °C, and the resulting reaction mixture was left stirring for 10 min. Then the reaction was left reach room temperature and 2-bromopropanoic acid ethyl ester (0.52 mL, 4.7 mmol) was added dropwise. After stirring overnight, the reaction mixture was diluted with water and then extracted with EtOAc (2x). The combined organic phases were

collected, dried over Na₂SO₄, filtered, and concentrated under reduced pressure. The residue was subjected to direct phase flash chromatography (cartridge: Biotage sfär Silica D 25 g, gradient conditions: EtOAc in CHX, from 0% to 60%, 8 CV) to afford compound **2h** (503 mg, 2.32 mmol, 54% yield) as a colourless oil. C₈H₁₁NO₄S; UPLC-MS acidic (method A) r.t. 0.75 min, MS (ESI) m/z= 218.1 [M+H]⁺.

Batch 3:

To a solution of thiazolidine-2,4-dione (2 g, 17.1 mmol) in dry DMF (10 mL), sodium hydride (as a 60% dispersion in mineral oil; 820 mg, 20.5 mmol) was added, and the reaction mixture was stirred at room temperature for 10 min. Then, 2-bromopropanoic acid ethyl ester (2 mL, 18 mmol) was added dropwise, and the resulting mixture was left stirring overnight. The reaction mixture was quenched with water and then extracted with EtOAc (3x). The organic phase was dried over Na₂SO₄, filtered and concentrated under *vacuum*. The residue was subjected direct phase flash chromatography (cartridge: Biotage sfär Silica D 25 g; gradient conditions: EtOAc in CHX, from 0% to 50%, 10 CV) to afford **2h** (3 g, 13.8 mmol, 81% yield) as a colourless oil. C₈H₁₁NO₄S; UPLC-MS acidic (method A) r.t. 0.77 min, MS (ESI) m/z= 218.1 [M+H]⁺.

Ethyl 2-[(5Z)-5-[(3,4-dihydroxyphenyl)methylidene]-2,4-dioxo-1,3-thiazolidin-3-yl]propanoate (1h)

Batch 1:

Compound **1h** was obtained from compound **2h** (63 mg, 0.29 mmol) and 3,4-dihydroxybenzaldehyde (40 mg, 0.29 mmol), by following the general procedure GP1 (conc. 0.18 M instead of 0.34 M), as a yellow solid (77 mg, 0.23 mmol, 79% overall isolated yield after purification by reversed phase flash chromatography); Cartridge: Biotage sfär C18 D 28 g; gradient conditions: MeCN in water, in presence of 0.1% HCOOH, from 2% to 100%, 10 CV.

¹H NMR (400 MHz, DMSO-*d*₆) δ 7.79 (s, 1H), 7.10 – 6.97 (m, 2H), 6.88 (d, J = 7.9 Hz, 1H), 5.09 (q, J = 7.1 Hz, 1H), 4.13 (qq, J = 7.1, 3.7 Hz, 2H), 1.50 (d, J = 7.2 Hz, 3H), 1.15 (t, J = 7.1 Hz, 3H). ¹³C NMR (100 MHz, DMSO-*d*₆) δ 169.05, 167.32, 165.36, 149.72, 146.44, 135.32, 124.90, 124.47, 117.01, 116.79, 115.85, 61.85, 50.52, 14.45, 14.39. C₁₅H₁₅NO₆S; UPLC-MS acidic (method A) r.t. 0.96 min, MS (ESI) m/z= 338.2 [M+H]⁺.

Batch 2:

Compound **1h** was obtained from compound **2h** (60 mg, 0.28 mmol) and 3,4-dihydroxybenzaldehyde (38 mg, 0.28 mmol), by following the general procedure GP1 (conc. 0.18 M instead of 0.34 M), as a yellow solid (77 mg, 0.23 mmol, 82% overall isolated yield

after purification by direct phase flash chromatography); Cartridge: Biotage sfär Silica D 25 g, gradient conditions: EtOAc in CHX, from 0% to 100%, 10 CV. C₁₅H₁₅NO₆S; UPLC-MS acidic r.t. 0.96 min, MS (ESI) m/z= 338.2 [M+H]⁺.

Batch 3:

Compound **1h** was obtained from compound **2h** (500 mg, 2.19 mmol) and 3,4-dihydroxybenzaldehyde (302 mg, 2.2 mmol), by following the general procedure GP1 (conc. 0.031 M instead of 0.34 M), as a yellow solid (634 mg, 1.88 mmol, 86% overall isolated yield after purification by direct phase flash chromatography); Cartridge: Biotage sfär Silica D 25 g, gradient conditions: EtOAc in CHX, from 0% to 80%, 10 CV. C₁₅H₁₅NO₆S; UPLC-MS acidic r.t. 0.96 min, MS (ESI) m/z= 338.1 [M+H]⁺.

Ethyl (2S)-2-[(5Z)-5-[(3,4-dihydroxyphenyl)methylidene]-2,4-dioxo-1,3-thiazolidin-3-yl]propanoate* (1l) and ethyl (2R)-2-[(5Z)-5-[(3,4-dihydroxyphenyl)methylidene]-2,4-dioxo-1,3-thiazolidin-3-yl]propanoate* (1m)

Compound **1h** (2nd batch: 77 mg, 0.23 mmol) was resolved by semi-preparative chiral HPLC to obtain the two separated enantiomers:

- First eluted enantiomer*: **1l** (26 mg, 0.078 mmol, 28% yield), e.e.= 100%, as a yellow solid. ¹H NMR (400 MHz, DMSO-*d*₆) δ 7.78 (s, 1H), 7.04 – 6.99 (m, 2H), 6.87 (d, J = 7.9 Hz, 1H), 5.09 (q, J = 7.1 Hz, 1H), 4.13 (qq, J = 7.0, 3.7 Hz, 2H), 1.50 (d, J = 7.1 Hz, 3H), 1.16 (t, J = 7.1 Hz, 3H). ¹³C NMR (100 MHz, DMSO-*d*₆) δ 169.06, 167.33, 165.36, 150.06, 146.53, 135.37, 124.97, 124.29, 116.91, 116.79, 115.63, 61.84, 50.52, 14.45, 14.39. C₁₅H₁₅NO₆S; UPLC-MS acidic (method A) r.t. 0.96 min, MS (ESI) m/z= 338.0 [M+H]⁺.
- Second eluted enantiomer*: **1m** (25 mg, 0.075 mmol, 27% yield), e.e.= 100%, as a yellow solid. ¹H NMR (400 MHz, DMSO-*d*₆) δ 7.78 (s, 1H), 7.06 – 6.96 (m, 2H), 6.86 (d, J = 8.0 Hz, 1H), 5.09 (q, J = 7.1 Hz, 1H), 4.13 (qq, J = 7.0, 3.7 Hz, 2H), 1.50 (d, J = 7.1 Hz, 3H), 1.16 (t, J = 7.1 Hz, 3H). ¹³C NMR (100 MHz, DMSO-*d*₆) δ 169.06, 167.34, 165.37, 150.03, 146.53, 135.37, 124.97, 124.30, 116.93, 116.79, 115.64, 61.84, 50.52, 14.45, 14.39. C₁₅H₁₅NO₆S; UPLC-MS acidic (method A) r.t. 0.96 min, MS (ESI) m/z= 338.0 [M+H]⁺.

Semipreparative chiral HPLC conditions and results: Column Chiralpak IC (25 x 2.0 cm, 5 μ), mobile phase: n-Hexane/(Ethanol + 0.1% HCOOH) 85/15 % v/v, flow rate 17 ml/min, DAD detection 220 nm, Loop 550 μL.

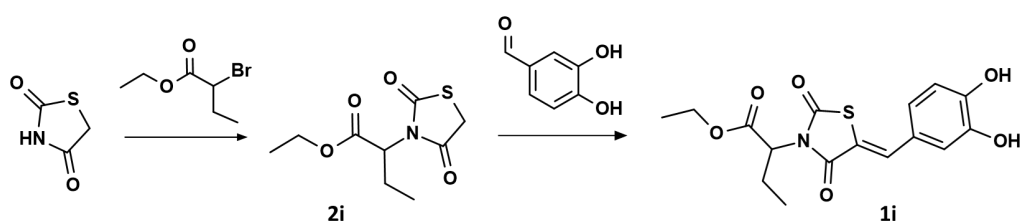
Analytical chiral HPLC conditions and results: Column Chiralpak IC (25 x 0.46 cm, 5 μ), mobile phase n-Hexane/(Ethanol + 0.1% HCOOH) 85/15 % v/v, flow rate (ml/min) 1.0, DAD 220 nm Loop 20 μ L.

1l chiral QC: Enantiomer 1 100 % a/a by UV (8.1 min), Enantiomer 2 Not detected.

1m chiral QC: Enantiomer 1 Not detected, Enantiomer 2 100 % a/a by UV (9.9 min).

*Single enantiomer of unknown absolute configuration. Stereochemistry arbitrarily assigned.

Synthesis of ethyl 2-[(5Z)-5-[(3,4-dihydroxyphenyl)methylidene]-2,4-dioxo-1,3-thiazolidin-3-yl]butanoate (1i)



Ethyl 2-(2,4-dioxo-1,3-thiazolidin-3-yl)butanoate (2i)

A solution of thiazolidine-2,4-dione (100 mg, 0.85 mmol) in dry DMF (2 mL) was cooled to 0 °C with an ice-bath, then sodium hydride (as a 60% dispersion in mineral oil; 27 mg, 1.11 mmol) was added and the mixture was left stirring for 15 min. Then the reaction was left reach room temperature and ethyl 2-bromobutanoate (0.13 mL, 0.85 mmol) was added. After stirring overnight, the reaction mixture was diluted with water and then extracted with EtOAc (2 x). The combined organic phases were collected, dried over Na₂SO₄, filtered, and concentrated under reduced pressure. The residue was subjected to direct phase flash chromatography (cartridge: Biotage sfär Silica D 10 g; gradient conditions: EtOAc in CHX, from 0% to 100%, 8 CV) to afford compound **2i** (100 mg, 0.43 mmol, 51% yield) as a white solid.

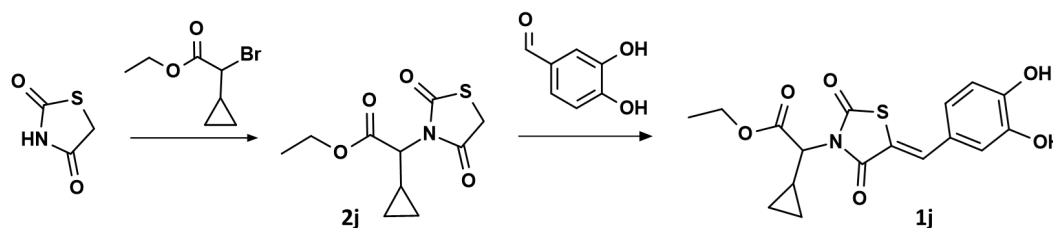
¹H NMR (400 MHz, DMSO-*d*₆) δ 4.73 (dd, *J* = 10.3, 5.0 Hz, 1H), 4.37 (d, *J* = 4.1 Hz, 2H), 4.18 – 4.03 (m, 2H), 2.11 – 1.98 (m, 1H), 1.97 – 1.83 (m, 1H), 1.15 (t, *J* = 7.1 Hz, 3H), 0.81 (t, *J* = 7.5 Hz, 3H). C₉H₁₃NO₄S; UPLC-MS acidic (method A) r.t. 0.87 min, MS (ESI) *m/z* = 232.1 [M+H]⁺.

Ethyl 2-[(5Z)-5-[(3,4-dihydroxyphenyl)methylidene]-2,4-dioxo-1,3-thiazolidin-3-yl]butanoate (1i)

Compound **1i** was obtained from compound **2i** (100 mg, 0.43 mmol) and 3,4-dihydroxybenzaldehyde (60 mg, 0.43 mmol), by following the general procedure GP1 (conc. 0.22 M instead of 0.34 M), as a yellow solid (150 mg, 0.427 mmol, 99% overall isolated yield after purification by direct phase flash chromatography); Cartridge: Biotage sfär Silica D 25 g, gradient conditions: EtOAc in CHX, from 0% to 100%, 10 CV.

¹H NMR (400 MHz, Chloroform -d) δ 7.79 (s, 1H), 7.05 (d, J = 2.1 Hz, 1H), 7.01 (dd, J = 8.3, 2.1 Hz, 1H), 6.95 (d, J = 8.3 Hz, 1H), 5.94 (s, 2H), 4.88 (dd, J = 10.5, 5.2 Hz, 1H), 4.24 (qq, J = 7.0, 3.6 Hz, 2H), 2.35 – 2.10 (m, 2H), 1.27 (t, J = 7.1 Hz, 3H), 0.94 (t, J = 7.5 Hz, 3H). ¹³C NMR (100 MHz, DMSO-*d*₆) δ 168.50, 167.57, 165.68, 149.93, 146.48, 135.69, 125.01, 124.34, 117.01, 116.79, 115.31, 61.78, 56.47, 21.42, 14.39, 10.82. C₁₆H₁₇NO₆S; UPLC-MS acidic (method A) r.t. 1.04 min, MS (ESI) m/z = 352.1 [M+H]⁺.

Synthesis of ethyl 2-cyclopropyl-2-[(5Z)-5-[(3,4-dihydroxyphenyl)methylidene]-2,4-dioxo-1,3-thiazolidin-3-yl]acetate (1j)



Ethyl 2-cyclopropyl-2-(2,4-dioxo-1,3-thiazolidin-3-yl)acetate (2j)

To a solution of thiazolidine-2,4-dione (50 mg, 0.43 mmol) in dry DMF (1 mL), sodium hydride (as a 60% dispersion in mineral oil; 11 mg, 0.47 mmol) was added at 0 °C, and the reaction mixture was left stirring for 10 min. Then the reaction was left reach room temperature and ethyl 2-bromo-2-(cyclopropyl) acetate (70 μL, 0.47 mmol) was added. After stirring overnight, the reaction mixture was quenched with water and then partitioned between EtOAc and water. The aqueous phase was extracted with EtOAc (2 x) and then the organic phases were collected, dried over Na₂SO₄, filtered and concentrated under reduced pressure. The residue was subjected to direct phase flash chromatography (cartridge: Biotage sfär Silica D 25 g; gradient conditions: EtOAc in CHX, from 0% to 100%, 10 CV) to afford compound **2j** (103 mg, 0.423 mmol, 99% yield) as a colourless oil.

¹H NMR (400 MHz, DMSO-*d*₆) δ 4.39 (d, J = 2.3 Hz, 2H), 4.15 – 4.10 (m, 2H), 1.58 – 1.47 (m, 1H), 1.24 – 1.12 (m, 4H), 0.76 – 0.67 (m, 1H), 0.63 – 0.56 (m, 1H), 0.42 (ddd, J = 8.1,

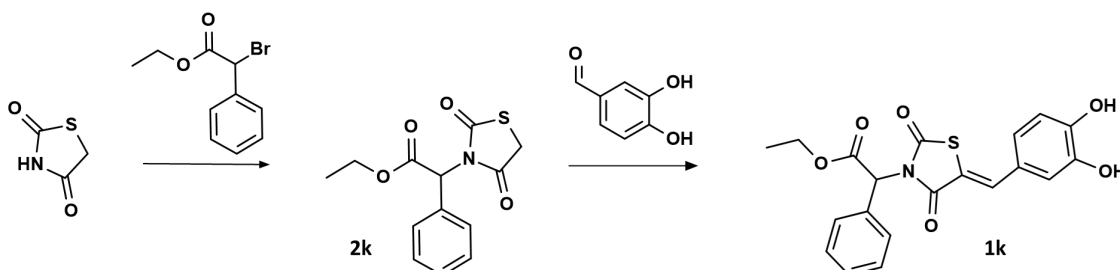
4.4, 2.2 Hz, 1H), 0.17 – 0.08 (m, 1H). C₁₀H₁₃NO₄S; UPLC-MS acidic (method A) r.t. 0.88 min, MS (ESI) m/z= 244.0 [M+H]⁺.

Ethyl 2-cyclopropyl-2-[(5Z)-5-[(3,4-dihydroxyphenyl)methylidene]-2,4-dioxo-1,3-thiazolidin-3-yl]acetate (1j)

Compound **1j** was obtained from compound **2j** (62 mg, 0.25 mmol) and 3,4-dihydroxybenzaldehyde (35 mg, 0.25 mmol), by following the general procedure GP1, as a yellow solid (66 mg, 0.18 mmol, 72% overall isolated yield after purification by trituration in MeOH, DCM, and Water).

¹H NMR (400 MHz, DMSO-*d*₆) δ 7.76 (s, 1H), 7.09 – 6.96 (m, 2H), 6.88 (d, J = 8.1 Hz, 1H), 4.59 (s, 2H), 3.66 – 3.61 (m, 2H), 3.60 – 3.51 (m, 4H), 3.46 – 3.41 (m, 2H). ¹³C NMR (100 MHz, DMSO-*d*₆) δ 168.09, 167.48, 165.54, 149.94, 146.46, 135.84, 125.04, 124.35, 117.03, 116.79, 115.40, 61.82, 61.09, 14.42, 11.36, 6.05, 2.87. C₁₆H₁₆N₂O₆S; UPLC-MS acidic (method A) r.t. 0.69 min, MS (ESI) m/z= 365.1 [M+H]⁺.

Synthesis of ethyl 2-[(5Z)-5-[(3,4-dihydroxyphenyl)methylidene]-2,4-dioxo-1,3-thiazolidin-3-yl]-2-phenylacetate (1k)



Ethyl 2-(2,4-dioxo-1,3-thiazolidin-3-yl)-2-phenylacetate (2k)

To a stirring suspension of thiazolidine-2,4-dione (50 mg, 0.43 mmol) in dry DMF (1 mL), sodium hydride (as a 60% dispersion in mineral oil; 11 mg, 0.47 mmol) was added under N₂ atmosphere at 0 °C, and the resulting reaction mixture was left stirring for 10 min. Then the reaction was left reach room temperature and 2-bromo-2-phenylacetic acid ethyl ester (0.08 mL, 0.47 mmol) was added. After stirring overnight, the reaction mixture was diluted with water and then extracted with EtOAc (2x). The combined organic phases were collected, dried over Na₂SO₄, filtered, and concentrated under reduced pressure. The residue was subjected to direct phase flash chromatography (cartridge: Biotage sfär Silica D 25 g, gradient conditions: EtOAc in CHX, from 0% to 100%, 10 CV) to afford compound **2k** (66 mg, 0.24 mmol, 55% yield) as a colourless oil.

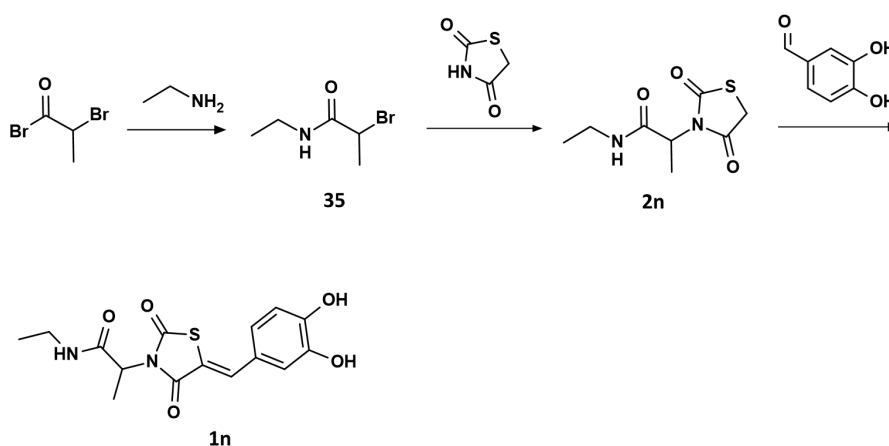
^1H NMR (400 MHz, $\text{DMSO-}d_6$) δ 7.47 – 7.26 (m, 5H), 6.05 (s, 1H), 4.49 – 4.33 (m, 2H), 4.22 – 4.11 (m, 2H), 1.17 (t, $J = 7.1$ Hz, 3H). $\text{C}_{13}\text{H}_{13}\text{NO}_4\text{S}$; UPLC-MS acidic (method A) r.t. 0.98 min, MS (ESI) $m/z = 280.0$ $[\text{M}+\text{H}]^+$.

Ethyl 2-[(5Z)-5-[(3,4-dihydroxyphenyl)methylidene]-2,4-dioxo-1,3-thiazolidin-3-yl]-2-phenylacetate (1k)

Compound **1k** was obtained from compound **2k** (63 mg, 0.2 mmol) and 3,4-dihydroxybenzaldehyde (28 mg, 0.2 mmol), by following the general procedure GP1 (conc. 0.14 M instead of 0.34 M), as a yellow solid (49 mg, 0.12 mmol, 60% overall isolated yield after purification by direct phase flash chromatography and then by reversed phase flash chromatography); *First column purification*: cartridge: Biotage sfär Silica D 25 g; gradient conditions: EtOAc in CHX, from 0% to 100%, 10 CV; *Second column purification*: cartridge: Biotage sfär C18 D 12 g; gradient conditions: MeCN in water, in presence of 0.1% HCOOH, from 2% to 100%, 10 CV.

^1H NMR (400 MHz, $\text{DMSO-}d_6$) δ 9.75 (s, 2H), 7.84 (s, 1H), 7.48 – 7.42 (m, 2H), 7.41 – 7.33 (m, 3H), 7.07 – 7.00 (m, 2H), 6.93 – 6.85 (m, 1H), 6.25 (s, 1H), 4.20 (q, $J = 7.1$ Hz, 2H), 1.18 (t, $J = 7.1$ Hz, 3H). ^{13}C NMR (100 MHz, $\text{DMSO-}d_6$) δ 167.35, 167.21, 165.31, 150.13, 146.50, 136.21, 134.06, 129.64, 128.95, 128.73, 125.17, 124.25, 117.02, 116.80, 115.02, 62.23, 58.15, 14.39. $\text{C}_{20}\text{H}_{17}\text{NO}_6\text{S}$; UPLC-MS acidic (method A) r.t. 1.10 min, MS (ESI) $m/z = 400.1$ $[\text{M}+\text{H}]^+$.

Synthesis of 2-[(5Z)-5-[(3,4-dihydroxyphenyl)methylene]-2,4-dioxo-thiazolidin-3-yl]-N-ethylpropanamide (1n)



2-bromo-N-ethylpropanamide (35)

To a stirring solution of ethylamine (0.72 mL, 1.43 mmol) in DCM (2 mL), TEA (0.4 mL, 2.86 mmol) was added. The reaction mixture was cooled to 0 °C, then 2-bromopropanoyl

bromide (0.1 mL, 0.96 mmol) was added dropwise. After 0.5 h, the reaction mixture was allowed to reach room temperature and left stirring for further 4 h. The reaction mixture was filtered. The filtrate was diluted with Et₂O (5 mL) and filtered again. The filtrate was concentrated under reduced pressure and then taken up in DCM (2 mL) and CHX (2 mL) and filtered again. The filtrate was concentrated under reduced pressure to afford compound **35** (260 mg, 0.96 mmol theoretical, yield considered as quantitative) as an orange crude, which was used directly in the subsequent step without any further purification.

¹H NMR (400 MHz, Chloroform-*d*) δ 6.36 (s, 1H), 4.43 - 4.37 (m, 1H), 3.32 (qd, J = 7.3, 5.7 Hz, 2H), 1.88 (d, J = 7.1 Hz, 3H), 1.18 (t, J = 7.3 Hz, 3H). C₅H₁₀BrNO; UPLC-MS acidic (method A) r.t. 0.49 min, MS (ESI) m/z= 180.0 and 182.0 [M+H]⁺.

2-(2,4-dioxo-1,3-thiazolidin-3-yl)-N-ethylpropanamide (2n)

To a stirring solution of thiazolidine-2,4-dione (86 mg, 0.73 mmol) in dry DMF (2 mL), sodium hydride (as a 60% dispersion in mineral oil; 32 mg, 0.81 mmol) was added at 0 °C. After 10 min, the reaction was left reach room temperature and compound **35** (260 mg, 0.960 mmol theoretical) was added. After stirring overnight, the reaction mixture was quenched with water and then partitioned between EtOAc and water. The aqueous phase was then extracted with EtOAc (2 x). The organic phases were collected, dried over Na₂SO₄, filtered, and concentrated under *vacuum*. The residue was purified by direct phase flash chromatography (cartridge: Biotage sfär Silica D 10 g; gradient conditions: EtOAc in CHX, from 0% to 60%, 8 CV) to afford compound **2n** (26 mg, 0.12 mmol, 12% yield) as a colourless oil. C₈H₁₂N₂O₃S; UPLC-MS acidic (method A) r.t. 0.46 min, MS (ESI) m/z= 217.1 [M+H]⁺.

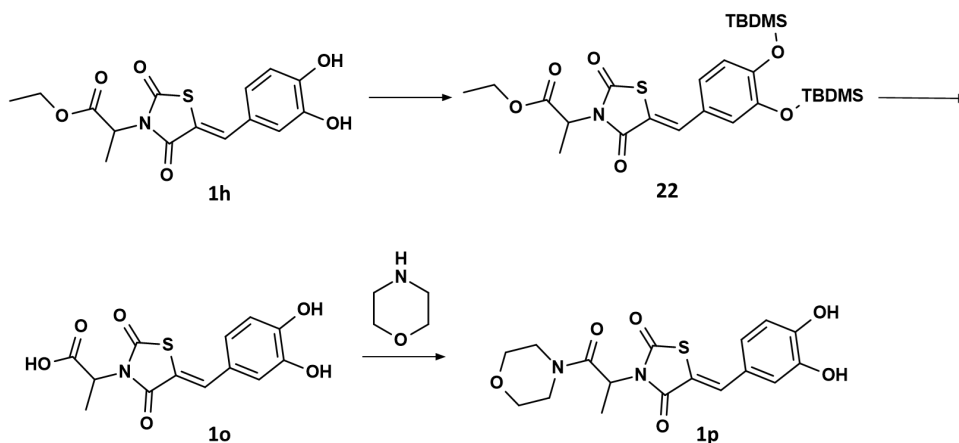
2-[(5Z)-5-[(3,4-dihydroxyphenyl)methylene]-2,4-dioxo-thiazolidin-3-yl]-N-ethylpropanamide (1n)

Compound **1n** was obtained from compound **2n** (25 mg, 0.12 mmol) and 3,4-dihydroxybenzaldehyde (17 mg, 0.12 mmol), by following the general procedure GP1 (conc. 0.124 M instead of 0.34 M), as a yellow solid (6 mg, 0.018 mmol, 15% overall isolated yield after purification by reversed phase flash chromatography); Cartridge: Biotage sfär Silica D 12 g, gradient conditions: MeCN in water, in presence of 0.1% HCOOH, from 2% to 60%, 10 CV.

¹H NMR (400 MHz, Methanol-*d*₄) δ 7.76 (s, 1H), 7.04 (d, J = 2.2 Hz, 1H), 6.98 (dd, J = 8.3, 2.2 Hz, 1H), 6.88 (d, J = 8.2 Hz, 1H), 4.96 (q, J = 7.2 Hz, 1H), 3.23 (q, J = 7.2 Hz, 2H), 1.60

(d, $J = 7.2$ Hz, 3H), 1.11 (t, $J = 7.2$ Hz, 3H). ^{13}C NMR (100 MHz, $\text{DMSO-}d_6$) δ 167.61, 167.55, 165.85, 149.63, 146.45, 134.16 (2C), 124.66, 124.57, 116.77, 51.80, 34.35, 15.08, 14.66. $\text{C}_{15}\text{H}_{16}\text{N}_2\text{O}_5\text{S}$; UPLC-MS acidic (method A) r.t. 0.75 min, MS (ESI) $m/z = 337.1$ $[\text{M}+\text{H}]^+$.

Synthesis of (5Z)-5-[(3,4-dihydroxyphenyl)methylene]-3-(1-methyl-2-morpholino-2-oxoethyl)thiazolidine-2,4-dione (1p)



Ethyl 2-[(5Z)-5-[(3,4-bis[(tert-butyldimethylsilyl)oxy]phenyl)methylene]-2,4-dioxo-1,3-thiazolidin-3-yl]propanoate (22)

A stirring solution of compound **1h** (634 mg, 1.9 mmol) and 4-dimethylaminopyridine (23 mg, 0.19 mmol) in dry DMF (3 mL) was placed under N_2 atmosphere. Then, TEA (0.65 mL, 4.7 mmol) and *tert*-butyldimethylsilyl chloride (708 mg, 4.7 mmol) were sequentially added and the resulting suspension was left stirring for 1 h at room temperature. The reaction was partitioned between EtOAc and $\text{NH}_4\text{Cl}_{\text{ss}}$, the organic phase was separated, washed with brine, dried over Na_2SO_4 , filtered, and concentrated under reduced pressure. The residue was purified by direct phase flash chromatography (cartridge: Biotage sfär Silica D 25 g; gradient conditions: EtOAc in CHX, from 0% to 80%, 12 CV) to afford compound **22** (1.06 g, 1.87 mmol, 99.7% yield) as a colourless oil.

^1H NMR (400 MHz, $\text{Chloroform-}d$) δ 7.79 (s, 1H), 7.02 (dq, $J = 4.7, 2.4$ Hz, 2H), 6.93 – 6.86 (m, 1H), 5.04 (q, $J = 7.2$ Hz, 1H), 4.30 – 4.15 (m, 2H), 1.65 (d, $J = 7.2$ Hz, 3H), 1.26 (t, $J = 7.1$ Hz, 3H), 1.00 (d, $J = 5.0$ Hz, 18H), 0.25 (d, $J = 3.5$ Hz, 12H). $\text{C}_{27}\text{H}_{43}\text{NO}_6\text{Si}_2\text{S}$; UPLC-MS acidic (method A) r.t. 1.88 min, MS (ESI) $m/z =$ No ionization.

2-[(5Z)-5-[(3,4-dihydroxyphenyl)methylene]-2,4-dioxo-thiazolidin-3-yl]propanoic acid (1o)

A mixture of compound **22** (910 mg, 1.61 mmol), glacial acetic acid (6 mL) and concentrated hydrogen chloride (3 mL, 36 mmol) was heated to 100 °C and left stirring for 2 h. The reaction was left reach room temperature, diluted with water and EtOAc. The organic phase was washed with NH₄Cl_{ss}, dried over Na₂SO₄, filtered, and concentrated under *vacuum*. The residue was purified by reversed phase flash chromatography (cartridge: Biotage sfär C18 D 12 g; gradient conditions: MeCN in water, in presence of 0.1% HCOOH, from 2% to 80%, 10 CV) to give the title compound **1o** (393 mg, 1.27 mmol, 79% yield), as a yellow solid.

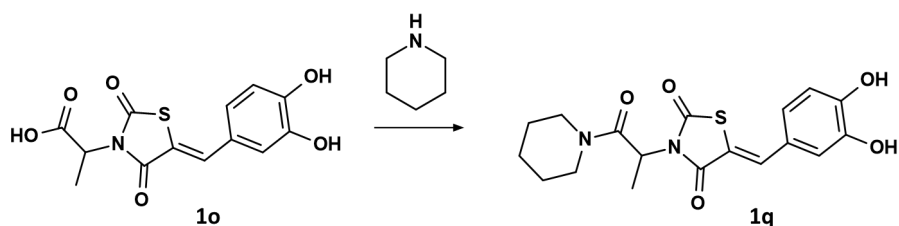
¹H NMR (400 MHz, DMSO-*d*₆) δ 13.19 (s, 1H), 9.91 (s, 1H), 9.50 (s, 1H), 7.77 (s, 1H), 7.05 – 6.98 (m, 2H), 6.89 (d, J = 8.1 Hz, 1H), 4.97 (q, J = 7.1 Hz, 1H), 1.50 (d, J = 7.2 Hz, 3H). C₁₃H₁₁NO₆S; UPLC-MS acidic (method A) r.t. 0.78 min, MS (ESI) m/z= 310.0 [M+H]⁺.

(5Z)-5-[(3,4-dihydroxyphenyl)methylene]-3-(1-methyl-2-morpholino-2-oxo-ethyl)thiazolidine-2,4-dione (1p)

A stirring solution of compound **1o** (30 mg, 0.1 mmol) in dry DMF (1 mL) was cooled to 0 °C, then DIPEA (20 μL, 0.1 mmol) was added followed by HATU (37 mg, 0.1 mmol). After 10 min, morpholine (10 μL, 0.1 mmol) was added and the resulting mixture was left stirring at room temperature for 4 h. The mixture was diluted with NH₄Cl_{ss} and extracted with EtOAc. The organic phase was separated, dried over Na₂SO₄, filtered, and concentrated under *vacuum*. The residue was purified by direct phase flash chromatography (Cartridge: Biotage sfär Silica D 10 g; gradient conditions: EtOAc in CHX, from 0% to 80%, 10 CV). The product containing fractions were collected and solvents were removed under reduced pressure. The residue (13 mg) was triturated in Et₂O to remove traces of tetramethylurea. The organic solvents were removed by filtration and the solid product was dried under *vacuum* to afford compound **1p** (11 mg, 0.03 mmol, 30% yield) as a yellow solid.

¹H NMR (400 MHz, DMSO-*d*₆) δ 7.74 (s, 1H), 7.05 – 6.97 (m, 2H), 6.87 (d, J = 8.0 Hz, 1H), 5.22 (q, J = 7.1 Hz, 1H), 3.67 – 3.42 (m, 8H), 1.51 (d, J = 7.1 Hz, 3H). ¹³C NMR (100 MHz, DMSO-*d*₆) δ 167.36, 166.92, 165.73, 149.68, 146.44, 134.93, 124.86, 124.52, 116.98, 116.78, 115.79, 66.48, 50.41, 42.42, 15.06. C₁₇H₁₈N₂O₆S; UPLC-MS acidic (method A) r.t. 0.74 min, MS (ESI) m/z= 379.2 [M+H]⁺.

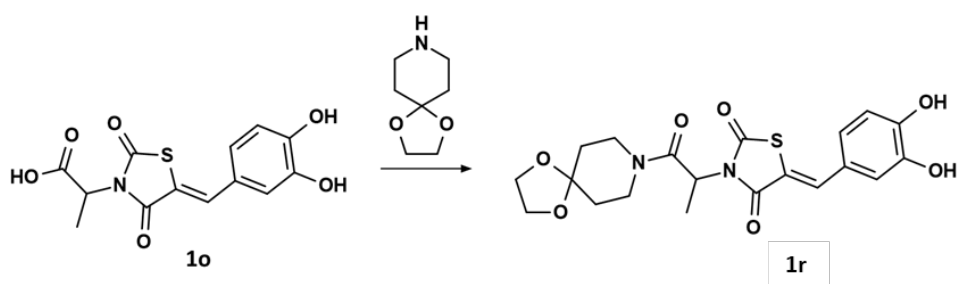
Synthesis of (5Z)-5-[(3,4-dihydroxyphenyl)methylene]-3-[1-methyl-2-oxo-2-(1-piperidyl)ethyl]thiazolidine-2,4-dione (1q)



A stirring solution of compound **1o** (30 mg, 0.1 mmol) in dry DMF (1 mL) was cooled to 0 °C, then DIPEA (40 μ L, 0.2 mmol) was added followed by HATU (37 mg, 0.1 mmol). After 10 min, piperidine (10 μ L, 0.1 mmol) was added and the resulting mixture was left stirring at room temperature for 4 h. The mixture was diluted with $\text{NH}_4\text{Cl}_{\text{ss}}$ and extracted with EtOAc. The organic phase was separated, dried over Na_2SO_4 , filtered, and the solvent was removed under *vacuum*. The residue was purified by direct phase flash chromatography (cartridge: Biotage sfär Silica D 10 g; gradient conditions: EtOAc in CHX, from 0% to 100%, 12 CV) to afford compound **1q** (18.5 mg, 0.05 mmol, 51% yield) as a yellow solid.

^1H NMR (400 MHz, Methanol- d_4) δ 7.78 (s, 1H), 7.03 (d, $J = 2.2$ Hz, 1H), 6.99 (dd, $J = 8.3, 2.2$ Hz, 1H), 6.88 (d, $J = 8.2$ Hz, 1H), 5.25 (q, $J = 7.0$ Hz, 1H), 3.88 – 3.65 (m, 1H), 3.42 – 3.33 (m, 2H), 3.30 – 3.21 (m, 1H), 1.74 – 1.57 (m, 4H), 1.56 (d, $J = 7.0$ Hz, 3H), 1.52 – 1.35 (m, 2H). ^{13}C NMR (100 MHz, DMSO- d_6) δ 167.30, 166.31, 165.72, 149.63, 146.44, 134.87, 124.84, 124.55, 116.99, 116.78, 115.84, 50.51, 46.28, 43.54, 26.17, 25.77, 24.37, 15.22. $\text{C}_{18}\text{H}_{20}\text{N}_2\text{O}_5\text{S}$; UPLC-MS acidic (method A) r.t. 0.88 min, MS (ESI) $m/z = 377.2$ $[\text{M}+\text{H}]^+$.

Synthesis of (5Z)-5-[(3,4-dihydroxyphenyl)methylene]-3-[2-(1,4-dioxo-8-azaspiro[4.5]decan-8-yl)-1-methyl-2-oxo-ethyl]thiazolidine-2,4-dione (1r)

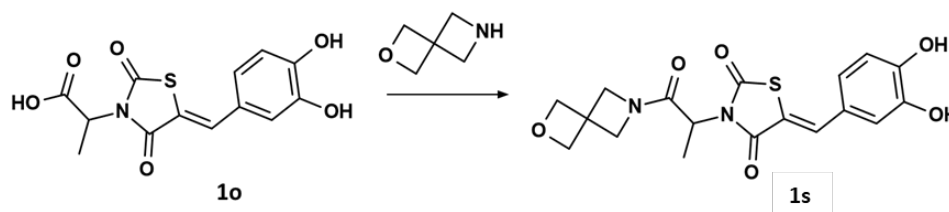


To a stirring solution of compound **1o** (55 mg, 0.18 mmol) in dry DMF (2 mL), HATU (67 mg, 0.18 mmol) was added at room temperature. After 10 min, DIPEA (60 μ L, 0.36 mmol) and 1,4-dioxo-8-azaspiro[4.5]decan-8-ylamine (25 mg, 0.18 mmol) were added and the resulting mixture was left stirring for 4 h. The mixture was diluted with $\text{NH}_4\text{Cl}_{\text{ss}}$ and extracted with EtOAc. The organic phase was separated, dried over Na_2SO_4 , filtered, and the solvent was

removed under *vacuum*. The residue was purified by direct phase flash chromatography (cartridge: Biotage sfär Silica D 10 g; gradient conditions: EtOAc in CHX, from 0% to 100%, 10 CV) to afford 18 mg of the title product as a yellow solid, which was further purified by reversed phase flash chromatography (cartridge: Biotage sfär C18 D 12 g; gradient conditions: MeCN in water, in presence of 0.1% HCOOH, from 2% to 60%, 10 CV) to give the title compound **1r** (13.3 mg, 0.031 mmol, 17% yield) as a yellow solid.

^1H NMR (400 MHz, DMSO- d_6) δ 7.75 (s, 1H), 7.10 – 6.96 (m, 2H), 6.86 (d, J = 7.9 Hz, 1H), 5.23 (q, J = 7.0 Hz, 1H), 3.87 (s, 4H), 3.38 – 3.27 (m, 4H), 1.72 – 1.53 (m, 2H), 1.52 – 1.37 (m, 2H), 1.48 (d, J = 6.9 Hz, 3H). ^{13}C NMR (100 MHz, DMSO- d_6) δ 167.29, 166.59, 165.68, 149.72, 146.44, 135.01, 124.92, 124.49, 116.98, 116.79, 115.69, 106.56, 64.29, 50.44, 43.40, 35.96, 15.23. $\text{C}_{20}\text{H}_{22}\text{N}_2\text{O}_7\text{S}$; UPLC-MS acidic (method A) r.t. 0.83 min, MS (ESI) m/z = 435.4 $[\text{M}+\text{H}]^+$.

Synthesis of (5Z)-5-[(3,4-dihydroxyphenyl)methylene]-3-[1-methyl-2-(2-oxa-6-azaspiro[3.3]heptan-6-yl)-2-oxo-ethyl]thiazolidine-2,4-dione (1s**)**

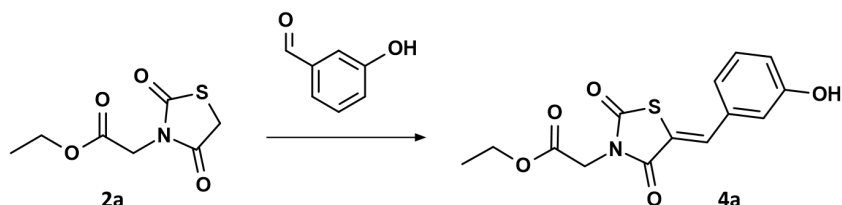


To a stirring solution of compound **1o** (55 mg, 0.18 mmol) in dry DMF (2 mL), HATU (67 mg, 0.18 mmol) was added at room temperature. After 10 min, DIPEA (60 μL , 0.36 mmol) and 2-oxa-6-azaspiro[3.3]heptane (18 mg, 0.18 mmol) were added and the resulting mixture was left stirring for 4 h. The mixture was diluted with $\text{NH}_4\text{Cl}_{\text{ss}}$ and extracted with EtOAc. The organic phase was separated, dried over Na_2SO_4 , filtered, and the solvent was removed under *vacuum*. The residue was purified by direct phase flash chromatography (cartridge: Biotage sfär Silica D 10 g; gradient conditions: EtOAc in CHX, from 0% to 100%, 10 CV, and then MeOH in EtOAc from 0% to 25%, 6 CV) to afford 30 mg of the title product as a yellow solid which was further purified by reversed phase flash chromatography (cartridge: Biotage sfär C18 D 12 g; gradient conditions: MeCN in water, in presence of 0.1% HCOOH, from 2% to 60%, 10 CV) to give the title compound **1s** (17 mg, 0.044 mmol, 25% yield) as a yellow solid.

^1H NMR (400 MHz, DMSO- d_6) δ 7.75 (s, 1H), 7.04 – 6.99 (m, 2H), 6.88 (d, J = 8.1 Hz, 1H), 4.96 (q, J = 7.1 Hz, 1H), 4.66 – 4.55 (m, 4H), 4.26 (d, J = 9.0 Hz, 1H), 4.12 – 4.03 (m, 2H), 4.00 (d, J = 10.3 Hz, 1H), 1.42 (d, J = 7.1 Hz, 3H). ^{13}C NMR (100 MHz, DMSO- d_6) δ

168.50, 167.08, 165.31, 149.62, 146.43, 135.06, 124.86, 124.58, 117.02, 116.78, 115.92, 80.20, 79.75, 60.25, 58.50, 49.69, 38.25, 14.21. C₁₈H₁₈N₂O₆S; UPLC-MS acidic (method A) r.t. 0.71 min, MS (ESI) m/z= 391.2 [M+H]⁺.

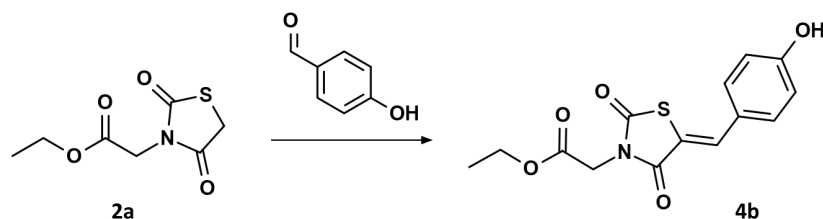
Synthesis of ethyl 2-[(5Z)-5-[(3-hydroxyphenyl)methylidene]-2,4-dioxo-1,3-thiazolidin-3-yl]acetate (4a)



Compound **4a** was obtained from compound **2a** (70 mg, 0.34 mmol) and 3-hydroxybenzaldehyde (46 mg, 0.38 mmol), by following the general procedure GP1, as a pale-yellow solid (64 mg, 0.208 mmol, 61% overall isolated yield after purification by reversed phase flash chromatography); Cartridge: Biotage sfär C18 D 12 g, gradient conditions: MeCN in water, in presence of 0.1% HCOOH, from 2% to 100%, 10 CV.

¹H NMR (400 MHz, DMSO-d₆) δ 9.91 (s, 1H), 7.91 (s, 1H), 7.35 (t, J = 7.9 Hz, 1H), 7.14 – 7.06 (m, 1H), 7.03 (t, J = 2.1 Hz, 1H), 6.92 (ddd, J = 8.3, 2.5, 0.9 Hz, 1H), 4.49 (s, 2H), 4.18 (q, J = 7.1 Hz, 2H), 1.22 (t, J = 7.1 Hz, 3H). ¹³C NMR (100 MHz, DMSO-d₆) δ 167.35, 167.13, 165.37, 158.41, 134.80, 134.34, 130.97, 121.96, 120.71, 118.72, 116.58, 62.11, 42.66, 14.40. C₁₄H₁₃NO₅S; UPLC-MS acidic (method A) r.t. 1.01 min, MS (ESI) m/z= 308.1 [M+H]⁺.

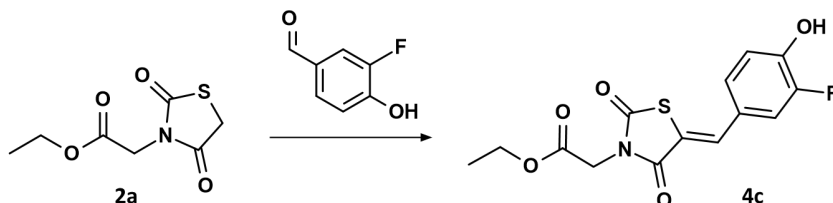
Synthesis of ethyl 2-[(5Z)-5-[(4-hydroxyphenyl)methylidene]-2,4-dioxo-1,3-thiazolidin-3-yl]acetate (4b)



Compound **4b** was obtained from compound **2a** (70 mg, 0.34 mmol) and 4-hydroxybenzaldehyde (46 mg, 0.38 mmol), by following the general procedure GP1, as a yellow solid (85.3 mg, 0.278 mmol, 81% overall isolated yield after purification by reversed phase flash chromatography); Cartridge: Biotage sfär C18 D 12 g, gradient conditions: MeCN in water, in presence of 0.1% HCOOH, from 2% to 100%, 10 CV.

^1H NMR (400 MHz, DMSO- d_6) δ 10.43 (s, 1H), 7.90 (s, 1H), 7.56 – 7.47 (m, 2H), 6.98 – 6.88 (m, 2H), 4.47 (s, 2H), 4.17 (q, J = 7.1 Hz, 2H), 1.21 (t, J = 7.1 Hz, 3H). $\text{C}_{14}\text{H}_{13}\text{NO}_5\text{S}$; UPLC-MS acidic (method A) r.t. 0.99 min, MS (ESI) m/z = 308.1 $[\text{M}+\text{H}]^+$.

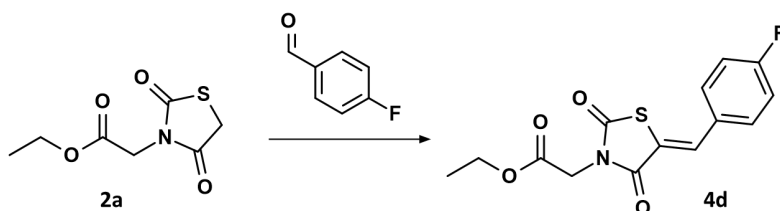
Synthesis of ethyl 2-[(5Z)-5-[(3-fluoro-4-hydroxyphenyl)methylidene]-2,4-dioxo-1,3-thiazolidin-3-yl]acetate (4c)



Compound **4c** was obtained from compound **2a** (70 mg, 0.34 mmol) and 3-fluoro-4-hydroxybenzaldehyde (49 mg, 0.35 mmol), by following the general procedure GP1, as a yellow solid (60.8 mg, 0.338 mmol, 54% overall isolated yield after purification by direct phase flash chromatography); *First column purification*: cartridge: Biotage sfär Silica D 10g; gradient conditions: EtOAc in CHX, from 0% to 50%, 10 CV; *Second column purification*: cartridge: Biotage sfär Silica D 10 g; gradient conditions: MeOH in DCM, from 0% to 10%, 10 CV.

^1H NMR (400 MHz, DMSO- d_6) δ 10.90 (s, 1H), 7.91 (s, 1H), 7.51 (dd, J = 12.4, 2.2 Hz, 1H), 7.34 (dd, J = 8.5, 2.2 Hz, 1H), 7.12 (t, J = 8.8 Hz, 1H), 4.48 (s, 2H), 4.17 (q, J = 7.1 Hz, 2H), 1.21 (t, J = 7.1 Hz, 3H). ^{13}C NMR (100 MHz, DMSO- d_6) δ 167.26, 167.16, 165.40, 152.60, 150.18, 148.63, 148.52, 133.94, 127.89, 124.67, 124.60, 119.19, 119.00, 118.10, 62.10, 42.64, 14.40. $\text{C}_{14}\text{H}_{12}\text{FNO}_5\text{S}$; UPLC-MS acidic (method A) r.t. 1.04 min, MS (ESI) m/z = 326.1 $[\text{M}+\text{H}]^+$.

Synthesis of ethyl 2-[(5Z)-5-[(4-fluorophenyl)methylidene]-2,4-dioxo-1,3-thiazolidin-3-yl]acetate (4d)

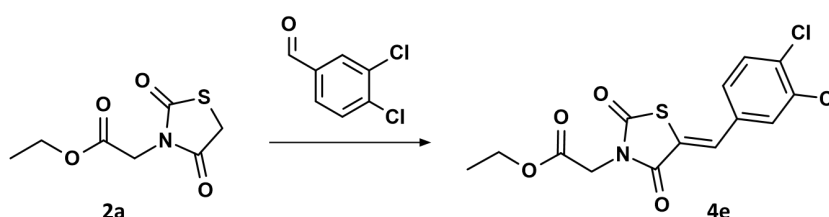


Compound **4d** was obtained from compound **2a** (70 mg, 0.34 mmol) and 4-fluorobenzaldehyde (43 mg, 0.35 mmol), by following the general procedure GP1, as a yellow solid (51.7 mg, 0.167 mmol, 49% overall isolated yield after purification by direct

phase flash chromatography); Cartridge: Biotage sfär Silica D 10 g, gradient conditions: EtOAc in DCM, from 0% to 50%, 10 CV.

^1H NMR (400 MHz, DMSO- d_6) δ 8.03 (s, 1H), 7.80 – 7.68 (m, 2H), 7.47 – 7.35 (m, 2H), 4.50 (s, 2H), 4.18 (q, $J = 7.1$ Hz, 2H), 1.22 (t, $J = 7.1$ Hz, 3H). ^{13}C NMR (100 MHz, DMSO- d_6) δ 167.20, 167.10, 165.33, 164.86, 162.36, 133.52, 133.31, 133.22, 129.89, 120.67, 117.20, 116.98, 62.11, 42.71, 14.40. $\text{C}_{14}\text{H}_{12}\text{FNO}_4\text{S}$; UPLC-MS acidic (method A) r.t. 1.16 min, MS (ESI) $m/z = 310.0$ $[\text{M}+\text{H}]^+$.

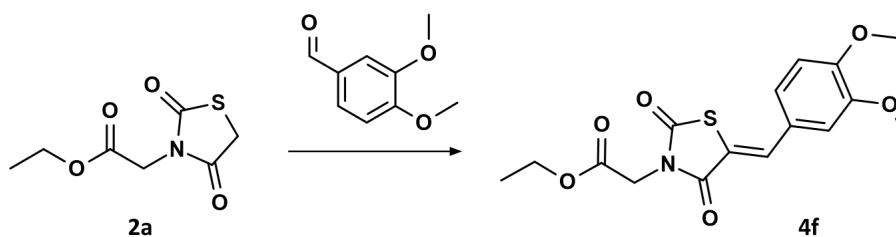
Synthesis of ethyl 2-[(5Z)-5-[(3,4-dichlorophenyl)methylidene]-2,4-dioxo-1,3-thiazolidin-3-yl]acetate (4e)



Compound **4e** was obtained from compound **2a** (50 mg, 0.25 mmol) and 3,4-dichlorobenzaldehyde (44 mg, 0.25 mmol), by following the general procedure GP1, as a yellow solid (52 mg, 0.144 mmol, 59% overall isolated yield after purification by direct phase flash chromatography); Cartridge: Biotage sfär Silica D 25 g, gradient conditions: EtOAc in CHX, from 0% to 50%, 10 CV.

^1H NMR (400 MHz, DMSO- d_6) δ 8.01 (s, 1H), 7.97 (d, $J = 2.1$ Hz, 1H), 7.83 (d, $J = 8.5$ Hz, 1H), 7.61 (dd, $J = 8.4, 2.1$ Hz, 1H), 4.50 (s, 2H), 4.18 (q, $J = 7.1$ Hz, 2H), 1.22 (t, $J = 7.1$ Hz, 3H). ^{13}C NMR (100 MHz, DMSO- d_6) δ 167.04, 166.80, 165.10, 133.92, 133.72, 132.92, 132.59, 131.99, 129.53, 123.27, 62.14, 42.79, 14.40. $\text{C}_{14}\text{H}_{11}\text{Cl}_2\text{NO}_4\text{S}$; UPLC-MS acidic (method A) r.t. 1.36 min, MS (ESI) $m/z = 360.0$ And 361.6 $[\text{M}+\text{H}]^+$.

Synthesis of ethyl 2-[(5Z)-5-[(3,4-dimethoxyphenyl)methylidene]-2,4-dioxo-1,3-thiazolidin-3-yl]acetate (4f)

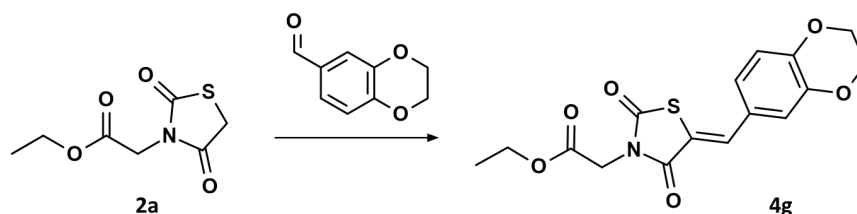


Compound **4f** was obtained from compound **2a** (70 mg, 0.34 mmol) and 3,4-dimethoxybenzaldehyde (58 mg, 0.35 mmol), by following the general procedure GP1, as a

yellow solid (95 mg, 0.269 mmol, 78% overall isolated yield after purification by direct phase flash chromatography); Cartridge: Biotage sfär Silica D 10 g, gradient conditions: EtOAc in CHX, from 0% to 50%, 10 CV.

^1H NMR (400 MHz, DMSO- d_6) δ 7.96 (s, 1H), 7.32 – 7.22 (m, 2H), 7.21 – 7.11 (m, 1H), 4.48 (s, 2H), 4.17 (q, J = 7.1 Hz, 2H), 3.84 (s, 3H), 3.82 (s, 3H), 1.21 (t, J = 7.1 Hz, 3H). ^{13}C NMR (100 MHz, DMSO- d_6) δ 167.41, 167.19, 165.43, 151.72, 149.45, 134.94, 125.83, 124.55, 117.79, 114.01, 112.63, 62.08, 56.20, 56.04, 42.62, 14.41. $\text{C}_{16}\text{H}_{17}\text{NO}_6\text{S}$; UPLC-MS acidic (method A) r.t. 1.11 min, MS (ESI) m/z = 352.1 $[\text{M}+\text{H}]^+$.

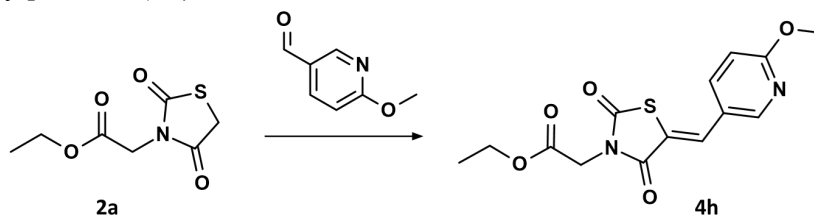
Synthesis of ethyl 2-[(5Z)-5-[(2,3-dihydro-1,4-benzodioxin-6-yl)methylidene]-2,4-dioxo-1,3-thiazolidin-3-yl]acetate (4g)



Compound **4g** was obtained from compound **2a** (70 mg, 0.34 mmol) and 2,3-dihydro-1,4-benzodioxin-6-carboxaldehyde (62 mg, 0.38 mmol), by following the general procedure GP1, as a yellow solid (85 mg, 0.242 mmol, 70% overall isolated yield after purification by reversed phase flash chromatography); Cartridge: Biotage sfär C18 D 12 g, gradient conditions: MeCN in water, in presence of 0.1% HCOOH, from 2% to 100%, 10 CV.

^1H NMR (400 MHz, DMSO- d_6) δ 7.90 (s, 1H), 7.20 – 7.14 (m, 2H), 7.04 (dd, J = 8.0, 0.7 Hz, 1H), 4.48 (s, 2H), 4.36 – 4.26 (m, 4H), 4.17 (q, J = 7.1 Hz, 2H), 1.21 (t, J = 7.1 Hz, 3H). ^{13}C NMR (100 MHz, DMSO- d_6) δ 167.29, 167.16, 165.41, 146.61, 144.24, 134.47, 126.46, 124.56, 119.58, 118.58, 118.33, 64.98, 64.43, 62.08, 42.63, 14.40. $\text{C}_{16}\text{H}_{15}\text{NO}_6\text{S}$; UPLC-MS acidic (method A) r.t. 1.15 min, MS (ESI) m/z = 350.1 $[\text{M}+\text{H}]^+$.

Synthesis of ethyl 2-[(5Z)-5-[(6-methoxy-3-pyridin-3-yl)methylidene]-2,4-dioxo-1,3-thiazolidin-3-yl]acetate (4h)

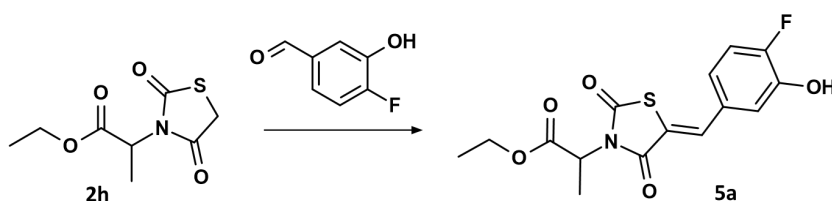


Compound **4h** was obtained from compound **2a** (70 mg, 0.34 mmol) and 6-methoxy-3-pyridinecarboxaldehyde (52 mg, 0.38 mmol), by following the general procedure GP1, as a

pale-yellow solid (68 mg, 0.212 mmol, 61% overall isolated yield after purification by reversed phase flash chromatography); Cartridge: Biotage sfär C18 D 12 g, gradient conditions: MeCN in water, in presence of 0.1% HCOOH, from 2% to 100%, 10 CV.

^1H NMR (400 MHz, DMSO- d_6) δ 8.57 (d, J = 2.6 Hz, 1H), 8.01 (s, 1H), 7.95 (dd, J = 8.8, 2.6 Hz, 1H), 7.02 (d, J = 8.7 Hz, 1H), 4.49 (s, 2H), 4.18 (q, J = 7.1 Hz, 2H), 3.94 (s, 3H), 1.21 (t, J = 7.1 Hz, 3H). ^{13}C NMR (100 MHz, DMSO- d_6) δ 167.12, 167.04, 165.25, 164.95, 151.38, 139.60, 131.66, 123.14, 119.57, 112.00, 62.11, 54.31, 42.72, 14.40. $\text{C}_{14}\text{H}_{13}\text{NO}_5\text{S}$; UPLC-MS acidic (method A) r.t. 1.10 min, MS (ESI) m/z = 323.1 $[\text{M}+\text{H}]^+$.

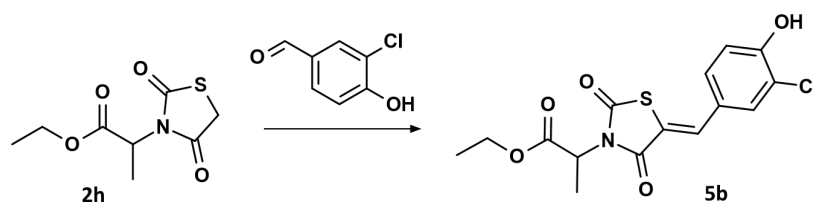
Synthesis of ethyl 2-[(5Z)-5-[(4-fluoro-3-hydroxy-phenyl)methylene]-2,4-dioxo-thiazolidin-3-yl]propanoate (5a)



Compound **5a** was obtained from compound **2h** (100 mg, 0.46 mmol) and 4-fluoro-3-hydroxy-benzaldehyde (65 mg, 0.46 mmol), by following the general procedure GP1 (conc. 0.46 M instead of 0.34 M), as a pale-yellow solid (122 mg, 0.36 mmol, 78% overall isolated yield after purification by direct phase flash chromatography); Cartridge: Biotage sfär Silica D 10 g, gradient conditions: EtOAc in CHX, from 0% to 40%, 10 CV.

^1H NMR (400 MHz, DMSO- d_6) δ 10.49 (s, 1H), 7.88 (s, 1H), 7.32 (dd, J = 11.1, 8.4 Hz, 1H), 7.23 (dd, J = 8.4, 2.3 Hz, 1H), 7.12 (ddd, J = 8.6, 4.3, 2.4 Hz, 1H), 5.11 (q, J = 7.1 Hz, 1H), 4.13 (qq, J = 6.9, 3.7 Hz, 2H), 1.51 (d, J = 7.2 Hz, 3H), 1.16 (t, J = 7.1 Hz, 3H). ^{13}C NMR (100 MHz, DMSO- d_6) δ 168.94, 167.04, 165.17, 146.26, 146.14, 133.89, 130.07, 123.17, 120.19, 119.02, 117.78, 117.59, 61.91, 50.71, 14.38 (2C). $\text{C}_{15}\text{H}_{14}\text{FNO}_5\text{S}$; UPLC-MS acidic (method A) r.t. 1.10 min, MS (ESI) m/z = 340.1 $[\text{M}+\text{H}]^+$.

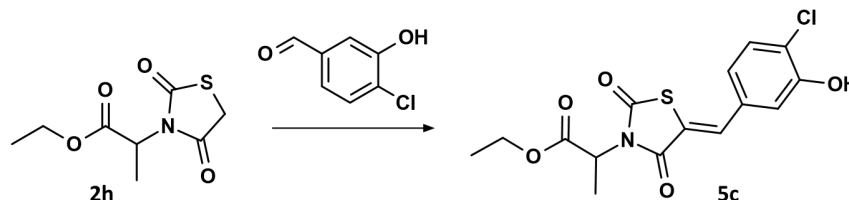
Synthesis of ethyl 2-[(5Z)-5-[(3-chloro-4-hydroxy-phenyl)methylene]-2,4-dioxo-thiazolidin-3-yl]propanoate (5b)



Compound **5b** was obtained from compound **2h** (100 mg, 0.46 mmol) and 3-chloro-4-hydroxybenzaldehyde (72 mg, 0.46 mmol), by following the general procedure GP1 (conc. 0.46 M instead of 0.34 M), as a pale-yellow solid (130 mg, 0.37 mmol, 80% overall isolated yield after purification by reversed phase flash chromatography); Cartridge: Biotage sfär C18 D 12 g, gradient conditions: MeCN in water, in presence of 0.1% HCOOH, from 2% to 100%, 10 CV.

¹H NMR (400 MHz, DMSO-d₆) δ 11.21 (s, 1H), 7.88 (s, 1H), 7.70 (d, J = 2.3 Hz, 1H), 7.45 (dd, J = 8.7, 2.3 Hz, 1H), 7.11 (d, J = 8.6 Hz, 1H), 5.10 (q, J = 7.1 Hz, 1H), 4.13 (qq, J = 7.2, 3.7 Hz, 2H), 1.50 (d, J = 7.2 Hz, 3H), 1.16 (t, J = 7.1 Hz, 3H). ¹³C NMR (100 MHz, DMSO-d₆) δ 168.98, 166.97, 165.21, 156.26, 133.58, 133.35, 130.51, 125.31, 121.21, 117.99, 117.86, 61.88, 50.65, 14.40 (2C). C₁₅H₁₄ClNO₅S; UPLC-MS acidic (method A) r.t. 1.13 min, MS (ESI) m/z= 356.0 and 358.0 [M+H]⁺.

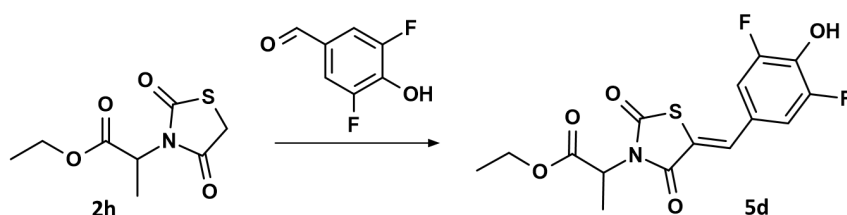
Synthesis of ethyl 2-[(5Z)-5-[(4-chloro-3-hydroxyphenyl)methylidene]-2,4-dioxo-1,3-thiazolidin-3-yl]propanoate (5c)



Compound **5c** was obtained from compound **2h** (100 mg, 0.46 mmol) and 4-chloro-3-hydroxy-benzaldehyde (72 mg, 0.46 mmol), by following the general procedure GP1 (conc. 0.46 M instead of 0.34 M), as a white solid (24 mg, 0.07 mmol, 15% overall isolated yield after purification by reversed phase flash chromatography and then by direct phase flash chromatography); *First column purification*: cartridge: Biotage sfär C18 D 12 g; gradient conditions: MeCN in water, in presence of 0.1% HCOOH, from 2% to 60%, 10 CV; *Second column purification*: cartridge: Biotage sfär Silica D 10 g; gradient conditions: EtOAc in CHX, from 0% to 80%, 12 CV.

¹H NMR (400 MHz, DMSO-d₆) δ 10.79 (s, 1H), 7.87 (s, 1H), 7.50 (d, J = 8.2 Hz, 1H), 7.21 (d, J = 2.2 Hz, 1H), 7.10 (dd, J = 8.4, 2.1 Hz, 1H), 5.12 (q, J = 7.1 Hz, 1H), 4.14 (qd, J = 7.1, 3.1 Hz, 2H), 1.51 (d, J = 7.2 Hz, 3H), 1.16 (t, J = 7.1 Hz, 3H). ¹³C NMR (100 MHz, DMSO-d₆) δ 168.92, 166.94, 165.13, 154.18, 133.62, 133.04, 131.26, 123.16, 123.01, 121.21, 117.22, 61.92, 50.75, 14.39, 14.36. C₁₅H₁₄ClNO₅S; UPLC-MS acidic (method A) r.t. 1.16 min, MS (ESI) m/z= 356.1 and 358.1 [M+H]⁺.

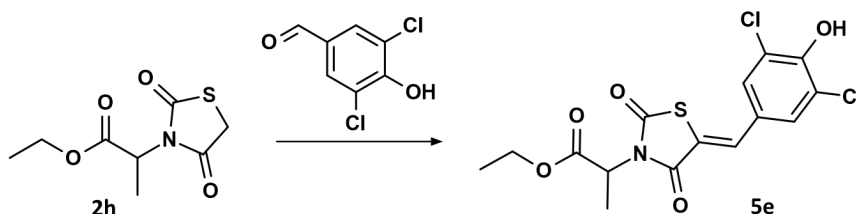
Synthesis of ethyl 2-[(5Z)-5-[(3,5-difluoro-4-hydroxy-phenyl)methylene]-2,4-dioxo-thiazolidin-3-yl]propanoate (5d)



Compound **5d** was obtained from compound **2h** (70 mg, 0.32 mmol) and 3,5-difluoro-4-hydroxy-benzaldehyde (51 mg, 0.32 mmol), by following the general procedure GP1, as a pale-yellow solid (75 mg, 0.21 mmol, 65% overall isolated yield after purification by reversed phase column chromatography). Cartridge: Biotage sfär C18 D 12 g, gradient conditions: MeCN in water, in presence of 0.1% HCOOH, from 2% to 100%, 10 CV.

^1H NMR (400 MHz, DMSO- d_6) δ 11.28 (s, 1H), 7.89 (s, 1H), 7.44 – 7.29 (m, 2H), 5.12 (q, $J = 7.1$ Hz, 1H), 4.14 (qq, $J = 7.1, 3.7$ Hz, 2H), 1.51 (d, $J = 7.1$ Hz, 3H), 1.16 (t, $J = 7.1$ Hz, 3H). ^{13}C NMR (100 MHz, DMSO- d_6) δ 168.92, 166.75, 165.08, 153.80, 151.38, 137.22, 132.80, 123.40, 119.90, 114.58, 114.51, 114.43, 114.35, 61.91, 50.74, 14.38 (2C). $\text{C}_{15}\text{H}_{13}\text{F}_2\text{NO}_5\text{S}$; UPLC-MS acidic r.t. 1.16 min, MS (ESI) $m/z = 358.0$ $[\text{M}+\text{H}]^+$.

Synthesis of ethyl 2-[(5Z)-5-[(3,5-dichloro-4-hydroxy-phenyl)methylene]-2,4-dioxo-thiazolidin-3-yl]propanoate (5e)

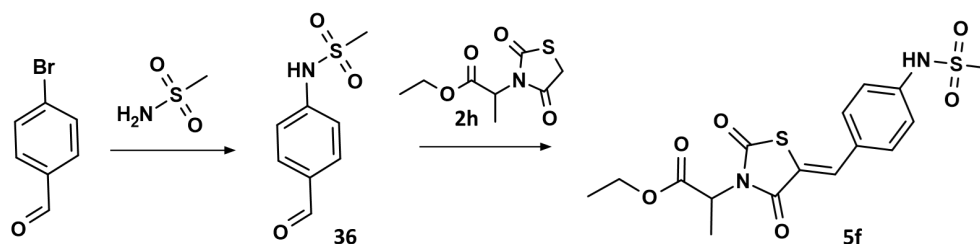


Compound **5e** was obtained from compound **2h** (100 mg, 0.46 mmol) and 3,5-dichloro-4-hydroxy-benzaldehyde (88 mg, 0.46 mmol), by following the general procedure GP1 (conc. 0.4 M instead of 0.34 M), as a pale orange solid (94 mg, 0.24 mmol, 52% overall isolated yield after purification by reversed phase flash chromatography).

Purification steps: After cooling the reaction mixture to room temperature, the precipitate was recovered by filtration. The filtrate was discarded, while the solid on the filter was washed with water, followed by DCM and MeOH. The residue was further purified by reversed phase flash chromatography (cartridge: Biotage sfär C18 D 12 g; gradient conditions: MeCN in Water, in presence of 0.1% HCOOH, from 2% to 100%, 10 CV) affording the title compound **5e**.

^1H NMR (400 MHz, DMSO- d_6) δ 11.18 (s, 1H), 7.88 (s, 1H), 7.64 (s, 2H), 5.11 (q, $J = 7.1$ Hz, 1H), 4.13 (qt, $J = 7.1, 3.6$ Hz, 2H), 1.51 (d, $J = 7.1$ Hz, 3H), 1.16 (t, $J = 7.1$ Hz, 3H). ^{13}C NMR (100 MHz, DMSO- d_6) δ 168.91, 166.60, 165.01, 151.93, 132.18, 130.80 (2C), 125.96, 123.36 (2C), 120.01, 61.91, 50.77, 14.38 (2C). $\text{C}_{15}\text{H}_{13}\text{Cl}_2\text{NO}_5\text{S}$; UPLC-MS acidic (method A) r.t. 1.29 min, MS (ESI) $m/z = 389.9$ and 391.9 $[\text{M}+\text{H}]^+$.

Synthesis of ethyl 2-[(5Z)-5-[[4-(methanesulfonamido)phenyl]methylene]-2,4-dioxo-thiazolidin-3-yl]propanoate (5f)



N-(4-formylphenyl)methanesulfonamide (36)

A stirring mixture of methanesulfonamide (154 mg, 1.62 mmol), potassium carbonate (374 mg, 2.7 mmol), 4-bromobenzaldehyde (250 mg, 1.35 mmol), tBuXPhos (11 mg, 0.03 mmol) and dry 2-Methyl-tetrahydrofuran (5 mL) was degassed with N_2 for 15 min. Then $[\text{Pd}(\text{allyl})\text{Cl}]_2$ (3 mg, 0.01 mmol) was added, and the reaction was heated to 80°C .⁷² After 3 h, the reaction was partitioned between water and EtOAc, the organic phase was separated, passed through a phase separator, and then concentrated under reduced pressure to afford compound **36** (269 mg, 1.35 mmol, 99.9% yield) as a brown solid. This crude was not further treated but used as such in the next experiment. $\text{C}_8\text{H}_9\text{NO}_3\text{S}$; UPLC-MS acidic (method A) r.t. 0.62 min, MS (ESI) $m/z = 200.0$ $[\text{M}+\text{H}]^+$.

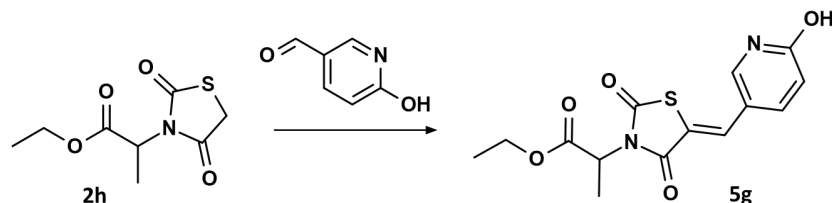
Ethyl 2-[(5Z)-5-[[4-(methanesulfonamido)phenyl]methylene]-2,4-dioxo-thiazolidin-3-yl]propanoate (5f)

Compound **5f** was obtained from compound **2h** (100 mg, 0.46 mmol) and compound **36** (130 mg, 0.65 mmol), by following the general procedure GP1 (conc. 0.23 M instead of 0.34 M), as a yellow solid (46 mg, 0.116 mmol, 25% overall isolated yield after purification by reversed phase flash chromatography). Cartridge: Biotage sfär C18 D 12 g, gradient conditions: MeCN in water, in presence of 0.1% HCOOH , from 2% to 60%, 10 CV.

^1H NMR (400 MHz, DMSO- d_6) δ 10.33 (s, 1H), 7.91 (s, 1H), 7.70 – 7.56 (m, 2H), 7.39 – 7.26 (m, 2H), 5.11 (q, $J = 7.1$ Hz, 1H), 4.14 (qt, $J = 7.1, 3.6$ Hz, 2H), 3.09 (s, 3H), 1.51 (d, $J = 7.2$ Hz, 3H), 1.16 (t, $J = 7.1$ Hz, 3H). ^{13}C NMR (100 MHz, DMSO- d_6) δ 168.98, 167.15, 165.28, 141.77, 134.08, 132.39 (2C), 127.62, 119.10 (2C), 118.64, 61.88, 50.66, 40.61,

14.39 (2C). C₁₆H₁₈N₂O₆S₂; UPLC-MS acidic (method A) r.t. 1.03 min, MS (ESI) m/z= 399.1 [M+H]⁺.

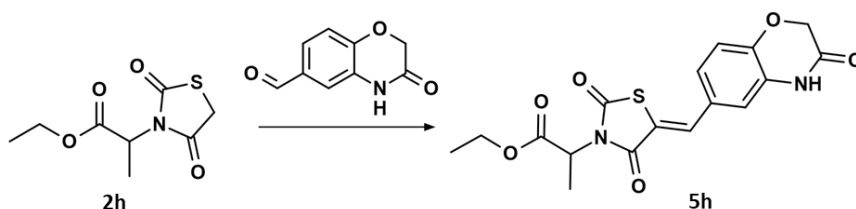
Synthesis of ethyl 2-[(5Z)-5-[(6-hydroxypyridin-3-yl)methylidene]-2,4-dioxo-1,3-thiazolidin-3-yl]propanoate (5g)



Compound **5g** was obtained from compound **2h** (100 mg, 0.46 mmol) and 6-Hydroxynicotinaldehyde (57 mg, 0.46 mmol), by following the general procedure GP1 (conc. 0.46 M instead of 0.34 M), as a white solid (89 mg, 0.28 mmol, 60% overall isolated yield after purification by filtration and trituration). *Purification steps:* After cooling the reaction mixture to room temperature, the precipitate was recovered by filtration. The filtrate was discarded, while the solid on the filter was washed with water, trituated in DCM and MeOH and dried under *vacuum* to afford the title product.

¹H NMR (400 MHz, DMSO-d₆) δ 12.27 (s, 1H), 8.06 (d, J = 2.8 Hz, 1H), 7.83 (s, 1H), 7.64 (dd, J = 9.7, 2.8 Hz, 1H), 6.49 (d, J = 9.7 Hz, 1H), 5.09 (q, J = 7.1 Hz, 1H), 4.13 (qq, J = 7.1, 3.7 Hz, 2H), 1.49 (d, J = 7.1 Hz, 3H), 1.15 (t, J = 7.1 Hz, 3H). ¹³C NMR (100 MHz, DMSO-d₆) δ 168.99, 166.74, 165.18, 161.71, 143.64, 138.83, 131.88, 121.21, 115.23, 112.31, 61.85, 50.62, 14.42 (2C). C₁₄H₁₄N₂O₅S; UPLC-MS acidic (method A) r.t. 0.80 min, MS (ESI) m/z= 323.1 [M+H]⁺.

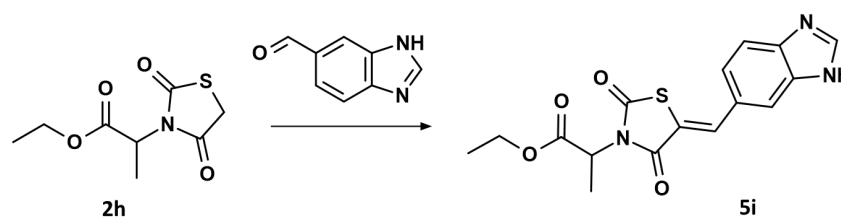
Synthesis of ethyl 2-[(5Z)-2,4-dioxo-5-[(3-oxo-4H-1,4-benzoxazin-6-yl)methylene]thiazolidin-3-yl]propanoate (5h)



Compound **5h** was obtained from compound **2h** (80 mg, 0.37 mmol) and 3-oxo-4H-1,4-benzoxazine-6-carbaldehyde (65 mg, 0.37 mmol), by following the general procedure GP1 (conc. 0.18 M instead of 0.34 M), as a pale-yellow solid (73 mg, 0.194 mmol, 53% overall isolated yield after purification direct phase flash chromatography). Cartridge: Biotage sfär Silica D 25 g, gradient conditions: EtOAc in CHX, from 0% to 50%, 10 CV.

^1H NMR (400 MHz, DMSO- d_6) δ 10.92 (s, 1H), 7.88 (s, 1H), 7.28 (dd, J = 8.5, 2.2 Hz, 1H), 7.17 (d, J = 2.2 Hz, 1H), 7.10 (d, J = 8.4 Hz, 1H), 5.11 (q, J = 7.1 Hz, 1H), 4.69 (s, 2H), 4.14 (qq, J = 6.9, 3.7 Hz, 2H), 1.51 (d, J = 7.2 Hz, 3H), 1.16 (t, J = 7.1 Hz, 3H). ^{13}C NMR (100 MHz, DMSO- d_6) δ 167.58, 165.82, 163.88, 141.46, 133.51, 132.31 (2C), 127.83, 119.32 (2C), 119.11, 66.37 (2C), 44.99 (2C), 43.00, 42.40. $\text{C}_{17}\text{H}_{16}\text{N}_2\text{O}_6\text{S}$; UPLC-MS acidic (method A) r.t. 1.03 min, MS (ESI) m/z = 377.1 $[\text{M}+\text{H}]^+$.

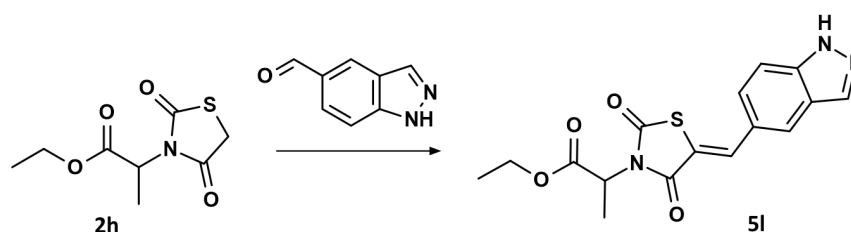
Synthesis of ethyl 2-[(5Z)-5-(1H-benzimidazol-5-ylmethylene)-2,4-dioxo-thiazolidin-3-yl] propanoate (5i)



Compound **5i** was obtained from compound **2h** (60 mg, 0.28 mmol) and 1H-benzimidazole-5-carbaldehyde (40 mg, 0.28 mmol), by following the general procedure GP1 (conc. 0.14 M instead of 0.34 M), as a pale-yellow solid (56 mg, 0.162 mmol, 59% overall isolated yield after purification by trituration in DCM).

^1H NMR (400 MHz, DMSO- d_6) δ 12.76 (s, 1H), 8.38 (s, 1H), 8.14 (s, 1H), 7.93 (d, J = 1.7 Hz, 1H), 7.75 (d, J = 8.4 Hz, 1H), 7.50 (dd, J = 8.5, 1.8 Hz, 1H), 5.13 (q, J = 7.1 Hz, 1H), 4.15 (qd, J = 7.1, 2.9 Hz, 2H), 1.52 (d, J = 7.1 Hz, 3H), 1.17 (t, J = 7.1 Hz, 3H). ^{13}C NMR (100 MHz, DMSO- d_6) δ 169.02, 167.26, 165.33, 145.18, 136.13 (2C), 130.82, 127.05, 124.91, 124.81, 120.77, 118.09, 61.89, 50.65, 14.43 (2C). $\text{C}_{16}\text{H}_{15}\text{N}_3\text{O}_4\text{S}$; UPLC-MS acidic (method A) r.t. 0.73 min, MS (ESI) m/z = 346.1 $[\text{M}+\text{H}]^+$.

Synthesis of ethyl 2-[(5Z)-5-(1H-indazol-5-ylmethylene)-2,4-dioxo-thiazolidin-3-yl] propanoate (5l)

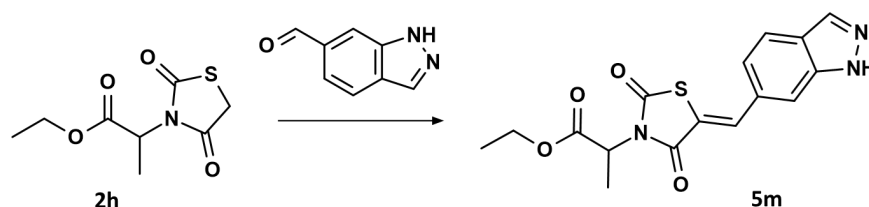


Compound **5l** was obtained from compound **2h** (100 mg, 0.46 mmol) and indazole-5-carboxaldehyde (67 mg, 0.46 mmol), by following the general procedure GP1 (conc. 0.23 M instead of 0.34 M), as a pale-yellow solid (78 mg, 0.23 mmol, 49% overall isolated yield

after purification by reversed phase flash chromatography); Cartridge: Biotage sfär C18 D 12 g, gradient conditions: MeCN in water, in presence of 0.1% HCOOH, from 2% to 100%, 10 CV.

^1H NMR (400 MHz, DMSO- d_6) δ 13.42 (s, 1H), 8.26 (d, J = 1.0 Hz, 1H), 8.16 – 8.14 (m, 1H), 8.12 (s, 1H), 7.74 – 7.68 (m, 1H), 7.62 (dd, J = 8.8, 1.7 Hz, 1H), 5.13 (q, J = 7.1 Hz, 1H), 4.14 (qq, J = 7.1, 3.7 Hz, 2H), 1.52 (d, J = 7.1 Hz, 3H), 1.17 (t, J = 7.1 Hz, 3H). ^{13}C NMR (100 MHz, DMSO- d_6) δ 169.02, 167.26, 165.33, 140.62, 135.73, 135.70, 128.07, 125.73, 125.24, 123.84, 118.06, 111.81, 61.89, 50.65, 14.39 (2C). $\text{C}_{16}\text{H}_{15}\text{N}_3\text{O}_4\text{S}$; UPLC-MS acidic (method A) r.t. 1.02 min, MS (ESI) m/z = 346.1 $[\text{M}+\text{H}]^+$.

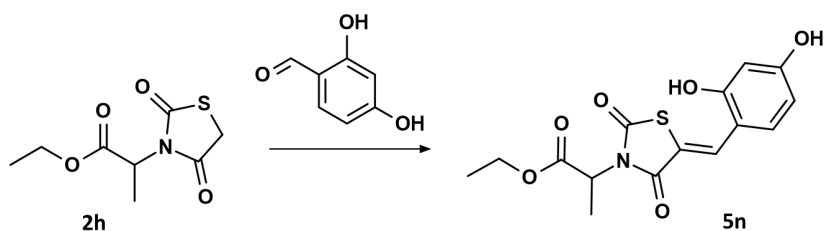
Synthesis of ethyl 2-[(5Z)-5-(1H-indazol-6-ylmethylene)-2,4-dioxo-thiazolidin-3-yl] propanoate (5m)



Compound **5m** was obtained from compound **2h** (100 mg, 0.46 mmol) and 1H-indazole-6-carboxaldehyde (67 mg, 0.46 mmol), by following the general procedure GP1 (conc. 0.23 M instead of 0.34 M), as a pale-yellow solid (62 mg, 0.18 mmol, 39% overall isolated yield after purification by reversed phase flash chromatography); Cartridge: Biotage sfär C18 D 12 g, gradient conditions: MeCN in water, in presence of 0.1% HCOOH, from 2% to 100%, 10 CV.

^1H NMR (400 MHz, DMSO- d_6) δ 13.41 (s, 1H), 8.20 – 8.14 (m, 2H), 7.93 (d, J = 8.4 Hz, 1H), 7.89 (s, 1H), 7.37 (dd, J = 8.5, 1.5 Hz, 1H), 5.14 (q, J = 7.1 Hz, 1H), 4.15 (qd, J = 7.1, 2.9 Hz, 2H), 1.53 (d, J = 7.1 Hz, 3H), 1.17 (t, J = 7.1 Hz, 3H). ^{13}C NMR (100 MHz, DMSO- d_6) δ 168.96, 167.11, 165.20, 140.32, 135.49, 134.31, 130.90, 124.16, 122.15, 121.86, 120.64, 113.51, 61.92, 50.74, 14.40 (2C). $\text{C}_{16}\text{H}_{15}\text{N}_3\text{O}_4\text{S}$; UPLC-MS acidic (method A) r.t. 1.05 min, MS (ESI) m/z = 346.1 $[\text{M}+\text{H}]^+$.

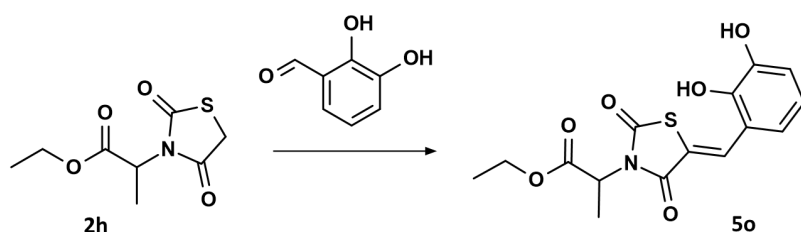
Synthesis of ethyl 2-[(5Z)-5-[(2,4-dihydroxyphenyl)methylene]-2,4-dioxo-thiazolidin-3-yl]propanoate (5n)



To a stirring solution of compound **2h** (200 mg, 0.87 mmol) and 2,4-dihydroxybenzaldehyde (121 mg, 0.88 mmol) in ethanol (2.2 mL), piperidine (43 μ L, 0.44 mmol) was added and the resulting mixture was heated under reflux for 9 h. After cooling the reaction mixture to room temperature, it was acidified with acetic acid (0.05 mL, 0.87 mmol) and then concentrated under *vacuum*. The residue was purified by reversed phase flash chromatography (cartridge: Biotage sfär C18 D 12 g; gradient conditions: MeCN in water, in presence of 0.1% HCOOH, from 2% to 80%, 10 CV) affording compound **5n** (68 mg, 0.2 mmol, 23% yield) as a yellow solid.

^1H NMR (400 MHz, DMSO) δ 10.56 (s, 1H), 10.26 (s, 1H), 8.11 (s, 1H), 7.29 – 7.17 (m, 1H), 6.50 – 6.38 (m, 2H), 5.07 (q, J = 7.1 Hz, 1H), 4.13 (qq, J = 7.2, 3.7 Hz, 2H), 1.49 (d, J = 7.2 Hz, 3H), 1.15 (t, J = 7.1 Hz, 3H). ^{13}C NMR (100 MHz, DMSO- d_6) δ 169.11, 167.58, 165.61, 162.68, 160.13, 130.90, 130.11, 114.11, 111.91, 109.02, 102.97, 61.80, 50.42, 14.48, 14.40. $\text{C}_{15}\text{H}_{15}\text{NO}_6\text{S}$; UPLC-MS acidic (method A) r.t. 0.96 min, MS (ESI) m/z = 338.4 $[\text{M}+\text{H}]^+$.

Synthesis of ethyl 2-[(5Z)-5-[(2,3-dihydroxyphenyl)methylene]-2,4-dioxo-thiazolidin-3-yl]propanoate (5o)

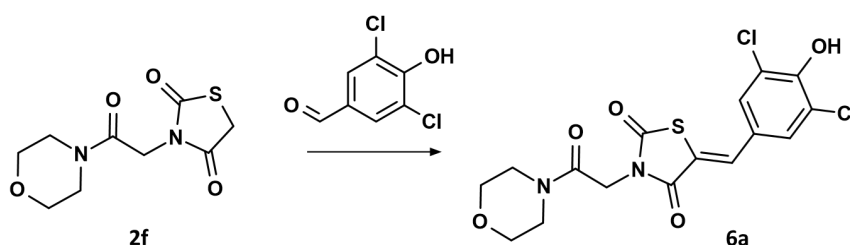


To a stirring solution of compound **2h** (200 mg, 0.87 mmol) and 2,3-dihydroxybenzaldehyde (121 mg, 0.88 mmol) in ethanol (2.2 mL), piperidine (43 μ L, 0.44 mmol) was added and the resulting mixture was heated under reflux for 9 h. After cooling the reaction mixture to room temperature, it was acidified with acetic acid (0.05 mL, 0.87 mmol) and then concentrated under *vacuum*. The residue was purified by reversed phase flash chromatography (cartridge: Biotage sfär C18 D 12 g; gradient conditions: MeCN in water, in presence of 0.1% HCOOH,

from 2% to 80%, 10 CV) affording compound **5o** (177 mg, 0.53 mmol, 60% yield) as a yellow solid.

^1H NMR (400 MHz, DMSO) δ 9.68 (s, 2H), 8.18 (s, 1H), 6.93 (dd, $J = 7.6, 1.7$ Hz, 1H), 6.85 (dd, $J = 8.0, 1.7$ Hz, 1H), 6.82 – 6.77 (m, 1H), 5.10 (q, $J = 7.1$ Hz, 1H), 4.14 (qt, $J = 7.1, 3.7$ Hz, 2H), 1.51 (d, $J = 7.2$ Hz, 3H), 1.16 (t, $J = 7.1$ Hz, 3H). ^{13}C NMR (100 MHz, DMSO- d_6) δ 169.02, 167.49, 165.43, 146.71, 146.36, 130.20, 120.78, 120.17, 119.18, 119.03, 118.36, 61.86, 50.57, 14.42 (2C). $\text{C}_{15}\text{H}_{15}\text{NO}_6\text{S}$; UPLC-MS acidic (method A) r.t. 1.01 min, MS (ESI) $m/z = 338.5$ $[\text{M}+\text{H}]^+$.

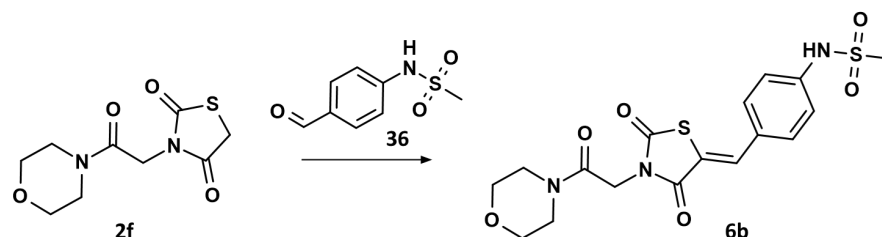
Synthesis of (5Z)-5-[(3,5-dichloro-4-hydroxy-phenyl)methylene]-3-(2-morpholino-2-oxoethyl)thiazolidine-2,4-dione (6a)



To a stirring solution of compound **2f** (70 mg, 0.23 mmol) and 3,5-dichloro-4-hydroxybenzaldehyde (44 mg, 0.23 mmol) in ethanol (0.6 mL), piperidine (10 μL , 0.12 mmol) was added and the resulting mixture was heated under reflux for 3 h. After cooling the reaction mixture to room temperature, the yellow precipitate was recovered by filtration, the filtrate was discarded and then the solid on the filter was washed with EtOH. To remove the residual traces of piperazine present in the batch (detected by NMR), the solid was washed with $\text{NH}_4\text{Cl}_{\text{ss}}$, water and CH_3CN and then dried under *vacuum* at 50 $^\circ\text{C}$ for 5 hrs. To remove the residual traces of NH_4Cl (detected by NMR), the solid was taken up with water and sonicated for 20 min. Then the solid precipitate was recovered by filtration and dried under *vacuum* at 50 $^\circ\text{C}$ for 18 hrs to afford the title compound **6a** (46 mg, 0.11 mmol, 47% yield) as a pale-yellow solid.

^1H NMR (400 MHz, DMSO- d_6) δ 7.85 (s, 1H), 7.64 (s, 2H), 4.61 (s, 2H), 3.67 – 3.61 (m, 2H), 3.60 – 3.56 (m, 2H), 3.56 – 3.51 (m, 2H), 3.46 – 3.41 (m, 2H). ^{13}C NMR (100 MHz, DMSO- d_6) δ 170.32, 165.35, 151.57, 149.39, 146.63, 143.25, 135.14, 125.38, 116.22, 110.96, 108.83, 60.94, 41.54, 14.57. $\text{C}_{16}\text{H}_{14}\text{Cl}_2\text{N}_2\text{O}_5\text{S}$; UPLC-MS acidic (method A) r.t. 0.99 min, MS (ESI) $m/z = 417.1$ $[\text{M}+\text{H}]^+$.

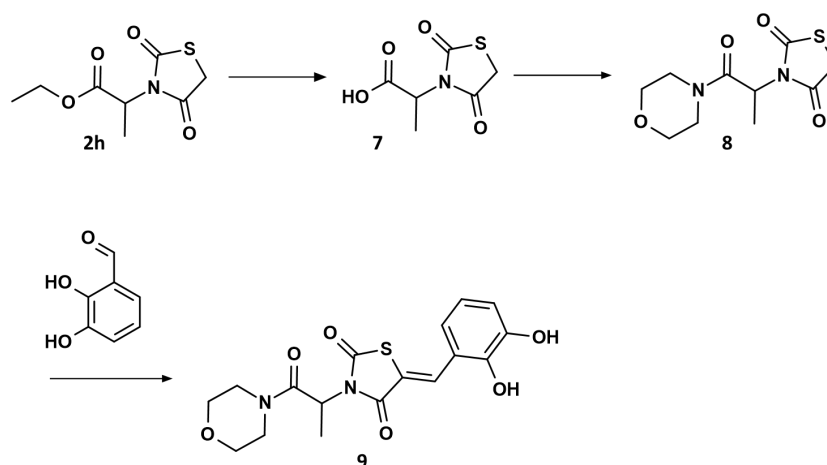
Synthesis of *N*-[4-[(*Z*)-[3-(2-morpholino-2-oxo-ethyl)-2,4-dioxo-thiazolidin-5-ylidene]methyl]phenyl]methanesulfonamide (6b**)**



To a stirring solution of compound **2f** (149 mg, 0.5 mmol) and compound **36** (140 mg, 0.7 mmol) in ethanol (4 mL), piperidine (30 μ L, 0.350 mmol) was added and the resulting mixture was heated under reflux for 3 h. After cooling the reaction mixture to room temperature, the yellow precipitate was recovered by filtration. The filtrate was discarded and the solid on the filter was washed with EtOH and then further purified by trituration in MeOH to afford compound **6b** (14.5 mg, 0.034 mmol, 5% yield) as a pale-yellow solid.

^1H NMR (400 MHz, DMSO- d_6) δ 10.30 (s, 1H), 7.89 (s, 1H), 7.66 – 7.59 (m, 2H), 7.37 – 7.27 (m, 2H), 4.61 (s, 2H), 3.64 (t, J = 4.7 Hz, 2H), 3.58 (t, J = 4.8 Hz, 2H), 3.58 – 3.51 (m, 2H), 3.44 (t, J = 4.7 Hz, 2H), 3.09 (s, 3H). ^{13}C NMR (100 MHz, DMSO- d_6) δ 168.98, 167.15, 165.28, 141.77, 134.08, 132.39 (2C), 127.62, 119.10 (2C), 118.64, 61.88, 50.66, 40.61, 14.39 (2C). $\text{C}_{17}\text{H}_{19}\text{N}_3\text{O}_6\text{S}_2$; UPLC-MS acidic (method A) r.t. 0.77 min, MS (ESI) m/z = 426.2 $[\text{M}+\text{H}]^+$.

Synthesis of (*SZ*)-5-[(2,3-dihydroxyphenyl)methylene]-3-(1-methyl-2-morpholino-2-oxo-ethyl)thiazolidine-2,4-dione (9**)**



2-(2,4-dioxothiazolidin-3-yl)propanoic acid (7**)**

A mixture of compound **2h** (500 mg, 2.3 mmol) in acetic acid (2 mL) and concentrated hydrochloric acid (1 mL, 12 mmol) was refluxed for 1 h. The reaction

was concentrated in vacuo and the residue partitioned between water and EtOAc. The aqueous phase was extracted with EtOAc (3 x), the organic phases were collected, dried over Na₂SO₄, filtered and concentrated in vacuo. The residue was purified by reversed phase flash chromatography (cartridge: Biotage sfär C18 D 12 g; gradient conditions: MeCN in water, in presence of 0.1% HCOOH, from 2% to 50%, 10 CV) to afford compound **7** (606 mg, yield considered as quantitative: 2.3 mmol theoretical. Purity: 55% w/w by NMR. Presence of DMSO: 45% w/w detected by NMR), as a colourless oil.

¹H NMR (400 MHz, DMSO-d₆) δ 13.06 (s, 1H), 4.81 (q, J = 7.2 Hz, 1H), 4.38 – 4.19 (m, 2H), 1.42 (d, J = 7.2 Hz, 3H). C₆H₇NO₄S; UPLC-MS acidic (method A) r.t. 0.52 min, MS (ESI) m/z= 189.95 [M+H]⁺.

3-(1-methyl-2-morpholino-2-oxo-ethyl)thiazolidine-2,4-dione (8)

To a solution of compound **7** (606 mg, 1.76 mmol) in dry DMF (3.5 mL), HATU (670 mg, 1.76 mmol) was added, and the resulting solution was left stirring for 10 min. Then DIPEA (0.46 mL, 2.64 mmol) and morpholine (0.15 mL, 1.76 mmol) were added and the resulting solution was left stirring at 25 °C for 4 h. The reaction mixture was diluted with NaHCO₃ and extracted with EtOAc (3 x). The organic phases were collected, dried over Na₂SO₄, filtered, and concentrated under reduced pressure. The residue was purified by direct phase flash chromatography (cartridge: Biotage sfär Silica D 10 g; gradient conditions: EtOAc in CHX, from 0% to 50%, 10 CV) to give compound **8** (391 mg, 1.51 mmol, 86% yield) as a white solid.

¹H NMR (400 MHz, Chloroform-d) δ 5.04 (q, J = 7.2 Hz, 1H), 3.97 (d, J = 2.8 Hz, 2H), 3.79 – 3.23 (m, 8H), 1.63 (d, J = 7.2 Hz, 3H). C₁₀H₁₄N₂O₄S; UPLC-MS acidic (method A) r.t. 0.49 - 0.52 min, MS (ESI) m/z= 259.0 [M+H]⁺.

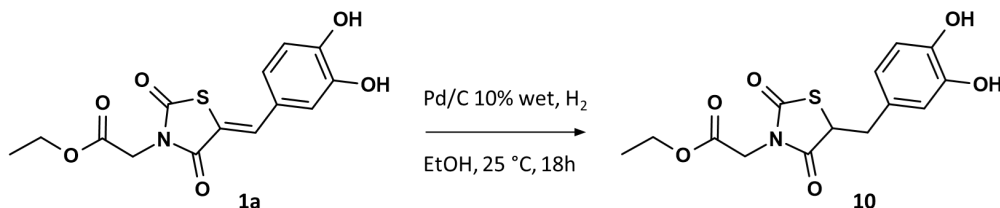
(5Z)-5-[(2,3-dihydroxyphenyl)methylene]-3-(1-methyl-2-morpholino-2-oxo-ethyl)thiazolidine-2,4-dione (9)

Compound **9** was obtained from compound **8** (40 mg, 0.16 mmol) and 2,3-dihydroxybenzaldehyde (22 mg, 0.16 mmol), by following the general procedure GP1 (conc. 0.16 M instead of 0.34 M), as a brown solid (13 mg, 0.034 mmol, 22% overall isolated yield after purification by reversed phase flash chromatography). Cartridge: Biotage sfär C18 D 12 g, gradient conditions: MeCN in water, in presence of 0.1% HCOOH, from 2% to 80%, 10 CV.

¹H NMR (400 MHz, DMSO-d₆) δ 9.61 (s, 1H), 8.16 (s, 1H), 6.91 (dd, J = 7.6, 1.7 Hz, 1H), 6.84 (dd, J = 8.0, 1.7 Hz, 1H), 6.78 (t, J = 7.8 Hz, 1H), 5.24 (q, J = 7.1 Hz, 1H), 3.63 – 3.43

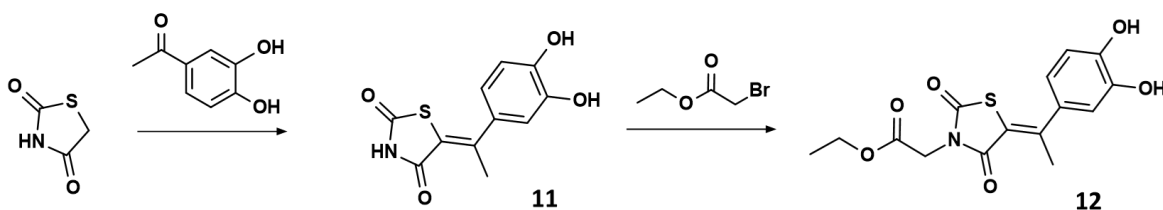
(m, 6H), 3.43 – 3.36 (m, 2H), 1.52 (d, J = 7.1 Hz, 3H). ¹³C NMR (100 MHz, DMSO-*d*₆) δ 167.53, 166.90, 165.83, 146.64, 146.33, 129.72, 120.88, 120.17, 119.13, 119.00, 118.26, 66.50 (2C), 50.51, 45.94, 42.87, 15.04. C₁₇H₁₈N₂O₆S; UPLC-MS acidic (method A) r.t. 0.80 min, MS (ESI) m/z= 379.1 [M+H]⁺.

Synthesis of ethyl 2-{5-[(3,4-dihydroxyphenyl)methyl]-2,4-dioxo-1,3-thiazolidin-3-yl} acetate (10)



Compound **1a** (0.17 mL, 0.06 mmol) was dissolved in dry ethanol (10 mL). The mixture was degassed with N₂, then Pd/C 10% wet (20 mg, 0.02 mmol) was added followed by molecular hydrogen (0.12 mg, 0.06 mmol). The reaction was stirred at 6 atm of hydrogen for 18 h. Then the mixture was filtered over a pad of Celite (packed and washed with EtOH) and concentrated under *vacuum*. The residue was purified by direct phase flash chromatography (cartridge: Biotage sfär Silica D 10 g; gradient conditions: EtOAc in CHX, from 0% to 60%, 10 CV) to afford compound **10** (16.8 mg, 0.052 mmol, 83% yield), as a colourless oil. ¹H NMR (400 MHz, Chloroform-*d*) δ 6.81 (d, J = 8.1 Hz, 1H), 6.76 (d, J = 2.1 Hz, 1H), 6.65 (dd, J = 8.1, 2.1 Hz, 1H), 5.50 (s, 2H), 4.49 (dd, J = 8.9, 4.3 Hz, 1H), 4.32 (s, 2H), 4.23 (q, J = 7.2 Hz, 2H), 3.41 (dd, J = 14.3, 4.3 Hz, 1H), 3.12 (dd, J = 14.3, 8.9 Hz, 1H), 1.30 (t, J = 7.2 Hz, 3H). C₁₄H₁₅NO₆S; UPLC-MS acidic (method A) r.t. 0.80 min, MS (ESI) m/z= 326.1 [M+H]⁺.

Synthesis of ethyl 2-[(5Z)-5-[1-(3,4-dihydroxyphenyl)ethylidene]-2,4-dioxo-1,3-thiazolidin-3-yl]acetate (12)



(5Z)-5-[1-(3,4-dihydroxyphenyl)ethylidene]-1,3-thiazolidine-2,4-dione (11)

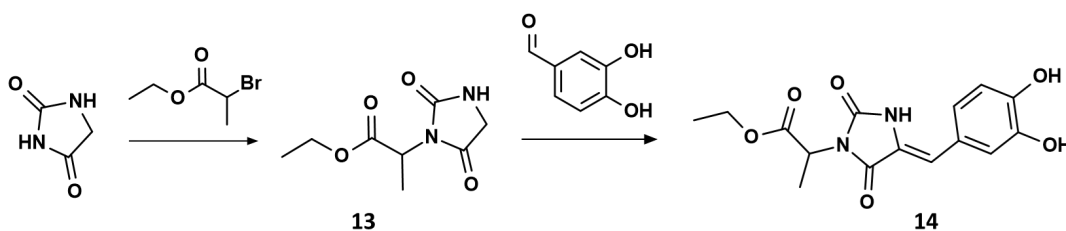
To a stirring suspension of thiazolidine-2,4-dione (100 mg, 0.85 mmol) and 1-(3,4-dihydroxyphenyl) ethanone (131 mg, 0.86 mmol) in dry toluene (4.6 mL), piperidine (42 μ L, 0.43 mmol) and acetic acid (20 μ L, 0.43 mmol) were added and the reaction was heated under reflux for 2 days. The mixture was allowed to reach room temperature and then partitioned between EtOAc and water. The organic phase was washed with brine and then dried over Na₂SO₄, filtered, and concentrated under reduced pressure. The residue was purified by reverse phase flash chromatography on a Biotage sfär C18 D 12 g (using as eluent a gradient of MeCN in water, in presence of 0.1% HCOOH, from 2% to 70%, 10 CV) to afford compound **11** (117 mg, 0.47 mmol, 55% yield) as an orange solid. ¹H NMR (400 MHz, DMSO-d₆) δ 12.11 (s, 1H), 9.40 (s, 1H), 9.22 (s, 1H), 6.83 (d, J = 2.1 Hz, 1H), 6.78 (d, J = 8.2 Hz, 1H), 6.73 (dd, J = 8.2, 2.1 Hz, 1H), 2.59 (s, 3H). C₁₁H₉NO₄S; UPLC-MS acidic (method A) r.t. 0.67 min, MS (ESI) m/z= 252.1 [M+H]⁺.

2-[(5Z)-5-[1-(3,4-dihydroxyphenyl)ethylidene]-2,4-dioxo-1,3-thiazolidin-3-yl]acetate (12)

To a stirring suspension of compound **11** (50 mg, 0.2 mmol) and potassium carbonate (55 mg, 0.4 mmol) in a mixture 3.5:1 of dry MeCN (3.5 mL) and DMF (1 mL), 2-bromoacetic acid ethyl ester (0.02 mL, 0.2 mmol) was added dropwise under nitrogen atmosphere at room temperature. After 18 h, the reaction was concentrated in vacuo and the residue partitioned between EtOAc and water. The aqueous phase was extracted with EtOAc (2 x), the organic phases were collected, dried over Na₂SO₄, filtered and concentrated under reduced pressure. The residue was subjected to direct phase flash chromatography (Cartridge: Biotage sfär Silica D 10 g; gradient conditions: EtOAc in CHX, from 0% to 50%, 10 CV) to afford compound **12** (30.6 mg, 0.091 mmol, 46% yield) as a yellow solid.

¹H NMR (400 MHz, DMSO-d₆) δ 6.87 (d, J = 1.9 Hz, 1H), 6.84 – 6.77 (m, 2H), 4.41 (s, 2H), 4.17 (q, J = 7.1 Hz, 2H), 2.66 (s, 3H), 1.21 (t, J = 7.1 Hz, 3H). ¹³C NMR (100 MHz, DMSO-d₆) δ 167.71, 167.38, 164.45, 153.01, 147.65, 145.94, 132.84, 119.21, 117.69, 116.21, 114.73, 61.98, 42.14, 22.38, 14.42. C₁₅H₁₅NO₆S; UPLC-MS acidic (method A) r.t. 0.92 min, MS (ESI) m/z= 338.2 [M+H]⁺.

Synthesis of ethyl 2-[(4Z)-4-[(3,4-dihydroxyphenyl)methylidene]-2,5-dioximidazolidin-1-yl]propanoate (14)



Ethyl 2-(2,5-dioximidazolidin-1-yl)propanoate (13)

To a stirring suspension of imidazolidine-2,4-dione (300 mg, 3 mmol) and potassium carbonate (456 mg, 3.3 mmol) in dry THF (9 mL), ethyl 2-bromopropanoate (0.37 mL, 3.3 mmol) was added at room temperature and the reaction was heated under reflux for 18 h. The mixture was allowed to reach room temperature and then partitioned between EtOAc and water. The organic phase was separated, dried over Na₂SO₄, filtered and concentrated under reduced pressure. The residue was subjected to direct phase flash chromatography (cartridge: Biotage sfär Silica D 10 g; gradient conditions: EtOAc in CHX, from 0% to 100%, 10 CV) to afford compound **13** (469 mg, 2.34 mmol, 78% yield) as a colourless oil. ¹H NMR (400 MHz, DMSO-d₆) δ 8.16 (s, 1H), 4.67 (q, J = 7.2 Hz, 1H), 4.10 (qd, J = 7.1, 2.1 Hz, 2H), 3.97 (d, J = 3.7 Hz, 2H), 1.42 (d, J = 7.2 Hz, 3H), 1.16 (t, J = 7.1 Hz, 3H). C₈H₁₂N₂O₄; UPLC-MS acidic (method A) r.t. 0.51 min, MS (ESI) m/z = 201.1 [M+H]⁺.

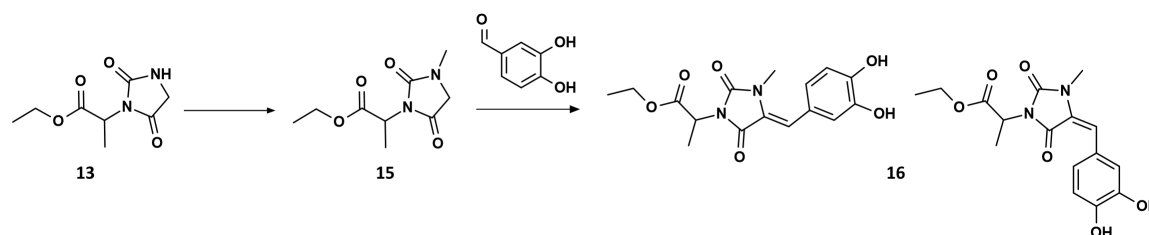
Ethyl 2-[(4Z)-4-[(3,4-dihydroxyphenyl)methylidene]-2,5-dioximidazolidin-1-yl]propanoate (14)

To a stirring suspension of 3,4-dihydroxybenzaldehyde (41 mg, 0.3 mmol) and compound **13** (60 mg, 0.3 mmol) in dry toluene (2 mL), piperidine (16 μL, 0.15 mmol) and acetic acid (10 μL, 0.15 mmol) were added at room temperature and the reaction was then heated under reflux for 18 h. Then, the reaction mixture was concentrated in vacuo and the residue partitioned between EtOAc and water. The organic phase was separated, dried over Na₂SO₄, filtered and concentrated under reduced pressure. The residue was subjected to direct phase flash chromatography (cartridge: Biotage sfär Silica D 25 g; gradient conditions: EtOAc in CHX, from 0% to 80%, 10 CV) to afford compound **14** (50 mg, 0.16 mmol, 52% yield) as a yellow solid.

¹H NMR (400 MHz, DMSO-d₆) δ 7.04 – 6.98 (m, 2H), 6.80 – 6.73 (m, 1H), 6.41 (s, 1H), 4.81 (q, J = 7.2 Hz, 1H), 4.12 (qd, J = 7.1, 2.1 Hz, 2H), 1.50 (d, J = 7.2 Hz, 3H), 1.16 (t, J = 7.1 Hz, 3H). ¹³C NMR (100 MHz, DMSO-d₆) δ 169.80, 163.85, 154.53, 147.40, 145.87,

124.37, 123.99, 122.27, 117.80, 116.29, 112.31, 61.67, 47.63, 15.03, 14.43. C₁₅H₁₆N₂O₆; UPLC-MS acidic (method A) r.t. 0.76 min, MS (ESI) m/z= 321.2 [M+H]⁺.

Synthesis of ethyl 2-[(4Z)-4-[(3,4-dihydroxyphenyl)methylene]-3-methyl-2,5-dioxoimidazolidin-1-yl]propanoate and ethyl 2-[(4E)-4-[(3,4-dihydroxyphenyl)methylene]-3-methyl-2,5-dioxoimidazolidin-1-yl]propanoate, obtained as a mixture of geometric isomers (16)



Ethyl 2-(3-methyl-2,5-dioxoimidazolidin-1-yl)propanoate (15)

To a stirring solution of compound **13** (100 mg, 0.49 mmol) in dry DMF (2 mL), potassium carbonate (68 mg, 0.49 mmol) was added at room temperature. After 10 min, iodomethane (30 μ L, 0.54 mmol) was added and reaction was left stirring at room temperature for 18 h. Then, the reaction was partitioned between EtOAc and water. The organic phase was separated, dried over Na₂SO₄, filtered and concentrated under reduced pressure. The residue was subjected to direct phase flash chromatography (cartridge: Biotage sfär Silica D 10 g; gradient conditions: EtOAc in CHX, from 0% to 80%, 10 CV) to afford compound **15** (97 mg, 0.45 mmol, 92% yield) as a yellow oil.

¹H NMR (400 MHz, DMSO-d₆) δ 4.68 (q, J = 7.2 Hz, 1H), 4.10 (q, J = 7.0 Hz, 2H), 4.03 (d, J = 2.9 Hz, 2H), 2.86 (s, 3H), 1.43 (d, J = 7.2 Hz, 3H), 1.16 (t, J = 7.1 Hz, 3H). C₉H₁₄N₂O₄; UPLC-MS acidic (method A) r.t. 0.57 min, MS (ESI) m/z= 215.1 [M+H]⁺.

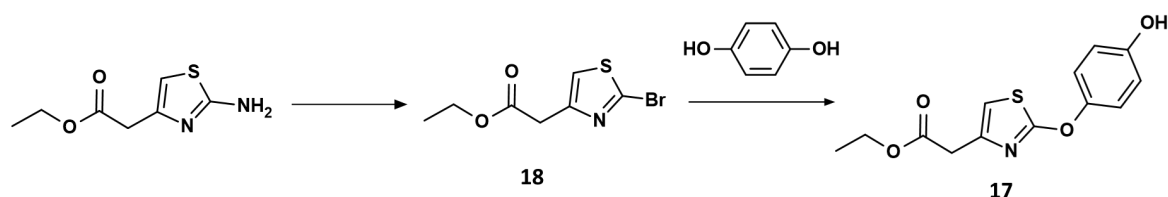
Ethyl 2-[(4Z)-4-[(3,4-dihydroxyphenyl)methylene]-3-methyl-2,5-dioxoimidazolidin-1-yl]propanoate and ethyl 2-[(4E)-4-[(3,4-dihydroxyphenyl)methylene]-3-methyl-2,5-dioxoimidazolidin-1-yl]propanoate, obtained as a mixture of geometric isomers (16)

To a stirring suspension of compound **15** (72 mg, 0.34 mmol) and 3,4-dihydroxybenzaldehyde (56 mg, 0.41 mmol) in dry toluene (2 mL), piperidine (20 μ L, 0.17 mmol) and acetic acid (10 μ L, 0.17 mmol) were added at room temperature and the reaction was heated for 18 h under reflux. After cooling to room temperature, the reaction mixture was partitioned between water and EtOAc (the black gummy solid residue was dissolved with 2 mL of DMSO and then added to the work up mixture). The organic phase was separated, dried over Na₂SO₄, filtered and concentrated under reduced pressure. The residue

was purified by reversed phase flash chromatography (cartridge: Biotage sfär C18 D 12 g; gradient conditions: MeCN in water, in presence of 0.1% HCOOH, from 2% to 80%, 10 CV) and then by direct phase flash chromatography (Cartridge: Biotage sfär Silica D 10 g, gradient conditions: EtOAc in CHX, from 0% to 80%, 10 CV) to afford compound **16** (35 mg, 0.104 mmol, 31% yield) as a brown solid and a mixture 1:2 of Z/E regioisomers. By NOE correlation it was possible to assign the regiochemistry to the two isomers: the minor isomer has the Z configuration, while the major isomer has the E configuration.

Minor isomer: ^1H NMR (400 MHz, DMSO- d_6) δ 6.81 (d, $J = 2.0$ Hz, 1H), 6.78 (d, $J = 8.1$ Hz, 1H), 6.76-6.73 (m, 1H), 6.69 (s, 1H), 4.89 – 4.83 (m, 1H), 4.14 (q, $J = 7.1$ Hz, 2H), 2.98 (s, 3H), 1.51 (d, $J = 7.2$ Hz, 3H), 1.18 (t, $J = 7.1$ Hz, 3H). Major Isomer: ^1H NMR (400 MHz, DMSO- d_6) δ 7.71 (d, $J = 2.1$ Hz, 1H), 7.31 (dd, $J = 8.5, 2.1$ Hz, 1H), 6.74 (d, $J = 8.3$ Hz, 1H), 6.43 (s, 1H), 4.86 (q, $J = 7.2$ Hz, 1H), 4.13 (q, $J = 7.1$ Hz, 2H), 3.15 (s, 3H), 1.51 (d, $J = 7.2$ Hz, 3H), 1.16 (t, $J = 7.1$ Hz, 3H). Mixture of isomers: ^{13}C NMR (100 MHz, DMSO- d_6) δ 169.69, 162.85, 160.90, 152.15, 147.53, 146.70, 145.31, 145.02, 127.63, 125.98, 124.55, 124.20, 123.30, 122.30, 119.83, 117.91, 117.36, 115.78, 115.51, 113.51, 61.67, 61.59, 48.14, 47.73, 30.85, 26.69, 14.93, 14.36. UPLC-MS acidic (method A) r.t. 0.81 and 0.83 min, MS (ESI) $m/z = 335.2$ $[\text{M}+\text{H}]^+$.

Synthesis of ethyl 2-[2-(4-hydroxyphenoxy)thiazol-4-yl]acetate (17)



Ethyl 2-(2-bromothiazol-4-yl)acetate (18)

To a solution of Copper (II) bromide (68 mg, 0.31 mmol) and 2-(2-amino-4-thiazolyl)acetic acid ethyl ester (100 mg, 0.54 mmol) in MeCN (4 mL), t-butyl nitrite (50 μ L, 0.4 mmol) was added and the reaction mixture was left stirring for 18 h at room temperature under N₂ atmosphere. The reaction mixture was diluted with DCM and washed with a 1M solution of HCl. The phases were separated, the aqueous phase was re-extracted with DCM (2 x), and the combined organic layers were dried over Na₂SO₄, filtered, and concentrated under reduced pressure. The residue was purified by direct phase flash chromatography (cartridge: Biotage sfär Silica D 10 g; gradient conditions: EtOAc in CHX, from 0% to 30%, 10 CV) to afford compound **18** (22 mg, 0.088 mmol, 16% yield) as a colourless oil.

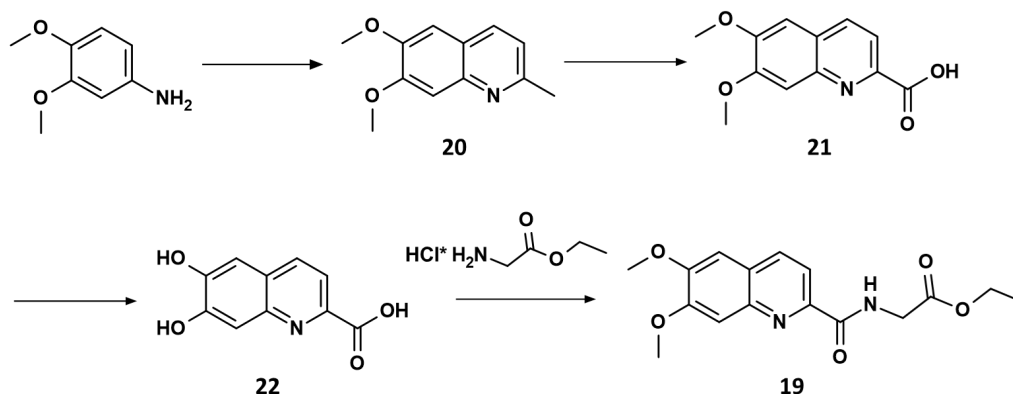
¹H NMR (400 MHz, DMSO-d₆) δ 7.55 (d, J = 0.8 Hz, 1H), 4.10 (q, J = 7.1 Hz, 2H), 3.82 (d, J = 0.9 Hz, 2H), 1.19 (t, J = 7.1 Hz, 3H). C₇H₈BrNO₂S; UPLC-MS acidic (method A) r.t. 0.89 min, MS (ESI) m/z= No ionization.

Ethyl 2-[2-(4-hydroxyphenoxy)thiazol-4-yl]acetate (17)

A mixture of hydroquinone (10 mg, 0.09 mmol), compound **18** (22 mg, 0.09 mmol) and potassium carbonate (12 mg, 0.09 mmol) in dry DMF (2 mL) was heated to 140 °C and left stirring at that temperature for 18 h under nitrogen atmosphere. The reaction mixture was left reach room temperature and then diluted with NH₄Cl_{ss} and EtOAc. The organic phase was separated, dried over Na₂SO₄, filtered, and concentrated under reduced pressure. The residue was purified by reversed phase flash chromatography (cartridge: Biotage sfär C18 D 12 g; gradient conditions: MeCN in water, in presence of 0.1% HCOOH, from 2% to 100%, 12 CV) to afford the title compound **17** (3 mg, 0.011 mmol, 12% yield), as a brown oil.

¹H NMR (400 MHz, Methanol-d₄) δ 7.14 – 7.08 (m, 2H), 6.87 – 6.81 (m, 2H), 6.80 – 6.74 (m, 1H), 4.17 (q, J = 7.1 Hz, 2H), 3.63 (d, J = 0.9 Hz, 2H), 1.26 (t, J = 7.1 Hz, 3H). C₁₃H₁₃NO₄S; UPLC-MS acidic (method A) r.t. 0.89 min, MS (ESI) m/z= 280.1 [M+H]⁺.

Synthesis of ethyl 2-[(6,7-dihydroxyquinoline-2-carbonyl)amino]acetate (19)



6,7-dimethoxy-2-methylquinoline (20)

To a stirring solution of ethyl vinyl ether (0.63 mL, 6.53 mmol) in dry toluene (10 mL), 3,4-dimethoxyaniline (500 mg, 3.26 mmol) and iodine (41 mg, 0.16 mmol) were added, and the resulting mixture was heated at 80 °C for 3 h. After cooling the reaction mixture to room temperature, it was diluted with Na₂S₂O₃ and extracted with EtOAc. The organic phase was separated, dried over Na₂SO₄, filtered and concentrated under reduced pressure. The residue was purified by direct phase flash chromatography (cartridge: Biotage sfär KP-Amino D 28 g; gradient conditions: EtOAc in CHX, from 0% to 100%, 10 CV) to afford compound **20** (130 mg, 0.64 mmol, 20% yield) as a yellow oil.

¹H NMR (400 MHz, DMSO-d₆) δ 8.04 (d, J = 8.3 Hz, 1H), 7.29 (s, 1H), 7.27 (s, 1H), 7.21 (d, J = 8.3 Hz, 1H), 3.90 (s, 3H), 3.88 (s, 3H), 2.58 (s, 3H). C₁₂H₁₃NO₂; UPLC-MS acidic (method A) r.t. 0.40 min, MS (ESI) m/z = 204.1 [M+H]⁺.

6,7-dimethoxyquinoline-2-carboxylic acid (21)

To a stirring solution of compound **20** (100 mg, 0.49 mmol) in pyridine (0.5 mL) selenium dioxide (164 mg, 1.48 mmol) was added, and the reaction mixture was heated at 115 °C for 4 h. After cooling the reaction mixture to room temperature, it was diluted with a 1M solution of HCl. Then, the aqueous phase was gradually neutralized by addition of a 1 M solution of NaOH and extracted with EtOAc at different pH (2-7). As most of the product remain in the aqueous phase, it was recollected with the organic phases and the resulting mixture was concentrated under reduced pressure. The residue was purified by reversed phase flash chromatography (cartridge: Biotage sfär C18 D 30 g; gradient conditions: MeCN in water, in presence of 0.1% HCOOH, from 2% to 40%, 7 CV) to afford compound **21** (53 mg, 0.23 mmol, 46% yield) as a yellow oil.

^1H NMR (400 MHz, DMSO- d_6) δ 12.97 (s, 1H), 8.33 (d, J = 8.4 Hz, 1H), 7.96 (d, J = 8.4 Hz, 1H), 7.49 (s, 1H), 7.44 (s, 1H), 3.97 (s, 3H), 3.96 (s, 3H). $\text{C}_{12}\text{H}_{11}\text{NO}_4$; UPLC-MS acidic (method A) r.t. 0.49 min, MS (ESI) m/z = 234.1 $[\text{M}+\text{H}]^+$.

6,7-dihydroxyquinoline-2-carboxylic acid (22)

A stirring solution of compound **21** (53 mg, 0.23 mmol) in hydrogen bromide (48% w/w in water; 0.08 mL, 0.680 mmol) was heated at 120 °C for 2 days. After cooling the reaction mixture to room temperature, the precipitation of an orange solid was observed. The orange solid was recovered by filtration to afford compound **22** (34 mg, 0.17 mmol, 73% yield).

^1H NMR (400 MHz, DMSO- d_6) δ 11.22 (br s, 1H), 10.83 (br s, 1H), 8.59 (d, J = 8.3 Hz, 1H), 8.01 (d, J = 8.3 Hz, 1H), 7.64 (s, 1H), 7.38 (s, 1H). $\text{C}_{10}\text{H}_7\text{NO}_5$; UPLC-MS acidic (method A) r.t. 0.20 - 0.36 min, MS (ESI) m/z = 206.1 $[\text{M}+\text{H}]^+$.

Ethyl 2-[(6,7-dihydroxyquinoline-2-carbonyl)amino]acetate (19)

To a stirring solution of compound **22** (34 mg, 0.17 mmol) in dry DMF (1 mL), HATU (63 mg, 0.17 mmol) and DIPEA (60 μL , 0.33 mmol) were added. The resulting solution was left stirring at room temperature for 10 min, then glycine ethyl ester hydrochloride (23 mg, 0.17 mmol) was added. After 45 min, water and $\text{NH}_4\text{Cl}_{\text{ss}}$ were added (pH = 7) and the mixture was extracted with EtOAc. The organic phase was washed with water and then concentrated under reduced pressure. The residue was purified by reversed phase flash chromatography (cartridge: Biotage sfär C18 D 12 g; gradient conditions: MeCN in water, in presence of 0.1% HCOOH, from 2% to 40%, 8 CV) to afford compound **19** (6 mg, 0.021 mmol, 13% yield) as a yellow solid.

^1H NMR (400 MHz, DMSO- d_6) δ 10.23 (s, 2H), 9.04 (t, J = 6.2 Hz, 1H), 8.18 (d, J = 8.4 Hz, 1H), 7.84 (d, J = 8.4 Hz, 1H), 7.34 (s, 1H), 7.19 (s, 1H), 4.14 (q, J = 7.1 Hz, 2H), 4.08 (d, J = 6.1 Hz, 2H), 1.22 (t, J = 7.1 Hz, 3H). ^{13}C NMR (100 MHz, DMSO- d_6) δ 167.02, 165.54, 163.79, 151.75, 131.66, 130.74 (2C), 126.13, 123.33, 120.64, 66.37 (2C), 45.00 (2C), 43.09, 42.41. $\text{C}_{14}\text{H}_{14}\text{N}_2\text{O}_5$; UPLC-MS acidic (method A) r.t. 0.69 min, MS (ESI) m/z = 291.2 $[\text{M}+\text{H}]^+$.

Synthesis of PROTACs

Capsule chemistry: Synple Chem technology

The Synple Chem technology is an automated flow-batch hybrid system which was employed in this project for the PROTAC synthesis. This technology consists of an automated synthesizer that uses commercially available reagent cartridges (Fig. 5.1). All the reagent cartridges consist of four different compartments, which are pre-filled with all the reagents needed for the reaction, plus the materials needed to isolate the product and a chip containing the reaction protocols (Fig. 5.2). The PROTAC cartridges and methods enable the user to rapidly prepare PROTAC analogues in an automated fashion and avoid the need for the manual manipulation of the difficult to handle partial PROTAC materials.



Figure 5.1: Synple Chem console and reagent cartridges (image adapted from: https://synplechem.com/images/2021/05/12/machinev_wlines.38_hp.jpg, 19/11/2022).

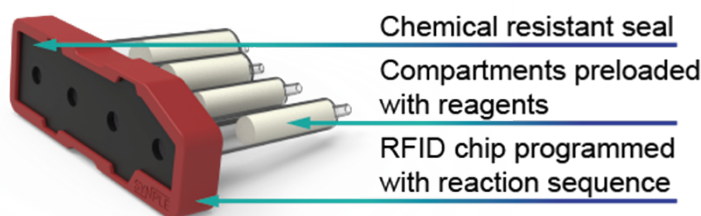


Figure 5.2: Synple Chem reagent cartridge (image adapted from: https://www.synplechem.com/images/2020/07/23/cartridge_info-03.png, 19/11/2022).

The first step of the process required the dissolution of the starting material in the required dry solvent. The solution was placed in a 40 mL reaction vial equipped with a magnetic stir bar. To start the reaction, the cartridge is simply scanned on the machine and the appropriate method for that cartridge loads automatically (there is also the possibility to modify defined parameters, e.g., reaction time, temperature) and the cartridge is inserted into the machine (Fig. 5.3). The system circulates the starting material solution between the vial and the first compartment of the cartridge. After the defined period of time, the solution is then circulated through the second, third and/or fourth compartment, if necessary - depending on the type of reaction run. During the process the individual reactions can take place in the cartridge itself or the reaction vial, which can serve as reactor.

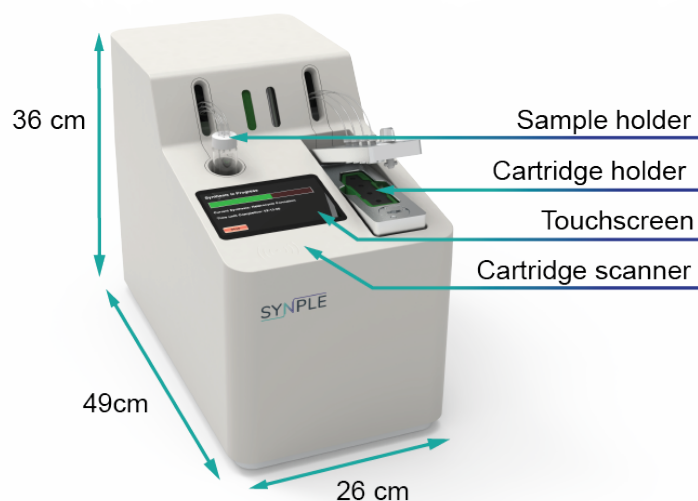
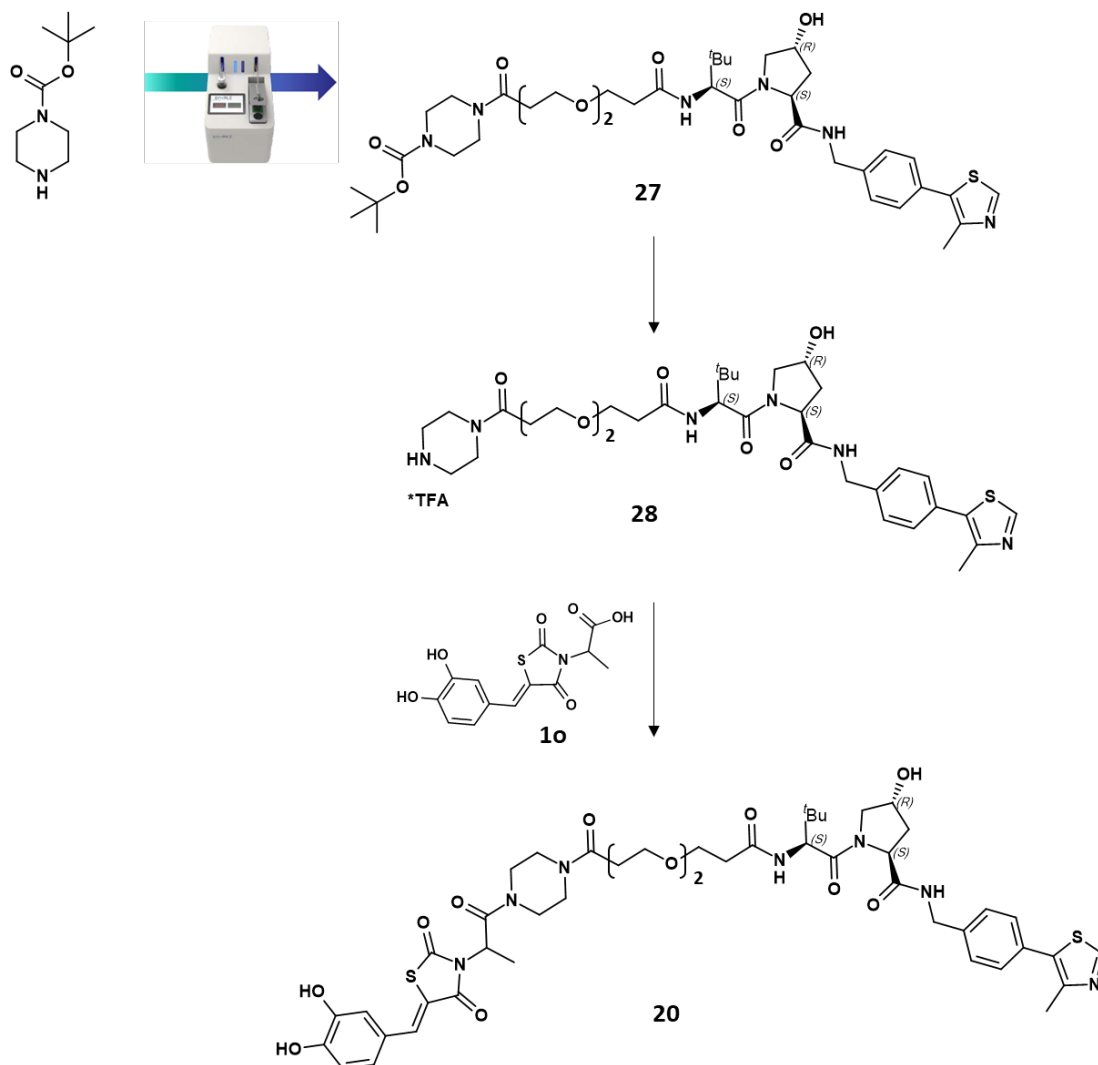


Figure 5.3: Synple Chem console (image adapted from: https://www.synplechem.com/images/2020/05/06/synple2_features-04.png, 19/11/2022).

VHL PROTAC

Synthesis of (2S,4R)-4-hydroxy-N-[[4-(4-methylthiazol-5-yl)phenyl]methyl]-1-[(2S)-3,3-dimethyl-2-[3-[2-[3-oxo-3-[4-[2-[(5Z)-5-[(3,4-dihydroxyphenyl)methylene]-2,4-dioxo-thiazolidin-3-yl]propanoyl]piperazin-1-yl]propoxy]ethoxy]propanoylamino]butanoyl]pyrrolidine-2-carboxamide (20)



Tert-butyl 4-[3-[2-[3-[(1S)-1-[(2S,4R)-4-hydroxy-2-[[4-(4-methylthiazol-5-yl)phenyl]methylcarbamoyl]pyrrolidine-1-carbonyl]-2,2-dimethyl-propyl]amino]-3-oxo-propoxy]ethoxy]propanoyl]piperazine-1-carboxylate (27)

Automated PROTAC formation by amidic coupling performed on the Synple Chem console. A 40 mL vial was charged with a solution of 1-Boc-piperazine (19 mg, 0.1 mmol) in dry DCM (4 mL), under N₂ atmosphere. The vial was placed on the console and connected to the console via a screw cap. The capsule with the desired reagents, P062-PEG2-AE-VHL {composed by three compartments, containing the silica supported carbonate, the solid

supported TEA, and the partial PROTAC reagent as an activated 2,3,5,6-tetrafluorophenyl ester (previously reported in Fig. 3.42): (2,3,5,6-tetrafluorophenyl) 3-[2-[3-[[[(1S)-1-[(2S,4R)-4-hydroxy-2-[[4-(4-methylthiazol-5-yl)phenyl]methylcarbamoyl] pyrrolidine-1-carbonyl]-2,2-dimethyl-propyl]amino]-3-oxo-propoxy]ethoxy]propanoate)} was inserted into the console and the capsule holder was closed. The reaction program was selected by scanning the chip on the capsule. The reaction started automatically upon initiation of the sequence. In the first step of the reactions sequence, the solution of 1-piperazinecarboxylic acid tert-butyl ester (19 mg, 0.1 mmol) in dry DCM (4 mL) circulated through compartment 3 to dissolve the partial PROTAC active ester, followed by rinsing with dry DCM. The solution containing the amine and the PROTAC active ester was stirred for 4 h at room temperature. In the second step (purification), the reaction mixture was slowly loaded to compartment 1 (Si-Carbonate) where the carbonate trapped the excess of active ester, leaving a solution containing only the desired product. The carbonate pad was rinsed with DCM and isopropanol to ensure the full release of the product. After completion of the reaction sequence, the solution in the vial was concentrated in vacuo to afford the crude product (154 mg). The residue was purified by direct phase flash chromatography (cartridge: Biotage sfär Silica D 10 g; gradient conditions: MeOH in EtOAc, from 0% to 25%, 10 CV) to afford compound **27** (28 mg, 0.04 mmol, 36% yield) as a colourless oil.

¹H NMR (400 MHz, Methanol-d₄) δ 8.89 (s, 1H), 7.51 – 7.47 (m, 2H), 7.46 – 7.41 (m, 2H), 4.62 – 4.54 (m, 3H), 4.53 – 4.48 (m, 1H), 4.38 (d, J = 15.5 Hz, 1H), 3.91 (d, J = 11.0 Hz, 1H), 3.82 (dd, J = 11.0, 3.9 Hz, 1H), 3.79 – 3.71 (m, 4H), 3.66 – 3.59 (m, 4H), 3.59 – 3.54 (m, 4H), 3.51 – 3.45 (m, 2H), 3.44 – 3.38 (m, 2H), 2.68 (t, J = 6.3 Hz, 2H), 2.61 – 2.51 (m, 2H), 2.50 (s, 3H), 2.29 – 2.19 (m, 1H), 2.10 (ddd, J = 13.3, 9.1, 4.5 Hz, 1H), 1.48 (s, 9H), 1.06 (s, 9H). C₃₉H₅₈N₆O₉S; UPLC-MS acidic (method A) r.t. 0.92 min, MS (ESI) m/z = 787.7 [M+H]⁺ and 394.4 [M+2H]²⁺.

(2S,4R)-1-[(2S)-3,3-dimethyl-2-[3-[2-(3-oxo-3-piperazin-4-ium-1-yl-propoxy)ethoxy]propanoylamino]butanoyl]-4-hydroxy-N-[[4-(4-methylthiazol-5-yl)phenyl]methyl]pyrrolidine-2-carboxamide; 2,2,2-trifluoroacetate (28)

A stirring solution of compound **27** (28 mg, 0.04 mmol) in dry DCM (0.5 mL) was cooled to 0 °C, then TFA (0.5 mL) was added and the reaction mixture was left reach room temperature. After 1 h, the reaction was concentrated under reduced pressure and the residue was taken up in toluene and concentrated again under *vacuum* to remove traces of trifluoroacetic acid. Compound **28** (35 mg, yield considered as quantitative: 0.04 mmol

theoretical. Purity: 90% A/a by UPLC) was obtained as a white solid and was used directly in the next step without further purification.

¹H NMR (400 MHz, Chloroform-d) δ 9.36 (d, J = 93.7 Hz, 2H), 9.06 (s, 1H), 7.54 – 7.46 (m, 1H), 7.41 (d, J = 8.3 Hz, 2H), 7.36 (d, J = 8.3 Hz, 2H), 7.07 (d, J = 8.4 Hz, 1H), 4.67 – 4.53 (m, 3H), 4.47 (d, J = 8.5 Hz, 1H), 4.35 (dd, J = 15.2, 5.3 Hz, 1H), 4.05 (d, J = 11.3 Hz, 1H), 4.00 – 3.82 (m, 3H), 3.82 – 3.68 (m, 5H), 3.65 – 3.51 (m, 5H), 3.39 – 3.19 (m, 2H), 3.16 – 2.98 (m, 2H), 2.73 – 2.64 (m, 2H), 2.56 (s, 3H), 2.55 – 2.50 (m, 2H), 2.36 – 2.22 (m, 2H), 1.01 (s, 9H). C₃₆H₅₁F₃N₆O₉S; UPLC-MS acidic (method A) r.t. 0.56 min, MS (ESI) m/z = 687.6 [M+H]⁺ and 344.5 [M+2H]²⁺.

(2S,4R)-4-hydroxy-N-[[4-(4-methylthiazol-5-yl)phenyl]methyl]-1-[(2S)-3,3-dimethyl-2-[3-[2-[3-oxo-3-[4-[2-[(5Z)-5-[(3,4-dihydroxyphenyl)methylene]-2,4-dioxo-thiazolidin-3-yl]propanoyl]piperazin-1-yl]propoxy]ethoxy]propanoylamino]butanoyl] pyrrolidine-2-carboxamide (20)

A solution of compound **1o** (12 mg, 0.04 mmol) in dry DMF (1.4 mL) was cooled to 0 °C, then HATU (15 mg, 0.04 mmol) was added, and the resulting mixture was left stirring for 10 min. Then, a solution of compound **28** (29 mg, 0.04 mmol) and DIPEA (20 μL, 0.11 mmol) in dry DMF (0.5 mL) was added and the resulting reaction mixture was left reach room temperature and stirring for a period of 2.5 h. Then, a solution of compound **1o** (12 mg, 0.04 mmol) and HATU (15 mg, 0.04 mmol) in dry DMF (0.2 mL) was added. After 2 h, the reaction was diluted with NH₄Cl_{ss} and EtOAc, the organic phase was washed with brine, separated, and passed through a phase separator. The organic solvents were removed under reduced pressure and the residue was purified by reversed phase flash chromatography (cartridge: Biotage sfär C18 D 12 g; gradient conditions: MeCN in water, in presence of 0.1% HCOOH, from 2% to 70%, 10 CV) to afford 9.5 mg of title product, that was further purified by preparative TLC (PLC silica gel 60 F₂₅₄ 0.5 mm [20 x 20 cm] plates, eluted with MeOH in EtOAc, 1:9) to afford the title product (6 mg) as a yellow solid. As this batch was not enough pure, was sent to semi-preparative HPLC purification to afford compound **20** (2 mg, 0.002 mmol, 5.68% yield) as a red solid.

¹H NMR (400 MHz, Methanol-d₄) δ 8.86 (s, 1H), 7.79 (s, 1H), 7.46 (d, J = 8.1 Hz, 2H), 7.40 (d, J = 8.2 Hz, 2H), 7.03 (s, 1H), 6.98 (d, J = 8.0 Hz, 1H), 6.88 (d, J = 8.2 Hz, 1H), 5.30 (q, J = 6.5 Hz, 1H), 4.66 (d, J = 6.3 Hz, 1H), 4.60 – 4.56 (m, 1H), 4.55 (s, 2H), 4.54 – 4.52 (m, 1H), 4.49 (s, 1H), 4.35 (d, J = 15.5 Hz, 1H), 3.88 (d, J = 11.1 Hz, 1H), 3.79 (dd, J = 11.0, 3.7 Hz, 1H), 3.74 – 3.36 (m, 14H), 2.64 (s, 2H), 2.56 – 2.48 (m, 2H), 2.46 (s, 3H), 2.22 (dd, J = 12.7, 7.9 Hz, 1H), 2.08 (ddd, J = 13.2, 9.2, 4.4 Hz, 1H), 1.57 (dd, J = 7.0, 3.2 Hz, 3H),

1.03 (s, 9H). C₄₇H₅₉N₇O₁₂S₂; UPLC-MS acidic (method A) r.t. 0.86 min, MS (ESI) m/z= 979.0 [M+H]⁺ and 490.0 [M+2H]²⁺.

Semipreparative HPLC conditions and results: Column XSelect CSH Prep. C18 (30 x 100, 5 μ), solvents: A = H₂O + 0.1 % HCOOH, B = MeCN, Loop 1 mL, Acquisition stop time: 15.0 min. Gradient:

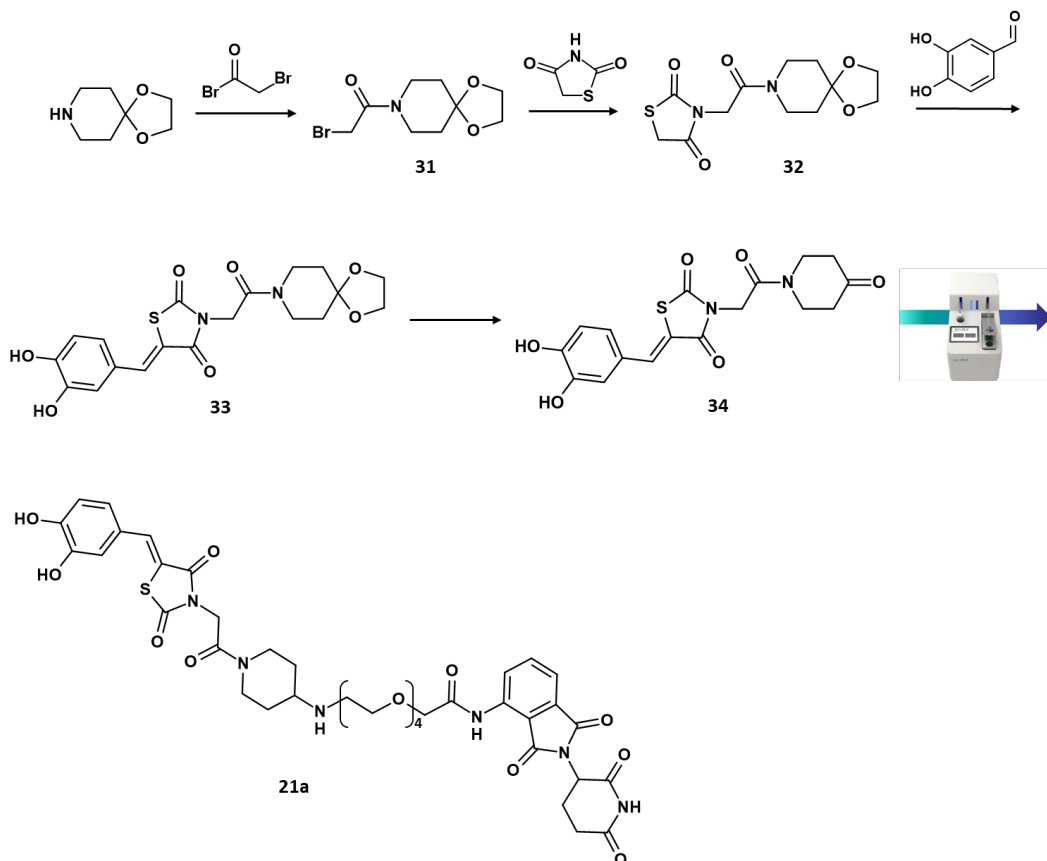
Time (min)	Flow Rate (ml/min)	% A	% B	Curve
initial	40.0	65.0	35.0	-
10.0	40.0	45.0	55.0	6
10.5	40.0	0.1	99.9	6
14.5	40.0	0.1	99.9	6
15.0	40.0	65.0	35.0	6

UV Conditions: UV detection range: 210 nm to 350 nm, acquisition rate: 1.0 spectra/s.

MS Conditions: Ionisation mode: Positive Electrospray (ES⁺), Scan Range : ES⁺ 100 to 900 AMU, Scan Duration : 0.50 seconds.

CRBN PROTACs

Synthesis of 2-[2-[2-[2-[2-[1-[2-[(5Z)-5-[(3,4-dihydroxyphenyl)methylene]-2,4-dioxo-thiazolidin-3-yl]acetyl]-4-piperidyl]amino]ethoxy]ethoxy]ethoxy]ethoxy]-N-[2-(2,6-dioxo-3-piperidyl)-1,3-dioxo-isoinдолin-4-yl]acetamide;2,2,2-trifluoroacetic acid (21a)



2-bromo-1-(1,4-dioxo-8-azaspiro[4.5]decan-8-yl)ethanone (31)

A solution of 1,4-dioxo-8-azaspiro[4.5]decan-8-yl ethanone (0.43 mL, 3.49 mmol) and 2-bromoacetyl bromide (0.37 mL, 4.19 mmol) in DCM (14 mL) was added to a solution of potassium carbonate (0.72 mL, 5.24 mmol) in water (14 mL) and the resulting mixture was vigorously stirred at room temperature for 18 h. The organic phase was filtered through a phase separator and then concentrated under reduced pressure to afford compound **31** (920 mg, 3.48 mmol, 99.7% yield) as a pale-yellow oil.

$^1\text{H NMR}$ (400 MHz, Chloroform- d) δ 3.99 (s, 4H), 3.88 (s, 2H), 3.76 – 3.68 (m, 2H), 3.61 – 3.54 (m, 2H), 1.87 – 1.76 (m, 2H), 1.75 – 1.66 (m, 2H). $\text{C}_9\text{H}_{14}\text{BrNO}_3$; UPLC-MS acidic (method A) r.t. 0.63 min, MS (ESI) m/z = 264.1 and 266.1 $[\text{M}+\text{H}]^+$.

3-[2-(1,4-dioxo-8-azaspiro[4.5]decan-8-yl)-2-oxo-ethyl]thiazolidine-2,4-dione (32)

To a stirring suspension of thiazolidine-2,4-dione (410 mg, 3.48 mmol) and potassium carbonate (963 mg, 6.97 mmol) in dry MeCN (20 mL), compound **31** (920 mg, 3.48 mmol) was added at room temperature under nitrogen atmosphere. After 18 h, the reaction was concentrated under *vacuum* and the residue was partitioned between DCM and water. The organic phase was passed through a phase separator and concentrated under reduced pressure to afford compound **32** (1.04 g, 3.46 mmol, 99 % yield) as an orange oil. This crude was used as such in the subsequent step without further purification.

¹H NMR (400 MHz, Chloroform-d) δ 4.43 (s, 2H), 4.04 (s, 2H), 3.98 (s, 4H), 3.69 (t, J = 6.0 Hz, 2H), 3.53 (t, J = 5.9 Hz, 2H), 1.78 (t, J = 5.9 Hz, 2H), 1.70 (t, J = 6.0 Hz, 2H). C₁₂H₁₆N₂O₅S; UPLC-MS acidic (method A) r.t. 0.58 min, MS (ESI) m/z= 301.2 [M+H]⁺.

(5Z)-5-[(3,4-dihydroxyphenyl)methylene]-3-[2-(1,4-dioxo-8-azaspiro[4.5]decan-8-yl)-2-oxo-ethyl]thiazolidine-2,4-dione (33)

To a stirring solution of compound **32** (500 mg, 1.66 mmol) and 3,4-dihydroxybenzaldehyde (230 mg, 1.66 mmol) in ethanol (4 mL), piperidine (82 μL, 0.83 mmol) was added and the reaction mixture was heated under reflux for 8 h. After cooling to room temperature, the reaction mixture was poured into water and acidified with acetic acid (4.0 mL, 66.94 mmol). The resulting precipitate was filtered off and washed with MeOH (10 mL) to give compound **33** (533 mg, 1.27 mmol, 76% yield) as a yellow solid.

¹H NMR (400 MHz, DMSO-d₆) δ 7.77 (s, 1H), 7.07 – 6.98 (m, 2H), 6.88 (d, J = 8.1 Hz, 1H), 4.61 (s, 2H), 3.93 (s, 4H), 3.54 (dt, J = 18.8, 6.0 Hz, 4H), 1.71 (t, J = 5.8 Hz, 2H), 1.58 (t, J = 6.0 Hz, 2H). C₁₉H₂₀N₂O₇S; UPLC-MS acidic (method A) r.t. 0.79 min, MS (ESI) m/z= 421.3 [M+H]⁺.

(5Z)-5-[(3,4-dihydroxyphenyl)methylene]-3-[2-oxo-2-(4-oxo-1-piperidyl)ethyl]thiazolidine-2,4-dione (34)

A suspension of compound **33** (513 mg, 1.22 mmol) in a mixture of MeCN (2 mL) and HCl 6 M (2.0 mL, 12 mmol) was left stirring at 80 °C for 4 h. After cooling the reaction to room temperature, precipitation of the title product as a yellow solid was observed. The solid was recovered by filtration and then was washed with MeCN and water to afford compound **34** (309 mg, 0.82 mmol, 67% yield) as a yellow solid.

¹H NMR (400 MHz, DMSO-d₆) δ 9.68 (s, 1H), 7.78 (s, 1H), 7.08 – 6.99 (m, 2H), 6.89 (d, J = 8.1 Hz, 1H), 4.69 (s, 2H), 3.84 (t, J = 6.3 Hz, 2H), 3.74 (t, J = 6.4 Hz, 2H), 2.55 – 2.51 (m,

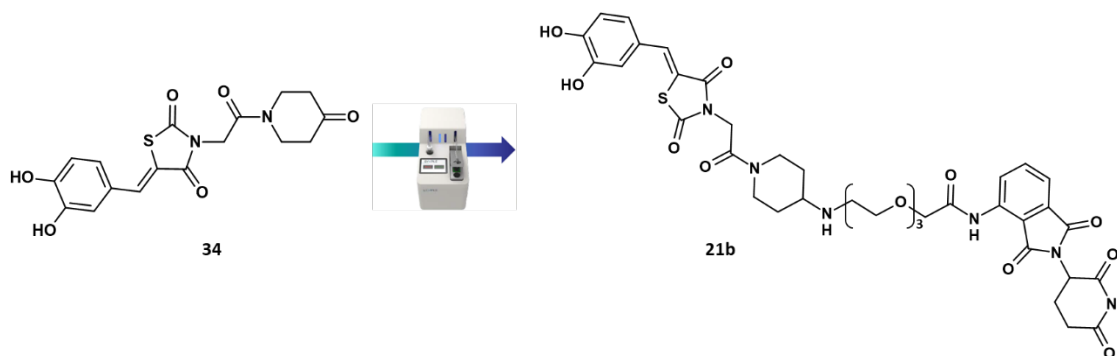
2H), 2.40 (t, J = 6.4 Hz, 2H). C₁₇H₁₆N₂O₆S; UPLC-MS acidic (method A) r.t. 0.69 min, MS (ESI) m/z= 377.3 [M+H]⁺.

2-[2-[2-[2-[2-[1-[2-[(5Z)-5-[(3,4-dihydroxyphenyl)methylene]-2,4-dioxo-thiazolidin-3-yl]acetyl]-4-piperidyl]amino]ethoxy]ethoxy]ethoxy]ethoxy]-N-[2-(2,6-dioxo-3-piperidyl)-1,3-dioxo-isoindolin-4-yl]acetamide;2,2,2-trifluoroacetic acid (21a)

Automated PROTAC formation by reductive amination performed on the Synple Chem console. A 40 mL vial was charged with a solution of compound **34** (38 mg, 0.1 mmol) in a mixture of dry DCM (3 mL) and HFIP (1 mL), under N₂ atmosphere. The vial was placed on the console and connected to the console via a screw cap. The capsule with the desired reagents, P004-CRBN-PEG4 {composed by four compartments, containing the silica supported cyanoborohydride, the solid supported TEA, a SCX and the partial PROTAC reagent, 2-[2-[2-[2-[2-[2-[(2,6-dioxo-3-piperidyl)-1,3-dioxo-isoindolin-4-yl]amino]-2-oxo-ethoxy]ethoxy]ethoxy] ethoxy]ethylammonium;2,2,2-trifluoroacetate, in form of amine salt} was inserted into the console and the capsule holder was closed. The reaction program was selected by scanning the chip on the capsule and the purification step of the sequence was manually disabled. The reaction started automatically upon initiation of the sequence. In the first step of the reactions sequence, the solution of compound **34** contained in the vial passed through compartment 4 to dissolve the amine salt of the partial PROTAC. The compartment is then rinsed into the vial with anhydrous DCM. The reaction mixture is then passed through compartment 2 (free basing agent) and then rinsed into the vial with anhydrous DCM. In the next step the solution was circulated through cartridge compartment 1 (reducing agent) at 2 mL/min at room temperature for 2.5 h. Then, compartment 1 was rinsed with DCM (5 mL) into the vial. As the purification step of the sequence was disabled, the machine provided the reaction product in solution in the reaction vial after the reduction step. After completion of the reaction sequence (11 hours), the solution in the vial was concentrated in vacuo and the residue was purified by reversed phase flash chromatography (cartridge: Biotage sfär C18 D 12 g; gradient conditions: MeCN in Water, in presence of 0.1% HCOOH, from 3% to 80%, 10 CV). The product containing fractions were collected and freeze-dried to afford 30 mg of the title product which was further purified by reversed phase flash chromatography (cartridge: Biotage sfär C18 D 12 g, gradient conditions; MeCN in Water, in presence of 0.05% TFA, from 3% to 35%, 10 CV). The product containing fractions were collected and freeze-dried to give compound **21a** (17 mg, 0.017 mmol, 17% yield) as a yellow solid and a trifluoroacetic acid salt.

^1H NMR (400 MHz, DMSO- d_6) δ 11.14 (s, 1H), 10.35 (s, 1H), 9.93 (s, 1H), 9.48 (s, 1H), 8.73 (d, $J = 8.4$ Hz, 1H), 8.53 (s, 2H), 7.87 (dd, $J = 8.5, 7.3$ Hz, 1H), 7.75 (s, 1H), 7.64 (dd, $J = 7.4, 0.8$ Hz, 1H), 7.10 – 6.96 (m, 2H), 6.89 (d, $J = 8.2$ Hz, 1H), 5.16 (dd, $J = 12.8, 5.5$ Hz, 1H), 4.66 (d, $J = 16.6$ Hz, 1H), 4.55 (d, $J = 16.5$ Hz, 1H), 4.41 – 4.26 (m, 1H), 4.22 (s, 2H), 4.10 – 3.93 (m, 1H), 3.77 (dd, $J = 5.8, 3.4$ Hz, 2H), 3.71 – 3.62 (m, 5H), 3.61 – 3.48 (m, 9H), 3.14 (d, $J = 13.7$ Hz, 3H), 2.90 (ddd, $J = 16.9, 13.7, 5.4$ Hz, 1H), 2.71 – 2.52 (m, 3H), 2.16 – 1.98 (m, 2H), 1.62 – 1.46 (m, 1H), 1.43 – 1.29 (m, 1H). $\text{C}_{42}\text{H}_{47}\text{F}_3\text{N}_6\text{O}_{16}\text{S}$; UPLC-MS acidic (method A) r.t. 0.63 min, MS (ESI) $m/z = 867.3$ $[\text{M}+\text{H}]^+$.

Synthesis of 2-[2-[2-[2-[[1-[2-[(5Z)-5-[(3,4-dihydroxyphenyl)methylene]-2,4-dioxo-thiazolidin-3-yl]acetyl]-4-piperidyl]amino]ethoxy]ethoxy]ethoxy]-N-[2-(2,6-dioxo-3-piperidyl)-1,3-dioxo-isoindolin-4-yl]acetamide;2,2,2-trifluoroacetic acid (21b)



Automated PROTAC formation by reductive amination performed on the Synple Chem console. A 40 mL vial was charged with a solution of compound **34** (38 mg, 0.1 mmol) in a mixture of dry DCM (3 mL) and HFIP (1 mL), under N_2 atmosphere. The vial was placed on the console and connected to the console via a screw cap. The capsule with the desired reagents, P003-CRBN-PEG3 (composed by four compartments, containing the silica supported cyanoborohydride, the solid supported TEA, a SCX and the partial PROTAC reagent, 2-[2-[2-[2-[[2-(2,6-dioxo-3-piperidyl)-1,3-dioxo-isoindolin-4-yl]amino]-2-oxo-ethoxy]ethoxy]ethoxy]ethyl ammonium;2,2,2-trifluoroacetate, in form of amine salt) was inserted into the console and the capsule holder was closed. The reaction program was selected by scanning the chip on the capsule and the purification step of the sequence was manually disabled. The reaction started automatically upon initiation of the sequence.

In the first step of the reactions sequence, the solution of compound **34** contained in the vial passed through compartment 4 to dissolve the amine salt of the partial PROTAC. The compartment is then rinsed into the vial with anhydrous DCM. The reaction mixture is then passed through compartment 2 (free basing agent) and then rinsed into the vial with anhydrous DCM. In the next step the solution was circulated through cartridge compartment

1 (reducing agent) at 2 mL/min at room temperature for 2.5 h. Then, compartment 1 was rinsed with DCM (5 mL) into the vial. As the purification step of the sequence was disabled, the machine provided the reaction product in solution in the reaction vial after the reduction step. After completion of the reaction sequence (11 hours), the solution in the vial was concentrated in vacuo and the residue was purified by reversed phase flash chromatography (cartridge: Biotage sfär C18 D 12 g, gradient conditions: MeCN in water, in presence of 0.05% TFA, from 3% to 35%, 10 CV). The product containing fractions were collected and freeze-dried to afford the title product **21b** (31 mg, 0.033 mmol, 33% yield) as a yellow solid and a trifluoroacetic acid salt.

¹H NMR (400 MHz, DMSO-d₆) δ 11.15 (s, 1H), 10.35 (s, 1H), 9.94 (s, 1H), 9.49 (s, 1H), 8.73 (d, J = 8.5 Hz, 1H), 8.56 (s, 2H), 7.88 (t, J = 7.9 Hz, 1H), 7.75 (s, 1H), 7.65 (d, J = 7.3 Hz, 1H), 7.10 – 6.96 (m, 2H), 6.89 (d, J = 8.1 Hz, 1H), 5.16 (dd, J = 12.8, 5.4 Hz, 1H), 4.65 (d, J = 16.6 Hz, 1H), 4.54 (d, J = 16.4 Hz, 1H), 4.34 (d, J = 13.1 Hz, 1H), 4.22 (s, 2H), 4.02 (d, J = 13.4 Hz, 1H), 3.78 (t, J = 4.6 Hz, 2H), 3.73 – 3.56 (m, 8H), 3.23 – 3.01 (m, 4H), 2.97 – 2.80 (m, 1H), 2.73 – 2.53 (m, 3H), 2.20 – 1.98 (m, 3H), 1.65 – 1.46 (m, 1H), 1.43 – 1.28 (m, 1H). C₄₀H₄₃F₃N₆O₁₅S; UPLC-MS acidic (method A) r.t. 0.63 min, MS (ESI) m/z= 823.3 [M+H]⁺.

6. REFERENCES

1. World Health Organization (WHO). Global Health Estimates 2020: Deaths by Cause, Age, Sex, by Country and by Region, 2000-2019. WHO; Accessed 20 November 2022. [who.int/data/gho/data/themes/mortality-and-global-health-estimates/ghe-leading-causes-of-death](https://www.who.int/data/gho/data/themes/mortality-and-global-health-estimates/ghe-leading-causes-of-death).
2. Mattiuzzi C, Lippi G. Current Cancer Epidemiology. *J Epidemiol Glob Health*. 2019;9(4):217. doi:10.2991/jegh.k.191008.001
3. Northcott PA, Jones DTW, Kool M, et al. Medulloblastomics: the end of the beginning. *Nat Rev Cancer*. 2012;12(12):818-834. doi:10.1038/nrc3410
4. Vasan N, Baselga J, Hyman DM. A view on drug resistance in cancer. *Nature*. 2019;575(7782):299-309. doi:10.1038/s41586-019-1730-1
5. Mariotto E, Viola G, Zanon C, Aveic S. A BAG's life: Every connection matters in cancer. *Pharmacol Ther*. 2020;209:107498. doi:10.1016/J.PHARMTHERA.2020.107498
6. Poletti A, Rein T, Wang C, Behl C, Stürner E. The Role of the Multifunctional BAG3 Protein in Cellular Protein Quality Control and in Disease. *Front Mol Neurosci*. 2017;10(177). doi:10.3389/fnmol.2017.00177
7. Behl C. Breaking BAG: The Co-Chaperone BAG3 in Health and Disease. *Trends Pharmacol Sci*. 2016;37(8):672-688. doi:10.1016/j.tips.2016.04.007
8. Kögel D, Linder B, Brunschweiler A, Chines S, Behl C. At the Crossroads of Apoptosis and Autophagy: Multiple Roles of the Co-Chaperone BAG3 in Stress and Therapy Resistance of Cancer. *Cells*. 2020;9(3):574. doi:10.3390/cells9030574
9. Rosati A, Ammirante M, Gentilella A, et al. Apoptosis inhibition in cancer cells: A novel molecular pathway that involves BAG3 protein. *Int J Biochem Cell Biol*. 2007;39(7-8):1337-1342. doi:10.1016/J.BIOCEL.2007.03.007
10. Gamerding M, Hajieva P, Kaya AM, Wolfrum U, Hartl FU, Behl C. Protein quality control during aging involves recruitment of the macroautophagy pathway by BAG3. *EMBO Journal*. 2009;28(7). doi:10.1038/emboj.2009.29

11. Lüders J, Demand J, Höhfeld J. The Ubiquitin-related BAG-1 Provides a Link between the Molecular Chaperones Hsc70/Hsp70 and the Proteasome. *Journal of Biological Chemistry*. 2000;275(7):4613-4617. doi:10.1074/jbc.275.7.4613
12. Rosati A, Graziano V, de Laurenzi V, Pascale M, Turco MC. BAG3: a multifaceted protein that regulates major cell pathways. *Cell Death Dis*. 2011;2(4). doi:10.1038/cddis.2011.24
13. Takayama S, Sato T, Krajewski S, et al. Cloning and functional analysis of BAG-1: A novel Bcl-2-binding protein with anti-cell death activity. *Cell*. 1995;80(2):279-284. doi:10.1016/0092-8674(95)90410-7
14. Reed JC. Bcl-2 and the regulation of programmed cell death. *Journal of Cell Biology*. 1994;124(1-2). doi:10.1083/jcb.124.1.1
15. Hockenbery DM. The bcl-2 oncogene and apoptosis. *Semin Immunol*. 1992;4(6).
16. Hockenbery D, Nuñez G, Milliman C, Schreiber RD, Korsmeyer SJ. Bcl-2 is an inner mitochondrial membrane protein that blocks programmed cell death. *Nature*. 1990;348(6299). doi:10.1038/348334a0
17. Coulson M, Robert S, Saint R. Drosophila starvin encodes a tissue-specific BAG-domain protein required for larval food uptake. *Genetics*. 2005;171(4). doi:10.1534/genetics.105.043265
18. Fang S, Li L, Cui B, Men S, Shen Y, Yang X. Structural insight into plant programmed cell death mediated by BAG proteins in *Arabidopsis thaliana*. *Acta Crystallogr D Biol Crystallogr*. 2013;69(6):934-945. doi:10.1107/S0907444913003624
19. Colinet H, Hoffmann A. Gene and protein expression of *Drosophila* Starvin during cold stress and recovery from chill coma. *Insect Biochem Mol Biol*. 2010;40(5). doi:10.1016/j.ibmb.2010.03.002
20. Doukhanina E v., Chen S, van der Zalm E, Godzik A, Reed J, Dickman MB. Identification and functional characterization of the BAG protein family in *Arabidopsis thaliana*. *Journal of Biological Chemistry*. 2006;281(27). doi:10.1074/jbc.M511794200

21. Takayama S, Xie Z, Reed JC. An evolutionarily conserved family of Hsp70/Hsc70 molecular chaperone regulators. *Journal of Biological Chemistry*. 1999;274(2). doi:10.1074/jbc.274.2.781
22. Arakawa A, Handa N, Ohsawa N, et al. The C-Terminal BAG Domain of BAG5 Induces Conformational Changes of the Hsp70 Nucleotide- Binding Domain for ADP-ATP Exchange. *Structure*. 2010;18(3). doi:10.1016/j.str.2010.01.004
23. Colvin TA, Gabai VL, Gong J, et al. Hsp70-Bag3 interactions regulate cancer-related signaling networks. *Cancer Res*. 2014;74(17). doi:10.1158/0008-5472.CAN-14-0747
24. Sondermann H, Scheußer C, Schneider C, Hohfeld J, Hartl F, Moarefi I. Structure of a Bag/Hsc70 Complex: Convergent Functional Evolution of Hsp70 Nucleotide Exchange Factors. *Science (1979)*. 2001;291(5508):1553-1557.
25. Fernández-Fernández MR, Valpuesta JM. Hsp70 chaperone: a master player in protein homeostasis. *F1000Res*. 2018;7:1497. doi:10.12688/f1000research.15528.1
26. Zhu H, Wu W, Fu Y, et al. Overexpressed BAG3 is a potential therapeutic target in chronic lymphocytic leukemia. *Ann Hematol*. 2014;93(3):425-435. doi:10.1007/s00277-013-1883-1
27. Bonelli P, Petrella A, Rosati A, et al. BAG3 protein regulates stress-induced apoptosis in normal and neoplastic leukocytes. *Leukemia*. 2004;18(2):358-360. doi:10.1038/sj.leu.2403219
28. Yang D, Zhou J, Wang H, Wang Y, Yang G, Zhang Y. High expression of BAG3 predicts a poor prognosis in human medulloblastoma. *Tumor Biology*. 2016;37(10). doi:10.1007/s13277-016-5197-5
29. Festa M, del Valle L, Khalili K, et al. BAG3 Protein Is Overexpressed in Human Glioblastoma and Is a Potential Target for Therapy. *Am J Pathol*. 2011;178(6):2504-2512. doi:10.1016/J.AJPATH.2011.02.002
30. Chiappetta G, Ammirante M, Basile A, et al. The antiapoptotic protein BAG3 is expressed in thyroid carcinomas and modulates apoptosis mediated by tumor necrosis factor-related apoptosis-inducing ligand. *Journal of Clinical Endocrinology and Metabolism*. 2007;92(3). doi:10.1210/jc.2006-1712

31. Chiappetta G, Basile A, Barbieri A, et al. The anti-apoptotic BAG3 protein is expressed in lung carcinomas and regulates small cell lung carcinoma (SCLC) tumor growth. *Oncotarget*. 2014;5(16). doi:10.18632/oncotarget.2261
32. Li N, Chen M, Cao Y, et al. Bcl-2-associated athanogene 3(BAG3) is associated with tumor cell proliferation, migration, invasion and chemoresistance in colorectal cancer. *BMC Cancer*. 2018;18(1):793. doi:10.1186/s12885-018-4657-2
33. Das CK, Linder B, Bonn F, et al. BAG3 Overexpression and Cytoprotective Autophagy Mediate Apoptosis Resistance in Chemoresistant Breast Cancer Cells. *Neoplasia*. 2018;20(3):263-279. doi:10.1016/j.neo.2018.01.001
34. Xiao H, Cheng S, Tong R, et al. BAG3 regulates epithelial-mesenchymal transition and angiogenesis in human hepatocellular carcinoma. *Laboratory Investigation*. 2014;94(3). doi:10.1038/labinvest.2013.151
35. Rosati A, Bersani S, Tavano F, et al. Expression of the antiapoptotic protein BAG3 is a feature of pancreatic adenocarcinoma and its overexpression is associated with poorer survival. *American Journal of Pathology*. 2012;181(5). doi:10.1016/j.ajpath.2012.07.016
36. Liao Q, Ozawa F, Friess H, et al. The anti-apoptotic protein BAG-3 is overexpressed in pancreatic cancer and induced by heat stress in pancreatic cancer cell lines. *FEBS Lett*. 2001;503(2-3):151-157. doi:10.1016/S0014-5793(01)02728-4
37. Bukau B, Weissman J, Horwich A. Molecular Chaperones and Protein Quality Control. *Cell*. 2006;125(3):443-451. doi:10.1016/j.cell.2006.04.014
38. Lüders J, Demand J, Höhfeld J. The Ubiquitin-related BAG-1 Provides a Link between the Molecular Chaperones Hsc70/Hsp70 and the Proteasome. *Journal of Biological Chemistry*. 2000;275(7):4613-4617. doi:10.1074/jbc.275.7.4613
39. Alberti S, Esser C, Höhfeld J. BAG-1—a nucleotide exchange factor of Hsc70 with multiple cellular functions. *Cell Stress Chaperones*. 2003;8(3):225. doi:10.1379/1466-1268(2003)008<0225:BNEFOH>2.0.CO;2
40. Singh R, Letai A, Sarosiek K. Regulation of apoptosis in health and disease: the balancing act of BCL-2 family proteins. *Nat Rev Mol Cell Biol*. 2019;20(3):175-193. doi:10.1038/s41580-018-0089-8

41. Boiani M, Daniel C, Liu X, Hogarty MD, Marnett LJ. The Stress Protein BAG3 Stabilizes Mcl-1 Protein and Promotes Survival of Cancer Cells and Resistance to Antagonist ABT-737. *Journal of Biological Chemistry*. 2013;288(10):6980-6990. doi:10.1074/JBC.M112.414177
42. Ammirante M, Rosati A, Arra C, et al. IKK γ protein is a target of BAG3 regulatory activity in human tumor growth. *PNAS*. 2010;107(16):7497-7502. doi:10.1073/pnas.0907696107
43. Li X, Colvin T, Rauch JN, et al. Validation of the Hsp70-Bag3 Protein-Protein Interaction as a Potential Therapeutic Target in Cancer. *Mol Cancer Ther*. 2015;14(3):642-648. doi:10.1158/1535-7163.MCT-14-0650
44. Li X, Srinivasan SR, Connarn J, et al. Analogues of the Allosteric Heat Shock Protein 70 (Hsp70) Inhibitor, MKT-077, As Anti-Cancer Agents. *ACS Med Chem Lett*. 2013;4(11):1042-1047. doi:10.1021/ml400204n
45. Shao H, Li X, Moses MA, et al. Exploration of Benzothiazole Rhodacyanines as Allosteric Inhibitors of Protein–Protein Interactions with Heat Shock Protein 70 (Hsp70). *J Med Chem*. 2018;61:6162-6177. doi:10.1021/acs.jmedchem.8b00583
46. Taylor IR, Duniak BM, Komiyama T, et al. High-throughput screen for inhibitors of protein–protein interactions in a reconstituted heat shock protein 70 (Hsp70) complex. *Journal of Biological Chemistry*. 2018;293(11):4014-4025. doi:10.1074/JBC.RA117.001575
47. Terracciano S, Lauro G, Russo A, et al. Discovery and synthesis of the first selective BAG domain modulator of BAG3 as an attractive candidate for the development of a new class of chemotherapeutics. *Chem Commun*. 2018;54:7613. doi:10.1039/c8cc03399d
48. Ruggiero D, Terracciano S, Lauro G, et al. Structural Refinement of 2,4-Thiazolidinedione Derivatives as New Anticancer Agents Able to Modulate the BAG3 Protein. *Molecules*. 2022;27(3):665. doi:10.3390/molecules27030665
49. Churcher I. Protac-Induced Protein Degradation in Drug Discovery: Breaking the Rules or Just Making New Ones? *J Med Chem*. 2018;61:444-452. doi:10.1021/acs.jmedchem.7b01272

50. Weathington NM, Sznajder JI, Mallampalli RK. The emerging role of the ubiquitin proteasome in pulmonary biology and disease. *Am J Respir Crit Care Med*. 2013;188(5).
51. Gao H, Sun X, Rao Y. PROTAC Technology: Opportunities and Challenges. *ACS Med Chem Lett*. 2020;11(3):237-240. doi:10.1021/acsmchemlett.9b00597
52. Hughes SJ, Ciulli A. Molecular recognition of ternary complexes: a new dimension in the structure-guided design of chemical degraders. *Essays Biochem*. 2017:61-505. doi:10.1042/EBC20170041
53. Pettersson M, Crews CM. PROteolysis TArgeting Chimeras (PROTACs) — Past, present and future. *Drug Discov Today Technol*. 2019;31:15-27. doi:10.1016/J.DDTEC.2019.01.002
54. Khan S, Zhang X, Lv D, et al. A selective BCL-XL PROTAC degrader achieves safe and potent antitumor activity. *Nat Med*. 2019;25(12):1938-1947. doi:10.1038/s41591-019-0668-z
55. Chessum NEA, Sharp SY, Caldwell JJ, et al. Demonstrating In-Cell Target Engagement Using a Pirin Protein Degradation Probe (CCT367766). *J Med Chem*. 2018;61(3):918-933. doi:10.1021/acs.jmedchem.7b01406
56. Ciulli A, Trainor N. A beginner's guide to PROTACs and targeted protein degradation. *Biochem (Lond)*. 2021;43(5):74-79. doi:10.1042/bio_2021_148
57. Troup RI, Fallan C, Baud MGJ. Current strategies for the design of PROTAC linkers: a critical review. *Explor Target Antitumor Ther*. 2020;1(5). doi:10.37349/etat.2020.00018
58. Niesen FH, Berglund H, Vedadi M. The use of differential scanning fluorimetry to detect ligand interactions that promote protein stability. *Nat Protoc*. 2007;2(9):2212-2221. doi:10.1038/nprot.2007.321
59. Bruce D, Cardew E, Freitag-Pohl S, Pohl E. How to Stabilize Protein: Stability Screens for Thermal Shift Assays and Nano Differential Scanning Fluorimetry in the Virus-X Project. *Journal of Visualized Experiments*. 2019;(144). doi:10.3791/58666

60. Kranz JK, Schalk-Hihi C. Protein Thermal Shifts to Identify Low Molecular Weight Fragments. In: *Methods Enzymol.* 2011;277-298. doi:10.1016/B978-0-12-381274-2.00011-X
61. https://www.reactionbiology.com/sites/default/files/styles/image_content_800_x_800_/public/Images/Content/Biophysical_Assay/SPR.png?itok=zduBba_f.
62. Hodgson E. Introduction to Biotransformation (Metabolism). In: *Hayes' Handbook of Pesticide Toxicology.* Elsevier; 2010:865-875. doi:10.1016/B978-0-12-374367-1.00036-7
63. Steiner K, Schwab H. Recent Advances in Rational Approaches for Enzyme Engineering. *Comput Struct Biotechnol J.* 2012;2(3):e201209010. doi:10.5936/csbj.201209010
64. Schweigert N, Zehnder AJB, Eggen RIL. Chemical properties of catechols and their molecular modes of toxic action in cells, from microorganisms to mammals. Minireview. *Environ Microbiol.* 2001;3(2):81-91. doi:10.1046/j.1462-2920.2001.00176.x
65. Marfat A. Indazole bioisostere replacement of catechol in therapeutically active compounds. WO1999023077A1
66. Wermuth CG, Ciapetti P, Giethlen B, Bazzini P. Bioisosterism. In: *Comprehensive Medicinal Chemistry II.* Elsevier; 2007:649-711. doi:10.1016/B0-08-045044-X/00051-1
67. Le S, Yasuoka C, Asahara H, Nishiwaki N. Dual Behavior of Iodine Species in Condensation of Anilines and Vinyl Ethers Affording 2-Methylquinolines. *Molecules.* 2016;21(7):827. doi:10.3390/molecules21070827
68. Sun Y. E3 Ubiquitin Ligases as Cancer Targets and Biomarkers. *Neoplasia.* 2006;8(8):645-654. doi:10.1593/neo.06376
69. Yang K, Zhao Y, Nie X, et al. A Cell-Based Target Engagement Assay for the Identification of Cereblon E3 Ubiquitin Ligase Ligands and Their Application in HDAC6 Degradation. *Cell Chem Biol.* 2020;27(7):866-876.e8. doi:10.1016/j.chembiol.2020.04.008

70. Fischer ES, Böhm K, Lydeard JR, et al. Structure of the DDB1–CRBN E3 ubiquitin ligase in complex with thalidomide. *Nature*. 2014;512(7512):49-53. doi:10.1038/nature13527
71. Lai AC, Toure M, Hellerschmied D, et al. Modular PROTAC Design for the Degradation of Oncogenic BCR-ABL. *Angewandte Chemie International Edition*. 2016;55(2):807-810. doi:10.1002/anie.201507634
72. Rosen BR, Ruble JC, Beauchamp TJ, Navarro A. Mild Pd-Catalyzed N-Arylation of Methanesulfonamide and Related Nucleophiles: Avoiding Potentially Genotoxic Reagents and Byproducts. *Org Lett*. 2011;13(10):2564-2567. doi:10.1021/ol200660s

7. ACKNOWLEDGEMENTS

I really want to thank Aptuit, the company I'm working for, my manager Daniele Andreotti and my tutor Colin Philip Leslie to give me this personal and very important opportunity. I also want to thank Professor Romeo Romagnoli, that let me be a member of his research team and makes this PhD work possible.

I also would like to thank all the colleagues and friends who supported me with their precious advice, brilliant ideas, and affection, they make every day better. A special thought also goes to my loved ones, they taught me to always believe in myself and follow my dreams.

“Twenty years from now you will be more disappointed by the things that you didn't do than by the ones you did do. So throw off the bowlines. Sail away from the safe harbor. Catch the trade winds in your sails. Explore. Dream. Discover”.

M. Twain

“The future belongs to those who believe in the beauty of their dreams”.

E. Roosevelt